Ovotransferrin: a multifunctional protein involved in the passive immunity of egg white

A thesis submitted to

THE UNIVERSITY OF READING '*The Faculty of Life Sciences*' in partial fulfilment of the requirements for the Degree of Doctor of Philosophy

&

INSTITUT AGRO '*École nationale supérieure des sciences agronomes, agroalimentaires, horticoles et du paysage*'

Spécialité : *Microbiologie, virologie et parasitologie*

Ecole doctorale Ecologie, Géosciences, Agronomie et Alimentation (EGAAL)

by

Julie Legros

October 2023

COLLEGE ECOLOGIE
DOCTORAL GEOSCIENCES
BRETAGNE AGRONOMIE ALIMENTATION

University of Reading

L'INSTITUT agro Rennes Angers

THESE DE DOCTORAT DE

L'INSTITUT AGRO RENNES-ANGERS

ECOLE DOCTORALE N° 600
Ecologie, Géosciences, Agronomie, Alimentation
Spécialité : Microbiologie, virologie et parasitologie

UNIVERSITY OF READING

Par
Julie LEGROS

Ovotransferrin: a multifunctional protein involved in the passive immunity of egg white

Thèse présentée et soutenue à Reading le 13 Décembre 2023
Unité de recherche : L'nstitut Agro Rennes-Angers, UMR 1253 STLO, INRAE, 35042, Rennes, France
School of Biological Sciences, University of Reading, Reading, United Kingdom
Thèse N° : I-862023-31

Composition du Jury :

Examinateurs :	Sheila MacIntyre	Maître de conférences, University of Reading Reading, United Kingdom
	Catherine Sarazin	Professeure, UMR 7025, CNRS, Université Picardie Jules Verne Amiens, France
Dir. de thèse :	Sophie Jan	Professeure, l'Institut Agro Rennes-Angers, UMR 1253 STLO, INRAE, Rennes, France
	Simon Andrews	Professeur, School of Biological Sciences, University of Reading, Reading, United Kingdom

To my beloved grandfather,
1927-2012

Acknowledgements

I wish to express my gratitude to the members of my viva committee Dr Sheila MacIntyre and Prof Catherine Sarazin for assessing my work. I also thank Prof Christina Nielsen-Leroux, Dr Geraldine Mulley, and Prof Thomas Croguennec for your advice and support during my thesis committees.

Thank you to my supervisors and co-supervisors: Prof Simon Andrews, Prof Sophie Jan, Dr Florence Baron, Dr Sylvie Bonnassie and Prof Françoise Nau for their advice and guidance throughout the past three years. Thank you, Marie-Françoise Cochet, for the upstream work you have accomplished and your help.

My thesis would not have been the same without all my colleagues from France and Reading. I would like to thank all of you for your support, help and, for sharing lunchtimes, coffee breaks and fun moments with me: Abdallah, Anne-Lise, Auxane, Bénédicte, Caroline, Clara, Cynthia, Fabien, Fabienne, Giovanni, James, Jacques, Joss, Laetitia, Marie-Emmanuelle, Noël, Saya and Sophie. I wish all of you the best.

I would also like to mention my friends, former colleagues and supervisor for your advice and precious support for several years. So many thanks to Julie, Nadia, Renan, Simon and Yoann.

My last thanks go to my family, especially my parents, who gave me the opportunity to follow my own way and always support my choices. And finally, my lovely grandparents for your love, generosity and being there for me throughout your lives. I miss you.

Original authorship

I confirm that this is my own work and the use of all material from other sources has been properly and fully acknowledged.

Julie Legros

Conflict of interests

This work is supported by the Regional Council of French Britany (Allocation de Recherche Doctorale, ARED) and by the Strategic Fund of the University of Reading. The author has no affiliations with or involvement in any organisation or entity with any financial interest, or non-financial interest in the subject matter or materials discussed in this report.

Publications

Legros, J.; Jan, S.; Bonnassie, S.; Gautier, M.; Croguennec, T.; Pezennec, S.; Cochet, M.-F.; Nau, F.; Andrews, S.C.; Baron, F. The Role of Ovotransferrin in Egg-White Antimicrobial Activity: A Review. *Foods* **2021**, *10*, 823.

foods

MDPI

Review

The Role of Ovotransferrin in Egg-White Antimicrobial Activity: A Review

Julie Legros [1,2], Sophie Jan [1], Sylvie Bonnassie [3], Michel Gautier [1], Thomas Croguennec [1], Stéphane Pezennec [1], Marie-Françoise Cochet [1], Françoise Nau [1], Simon C. Andrews [2] and Florence Baron [1,*]

Draft in preparation for submission

Legros, J.; Bonnassie, S.; Cochet, M.-F.; Jan, S.; Andrews, S.C; Baron, F. Impact of ovotransferrin on the integrity of *Salmonella* Enteritidis membranes under egg-white conditions

Poster presentations

Julie Legros, Louis Julien, Sophie Jan, Sylvie Bonnassie, Michel Gautier, Simon Andrews, Florence Baron. Impact of the level of ovotransferrin saturation by iron on the growth of *Salmonella* Enteritidis in egg white. Microbes, 16th National congress of the microbiology society (SFM), Sept 21, Nantes, France.

Julie Legros, Sylvie Bonnassie, Sophie Jan, Simon Andrews, Florence Baron. Ovotransferrin induces membrane depolarization of *Salmonella* Enteritidis under egg white conditions, International symposium *Salmonella* & salmonellosis (I3S), June 22, Saint-Malo, France.

Julie Legros, Sylvie Bonnassie, Marie-Françoise Cochet, Sophie Jan, Simon Andrews, Florence Baron. Understanding the antimicrobial activity of ovotransferrin in egg white toward *Salmonella* Enteritidis, Microbiology Society – Annual Conference, April 23, Birmingham, United Kingdom.

Oral communications

Julie Legros. My thesis in 150 seconds. Agreenium international research facility (EIR-A), April 21, Online, France

Julie Legros. Ovotransferrin, an antimicrobial egg white protein causes membrane damage in *Salmonella* Enteritidis in addition to iron restriction. SBS research conference, September 2022, Reading, United Kingdom

Julie Legros. Ovotransferrin, a multifunctional protein involved in the passive immunity of egg white. EGAAL Scientific days, June 2023, Rennes, France

Students supervision

- Iestyn Davies, Undergraduate student, Final year project (Oct-Dec 2022)
- Cynthia Martins Da Silva Tores, Msc (Apr-Jul 2023)
- Will Evans, Undergraduate student, Final year project (Oct-Dec 2023)

Demonstration

At the University of Reading

1st year undergraduate:

- **Introductory microbiology:** Teaching elementary skills in microbiology to isolate and identify bacteria from different samples. (36h)

- **Bacteriology and virology**: Enumeration and observation of bacteria and bacteriophage diversity from water samples. Isolation and identification of bacterial species from soil samples. (12h)

- **Building Block of Life**: Teaching how to perform a PCR. (4h)

2nd year undergraduate:

- **Bacterial cell**: Teaching how to perform and analyse transposon mutagenesis but also to demonstrate evolutionary principles using biofilm formations. (12h)

- **Infectious diseases**: Teaching microbiology techniques used in disease diagnosis and how to perform purification of bacteriophages and plaque assays. (78h)

Table of contents

List of abbreviations

Amp	Ampicillin
AvBD11	Avian β-defensin 11
BHI	Brain Heart Infusion
B-PER	Bacterial Protein Extraction Reagent
BPI	Bactericidal permeability-increasing proteins
CCCP	Carbonyl cyanide m-chlorophenyl hydrazone
Ct	Cycle threshold
DIP	2,2-Dipyridyl
$DiSC_3(5)$	3,3'-Diopropylthiadicarbocyanine Iodide
DMSO	Dimethylsulfoxide
EDTA	Ethylenediaminetetraacetic acid
Ent	Enterobactin
EU	European Union
EW	Egg white
EWF	Egg-white filtrate
EWMM	Egg white Model Medium
Ex-FABP	Extracellular fatty-acid-binding-protein
EY	Egg yolk
FAO	Food and Agriculture Organization of the United Nation
Hepes	(4-(2-hydroxyethyl)-1-piperazineethanesulfonic acid)
IPTG	Isopropyl-β-D-thiogalactopyranoside
IVET	In Vivo Expression Technology
LB	Luria-Bertani Broth
LPS	Lipopolysaccharides
ONP	o-nitrophenol
ONPG	Ortho-nitrophenyl-β-galactopyranoside
OT	Ovotransferrin
OVAX	Ovalbumin-related protein X
PCR	Polymerase Chain Reaction
pmf	proton motive force
Psp	Phage Shock Protein
qRT-PCR	Real-Time Quantitative Reverse Transcription PCR
RFU	Relative Fluorescent Unit
Sal	Salmochelin
SM	Synthetic Medium
SOC	Super Optimal broth with Catabolite repression
TCA	Tricarboxylic acid cycle
TS	Tryptone Salt
TSA	Tryptone Soya Agar
TSB	Tryptone Soya Broth
TSS	Transcription Start Site
WHO	World Health Organization
X-Gal	5-Bromo-4-Chloro-3-Indolyl β-D-Galactopyranoside

Chapter 1.
Bibliographic study

1.1. *Salmonella*: Introduction

1.1.1. General characteristics of *Salmonella*

Salmonella belongs to the family *Enterobacteriaceae* in the class *Gammaproteobacteria*. It is a Gram-negative rod-shaped bacterium (2-3 x 0.4-0.6 µm), non-sporulating and motile due to the presence of peritrichous flagella (Figure 1.1A and 1.1.B) (Minamino et al., 2018). From a biochemical point of view, *Salmonella* is a facultative anaerobe and oxidase negative, and is able to reduce nitrate to nitrites, synthesise hydrogen sulphide, and produce hydrogen and carbon dioxide by breaking down D-glucose (D'Aoust & Maurer, 2007). *Salmonella* grows at the optimum temperature of 35 to 37 °C, pH of 6.5 to 7.5, and at an a_w of 0.94 to 0.99. However, depending on the serovar, *Salmonella* can survive in more extreme conditions such as at temperatures between 2 and 54 °C, a pH of 4 to 9, and an a_w lower than 0.2 (Gray & Fedorka-Cray, 2002).

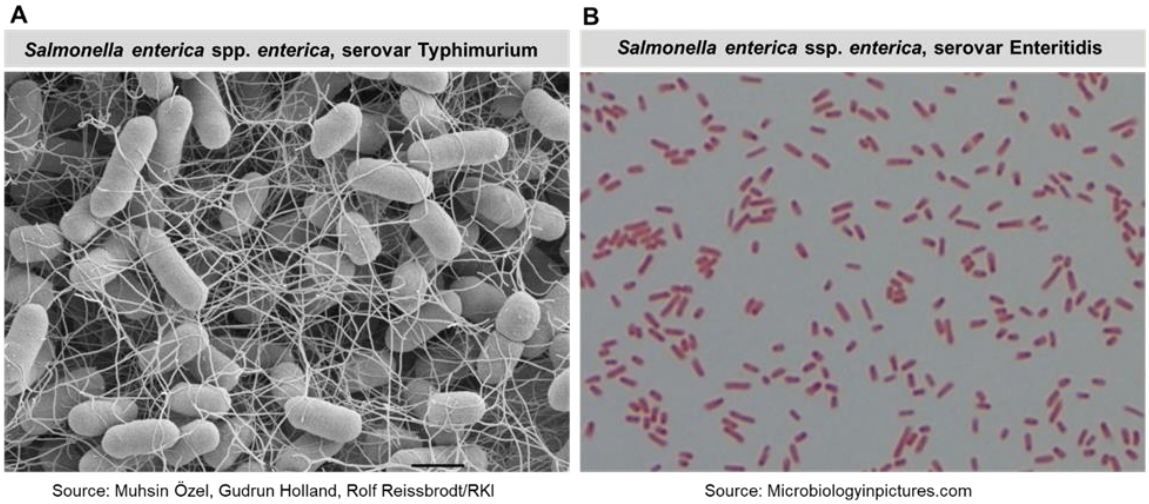

Figure 1.1. Cell morphology of *Salmonella.* (A) *Salmonella enterica* ssp. *enterica*, serovar Typhimurium, colony, observed by scanning electron microscopy (https://www.rki.de); scale bar is 1 µm. (B) Gram stain of *Salmonella enterica* ssp. *enterica*, serovar Enteritidis from a liquid culture (tryptic soy broth) (https://www.microbiologyinpictures.com).

1.1.2. A sophisticated nomenclature

The first *Salmonella*, known as Typhoid bacillus, was observed by Erberth in 1880 from patients with Typhoid fever. The organism was initially named *Bacillus choleraesuis* but was renamed *Salmonella choleraesuis* by Lignières in 1900 in honour to D.E. Salmon (Lignieres, 1900). Indeed, this American isolated *Salmonella* from a porcine intestine in 1894 (Smith, 1894). This name was often confused with *Vibrio cholera* so was changed again to definitively become *Salmonella enterica* in 1986 (Penner, 1988). However, for many years, the nomenclature of *Salmonella* has continued to evolve up to 2007. Currently, over 2500 serovars have been identified and named under the Kauffmann-White scheme, recommended by the World Health Organization (WHO) (Grimont & Weill, 2007, Figure 1.2). Based on the phylogeny, the genus *Salmonella* is divided into two species: *Salmonella bongori* and *Salmonella enterica* (Trüper, 2005). These species are classified into subspecies, one for *Salmonella bongori* (ssp. V) and six for *Salmonella enterica* (ssp. I *enterica*, ssp. II *salamae*, ssp. IIIa *arizonae*, ssp. IIIb *diarizonae*, ssp. IV *houtenae* and ssp. VI *indicae*). Each subspecies is organised into serovars using antigenic formulae. Introduced by Kauffman in 1966, the method is based on the identification of O and H antigens. The O antigen (or 'somatic' antigen), is the principal component of the lipopolysaccharides that are located on the outer membrane of *Salmonella*. The H antigens are involved in the activation of the host immune responses and are divided into two types according to flagella-phase variation whereby two alternative flagellin genes are expressed (phase 1, *fliC*; and phase 2, *fljB*). Subspecies I *enterica* is subdivided into two categories, typhoidal (infects humans) and non-typhoidal *Salmonella* (infects humans and animals). The last

group is composed of more than 1500 serovars including *Salmonella enterica* ssp. *enterica* serovar Enteritidis. In 1987, 27 phage types were identified among *S*. Enteritidis serovars (Ward et al., 1987), including PT4, PT8, and PT13a, involved in many outbreaks worldwide (Pan et al., 2009).

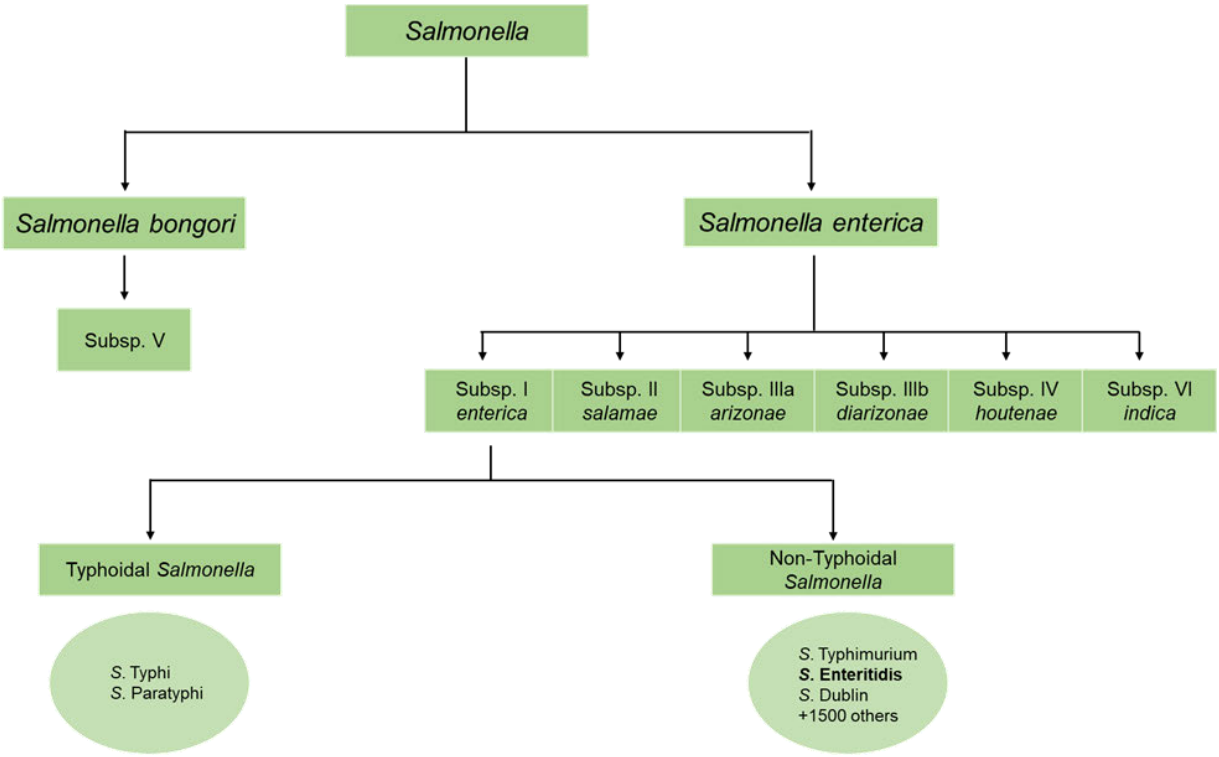

Figure 1.2. *Salmonella* nomenclature. Classification of *Salmonella* according to Grimont and Weill 2007; adapted from Achtman et al, (2012).

1.1.3. *Salmonella* cause Human and animal diseases

Non-typhoidal *Salmonella* is a zoonotic agent and the second most important pathogen responsible for foodborne diseases after *Campylobacter* (EFSA & ECDC, 2022). It provokes gastrointestinal disorders leading in some cases to hospitalisation and death. In 2020, 52,702 cases of salmonellosis were reported in the EU. Brexit and the pandemic of COVID-19 reduced the number of cases. Indeed, from 2016 to 2019 around 90,000 cases of salmonellosis were reported each year, of which 10,000 were in the United Kingdom and 8,000 in

France (EFSA & ECDC, 2022). In the EU, 694 foodborne outbreaks of *Salmonella* were registered in 2020 and the most important food vehicle involved was eggs and egg products. Furthermore, most foodborne diseases were caused by *S*. Enteritidis (79.7%) (EFSA & ECDC, 2022). Indeed, since the early 20th century, contamination of poultry flocks with *Salmonella* has been a real curse. It all began when the two serovars, *Salmonella* Pullorum and *Salmonella* Gallinarum emerged and induced economic losses in poultry flocks in the United States and Europe (Bullis, 1977). Thus, surveillance and eradication programs were introduced in the 1930s, including testing and control measures. But the eradication of these serovars has been complicated by the competitive exclusion between *S*. Gallinarum and *S*. Enteritidis which has resulted in increased *S*. Enteritidis transmission such that this serovar has become a major concern for food safety (Barrow et al., 2012, for a review). In order to prevent and control *Salmonella* outbreaks in poultry flocks, specific rules were established worldwide. Different measures of prevention were implemented including safe access to water, safe food handling, public education and vaccination (Whitehead & Roberts, 2014). Since 2003, Salmonellosis monitoring is determined by regulation (EC) No. 2160/2003 in the EU and at every stage of the production, the control and detection of *Salmonella* are strictly managed.

1.1.4. Transmission routes of *Salmonella* in eggs

Eggs can be infected by *Salmonella* in two different ways, vertical or horizontal (Figure 1.3). The poultry environment is the main factor responsible for horizontal transmission. Such contamination can take place after oviposition, from the nest boxes, the hatchery environment, and during storage and transport of eggs. Environmental conditions including temperature and humidity may

facilitate the horizontal contamination of eggs by bacteria from sources such as organic material which are a rich in nutrients for bacterial growth and survival on the eggshell. Moreover, the integrity of the eggshell is a key factor influencing *Salmonella* contamination. Indeed, a cracked eggshell is more likely to facilitate the penetration of bacteria through the egg (Gantois et al., 2009a; Jan & Baron, 2017; Baron et al., 2023).

The other route of contamination, known as vertical contamination, originates from the infection of the reproductive organs with *Salmonella*. The oviduct is composed of five parts: the infundibulum, magnum, isthmus, uterus and vagina (Figure 1.3). All these parts possess a specific function during egg formation and can be colonised by *Salmonella* carried in macrophages, from the intestine (Gantois et al., 2009a).

The most important route used by *S*. Enteritidis to contaminate eggs remains unclear as some authors suggest the horizontal route (Barrow & Lovell, 1991; Bichler et al., 1996) whilst others indicate the vertical (Gast & Beard, 1990; Miyamoto et al., 1997). However, vertical contamination is considered by WHO and FAO (Food and Agriculture Organization of the United Nations) as the major route of *S*. Enteritidis contamination; this is because it is easier to control and reduce horizontal contamination by disinfection and contamination-restriction methods (WHO & FAO, 2002). The frequency of vertical transmission is tough to estimate, nevertheless, in 2020, *Salmonella* was found in 1323 (3.3%) of hen laying flocks in the EU. Among these cases, 533 were positive to the target serovars, 76% were associated with *S*. Enteritidis and 24% to *S*. Typhimurium (EFSA & ECDC, 2022).

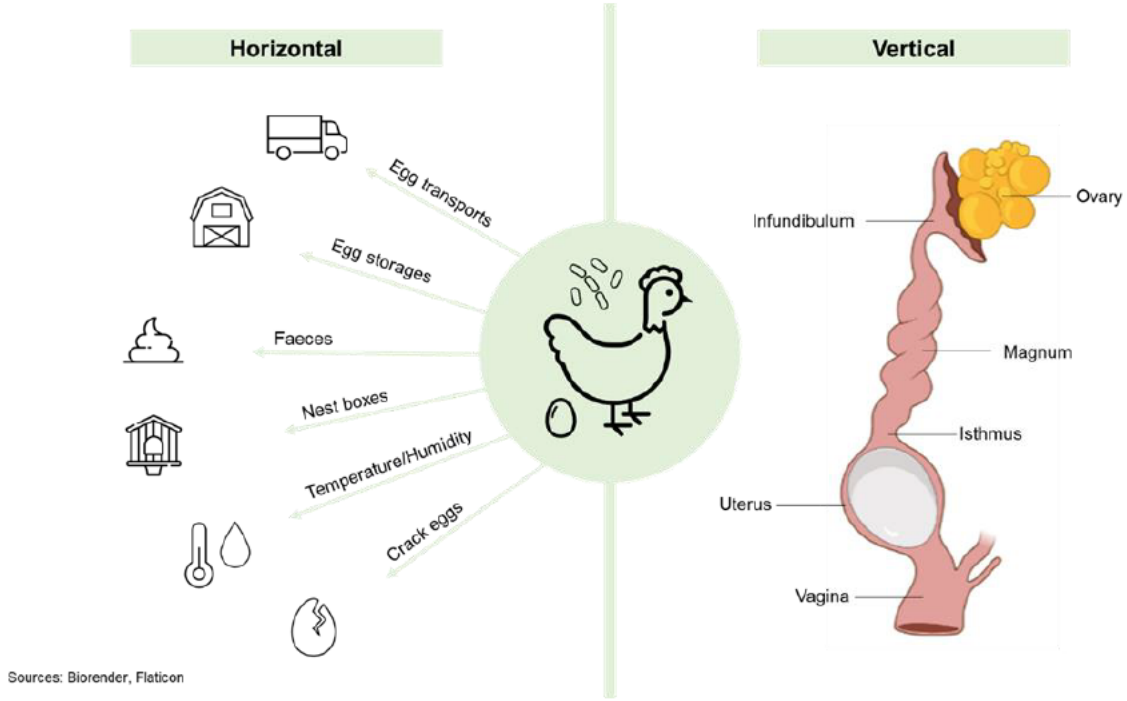

Figure 1.3. Schematic diagram summarising the horizontal and vertical transmission of *Salmonella* in eggs, according to Gantois et al. (2009a).

1.2. Hen egg characteristics

The whole egg is composed of 60% of egg white (EW) and 30% of egg yolk (EY), surrounded by the shell representing 10% of the total egg weight (Nys & Sauveur, 2004). However, these proportions vary depending on the age of the hens, their alimentation and breeding environmental conditions. The composition of the EW, EY and whole egg are described in Table 1.1. From the farm to fork, eggs are exposed to several microorganisms and the risk of contamination is real. However, the eggshell and EW form a barrier to prevent bacterial invasion.

Table 1.1. Composition of EW, EY and the whole egg (without eggshell) in g for 100 g of egg according to Nys & Sauveur (2004).

	EW	EY	Whole egg
Water	88.6	49	74.4
Proteins	10.6	16.1	12.3
Carbohydrates	0.8	0.5	0.7
Lipids	0.1	34.5	11.9
Minerals	0.5	1.6	7
Vitamins	0.008	0.01	0.004

1.2.1. Eggshell

The eggshell is essential to protect the embryo against physical and biological risks emanating from the environment, including bacterial invasion. The eggshell is essentially composed of proteins and a low amount of carbohydrates and lipids (Burley & Vadehra, 1989). The cuticle is the outermost layer and therefore the first line of defence of the egg (Figure 1.4). However the cuticle is not only a physical barrier, it also contains antimicrobial proteins such as lysozyme, ovotransferrin (OT) and ovocalyxin-32, the activity of which has been demonstrated against *B. subtilis*, *P. aeruginosa* and *S. aureus* (Wellman-Labadie et al., 2008). Over time and due to poor egg handling, the cuticle may rupture, allowing bacteria to penetrate the pores of the shell. Three other layers shape the shell membranes: the shell, and the outer and the inner shell membranes, forming a well-organised meshwork of fibres (Parsons, 1982), carrying traces of antimicrobial molecules such as lysozyme (Hincke et al., 2000; Wellman-Labadie et al., 2008).

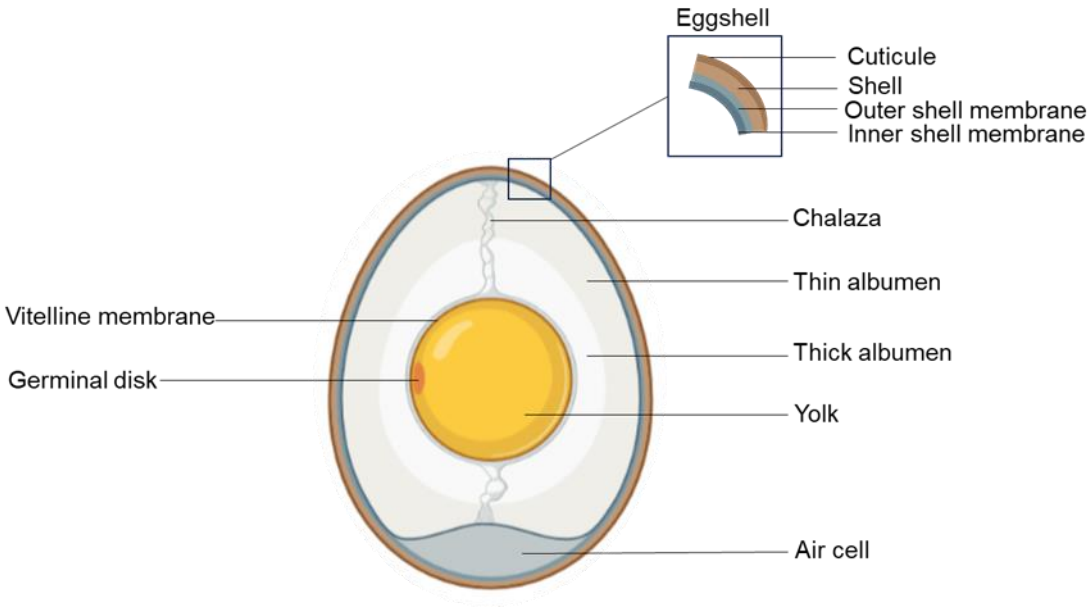

Figure 1.4. Structure of hen egg. The eggshell is composed of four parts (the cuticule, the outer and inner shell membrane). The EY is separated from the EW by the vitelline membrane and is attached to the eggshell thanks to the chalaza. Around EY, the EW is divided in several thin and thick layers (Designed with Biorender).

1.2.2. Egg white

Although the eggshell is the first line of defence against bacterial invasion, it can crack and allow bacteria to reach the EW. However, EW is a heterogenous and viscous medium (5 mPa.s^{-1} at 20 °C and a shear rate of 400 s^{-1}) (Lang & Rha, 1982), with an alkaline pH (pH increases from 7.8 to 9.3 a few days after laying) (Sauveur, 1988) and is composed of several proteins some of which have antimicrobial properties that limit bacterial growth and migration into the egg yolk. (Baron et al., 2016 for a review).

1.3. Egg white proteins with antimicrobial properties

EW is composed of several proteins, some of which are known for their antimicrobial properties. It should be noted that there is no strong evidence of such antimicrobial activity for all EW proteins. The mechanism of action of each

predicted or confirmed antimicrobial protein is described below (Baron et al., 2016 for a review).

1.3.1. Peptidoglycan hydrolysis

Lysozyme is the best-described antimicrobial EW protein, present at 3.5 g/L and belonging to the hydrolase family. Lysozyme targets the peptidoglycan of the bacterial cell wall by cleaving the glycosidic bonds (β1-4) between the N-acetylglucosamine and N-acetylmuramic residues. Two other mechanisms of action of lysozyme have been described. Lysozyme can also inhibit DNA and RNA synthesis of *E. coli* at 37 °C, pH 7.4, as reported by Pellegrini et al. (2000). The ability of lysozyme to form pores through the outer membrane was also suggested since it has been shown that the EW protein induced inner and outer membrane permeabilisation of *E. coli* at 37 °C, pH 7, by measuring the β-lactamase and β-galactosidase activity (Derde et al., 2013). Lysozyme activity has a direct bactericidal action against both Gram-negative and Gram-positive bacteria (Pellegrini et al., 1992). However, the activity of lysozyme against *S*. Enteritidis membranes under EW conditions remains unknown. Nevertheless, Baron et al. (1997) observed neither bactericidal or bacteriostatic activity of lysozyme on *S*. Enteritidis growth in EW at 30 °C.

1.3.2. Iron-chelating activity

OT is the only iron-chelating protein in EW and it is described as the main factor responsible for the antimicrobial activity of EW (Legros et al., 2021 for review). This is the subject of this study and will be further described later in this chapter.

1.3.3. Vitamin-chelating activity

With respect to proteins that chelate vitamins, avidin can form a complex with biotin and induce a vitamin deprivation, that may result in a bacteriostatic effect (Banks et al., 1986). Indeed, biotin is an enzyme cofactor, involved in different metabolism pathways such as fatty acid synthesis, amino acid metabolism and the tricarboxylic acid cycle, and in this way is essential for bacteria survival. However, it was described that several bacteria are able to synthesise biotin *de novo* or to export it into their environment (Beckett, 2007). Two other vitamin-chelating proteins are present in EW (riboflavin-binding protein and thiamine-binding protein), but no evidence of their antimicrobial functions has been described (Mann, 2007; Muniyappa & Adiga, 1979).

1.3.4. Protease inhibitors

EW is composed of several proteins with demonstrated protease inhibitor activity against pathogens. This is the case of ovostatin, cystatin and ovalbumin-related protein X (OVAX). It has been shown that ovostatin possesses antimicrobial activity against pathogenic bacteria producing proteases responsible for corneal ulcers, at 25 and 37 °C in tris-hydrochloride buffer (pH 7.5) (Molla et al., 1987). The bactericidal activity of chicken EW cystatin against Gram-positive bacteria at 37 °C was highlighted using radial diffusion assay, but its mechanism of action remains unknown (Wesierska et al., 2005). Using the same method, it has also been shown that OVAX is able to inhibit *S*. Enteritidis and *Listeria monocytogenes* at 37 °C (Réhault-Godbert et al., 2013). However, several other protease inhibitors were identified in EW (ovoinhibitor, ovomucoid, ovalbumin related protein Y, heparin cofactor, and proteins similar to pancreatic

secretory trypsin inhibitor and to Kunitz-like protease inhibitor) for which antimicrobial activity evidence has not yet been published (Baron et al., 2016).

1.3.5. Bactericidal permeability-increasing proteins

Currently, no evidence for the antimicrobial activity of BPI has been published. However, three BPIs were found in EW (Tenp, BPIL2 and Similar-to-BPI) and they potentially could induce bacterial membrane damage. Indeed, homology between the C-terminus of the Tenp amino-acid sequence and the BPI2 domain of the BPI/lipopolysaccharide-binding protein was found (Guérin-Dubiard et al., 2006), suggesting a similar activity in binding the lipopolysaccharide of the Gram-negative outer membrane (Bingle & Craven, 2004).

1.3.6. Defensins

Defensins are peptides present in all living organisms and are known for their antimicrobial activity (Lehrer et al., 2005). Two defensins have been found in EW: AvBD11 and Gallin. The antimicrobial activity of AvBD11 (purified from the vitellin membrane) has been demonstrated against *S*. Enteritidis, *S* Typhimurium *L. monocytogenes*, *E. coli* and *Staphylococcus aureus* at 37 °C using radial diffusion assay (Hervé-Grépinet et al., 2010). The second defensin, named Gallin, can also inhibit the growth of *E. coli* at 37 °C in Luria-Bertani (LB) broth (Gong et al., 2010).

1.3.7. Lipocalins

Lipocalins have been identified in EW and three types can be distinguished: Extracellular fatty-acid-binding-protein (Ex-FABP), chondrogenesis-associated lipocalin and α-1-ovoglycoprotein (D'Ambrosio et al.,

2008; Desert et al., 2001; Guérin-Dubiard et al., 2006; Mann, 2007; Mann & Mann, 2011). Several studies reported the ability of some lipocalins to sequester siderophores and inhibit bacterial growth of *E. coli* and *B. subtilis* (Correnti et al., 2011; Garénaux et al., 2013). The effect of EW lipocalins on *S*. Enteritidis growth was reported by Julien et al. (2020). The authors show that Ex-FABP was able to sequester the enterobactin (Ent) but not its glycosylated derivate, salmochelin (Sal), whereas the other two lipocalins showed no such activity (Julien et al., 2020).

1.4. Ovotransferrin

1.4.1. Structure

OT, also called conalbumin, is a monomeric glycoprotein belonging to the transferrin family that represents 13% (170 µM in EW) of total EW protein. Transferrins are extracellular glycoproteins involved in iron homeostasis, and they appear to have arisen from a common ancestorial gene through a gene duplication and fusion event that generated an encoded protein with two homologous lobes, each binding a single iron atom (Palmiter et al., 1978). Four major types of iron-binding transferrin are known: Blood transferrin (serotransferrin); milk lactotransferrin (lactoferrin); membrane-associated melanotransferrin; and EW OT (Crichton, 1990). Although these four types of transferrin have distinct physiological roles, they all serve to control iron levels in biological fluids and thus possess conserved characteristics. Production of OT in eggs is enabled as the gene is under the control of steroid hormones (oestrogen, progestins, glucocorticoids, and androgens; Palmiter et al., 1978), which provides a high-level OT secretion into the EW during its biosynthesis.

From a structural point of view, hen OT is composed of a single 686 amino acid residue polypeptide with a molecular mass of around 77.7 kDa and has an isoelectric point of 6 (Jeltsch & Chambon, 1982; Kurokawa et al., 1995). The two lobes of OT (referred to as the N- and C-terminal lobes) each consist of two α/β domains (N1 and N2, and C1 and C2, respectively) of ~160 residues that are connected via two anti-parallel β-strands (Kurokawa et al., 1999; Phelps & Antonini, 1975). The amino acid sequences of the two lobes are similar, with a sequence identity of 37.4% (Williams, 1968). A nine amino acid residue α-helix connects the two lobes (Figure 1.5).

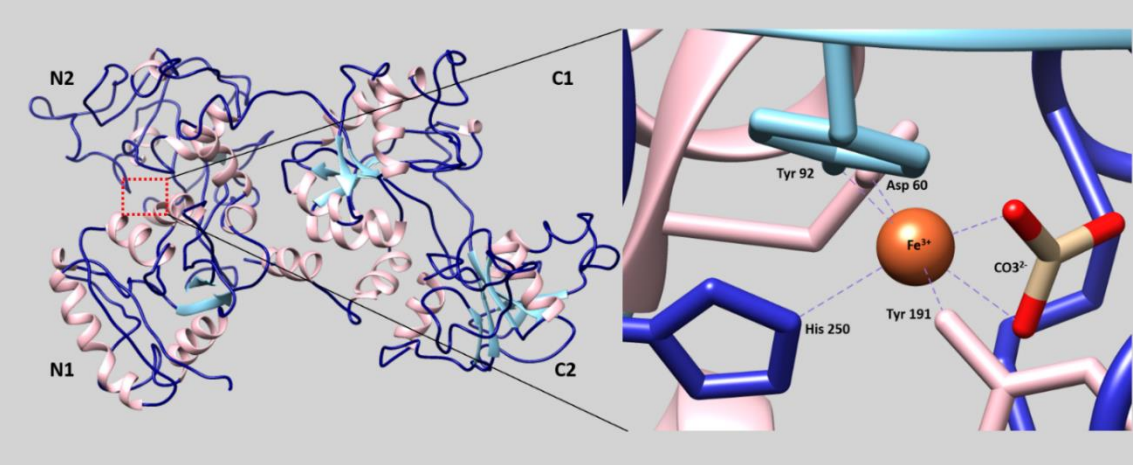

Figure 1.5. Representation of the tertiary structure of OT. The subdomains of each lobe are indicated by N1, N2, C1, and C2. On the left, an enlargement of the binding site of the N lobe shows the binding of iron by its six ligands. The images were produced using the UCSF chimera package (Pettersen et al., 2004) from the tertiary structure of the OT (PDB ID: 1AIV) (Kurokawa et al., 1999) (Legros et al., 2021).

The two iron-binding sites are located in the interdomain cleft in each of the corresponding lobes (Figure 1.5). Each lobe reversibly binds one Fe^{3+} cation along with one CO_3^{2-} anion. Thus, two iron ions can bind to OT in the presence of bicarbonate (Phelps & Antonini, 1975). The interdomain clefts are in an open configuration under iron-free conditions but adopt a closed conformation when they engage iron (Anderson et al., 1990; Grossmann et al., 1992). Binding of

each iron atom is achieved via six ligands: Two are oxygen atoms from the bidentate carbonate ion and the four others are amino acid residues (Asp 60/395, Tyr 92/431, Tyr 191/524, and His 250/592, for the N-/C-lobes, respectively) (Guha Thakurta et al., 2003; Kurokawa et al., 1995, 1999; Mizutani, 1999). The N- and C-lobes have distinct iron-affinity constants of 1.5×10^{14} and 1.5×10^{18} M^{-1}, respectively (Kurokawa et al., 1995). This difference in iron affinity has been ascribed to lobe-specific amino acid residue interactions within the domains (Kurokawa et al., 1999). Iron-free OT (apo-form) is more sensitive to physical, thermal, and chemical treatments than iron-bound OT (holo-form) (Azari & Feeney, 1958). Ko and Ahn (2008) studied the effect of the addition of iron (25–300% saturation) to OT and found that 200% saturation prevented the denaturation of OT with ethanol (Ko & Ahn, 2008). In addition to iron, OT is able to bind other divalent cations such as chromium, copper, manganese, zinc, nickel, cobalt, and cadmium, but with lower affinities than for iron (Tan & Woodworth, 1969).

1.4.2. Role of ovotransferrin in iron deficiency

1.4.2.1. The requirement for iron

Iron is essential for all forms of life, including bacteria, since it is involved in many cellular processes such as respiration, DNA synthesis, redox-stress resistance, and the tricarboxylic acid cycle (TCA) (Andrews et al., 2003). Concentrations varying from 0.1 to 10 µM are typically needed for optimal bacterial growth (Andrews et al., 2003). Iron is found in two major forms, either oxidized ferric iron (Fe^{3+}) or the reduced ferrous form (Fe^{2+}). The ferric form is the most abundant under aerobic environmental conditions. However, ferric iron displays much lower solubility than the ferrous form (10^{-18} and 0.1 M at pH 7,

respectively) (Andrews et al., 2003). On the other hand, the ferrous form is predominant and more stable in anaerobic environments, as well as under acid conditions.

The addition of iron was shown, as early as 1944, to counteract bacterial growth inhibition in EW. This effect was observed for several microorganisms, including *E. coli*, *Shigella dysenteriae*, and *S. aureus* (Shade & Caroline, 1944). In 1946, OT was identified as the key factor limiting bacterial growth in EW (Alderton et al., 1946). Assuming that (i) one mole of OT is able to bind two moles of iron, and (ii) EW contains around 3.6 to 18 µM of iron (*Ciqual*, 2021; Nau et al., 2010a; Nys & Sauveur, 2004; Sauveur, 1988; Stadelman & Cotterill, 1995), it can be assumed that OT is 1.07 to 5.4% iron-saturated suggesting that there would be virtually no free iron in EW. Several studies have validated the iron-restriction role of OT on bacterial growth. This effect was tested with different species, including *Pseudomonas fluorescens*, *Proteus vulgaris, Proteus melanovogenes*, and *Aerobacter cloacae* (Garibaldi, 1960). Garibaldi et al. (1960) showed that the bacterial population increased up to 8 $\log_{10}$ CFU/mL in a few days at 28 °C after the addition of iron at a concentration higher than the saturating concentration of OT in EW (addition of 20 mg/L of free Fe^{2+}, leading to a 105% theoretical value of OT saturation). Lock and Board (1992) showed that different *Salmonella* serotypes were able to remain viable in EW at 20 °C and 30 °C for 42 days, and that the subsequent addition of 8 mg/L of ferric ammonium citrate (40 % theoretical OT saturation) induced growth by 4 $\log_{10}$ at both temperatures (Lock & Board, 1992). Baron et al. (1997) used egg white filtrate (EWF) (obtained by EW ultrafiltration at a molecular weight cut-off of 10 kDa) combined with individual EW proteins to investigate which EW protein contributes to the antimicrobial

activity of EW (Baron et al., 1997). Only the addition of OT resulted in a bacteriostatic impact on *S*. Enteritidis. Further, the authors showed that the addition of iron at 110% OT saturation enhanced *Salmonella* growth by 4 $\log_{10}$ at 30 °C. Such studies demonstrate the major role of OT in the anti-*Salmonella* effect of EW through its iron deprivation action. Thus, OT, like other transferrins, in addition to its host-iron transport and storage role, has a clear role in limiting the access of pathogenic bacteria to iron. However, bacteria have developed various mechanisms to sequester or scavenge iron from the host environment and from host-chelating proteins such as transferrins.

1.4.2.2. Iron metabolism in bacteria

Intracellular iron concentration must be finely regulated, and a balance between iron uptake and storage must be maintained to ensure bacterial survival. When iron is restricted in the environment, bacteria often respond by secreting high-affinity iron-chelating molecules called siderophores (Griffiths, 1983) which have affinity constants for iron between 10^{30} and 10^{52} M^{-1} (Andrews et al., 2003). Over 500 siderophores are known and they are divided into several families according to the functional groups utilized in iron binding. The three major families are the catecholate, hydroxamate and α-hydroxycarboxylate siderophores. The Enterobacteriaceae secrete Ent (also called enterochelin), which belongs to the catecholate family. Depending on the species or strain, Enterobacteriaceae also secrete Sal (glucosylated Ent), aerobactin (dihydroxamate) and yersiniabactin (a five-member heterocyclic siderophore) (Andrews et al., 2003).

The synthesis of siderophores takes place in the cytosol. Figure 1.6 shows the proteins involved in the iron-acquisition systems of *S*. Enteritidis. The enzymes required for Ent synthesis are encoded by the *ent* genes (Gehring et al., 1998). Ent also acts as the precursor of Sal synthesis. The glucosylation of Ent, to form Sal, requires the product of the *iroB* gene (Bäumler et al., 1998). It is important to emphasise that the glucosylation of Ent is a virulence strategy since it allows circumvention of the capture of Ent by siderocalin (also named lipocalin 2), a host innate immunity protein in human serum (Devireddy et al., 2005). Siderocalin inhibits Ent-mediated bacterial growth during infection through its ferri-Ent sequestration activity (Goetz et al., 2002). Aerobactin synthesis is enabled by the *iucABCD* gene products, but this capacity is only found in some Enterobacteriacea (Carbonetti & Williams, 1984). Following synthesis, siderophores are secreted into the environment via specific exporters (Figure 1.6). In Gram-negative bacteria, the resulting ferri-siderophore complexes are transported across the outer-membrane (OM) by high-affinity and highly-specific OM receptors (e.g. FepA for Ent). Subsequent translocation into the periplasm requires the energy-transducing TonB-ExbBD complex which utilises the proton motive force (pmf) of the cytoplasmic membrane to drive ferri-siderophore transport (Skare et al., 1993). Ferri-siderophores are transported from the periplasm through the cytoplasmic membrane via a periplasmic-binding protein-dependent ABC-binding cassette permease (e.g. FepBDGC for Ent). In the case of ferri-Ent, Ent esterase (Fes) facilitates iron release through degradation into dihydroxbenzoylserine units (Lin et al., 2005). The reduced, ferrous form of iron can be acquired by *Salmonella* and other Enterobacteriaceae through the FeoABC (or SitABCD, which has preference for Mn^{2+}) system, in particular under

anaerobic conditions (Carbonetti & Williams, 1984). Ferrichrome and ferrioxamine are not synthesised by *Salmonella* but they can be recognised via specific receptors (Figure 1.6) and utilised for iron acquisition by *Salmonella* (Luckey et al., 1972).

Iron uptake by Enterobacteriaceae is finely controlled by the ferric uptake regulator (Fur) protein, which acts as the global regulator of iron homeostasis according to cellular iron availability (Troxell & Hassan, 2013, for a review). Fur represses iron-uptake systems, but also activates the expression of other genes (Hantke, 2001) by either direct or indirect mechanisms, the latter involving repression of the small regulatory non-coding RNA, RyhB (Masse & Gottesman, 2002). Genes repressed by Fur include those involved in iron transport and biosynthesis of siderophores; those induced include genes encoding iron storage, redox stress response, TCA cycle, and glycolysis functions. Furthermore, when bacteria are subject to iron restriction they can reduce their iron requirements by replacing iron-dependent proteins with non-iron alternatives and by down regulation of iron-demanding systems (“iron rationing”); they can also utilise intracellular iron stores in place of external iron (Troxell & Hassan, 2013, for a review).

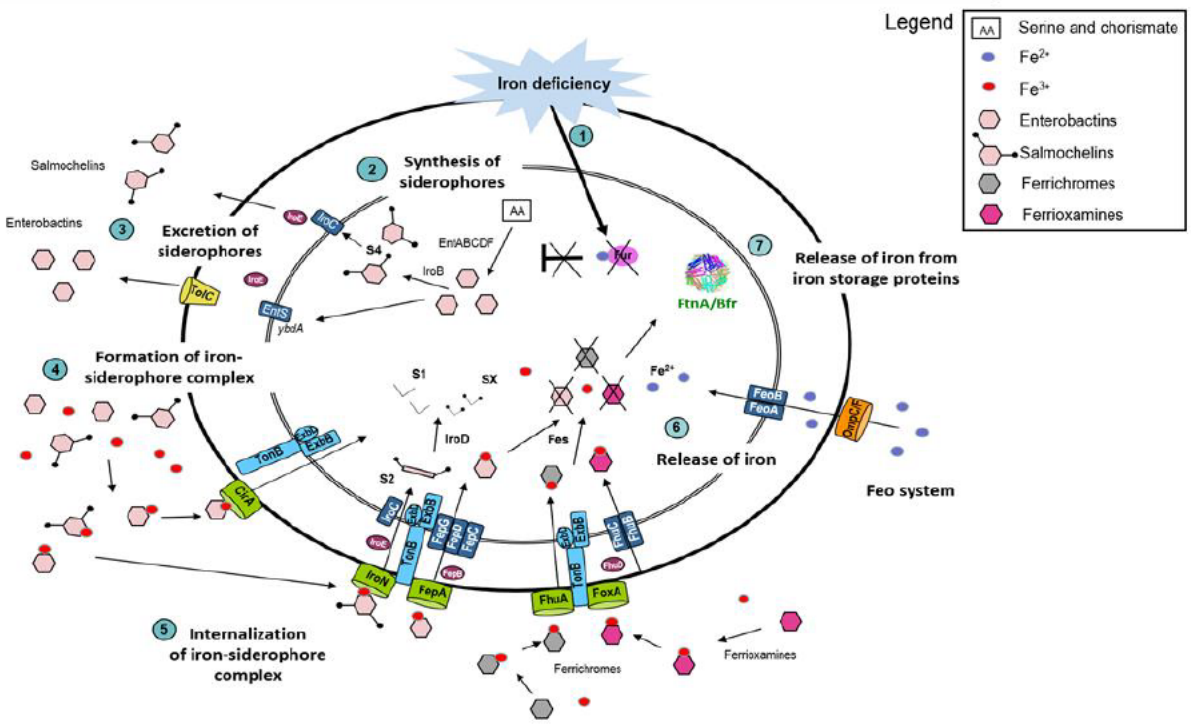

Figure 1.6 The different pathways of iron acquisition and storage in *S.* Enteritidis. (1) Iron deficiency induces derepression by the Fur regulator, leading to transcriptional upregulation of the genes under its control, in particular the genes encoding enzymes required for the production of siderophores. Salmonella is able to synthetize and/or use several siderophores: Ent, Sal, ferrichrome, and ferrioxamine. (2) In the first step, Ent is synthetised using serine and chorismate as precursors. This step is catalysed by EntABCDF enzymes (Gehring et al., 1998). Then, Ent is transported into the environment by EntS and TolC or used as a precursor in the production of Sal S4 via the glycosyltransferase IroB (Bister et al., 2004). (4) Once in the environment, the siderophores chelate ferric iron. (5) The siderophore-iron complexes (ferri-Ent and ferri-Sal, and the exogenous siderophores ferrichrome and ferrioxamine) are recognised by specific receptors present in the bacterial OM (CirA and FepA for Ent, IroN for Sal, FhuA for ferrichromes, and FoxA for ferrioxamine) (Hantke, 2001). Then, the TonB-ExbBD, an energy-transducing complex, drives siderophore internalization into the periplasm. Once in the cytoplasm, Sal is linearised into the S2 form by IroE, an esterase (Luckey et al., 1972). The passage through the inner membrane is achieved by the FepBDGC transporter for both Sal and Ent (Chenaul & Earhart, 1992; Langman et al., 1972). On the other hand, ferrichromes and ferrioxamines use the FhuBCD transporter to pass through the inner membrane (Rohrbach et al., 1995). (6) Inside the cytoplasm, the iron-siderophore complexes are dissociated by esterases: Fes converts tricyclic Ent into monomeric units; IroD act on the linear, trimeric S2 from of Sal (H. Lin et al., 2005) to generate mono (S1) or dimeric (SX) products from which iron can be released more readily. Finally, iron can be utilised for metabolism or (7) stored by ferritin (FtnA) or bacterioferritin (Bfr) (Andrews, 1998). To acquire Fe^{2+}, *S.* Enteritidis primarily uses the FeoABC system (Hantke, 2001; Rohrbach et al., 1995), which allows iron to be imported across the inner membrane from the periplasm; the OmpC and OmpF porins allow passive diffusion of ferrous iron across the OM (Gerken et al., 2020). (Legros et al., 2021)

1.4.2.3. Capacity of siderophores to capture iron from ovotransferrin

By chelating iron, OT leads to iron deficiency and to activation of high-affinity iron-acquisition systems. Studies on the impact of OT-dependent iron restriction on the growth of *E. coli* and *S*. Enteritidis at 37 °C in Trypticase Soy Broth medium (TSB, pH 7) showed that OT (5 g/L) induces expression of siderophore outer-membrane receptor proteins (Chart et al., 1986; Chart & Rowe, 1993). Further, OT (1 g/L) severely impaired the minimal medium growth of *E. coli* mutants (Δ*fes* Δ*iroD* and Δ*fes* Δ*iroD* Δ*iroE*) lacking the esterases required for release of iron from Ent and Sal. However, the growth of single esterase mutants was similar to that of the wild type (Caza et al., 2015). These studies highlight the ability of OT to trigger induction of ferri-siderophore acquisition systems and demonstrate that the function of only one such system is required to enable bacteria to counter the growth restriction imposed by OT in laboratory media.

Recent studies, using a range of approaches, show that iron-acquisition genes are amongst the most highly induced when *S.* Enteritidis is exposed to EW. Baron et al. (2017) used microarray analysis to study the global transcriptomic response of *S*. Enteritidis to egg white model medium (EWMM) (10% of EW in EWF) (Baron et al., 2017). RNA-Seq analysis was used by Huang et al. (2019) to study the global gene-expression response of *S*. Enteritidis incubated in distilled water with 80% EW (Huang et al., 2019). Qin et al. (2019) used iTRAQ-based proteomics to examine protein secretion by *S*. Enteritidis in LB medium with 0 to 80% EW (Qin et al., 2019). All three studies found high-level induction of genes (or protein synthesis) related to Ent (*entABCEFH*) and Sal (*iroBCDEN*) biosynthesis, and to the internalisation of iron-siderophores complexes (e.g. *fepABCDG*, *cirA*, *fhuABCDE*, *tonB* and *exbBD*). These studies

clearly show that siderophore-related genes/proteins are strongly induced by *S.* Enteritidis upon exposure to EW. However, such studies do not indicate whether siderophore production and utilisation provide any advantage for the survival and/or growth of *S.* Enteritidis in EW.

An insightful study investigated the impact of combined deletion of both the ferrous and ferric uptake systems on the survival of *S*. Enteritidis in EW at 37 °C (Kang et al., 2006). Thus, a double Δ*entF* Δ*feoAB* mutant (lacking any effective high-affinity iron transport activity), was able to survive similarly to the wildtype (WT) in EW at 37 °C, but after 70 h incubation, the mutant displayed a 2 $\log_{10}$ reduction in viable cells with respect to the wildtype. Although the addition of iron to the EW (at 110% OT saturation) enhanced growth of the mutant (and WT), the single Δ*entF* and double Δ*entF* Δ*feoAB* mutants exhibited an extended growth lag, as well as reduced overall growth in comparison to the WT (3 to 5 $\log_{10}$ reduction, respectively). These results suggest that the production of siderophores by *S.* Enteritidis in EW provides an advantage, especially when OT is iron saturated such that iron availability is increased. Importantly, the siderophore-producing WT was unable to grow in EW in the absence of iron supplementation. This suggests that *S*. Enteritidis is unable to access iron bound to OT in EW, despite its siderophore-production capacity. Indeed, EW carries sufficient iron (3.6 to 18 µM; Ciqual, 2021; Nau et al., 2010a; Nys & Sauveur, 2004; Sauveur, 1988; Stadelman & Cotterill, 1995) to support bacterial growth, but this iron is likely to be almost entirely chelated by OT since (as indicated above) it is present in considerable molar excess. Thus, bacterial growth within EW requires a suitable mechanism to acquire iron from OT.

Garibaldi (1970) showed that the direct provision of siderophore compounds can overcome the bacteriostatic effect of EW to allow rapid growth for *S.* Typhimurium and *Pseudomonas ovalis* (Garibaldi, 1970). Neither species could grow in EW, even when iron was added at up to 4 µg/mL, a concentration that is below that required to saturate OT (~20% iron saturation was achieved). However, rapid growth was observed when siderophore-containing extracts were added to EW, even without co-supplementation with iron (Garibaldi, 1970). These results therefore suggest that the levels of siderophore produced by bacteria in EW may be insufficient to enable effective competition with OT for iron such that the siderophore-production capacity of bacteria may provide no growth benefit.

As indicated above, three lipocalins have been identified in EW (D'Ambrosio et al., 2008; Desert et al., 2001; Guérin-Dubiard et al., 2006; Mann, 2007; Mann & Mann, 2011). One of them, Ex-FABP, has been demonstrated to possess a siderophore-sequestering activity (Julien et al., 2020). However, although Ex-FABP can sequester Ent, it displays no activity against the di-glucosylated derivative of Ent, Sal (Correnti et al., 2011; Julien et al., 2020). The addition of Ex-FABP at the concentration found in EW (5 µM) caused defective growth (1.5–2-fold reduction of OD 600 nm) of an *S*. Enteritidis *iro* (Ent^+, Sal^-) mutant using Ent as sole siderophore in an iron-restricted medium (LB with 2-2′ dipyridyl; DIP, a strong iron chelator) compared to the WT (Julien et al., 2020). Thus, the sequestration of Ent by Ex-FABP reduced the bacterial iron-scavenging capacity. An *entB* mutant (unable to produce any siderophore) propagated under the same conditions exhibited a major growth defect (4-fold and 2-fold OD reduction cf. the WT and *iro* mutant, respectively). Thus, Sal production allows *S.* Enteritidis to overcome the growth inhibition that results from Ent sequestration

by Ex-FABP under iron restriction. These findings suggest that the presence of Ex-FABP in EW at ~5 µM may limit the ability of siderophores, such as Ent, to support growth in EW.

1.4.3. Role of ovotransferrin in bacterial membrane perturbation

1.4.3.1. Bacterial envelope: structure

Bacterial envelope is the most important part of the bacteria conferring it, its shape and integrity. Other vital functions are associated to the bacterial envelope, though. Indeed, it is a physical barrier against antimicrobial agents, but it has also a role in transport, enabling small molecules or macromolecules to transit in and out of the cell (Silhavy et al., 2010 for a review). There are two different types of bacterial envelopes which can be distinguished by Gram staining, single or double membrane. Another category of bacterial envelope is affiliated with the Archaea but cannot be distinguished by Gram staining. Only the envelope of the Gram-negative bacteria will be described below since *S*. Enteritidis is the subject of this thesis. The Gram-negative bacterial envelope is composed of two distinct lipid-bilayer membranes: the outer and the inner membrane (Figure 1.7). Several efflux pumps and transporters span both the inner and outer membranes, expelling harmful molecules, or allowing the transport of essential compounds for bacterial growth, respectively. Molecules called LPS are localised to the outer leaflet of the outer membrane. They are composed of three parts: the lipid A; the core; and the O-antigen. The LPS is negatively charged resulting from the presence of numerous phosphate groups in the lipid A and core oligosaccharide regions, which are bridged by divalent cations (Ca^{2+} and Mg^{2+}) (Wang & Quinn, 2010). Only the inner leaflet of the outer membrane is composed of phospholipids, whereas for the inner membrane both

the inner and outer leaflets consist of a phospholipids. In *Salmonella* and other Gram-negative bacteria, different types of phospholipids are present in membrane: around 75-80% is phosphatidylethanolamine, 5-20% is phosphatidylglycerol, 1-5% is cardiolipin and <1% is phosphatidylserine (Rana et al., 1991; Kobayashi et al., 2007). Between the two membranes, a thin layer of peptidoglycan is linked to the outer membrane by Braun's lipoproteins (Braun, 1975). The peptidoglycan is composed of repeating units of N-acetylglucosamine and N-acetylmuramic acid, crosslinked by pentapeptide side chains (Vollmer et al., 2008).

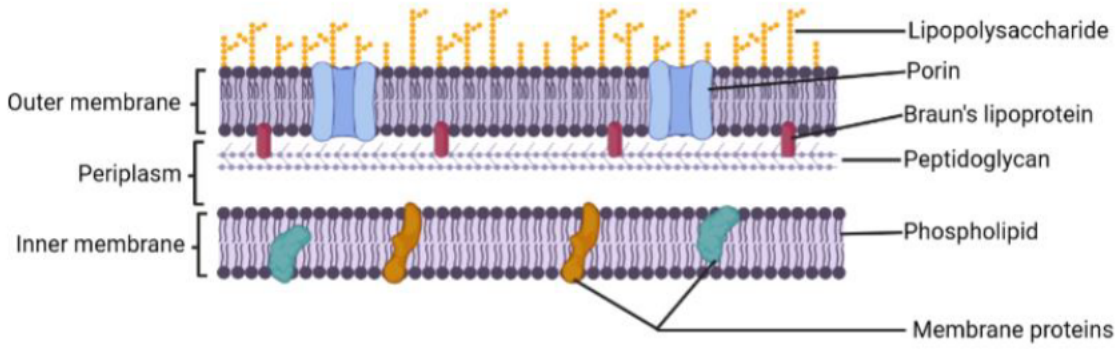

Figure 1.7. Envelope structure of Gram-negative bacteria (designed with Biorender)

1.4.3.2. System involved in the bacterial envelope repairs

Bacterial envelopes are exposed to a multitude of environmental factors, such as pH, temperature, osmotic stress, pressure, and chemicals such as antibiotics, antimicrobial peptides and detergents. The bacterial cell envelope is the first target of antimicrobial agents and bacteria have developed different systems to repair membrane damage (RpoE-, CpxAR-regulated systems, Regulator of capsule synthesis (Rcs), Bacterial adaptative response (Bae) system and Phage Shock Proteins (Psp)) (Hews et al., 2019).

1.4.3.2.1. RpoE

In *E. coli*, stress conditions such as heat or osmotic shock can induce outer membrane and periplasmic protein misfolding (Duguay & Silhavy, 2004). Consequently, the extra-cytoplasmic function sigma factor (σE) encoded by *rpoE* is activated to induce genes required to maintain the integrity of outer membrane components (Duguay & Silhavy, 2004). RpoE is one of the most important alternative sigma factors and is part of four-gene operon (*rpoE*, *rseA*, *rseB* and *rseC*). Under normal conditions, to prevent its association with the RNA polymerase, σE is bound to RseA. Misfolding of outer membrane proteins are recognised by binding to the inner membrane protease, DegS; this lead to the cleavage of RseA (Ades et al., 1999; Collinet et al., 2000). This step allows a second cleavage of RseA by a second protease, RseP, facilitating the release of σE into the cytoplasm (Akiyama et al., 2004). Once free in the cytoplasm, σE becomes associated with RNA polymerase which in turn activates the regulon. The induction of σE-dependent genes leads to the upregulation of the outer-membrane protein folding pathways, and also of the genes involved in LPS biogenesis and transport (Mitchell & Silhavy, 2019). In *Salmonella*, it has been shown that RpoE can promote, under hyperosmotic stress, flagellar gene expression (Du et al., 2011). A deletion of *rpoE* in *S*. Typhimurium increases the resistance to antimicrobial agents (Xie et al., 2016).

1.4.3.2.2. CpxAR

Another system involved in the maintenance of the integrity of the bacterial membranes is the two-component system, CpxAR. A defect in protein secretion across the inner membrane or the secretion of a misfolding protein lead to the autophosphorylation of CpxA histidine kinase domain. The phosphate group is

then transferred to CpxR which leads to the upregulation of several chaperones and proteases. These allow the degradation or refolding of the misfolded proteins. It has been shown that CpxAR is involved in the virulence of *S. enterica* (Humphreys et al., 2004). Furthermore, many genes under the control of Cpx system were up regulated by *S*. Enteritidis after EW exposure (Baron et al., 2017, 2020; Gantois et al., 2008; Huang et al., 2019; Qin et al., 2019).

1.4.3.2.3. Bacterial adaptative response (Bae) system

The Bae system is a two-component system located into the inner membrane and composed of the sensor histidine kinase, BaeS, and the response regulator, BaeR (Nagasawa et al., 1993). BaeS is activated after exposure to toxic molecules (e.g. ethanol, indole, nickel chloride) and induces its autophosphorylation and the transfer of the phosphate group to BaeR (Mitchell & Silhavy, 2019). In response to the corresponding toxic molecules, BaeR causes the upregulation of genes that protect the membrane, such as a periplasmic chaperone (Spy) and efflux pumps (Nagakubo et al., 2002; Nishino et al., 2005).

1.4.3.2.4. Regulator of capsule synthesis (Rcs) system

The Rcs system responds to various membrane alterations affecting membrane fluidity, the LPS, peptidoglycan biosynthesis and lipoprotein trafficking (Mitchell & Silhavy, 2019). Rcs is composed of RcsF, an outer membrane sensor protein, which is, in normal conditions, repressed by IgaA (an inner membrane protein). IgaA interacts with a complex phosphorelay (composed of a histidine kinase RcsC, the phosphotransferase RcsD and the response regulator RcsB) preventing the autophosphorylation of RcsC. Under stress conditions, the interaction between IgaA and the phosphorelay is repressed by RcsF, leading to the phosphorylation cascade of RcsC, RcsD and RcsB (Wall et al., 2018). This

latter can act as a homodimer or a heterodimer (with RcsA, which is not regulated by phosphorylation) and is responsible for the transcription of several genes involved in flagellar motility (Francez-Charlot et al., 2003), and capsule and biofilm formation in *E. coli* (Ferrières et al., 2007; Wehland & Bernhard, 2000).

1.4.3.2.5. Phase shock protein (Psp)

Another system that enables maintenance of the integrity of the bacterial membranes is the phage shock protein (Psp) system. This protein was first discovered by Brissette et al. (1990) during *E. coli* infection by a filamentous phage. Seven genes compose the *psp* regulon*: pspABCDE*, *pspF* and *pspG* (located at a different locus). The biological function of PspA is to block proton leakage by binding inner membrane phospholipids (Kleerebezem et al., 1996; Kobayashi et al., 2007a). PspF is a DNA-binding transcriptional activator of the *psp* genes (Jovanovic et al., 1996). Both inner membrane proteins, PspB and PspC, have a role in controlling the *psp* gene transcription (Kleerebezem et al., 1996). However, the role of *pspD*, *pspE* and *pspG* remain little understood but they appear to be accessory genes as they are not conserved in all organisms (Darwin, 2005). Under physiological conditions, PspA binds to PspF and thus acts as a negative regulator of PspF via protein-protein interaction (Joly et al., 2009). Under stress conditions, a signal is sent to PspB and PspC which act as sensors and interact with PspA (Weiner et al., 1991). Then, PspF is released which allows the activation of the transcription of *pspABCDE* and *pspG* (Weiner et al., 1991) (Figure 1.8).

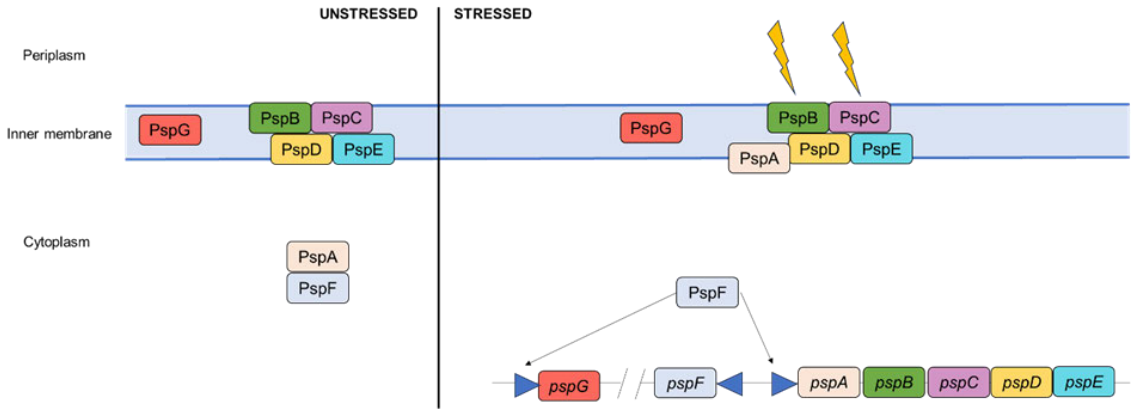

Figure 1.8. Regulation of *psp* genes in *E. coli*. PspA and PspF associate under physiological conditions and the transcription of *pspA* and *pspG* are repressed. When bacterial membrane is subjected to stress, such as a dissipation of the pmf, PspF is released and can then act as an activator of *pspA-E* and *pspG* transcription.

1.4.3.3. Evidence for a direct interaction of ovotransferrin with the bacterial membrane

Several antimicrobial mechanisms other than, or in addition to, iron restriction have been assigned to OT. Valenti et al. (1985) showed that iron saturation of OT had no impact on its antimicrobial activity against *Candida albicans* and suggested a complex mechanism involving a direct interaction between OT and *Candida* cells. This assumption was supported by the microscopic observation that OT induces cell aggregation (Valenti et al., 1985). The need for direct interaction in order to elicit this effect was confirmed when separation of OT from *C. albicans* cells using a dialysis membrane prevented the antimicrobial activity (Valenti et al., 1986). However, the manner in which OT directly interacts with *C. albicans* cells remains unknown. In addition, transferrin and lactoferrin have been shown to mediate damage to the outer membrane of Gram-negative bacteria (Ellison et al., 1988). Indeed, chelation of divalent cations is known to permeabilise the outer membrane of Gram-negative bacteria, making it more permeable to antimicrobial compounds (Leive, 1974; Nikaidoi & Vaara,

1985). According to Ellison et al. (1988), human transferrin and lactoferrin can chelate the divalent ions present on the surface of the outer membrane of *E. coli* (Ellison et al., 1988). The similarities between the properties of OT, and human transferrin and lactoferrin suggest that OT may act similarly in sequestering divalent ions from the outer membrane, leading to membrane destabilisation. Direct binding of OT to the bacterial outer surface is suggested by treatment of *Bordetella pertussis* under iron-restriction conditions which resulted in co-association of OT with the outer-membrane protein fraction (Redhead et al., 1987), indicating direct binding of OT to an outer-membrane protein.

Further evidence for interaction of OT with the bacterial membrane was provided by Aguilera et al. (2003) who showed that OT can permeabilise the inner membrane of *E. coli* (for both whole cells and derived liposomes) resulting in selective leakage of K^+ ions (but not Na^+ or H^+). The potassium permeabilisation resulted in abolition of Δψ but not ΔpH, and a consequential dissipation of the pmf, which decreased from −198 to −56 mV (Aguilera et al., 2003). The pmf is derived from the sum of the transmembrane electric potential (ΔΨ) and proton gradient (ΔpH) and drives the production of energy by the F_0F_1-ATPase through phosphorylation of ADP to ATP (Mitchell, 1966). Thus, loss of pmf, as caused by membrane destabilisation, impairs energy generation. Such disruption also allows ions to freely diffuse across the membrane along concentration gradients. An intact cytoplasmic membrane supports cytosolic homeostasis, efficient energy production, and pmf-dependent transport and motility functions, whereas dysfunction of the cytoplasmic membrane can lead to cell death.

1.4.3.4. Bacterial membrane perturbation in the natural context of egg white

Exposure of *E. coli* and *S.* Enteritidis to EW has also been shown to elicit membrane damage (Huang et al., 2019; Jan, et al., 2013). Atomic force microscopy (Jan, et al., 2013) and transmission electronic microscopy (Huang et al., 2019) demonstrated that EW induces disruption of the cell envelop and leakage of intracellular contents. However, the EW components specifically responsible for this membrane perturbation are not yet defined. The observed membrane damage is well reflected by the induction of a set of cell-envelop stress genes in response to exposure of *S*. Enteritidis to EW and by the EW sensitivity of mutants with defects in cell envelope systems. Approaches used to demonstrate such effects have included *in vivo* expression technology (IVET) (Gantois et al., 2008), microarray- and RNAseq-based transcriptomic analysis (Baron et al., 2017; Huang et al., 2019), quantitative proteomics (Qin et al., 2019), directed mutagenesis (Gantois et al., 2008; Huang et al., 2020; Qin et al., 2019), random mutagenesis (Clavijo et al., 2006), and microarray-based transposon-library screening (Raspoet et al., 2014).

Many of the *S.* Enteritidis genes/proteins highlighted by these studies have roles in periplasm homeostasis and degradation of abnormal proteins (Baron et al., 2017; Huang et al., 2019), membrane permeability and replacing the general-diffusion porins with porins of smaller pore-size (Baron et al., 2017; Clavijo et al., 2006), maintenance of cell envelope integrity (Baron et al., 2017; Huang et al., 2019, 2020; Qin et al., 2019), LPS biosynthesis (Clavijo et al., 2006; Gantois et al., 2008; Raspoet et al., 2014), cell-wall integrity and biosynthesis (Gantois et al., 2008), remodelling of the peptidoglycan (Baron et al., 2017; Huang et al.,

2020), and removal of antimicrobial compounds through multidrug-efflux (Baron et al., 2017; Huang et al., 2019). The majority of these genes are under the control of the CpxAR regulator (section 1.4.3.2.2). Deletion of the CpxAR-encoding genes has demonstrated that CpxAR is a key regulator for *S.* Enteritidis survival under the natural alkaline conditions of EW at 37 °C (Huang et al., 2019). The observed induction of the CpxAR-regulated genes in EW is consistent with an attempt by *S.* Enteritidis to combat the antimicrobial EW components that mediate envelope damage. There are several EW components that cause damage to the bacterial envelope, and these could therefore contribute to induction of CpxAR-regulated genes by EW. Such components include: Avian β-defensin 11 (AvBD11) (Hervé-Grépinet et al., 2010); gallin (Gong et al., 2010); lysozyme; and OT. In addition, there are likely to be other EW proteins or peptides with unknown function that also act on the bacterial envelope to induce the CpxAR regulon (Baron et al., 2016). Important new insight into the components of EW responsible for induction of the CpxAR controlled genes in *S*. Enteritidis was recently obtained by utilisation of EWF (3 and 10 kDa cut-off membranes) (Huang et al., 2020) whereby similar CpxAR responses were achieved with EW and EWF. Thus, since the filtrates lacked OT yet still induced the CpxAR regulon, it is clear that neither OT nor any other protein above 3 kDa are strictly required for the observed CpxAR induction.

In contrast to the induction of the CpxAR regulon by EW, the *psp* genes of *S.* Enteritidis were only induced by EW when proteins of >10 kDa were present (Baron et al., 2020). Upon EW exposure, the *psp* genes where shown to be subject to rapid (≤7 min) up-regulation followed by an expression decrease from 25–45 min (Baron et al., 2017). In apparent contradiction to this finding, Huang

et al. (2020) failed to observe any induction of the *psp* genes by EW (Huang *et al*., 2020); this discrepancy likely arises from the longer incubation times (6 and 24 h) employed.

To further explore any pmf disruption effect caused by EW proteins, Baron et al. (2020) tested the membrane depolarisation of *S.* Enteritidis (Baron et al., 2020) using the $diSC_3(5)$ fluorescent dye method (Baron et al., 2020; Epand et al., 2010). This study showed a significant increase in the fluorescence of *S.* Enteritidis upon incubation in EW, but not in EWF where EW proteins of >10 kDa were absent (Baron et al., 2020). The authors concluded that the proteins (>10 kDa) present in EW are responsible for the observed depolarisation of the bacterial membrane (Baron et al., 2020). Although the identity of the proteins involved has not yet been determined, it was suggested that OT may play a part since previous studies have shown a disruptive effect of OT on bacterial membranes (Aguilera et al., 2003; Ellison et al., 1988) and the electrochemical potential of the cytoplasmic membrane of *Bacillus cereus* (Baron et al., 2014).

To conclude, it is likely that OT, like other transferrin-family members, is able to chelate divalent ions present on the surface of the outer membrane of Gram-negative bacteria and provoke membrane perturbation, probably by direct contact. The bacterial membrane perturbation effects induced by OT include membrane permeabilisation to potassium and dissipation of the pmf. In addition, several studies have shown that EW induces the expression of *S.* Enteritidis genes (and/or the production of proteins) involved in the envelope-damage response, maintenance of membrane integrity, and pmf restoration. The mechanism(s) by which OT induces perturbation of bacterial envelopes, under the specific conditions found in EW, remain(s) to be clarified. Understanding

these mechanisms, and the contribution that the specific conditions of EW play in OT-induced bacterial membrane perturbations, would be expected to greatly support research aimed at optimising the control of egg contamination.

1.4.4. Impact of egg-white conditions on ovotransferrin

1.4.4.1. Impact of egg white pH

In EW, the pH increases from 7.8 to 9.3 a few days after laying (Sauveur, 1988). This is caused by the loss of CO_2 through the pores of the eggshell (Sharp & Powell, 1931). The maintenance of intracellular pH around its optimum value (7.4 to 7.8; Booth, 1985; Padan et al., 1976, 1981) is essential for many biological functions, particularly for bacterial enzymatic activities and the status of membranes. Excessive differences in pH between the environment and the bacterial cytoplasm can lead to energetically unfavourable conditions for growth (Jin & Kirk, 2018). The impact of EW pH on bacterial behaviour has been much reported. At 39.5 °C, Tranter and Board (1984) showed a bactericidal effect on *E. coli* incubated at pH 9.3, while bacteriostasis was observed at pH 7.8 (Tranter & Board, 1984). At 37 °C, bacteriostasis was reported by Kang *et al*. (2006) for *S*. Enteritidis incubated at pH 9.0, although growth was seen at pH 8.0 (Kang et al., 2006). At 20 °C, a one-$\log_{10}$ reduction of *S*. Enteritidis growth was observed at pH 9.3 compared to 8.2 (Messens et al., 2004). Alabdeh et al. (2011) showed that alkalinisation (increase in pH from 7.8 to 9.3) potentiates the antibacterial effect of EW on *E. coli* and *S.* Enteritidis at temperatures that are growth permissive (between 20–37 °C) or bactericidal (above 40 °C) (Alabdeh et al., 2011). However, at 39.5 °C the addition of 20 µg/mL iron to EW (corresponding to 105% OT saturation) overcame the bactericidal effect at pH 9.0 and the

bacteriostatic effect at pH 7.8 for *E. coli* (Tranter & Board, 1984), with iron supporting better growth at pH 7.8 than at pH 9.

The impact of pH (from 6.5 to 9) on iron-binding by OT has been studied by Okamoto et al. (2004). They showed that lobe preference for initial iron binding is highly dependent on pH (Okamoto et al., 2004). However, it remains unknown whether the pH of EW (7.8 or 9.3) influences the overall metal-chelating activity of OT. Another pH impact of relevance is influence on the interaction between EW proteins and the bacterial outer membranes. Figure 1.9 shows a structural model of apo-OT (PDB ID: 1AIV) with its molecular surface coloured by the electrostatic potential calculated at pH 7.0, 8.0 or 9.0. This model indicates that the few positively charged areas present on the surface of OT at pH 7.0 are almost completely lost at pH 9.0. Therefore, OT appears to be negatively charged at alkaline pH, whatever the surface area considered.

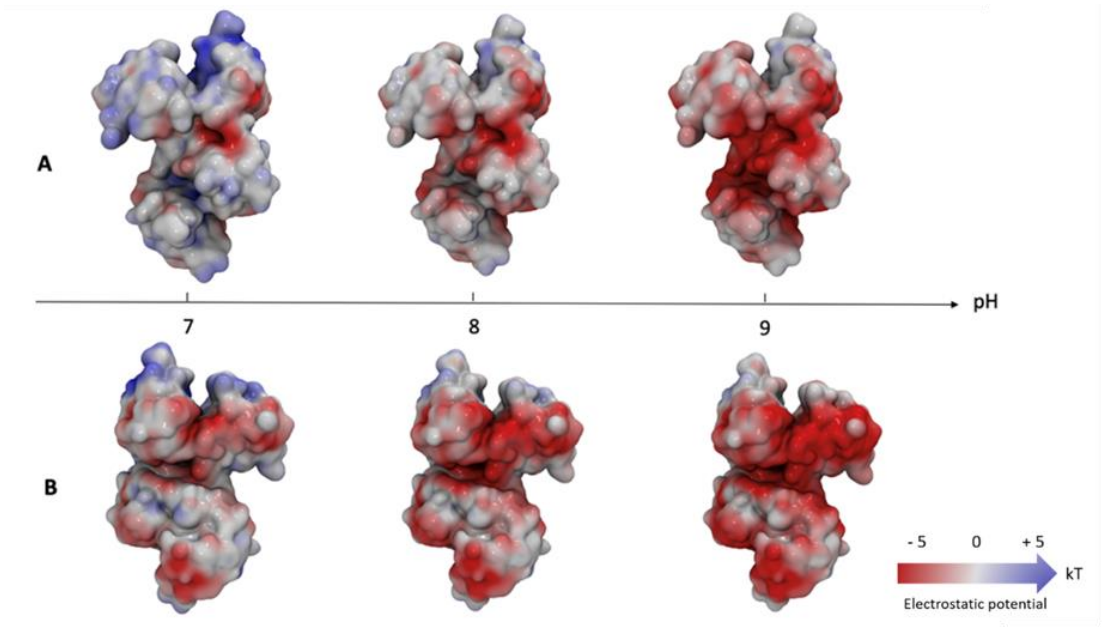

Figure 1.9. Prediction of electrostatic charge distribution at the surface of OT. Each representation (A) and (B) corresponds to a rotation of the molecule by 180° around the vertical axis. Charges were computed at each pH using the PDB2PQR tool (Dolinsky et al., 2004) and the electrostatic potential of the protein surface was estimated with the APBS tool (Baker et al., 2001), using a specific server (https://server.poissonboltzmann.org/ (accessed on 15 January 2021). The molecule was visualised using the VMD software (Humphrey et al., 1996). The surface of each molecule is coloured according to the electrostatic potential, from −5 kT (red) to +5 kT (blue), via 0 kT (white), where k is the Boltzmann constant and T the absolute temperature. (Legros et al., 2021)

The impact of the pH-related change in surface charge on OT function (e.g., interaction with bacterial surfaces and or metals ions) remains largely unexplored. Moreover, it was shown that OT provokes a stronger depolarisation of the cytoplasmic membrane of the Gram-positive *B. cereus* at pH 9.3 than at neutral pH (Baron et al., 2014). The precise influence of EW pH on the membrane perturbation activity of OT requires further investigation (especially for *S.* Enteritidis).

1.4.4.2. Impact of the ionic composition of egg white

Studies investigating the antimicrobial activity of OT have been performed mainly in minimal or rich model media under a range of iron regimes. However, Baron et al. (1997) investigated the effect of OT under the ionic environment of

EW by utilising EWF (free of >10 kDa EW proteins) and found that OT exerts a major antibacterial impact on *S.* Enteritidis (Baron et al., 1997). However, it should be pointed out that the ion concentration of EW (Table 1.2) is variable and the influence of metal ions other than iron has not been explored. Indeed, OT is able to bind iron, chromium, copper, manganese and zinc, and aluminium (listed in respective order of decreasing affinity) (Aasa et al., 1963; Evans et al., 1977; Hirose et al., 1996; Tan & Woodworth, 1970; Warner & Weber, 1953). Valenti et al. (1987) found that 100% saturation of OT with zinc increases its bacteriostatic activity in BHI medium at 37 °C, but that saturation of OT with iron reverses the antimicrobial effect of the Zn-OT complex (Valenti et al., 1987). These authors showed that iron, copper and zinc ions are in competition for the same binding site in OT, but they failed to explain why the bacteriostatic activity of OT is enhanced by complexation with zinc (Valenti et al., 1987). The role for EW metals (Table 1.2) in the antimicrobial activity of OT has not yet been fully studied. The investigation of such effects is complicated by the need to consider changes in EW metal content during the course of egg storage since fluxes of minerals are observed due to metal migration from the egg yolk through the vitelline membrane (Réhault-Godbert et al., 2019). This could have an impact on EW metal content and, consequently, on the antimicrobial activity of OT. In addition, the ion content of eggs is influenced by diet such that variations of 28% are observed for manganese and zinc, 40% for copper, and 12% for iron (Grittins & Overfield, 1991).

Table 1.2. Mineral and glucose composition of EW

	Minimal concentration in EW (mM)*	Maximal concentration in EW (mM)*
Sodium	67.424	80.908
Sulfur	50.834	56.136
Chloride	-	49
Potassium	35.807	44.247
Phosphorus	4.1971	7.1028
Magnesium	3.7029	4.9372
Calcium	1.2476	2.9942
Iron	0.0036	0.0179
Zinc	0.0015	0.0185
Copper	0.0029	0.0058
Manganese	0.0013	0.0020
Glucose	-	25

* The values are obtained from: Ciqual, 2021; Nau et al., 2010b; Nys & Sauveur, 2004; Sauveur, 1988; and Stadelman & Cotterill, 1995. Whereas chloride, sodium, and potassium are mainly free in solution, sulphur is a constituent element of EW proteins. Calcium and magnesium are partly bound to proteins and heterogeneously distributed between thick and thin EW.

According to the concentration ranges detected in EW (Table 1.2), OT appears to be only 1.07 to 5.4% saturated for iron, 0.48 to 5.4% for zinc, 0.87 to 1.74% for copper, and 0.38 to 0.60% for manganese; this gives a maximum total metal saturation of ~13%, which leaves a considerable 87% residual chelation capacity.

Bicarbonate is present in EW at around 55 mM and originates from the mother hen's blood, as is the case for other ions that enrich EW during hydration in the hen's uterus (Brooks & Pace, 1938; Mongin & Lacassagne, 1966). Valenti et al. (1981) showed that the addition of 50 mM bicarbonate increases the antimicrobial activity of a 10 g/L OT solution towards Staphylococci and *E. coli* incubated in BHI medium at 37 °C (Valenti et al., 1981), presumably due to the dependence of metal-complex formation on the co-binding of anions such as bicarbonate (Guha et al., 2003). Similar results were obtained with *E. coli* O157:H7 and *Listeria monocytogenes* incubated with 100 mM bicarbonate in BHI

at 37 °C (Valenti et al., 1981). The combination of high bicarbonate and relatively low iron with OT in EW would be expected to greatly support the metal-chelation activity of OT, ensuring very low access to iron for bacterial invaders.

The mineral composition of EW may support the integrity of the outer membrane due to the presence of divalent cations such as Ca^{2+} and Mg^{2+} that are bound to the LPS and contribute to resistance against antimicrobial agent. It remains unclear whether OT within EW has the capacity to remove these cations from bacterial outer membranes and if any such activity results in perturbation of the outer membrane. In conclusion, the mineral composition of EW may have an impact on the antimicrobial activity of OT. This possibility requires further exploration, especially in view of the potential for optimising the antimicrobial activity of OT through influencing the ionic composition of EW by suitably adjusting hen feeding and/or egg-storage practices.

1.4.4.3. Impact of viscosity and the heterogeneous structure of egg white

EW has a viscosity of 5 $mPa.s^{-1}$ at 20 °C and a shear rate of 400 s^{-1}, which corresponds to a highly viscous medium (Lang & Rha, 1982). However, EW viscosity is not homogeneous with respect to its three distinct layers: the two layers of low-viscosity (thin) EW, one located near the EY and the other close to the eggshell; and a layer of high-viscosity (thick) EW sandwiched in between the "thin" layers. The thick EW can be 40 times more viscous than the thin EW (Lang & Rha, 1982) due to the presence of ovomucin, which forms filamentous super-aggregates (Robinson & Monsey, 1972, 1975). The viscosity of EW decreases during egg storage due to biochemical changes (not yet completely understood) involving ovomucin (Brooks & Hale, 1959; Cotterill & Winter, 1955; Kato et al., 1979, 1981; Robinson & Monsey, 1972; Sato et al., 1976) which might impact

infection potential. It is likely that the viscosity of EW and the presence of heterogeneous rheological fractions (thin and thick layers) hinder bacterial infection by limiting motility resulting in reduced access to nutrients and dissemination throughout the egg. Moreover, several authors have suggested that iron-OT complexes are probably not distributed uniformly within EW (Baron et al., 1997; Li-Chan, 1989). It can be assumed that EW viscosity and its heterogeneous structure will have an impact on bacterial contamination, and on the interaction between bacteria and OT.

1.4.4.4. Impact of the presence of other egg-white proteins

Synergistic or antagonistic effects may occur between OT and other EW proteins. Cooperation between lysozyme and lactoferrin has already been established for anti-microbial effects on Gram-negative bacteria (Ellison & Giehl, 1991; Facon & Skura, 1996; Suzuki et al., 1989). The hydrolysis activity of lysozyme results in lysis of Gram-positive bacteria under conditions where the internal osmotic pressures exceed that externally. However, the outer-membrane surface of Gram-negative bacteria protects bacteria from lysozyme activity. The lysozyme resistance of Gram-negative bacteria can be impaired by the addition of molecules that chelate the divalent ions of the LPS layer, allowing peptidoglycan lysis and membrane damage (Branen & Davidson, 2004; Samuelson et al., 1985; Ko et al., 2008). A synergistic effect of lactoferrin and lysozyme has been observed in 1% of peptone medium (Suzuki et al., 1989; Ellison & Giehl, 1991). According to Ko et al. (2008), the addition of 2.5 to 3 g/L lysozyme to a 20 g/L OT solution exerts a synergistic bacteriostatic effect on *L. monocytogenes* (a Gram-positive bacterium) in BHI (pH 7) medium at 37 °C, but only in the presence of 100 mM bicarbonate (Ko et al., 2008). In contrast, at

35 °C and in the same medium, no significant difference in bacterial growth was observed when *E. coli* (Gram negative) was incubated with OT (20 g/L with 100 mM bicarbonate) with or without 1 g/L lysozyme (Ko et al., 2008). However, these studies did not consider the synergistic effects of lysozyme and OT under conditions that reflect those of EW (i.e., at 13 and 3.5 g/L for OT and lysozyme, respectively, and at alkaline pH and with relevant mineral levels).

Other work has shown that genes encoding proteins involved in the inhibition of lysozyme activity (lysozyme inhibitor encoded by *ydhA* and *SEN1802*) are induced when *S.* Enteritidis is incubated with EW proteins (45 min at 45 °C) (Baron et al., 2020). It was suggested that exposure of *S.* Enteritidis to EW proteins at 45 °C causes permeabilisation of the outer membrane (through chelation of the divalent cations of the LPS layer by OT) which enabled lysozyme to gain access to the peptidoglycan, stimulating the induction of the expression of the lysozyme inhibitor gene in response (Baron et al., 2020).

The possible synergy between OT and lysozyme (or other EW components) in mediating antibacterial activity remains to be clarified under the natural conditions of EW. Such insight would enhance understanding of the antimicrobial activity of EW and EW preservation processes. Understanding the complex and effective synergy of EW proteins represents a strong basis to consider practical applications (such as hen selection and egg storage) for increasing antimicrobial EW defence and enhancing egg safety.

1.4.4.5. Impact of ovotransferrin-derived peptides

In addition to the antimicrobial role of native OT, antimicrobial peptides derived from OT have also been identified. The acid hydrolysis of OT yielded a

cationic peptidic fragment (OTAP.92) which exhibited a wider antimicrobial spectrum than native OT. The OTAP.92 peptide was found to kill bacteria by disrupting the function of the cytoplasmic membrane (Ibrahim et al., 2000). More recently, another peptide, designated OVTp12, was isolated from OT (by pepsin hydrolysis) and found to increase the membrane permeability of bacteria (Ma et al., 2020). However, although these OT fragments display clear antibacterial activity, their relevance to EW immunity is uncertain since they are unlikely to be present given the absence of the corresponding hydrolysis processes.

Nevertheless, protein degradation may occur during egg storage. An SDS-PAGE analysis highlighted the presence of proteolytic fragments after five-day storage of eggs at 37 °C (Réhault-Godbert et al., 2013), and peptides derived from the proteolytic degradation of OT were identified by mass spectrometry (Réhault-Godbert et al., 2013). Liu *et al*. (2018) showed that the overall protein content of EW gradually decreases during egg storage at room temperature, with a corresponding increase in peptide content (Liu et al., 2018). In the <3 kDa EW fraction, a significant increase in peptide content was observed after 21 days of egg storage, and after 56 days, the peptide level was increased by 17-fold with respect to those of fresh eggs. Six OT-derived peptides were subsequently identified in the <3 kDa EW fraction from day 56. The authors suggested that storage at room temperature impacts OT in a fashion that leads to its consequential degradation to generate the observed peptides (Liu et al., 2018). However, it remains unclear whether these OT-derived peptides have antibacterial activity under EW conditions and what mechanism drives their formation.

1.4.4.6. Impact of egg processing and technological factors

During egg production, storage and processing, and egg-product manufacture, any operation that introduces iron (or other metals) or impairs OT activity can potentially suppress the bacteriostatic activity of EW. It is generally recognised that egg quality is influenced by egg-production processes (housing systems, breeding practice, hen age and hen nutrition), but the levels of the major egg components, including EW proteins (and OT), are relatively stable (Réhault-Godbert et al., 2019). However, the mineral content of eggs can be altered by the hen diet (Réhault-Godbert et al., 2019). Egg contents are particularly impacted by egg-storage factors such as temperature and duration. Shell eggs are generally consumed within 28 days after laying. During this period, eggs are stored at various temperatures depending on the site of storage (laying farm, conditioning centre, food store, consumers' home) and might be subject to different temperatures generally ranging between 20 °C (ambient temperature) and 4 °C (refrigeration temperature). During egg aging, gas exchange (loss of CO_2) with the external environment leads to EW alkalinisation. In addition, the thick-layer content and viscosity of the EW decrease, and the degradation of the vitelline membrane allows mineral transfer between the albumen and yolk (Réhault-Godbert et al., 2019).

When eggs are incorporated into commercial foodstuffs, manufacturers utilise ready-to-use egg products. EW is widely used as an ingredient in various food products due to its whipping (cakes, meringues and confections) and textural properties (sausages, terrines). The transformation of shell eggs into safe-liquid or spray-dried EW with extended shelf life requires technological operations that could impact the antibacterial activity of OT. The first step of EW-

product manufacturing involves breaking the eggshell and separation of EW from EY. The integrity of the vitelline membrane is important at this point to ensure that the yolk is retained within the vitelline membrane to thus avoid any contamination of EW with EY. Baron et al. (1999) showed that the presence of yolk in EW enhances *Salmonella* growth due to increased iron availability and OT saturation (Baron et al., 1999). They observed that EW collected (just after breaking) from several factories allows *Salmonella* growth at similar levels to that observed experimentally in EW containing 0.7% yolk. These findings highlight the need to ensure that the egg breakage and yolk separation processes are carefully controlled (considering factors such as egg quality, egg age, processing parameters and operator vigilance) to avoid yolk contamination.

After egg breakage, the isolated liquid EW is pasteurised to enhance food safety. However, the heat treatment employed must be mild (traditionally 57 °C for 2 to 6 min) because of the thermal fragility of EW, and such mild treatment is insufficient for effective *Salmonella* elimination (Baron & Jan, 2011). However, dried EW (powder) is used in place of liquid EW by many sectors of the food industry for practical reasons (e.g., room storage and microbiological stability due to low water activity) which include the possibility of applying a much stronger and more effective heat treatment (incubation at 67 or 75 °C for 15 days) to the dried-egg product (Baron & Jan, 2011). Heat treatment of EW powder has the dual advantage of ensuring effective *Salmonella* elimination and improvement of the functional properties (whipping and gelling) of the dried EW functional properties that are important for various foodstuffs including cakes, meringues and surimi (Baron & Jan, 2011). The EW drying process involves pumping and atomization (aerosol generation) and is considered to cause only minor changes

to the EW proteins (Baron et al., 2003). Nevertheless, Baron et al. (1999) showed that this pasteurisation process results in a dramatic loss of bacteriostatic activity for EW when it is subsequently reconstituted such that a rapid growth of *Salmonella* is observed in the reconstituted EW (comparable to that obtained in optimum growth medium) (Baron et al., 1999). This effect likely arises from the heat lability of OT, which was found to possess the lowest heat stability of all the major EW proteins, with a denaturation temperature of 60 °C at pH 9 (for apo-OT) (Lin et al., 1994). Indeed, Baron et al. (2003) subsequently demonstrated that the observed loss of bacteriostatic activity is attributable to the thermal denaturation of OT during pasteurisation resulting in a reduction in its iron chelation activity (Baron et al., 2003).

It is therefore clear that technological factors applied during EW product manufacturer can modify OT activity, especially when iron is introduced, or thermal treatment is applied. This is also the case when EW protein is incorporated into other foods as an ingredient and then exposed to technological processes within the subsequent food chain.

1.5. Aim of this study

Considering all the above findings, the role of OT and the response of *S*. Enteritidis to the EW antimicrobial activity requires further investigation. Indeed, the factors affecting the ability of *S*. Enteritidis to survive in the poor-iron environment of EW remain unclear. Furthermore, the ability of OT to induce *S*. Enteritidis membrane damage has not been clearly demonstrated in EW and is based on the assumption that all transferrins have this capacity. Thus, this study is divided in three main parts.

- **Iron-chelating activity of OT.** In the first results chapter, using an enumeration method, the antimicrobial action of OT, due to its iron-chelating activity, against *S*. Enteritidis was studied. The capacity of *S*. Enteritidis to acquire iron in the iron deficient environment of EW was investigated using a strain unable to produce siderophores. Finally, the ability of S. Enteritidis to use exogenous siderophores to counteract iron restriction imposed by OT was explored.
- **OT and bacterial membrane damage.** In the second results chapter, the role of EW as well as OT to induce *S*. Enteritidis membrane damage was explored. The cooperation between OT and lysozyme was also studied. Thus, permeabilisation of the inner and outer membrane was measured by spectrophotometry and depolarisation of the inner membrane by spectrofluorimetry.
- ***S*. Enteritidis response to membrane damage.** In the third results chapter, different molecular-genetic approaches were used to study the regulation of the *psp* genes involved in the maintenance of the pmf, by EW and OT. Thus, transcriptional fusions were constructed and used to measure the promoter activity. Furthermore, expression of *psp* genes was also studied by qRT-PCR.

Chapter 2.
Material and methods

2.1. Materials

2.1.1. Bacterial strains

All the bacterial strains used in this study were described in Table 2.1. *Salmonella enterica* subsp*. enterica* serovar Enteritidis (*S*. Enteritidis) PT4-125109, also called NCTC13349 (genome accession number: AM933172) was kindly donated by Matthew McCusker from the Center for Food Safety and Food Borne Zoonomics, Veterinary Sciences Centre of the University College Dublin, Ireland. From this strain, the *S*. Enteritidis (pBBC129) was engineered for this study (Appendix 1) and used to investigate the impact of OT on the permeabilisation of *S*. Enteritidis membranes. The mutant PT4-125109 Δ*entB* was constructed previously by Dr Louis Julien (Julien et al., 2020) and was used to study the impact of the iron-chelating activity of OT on *S*. Enteritidis under EW conditions.

The *lacZ* transcriptional fusions were constructed using *E. coli* TOP10 competent cells from Invitrogen (Walthman, United States). This strain is known for its high transformation efficiency due to a mutation in the gene *endA*, a non-specific endonuclease I, and a mutation in the gene *recA*, responsible for DNA homologous recombination. All strains were stored as seed stocks at -80 °C in L-broth with 20% (v/v) glycerol (Fisher Scientific, Hampton, United States) in cryovials.

Table 2.1. Bacterial strains used in this study

Strain	Genotype	Source
	Escherichia coli	
E. coli TOP10	F^-, *mcrA* Δ(*mrr-hsdRMS-mcrBC*) Φ80*lacZΔM15 ΔlacX74 recA1 araD139* Δ(*ara leu*)7697 *galU galK rpsL* (Str^R) *endA1 nupG*	Invitrogen
	Salmonella enterica serovar Enteritidis	
PT4-125109 (NCTC13349)	Wild type	McCusker, Dublin, Ireland
PT4-125109 Δ*entB*	PT4-P125109 ΔentB::cat	Julien et al., 2020
S. Enteritidis(pBBC129)	β-galactosidase positive	Dr Sylvie Bonnassie for this study

2.1.2. Plasmids

The plasmids used in this study are listed in Table 2.2. The plasmid vector pJET1.2/blunt was used for the *lacZ*-fusions, as an intermediate before cloning DNA fragments into the final plasmid. It possesses the gene *eco471R* (encoding for a restriction enzyme) located in the ligation region. In the case of a re-circularisation of the plasmid without DNA insert, this gene is functional, resulting in a lethal phenotype and in this way, increasing the efficiency of transformant screening. The plasmid pRS1274 was used as the final *lacZ*-fusion vector. It is a medium copy number plasmid, containing an ampicillin resistance cassette and a non-expressed operon lactose (lacking a functional promoter). This vector was used in the engineering of *psp-lacZ* transcriptional fusions.

Table 2.2. Plasmids used in this study

Plasmid	Size (bp)	Genotype	Resistance	Source
Plasmid used for cloning				
pJET1.2/blunt	2,974	Cloning vector	Amp	ThermoScientifc™
pRS1274	10,752	*bla-TI*$_4$, *Bam*HI-*Sma*I-*Eco*RI, *'lacZYA*	Amp	Simons et al., 1987
pJET1.2/blunt containing target regions from *S.* Enteritidis PT4-125109				
pJET1.2-*pspA*	3,336	putative phage shock protein A	Amp	This study
pJET1.2-*pspF*	3,336	putative phage shock protein F		
pJET1.2-*pspG*	3,243	putative phage shock protein G		
pRS1274 containing target regions from *S.* Enteritidis PT4-125109				
pRS1274-*pspA-lacZ*	11,114	putative phage shock protein A	Amp	This study
pRS1274-*pspF-lacZ*	11,114	putative phage shock protein F		
pRS1274-*pspG-lacZ*	11,021	putative phage shock protein G		

2.1.3. Primers

Different pairs of primers were used in this study for DNA amplification, qRT-PCR or Sanger sequencing. Primers are presented in Tables 2.3, 2.4 and 2.5.

Table 2.3. Primers used for DNA amplification

Gene		Sequence (5' - 3')*	%GC	Length (nuc)	Tm (°C)	Amplicon (bp)
pspA	F	GAGGGATCCCGCCAAGCCCACGT TTACAGGAATTT	50	26	66.4	362
	R	CACGAATTCCTGCTTGCTGGCTGG TTGATGTCC	58.3	24	66.5	
pspF	F	GAGGGATCCCGGGAGACTTGTTC CAGTACTTCAA	48	25	62.5	362
	R	CACGAATTCCCAGCGTATCTTCCA TCTCCTGAAT	48	25	62.3	
pspG	F	GAGGGATCCCGATGTATCCCTATA TTGAGCGTGA	44	25	60.2	457
	R	CACGAATTCCAGAATGCCCAGCAA GGAGA	55	20	60	

*Underlined nucleic acids correspond to the restriction enzyme site *Bam*HI (GGATCC) or *Eco*RI (GAATTC)

Table 2.4. Primers used for Sanger sequencing

Name		Sequence (5' - 3')	%GC	Length (nuc)	Tm (°C)
pJET1.2/blunt	F	CGACTCACTATAGGGAGAGCGGC	61	24	63
	R	AAGAACATCGATTTTCCATGGCAG	42	24	64.18
pRS1274	F	GGATTTGAACGTTGCGAA	44.4	18	49.28
	R	AAGTTAAAATGCCGCCAG	44.4	18	48.11

Table 2.5. Primers used for qRT-PCR

Genes		Sequence (5' - 3')	Length (bp)	Tm (°C)	%GC
asmA	F	GTTTGCGGCGTCAGTTGAAT	20	60	50
	R	AACTCAGCATCCTTTCCGGG	20	60	55
emrA	F	CAGACTGACGCCAAACAAGC	20	60	55
	R	CGATATTCGCCTGCAACTGC	20	60	55
pspA	F	GAAGTCACGCTGGTGGATGA	20	60	55
	R	TCAAGCTGACGACGGACATC	20	60.1	55
pspG	F	GTCTCCTTGCTGGGCATTCT	20	60	55
	R	CAGCAGTAGCCACGGTAACA	20	60	55

2.1.4. Culture medium

2.1.4.1. Standard bacterial growth medium

Tryptone Soya Broth (TSB, Sigma-Aldrich, St Louis, United States) was used for *S.* Enteritidis, and Luria-Bertani (LB; 10 g/L tryptone, 5 g/L yeast extract, 5 g/L NaCl) for *E. coli* cultures. Agar (15 g/L) was added to obtain solid media. Super optimal broth with catabolite repression (SOC; 5 g/L yeast extract, 20 g/L tryptone, 10 mM NaCl, 2.5 mM KCl, 10 mM $MgCl_2$, 20 mM glucose) was used for transformation (section 2.2.6.1) and electroporation (section 2.2.16). All media were sterilised by autoclaving (21 min at 120 °C).

2.1.4.2. Preparation of sterile egg white

EW was prepared from eggs obtained from a conventional hen housing system. Eggshell surfaces were sanitized with absolute alcohol. Residual alcohol was removed by briefly flaming the eggshell. Eggshells were then broken, under sterile conditions, and the collected EW was aseptically homogenised with an Ultra-Turrax® Disperser DI25 Basic (Ika, Grosseron, Saint-Herblain, France) for 1 min at 9500 x rpm. The pH of EW was measured at 9.3 ± 0.1 and its sterility was checked by the addition of 1 mL EW into melted Tryptone Soya Agar (TSA; Biokar Diagnostics, Pantin, France) in a Petri dish. The plate was incubated for 24 h at 37 °C. After incubation, EW sterility was confirmed by the absence of colonies on the plate. The EW was used either directly (EW) or diluted at 10% (v/v) in either egg-white filtrate (EWF; EWF with 10% EW) or synthetic medium (SM; SM with 10% EW).

2.1.4.3. Preparation of egg-white filtrate

EWF was prepared according as previously described (Baron et al., 1997) by ultrafiltration, using a pilot unit (TIA, Bolène, France) equipped with a membrane with a molecular weight cut-off of 10 kDa. EWF was sterilised by filtration (Nalgene® filter unit, pore size < 0.2 µm, Osi, Elancourt, France). The pH of EWF was checked (9.3 ± 0.1).

2.1.4.4. Preparation of synthetic medium

SM was developed according to the composition of EW and EWF (section 3.7.1). It was prepared by adding the following in the order given: 1 mM of $(NH4)_2SO_4$ (Panreac, Barcelone, Spain), 2 mM of Na_2HPO4 (Merk, Darmstadt, Germany), 40 mM of KCl (Merk), 20 mM of glucose (Merk), 2 mM of $MgCl_2$ (Merk), 0.25 mM of $CaCl_2$ (Sigma), 55 mM of sodium carbonate buffer, pH 9.3. The final

volume was completed with ultrapure water, the pH was checked at 9.3 ± 0.1. The SM was then sterilised by filtration (Nalgene® filter unit, pore size <0.2 µm).

2.1.5. Chemicals

2.1.5.1. Ovotransferrin

Apo-OT was purchased from Sigma and is substantially iron free. OT was prepared in EWF or in SM at different concentrations, ranging from 1.3 to 13 g/L corresponding to 10 and 100% of the theoretical concentration found in EW. For some experiments, ferric citrate (Sigma) was added to obtain a theoretical OT saturation from 10 (33.4 µM) to 110% (367 µM). The pH was measured at 9.3 ± 0.1 and OT solutions were sterilised by filtration (Nalgene® filter unit, pore size <0.2 µm).

2.1.5.2. Lysozyme

Hen lysozyme was purchased from Sigma and was prepared in SM at 3.5 g/L (its concentration found in EW) or at 0.35 g/L (10% of its concentration found in EW). Lysozyme solutions were sterilised by filtration (Nalgene® filter unit, pore size <0.2 µm).

2.1.5.3. Iron

Iron citrate (Sigma) was used to saturate OT. The powder was dissolved in ultrapure water and pH was adjusted to 7. Then the solution was sterilised by filtration (Nalgene® filter unit, pore size <0.2 µm) and stored at 4 °C in the dark before use. For some experiments, ferric citrate was added to EW or OT solutions to obtain iron saturation of OT. Assuming that one mole of OT can bind two moles of iron, the amount of iron required to saturate OT was calculated to reach 10 to 300% OT saturation by iron. Thus, according to Legros et al. (2021), 18.7 mg of

iron is required to saturate at 100% the OT present in 1 L of EW (i.e. 334 µM of iron).

2.1.5.4. Enterobactin

Ent was purchased from Sigma and used in the section 3.8 to study the capacity of *S*. Enteritidis to use exogenous siderophore under EW conditions. Ent was prepared at the concentration of 1.5 mM in 40% DMSO dimethylsulfoxide (DMSO) (Sigma) and used at the final concentration of 10 µM in SM with 1.3 g/L of OT.

2.1.5.5. Antibiotics

Ampicillin (Fisher Scientific, Hampton, United States) was dissolved in ultrapure water and used at the final concentration of 100 µg/mL to select *E*. *coli* and *S*. Enteritidis transformants during the *psp-lacZ* fusions construction and for the growth of S. Enteritidis (pBBC129).

2.1.5.6. DNA and RNA ladder

Nucleic acids were visualised by agarose gel electrophoresis using UV-induced fluorescence in the presence of 1X Gel Red® (Cambridge Bioscience, Cambridge, United Kingdom). The 1 kb and 100 bp RiboRuler DNA ladder (Thermo Scientific™, Waltham, United States) and the RiboRuler high-range RNA ladder (Thermo Scientific™) were used to estimate the size of nucleic acids (Figure 2.1). Each ladder was prepared following the recommendation of the manufacturer.

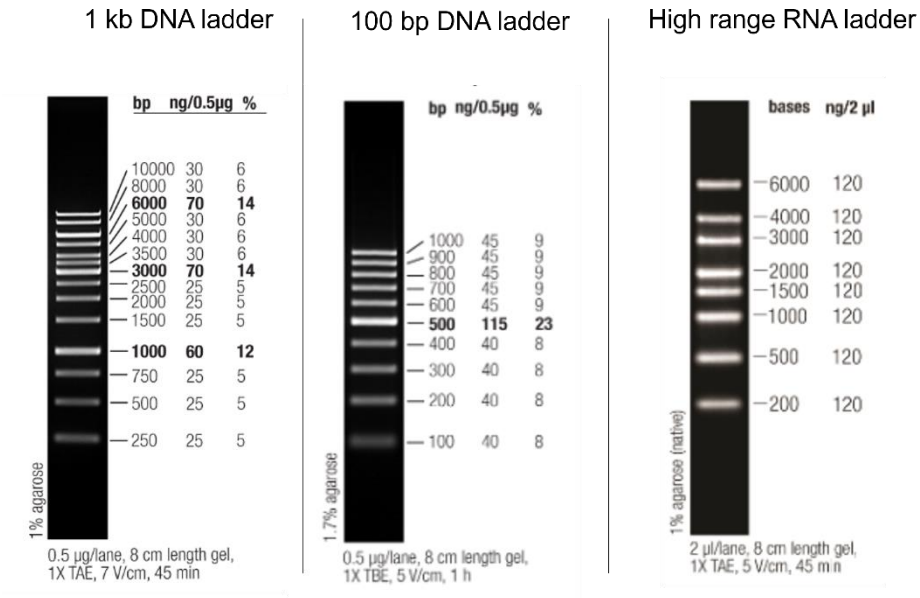

Figure 2.1. Acid nucleic ladders. DNA and RNA RiboRuler ladders (Thermo Scientific™) were used to determine the size of nucleic acids (Source: https://www.thermofisher.com).

2.1.5.7. Protein ladder

Proteins were visualised by SDS-PAGE and their sizes were estimated by comparison with a precision Plus Protein™ Biorad 250 kDa ladder (Biorad, Hercules, United States) (Figure 2.2).

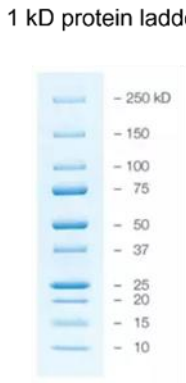

Figure 2.2. Protein ladder. Plus Protein™ 250 kDa ladder (Biorad) was used to determine the size of proteins by SDS-PAGE (Source: https://www.bio-rad.com).

2.1.5.8. Restriction and polymerisation enzyme

The restriction enzymes *Bam*HI (GGATCC) (FastDigest, Thermo Scientific™) and *Eco*RI (GAATTC) (FastDigest, Thermo Scientific™) were used to clone the putative promoter regions of the *psp* genes into the *lacZ*-fusion vector during the construction of *psp-lacZ* fusions, according to the manufacturer's instructions.

Phusion™ High-Fidelity DNA Polymerase (Thermo Scientific™) was used to amplify genomic DNA by PCR (section 2.2.9).

2.2. Methods

2.2.1. Bacterial inoculation and incubation

S. Enteritidis was propagated (two passages) in 9.8 mL of TSB (with ampicillin if necessary) for 24 h at 37 °C without shaking. The culture was centrifuged for 5 min at 7000 x rpm and the pellet was washed three times in 10 mL of tryptone salt (TS, 8.5 g/L NaCl, 1 g/L tryptone). The bacterial cells were diluted in TS to obtain the desired cell density. In a 96-well plate, 800 µL of the growth medium were added and the bacteria were inoculated at 2% v/v. The 96-well plates were incubated for 24 h at 30 °C in a water bath. TSB was used as a control.

2.2.2. Enumeration

After incubation (or just after inoculation to determine the number of inoculated cells), bacterial cells were enumerated using a rapid and cost-effective method, according to Baron et al. (2006). Briefly, in 96-well plates, 10-fold dilutions were prepared in TS in a final volume of 200 µL. In 24-well plates, a volume of 50 µL of each dilution was added with 400 µL of molten tryptone soy

agar (TSA, Sigma) at 50 ˚C. The plates were incubated for 24 h at 37 °C. Then, colonies were counted and the number of CFU per mL was determined and expressed in Log10 CFU/mL using the following formula:

$$CFU/mL = \frac{Number\ of\ CFU * Dilution\ factor * 1000}{Volume\ of\ sample\ plate\ (\mu L)}$$

2.2.3. Membrane permeabilisation

Membrane permeabilisation was determined spectroscopically using a method adapted from Lehrer et al. (1988) and Derde et al. (2013). As previously described for *E. coli* ML-35p, β-lactamase and β-galactosidase activities were measured to detect outer and inner membrane permeabilisation, respectively (Derde et al., 2013; Lehrer et al., 1988; Turner et al., 1998). For this experiment, *S*. Enteritidis (pBBC129) was used (Appendix 1) to allow production of β-galactosidase since *S*. Enteritidis (NCTC13349) does not carry *lacZ*.

After propagation as previously described (section 2.2.1), cells were centrifugated at 4000 rpm for 7 min at 15 °C, washed three times with TS and then the OD_{600nm} (Colourwave Colorimeter WPA CO7500, Biochrom, Holliston, United States) was adjusted to 0.35 in the same buffer.

In a 96-well plate, 30 mM of nitrocefin (Sigma) or 2.5 mM of ortho-nitrophenyl-β-galactopyranoside (ONPG) (Sigma), prepared in 10 mM phosphate buffer (pH 7.4), were added to the media. Then, the bacteria (prepared as described above) were added at 1/10 of the 300 µL final volume. Polymyxin B (50 µg/mL) (Sigma), a polypeptide antibiotic, was used as a positive control for the permeabilisation of the outer membrane. Melittin (15 µg/mL) (Sigma), an amphipathic cytotoxin derived from bee venom, was used as a positive control for the permeabilisation for the inner membrane. The plate was then incubated in

a Spectramax M2 spectrophotometer (Molecular Devices, San Jose, United States) at 30 °C for 5 h. Absorbance values were read at 490 and 405 nm to measure HP nitrocefin release (for outer membrane permeabilisation) and ONP release (for inner membrane permeabilisation), respectively. The maximal absorbance of the ONP is between 400 and 420 nm (Lehrer et al., 1988). According to Derde *et al*. (2013), the intersection of the baseline and the tangent identifies the lag time (delay between outer and inner membrane permeabilisation). Using the following formula: ΔA_{nm}/30min, the enzyme activity was expressed in milli-A_{nm}/min units (Figure 2.3).

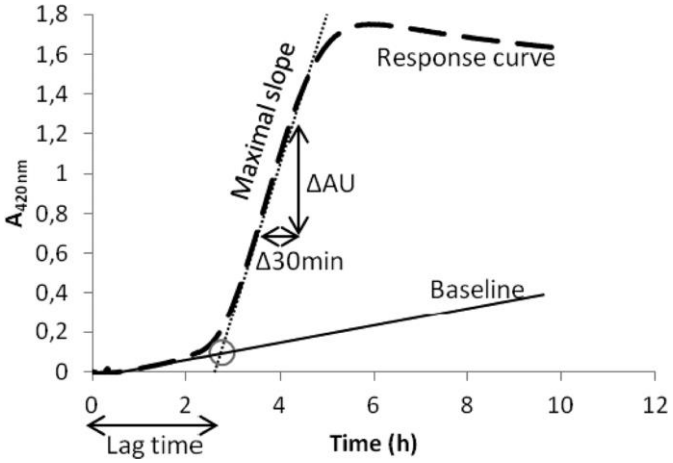

Figure 2.3. Example quantification of inner membrane permeabilisation (β-galactosidase activity) using maximal slope and lag time. ΔAU (measured at 420 nm) corresponds to the difference between the two absorbance points chosen for the calculation. (Taken from Derde et al., 2013).

2.2.4. Membrane depolarisation

A spectrofluorescent method adapted from Epand et al. (2010) was used to detect depolarisation of the inner membrane of *S*. Enteritidis. A change in membrane potential was detected using 3,3'-diopropylthiadicarbocyanine Iodide ($DiSC_3(5)$), a lipophilic potentiometric dye. Bacteria were grown as previously described (section 2.2.1) and then ten-fold diluted in TSB and incubated for 3.5 h at 37 °C. Bacteria were centrifuged (5,600 g for 7 min at 15 °C) and washed three

times in Hepes buffer (5 mM Hepes, 5 mM glucose, pH 7.2) before being resuspended in the same buffer to reach OD_{600nm} of 0.5. The cells were then charged using 20 µM of $DiSC_3(5)$ solution and 100 mM KCl, to balance cytoplasmic and external K^+ concentrations. The mix was incubated for 15 min at 37 °C in the dark to stabilise the dye signal. Then, cells charged with $DiSC_3(5)$ were diluted 10 times in various media and incubated for 10 min at 30 °C. Fluorescent measurements corresponding to the disruption of the membrane potential gradient ($\Delta\Psi$) were made using a spectrofluorometer (Molecular Devices Spectra, MAX Gemini XS) at an excitation wavelength of 622 nm and an emission wavelength of 670 nm. Results were expressed in Relative Fluorescent Units (RFU).

2.2.5. SDS-PAGE

SDS-PAGE was used to check the purity of two batches of OT powder (one provided by Sigma-Aldrich and the second by Liot industry (Pleumartin, France). Each sample was tested at the concentrations of 12.5 and 50 µM. Samples were diluted in Laemmli buffer 2X (Biorad) and then boiled for 3 min at 95 °C. A volume of 10 µL of each sample was loaded in a Mini-PROTEAN® TGFTM precast gel containing 4 to 20% acrylamide and run for 30 min at 200 V in 10X Tris/Glycine/SDS migration buffer (Biorad). The Precision Plus Protein™ Biorad 250 kDa ladder was loaded in the same gel. The proteins were then fixed with 20% of trichloroacetic acid (TCA) for 1 h in a rotating shaker. The gel was washed three times with distilled water for 5 min before being stained with Bio-Safe Coomassie Stain G250 (Biorad), overnight, under shaking. Finally, the gel was detained overnight in 20% ethanol and scanned using an ImageScanner III (GE Healthcare, Chicago, United States) system.

2.2.6. Chemically competent cells

2.2.6.1. *E. coli* TOP10

A single colony of *E. coli* TOP10 was inoculated in 3 mL of LB and incubated overnight at 37 °C and 250 rpm. One mL of overnight culture was inoculated in 100 mL of LB in a 250 mL Erlenmeyer flask which was incubated at 37 °C and 250 rpm until an OD_{600} of 0.5 was achieved. The culture was then placed on ice for 20 min and equally divided into two 45 mL Falcon tubes. Tubes were centrifugated for 10 min at 4 °C and 4000 rpm. The supernatants were discarded and the pellets were resuspended in 20 mL of ice-cold 0.1 M $CaCl_2$ (Fisher Scientific). The bacterial cultures were then incubated on ice for 30 min and centrifuged for 10 min at 4 °C, 4 000 rpm. The supernatants were discarded and the pellets were resuspended and combined in 4 mL of ice-cold 0.1 M $CaCl_2$ containing 15% glycerol. Finally, 200 µL volumes of the resulting competent cells were aliquoted into Eppendorf tubes and stored at -80 °C.

The required 200 µL aliquot were defrosted on ice prior to being used for transformation. Competent cells were incubated with 5 µL of ligation product or 1 µL of plasmid DNA for 30 min on ice. Cells were then subjected to a thermal shock to increase the permeability of the cell wall by first incubating for 45 sec at 42 °C using a water bath and then directly immersing the tubes in ice for 5 min. A 250 µL volume of SOC medium was added and the bacteria were incubated for 1 h at 37 °C in a rotary shaker for post-transformation induction of antibiotic resistance. After that, 100 µL of bacteria were spread on an LB plate containing the appropriate antibiotic and 40 µg/mL of X-Gal (5-Bromo-4-Chloro-3-Indolyl β-D-Galactopyranoside) (ThermoScientific™). Finally, plates were incubated for 24 h at 37 °C.

2.2.6.2. *S*. Enteritidis electrocompetent cells

A single colony was inoculated overnight in 5 mL of TSB at 37 °C and 250 rpm, and then 1 mL of this culture was combined with 10 mL of TSB in an 250 mL Erlenmeyer flask. The mixture was incubated at 37 °C and 250 rpm until the OD_{600} reached 0.6 and then the flask was heated at 50 °C for 25 min in a water bath (to heat-inactivate the host restriction systems). After 2 min on ice, the bacterial cells were centrifuged for 10 min at 4 °C and 4200 rpm, and the supernatant was discarded. The pellets were washed twice with 10 mL of ice-cold 10% glycerol and centrifuged for 10 min at 4200 rpm and 4 °C. A volume of 60 µL of ice-cold GYT (10% glycerol, 0.125% yeast extract, 0.25% tryptone) was used to resuspend the pellet. The electrocompetent cells were stored at -80°C.

2.2.7. Extraction and purification of nucleic acids

2.2.7.1. Plasmid miniprep

Transformants were incubated overnight in 15 mL Falcon tubes containing 3 mL of LB with ampicillin at 37 °C and 250 rpm. Then, plasmid DNA was extracted using a GeneJET Plasmid Miniprep Kit (Thermo Scientific™) using the entire 3 mL culture. The culture was centrifuged for 5 min at 10 000 rpm, the supernatant was discarded and the pellet was resuspended in 250 µL of resuspension solution (containing RNase A) by pipetting up and down. A 250 µL volume of Lysis solution was added to previous suspension which was then mixed thoroughly by inverting the tube several times until the solution became viscous. A 350 µL volume of neutralisation solution was added and the tube was mixed by inverting 4-6 times. The resultant ruptured cells were centrifuged for 5 min at 10 000 rpm to remove cell debris and precipitated chromosomal DNA. The supernatant was transferred to the GeneJET spin column, avoiding transfer of

the white precipitate. The column was centrifuged for 1 min at 10 000 rpm and the flow-through was discarded. The column was washed twice with 500 µL of wash solution (containing absolute ethanol) and was centrifuged for 1 min at 10 000 x rpm between each washing. Then, the empty column was centrifuged, to remove the residual wash solution, for a further 1 min at 10 000 rpm. The column was transferred into a fresh sterile Eppendorf tube and 50 µL of RNase/DNase-free water were added. The column was incubated for 3 min at room temperature and then centrifuged for 2 min at 10000 rpm. The size of the isolated plasmid DNA was checked by agarose gel electrophoresis (and restriction digest) and plasmid concentration was measured using a Denovix (DS-11 FX+, Wilmington, United States) before being stored at -20 °C.

2.2.7.2. Total DNA extraction

Bacteria were cultured overnight in 15 ml Falcon tubes containing 3 mL of TSB at 37 °C and 250 rpm to give up to $2x10^9$ bacterial cells. The culture was centrifugated for 10 min at 5000 rpm, the supernatant was discarded, and the pellet was used for DNA purification using a GeneJET Genomic DNA Purification Kit (Thermo Scientific™). The pellet was resuspended in 180 µL of digestion solution and 20 µL of Proteinase K, and was then mixed thoroughly by vortexing. The sample was incubated at 56 °C for 1 h in a rotary heater block until the cells were completely lysed (~30 min). Then, a 20 µL volume of RNase A was added and the solution was mixed by vortexing and incubated for 10 min at room temperature. A volume of 200 µL of Lysis Solution was added to the sample and mixed by vortexing until a homogeneous mixture was obtained. This step was followed by the addition of 400 µL of ethanol and the sample was again mixed by vortexing. The lysate was transferred to a GeneJET Genomic DNA Purification

Column which was then was centrifugated for 1 min at 10000 rpm. The column was washed with 500 µL of Wash Buffer I and then centrifuged for 1 min at 10000 rpm, and then washed a second time with 500 µL of Wash Buffer II and centrifuged for 3 min at 10000 rpm. The column was placed in a fresh sterile Eppendorf tube and 50 µL of RNase/DNase-free water were added to the centre of the column. The column was incubated for 3 min at room temperature and centrifugated 1 min at 10000 rpm to elute genomic DNA. Finally, the DNA concentration was measured using a Denovix and the integrity of the isolated gDNA was tested by agarose electrophoresis. The gDNA was stored at -20 °C.

2.2.7.3. Total RNA extraction

After overnight culture, *S*. Enteritidis was subcultured in TSB and incubated at 37 °C, without shaking, until an OD_{600} of 0.4–0.5 was reached. The culture was divided into 1 mL volumes which were centrifugated for 2 min at 5000 rpm. The supernatants were discarded, and the pellets were washed with 1 mL of SM and centrifugated once again for 2 min at 5000 rpm. Supernatants were removed and pellets were resuspended in different media (TSB, SM, SM with 10% EW, SM with 13 g/L or 1.3 g/L of OT at various iron saturation levels). Samples were incubated at 30 °C without shaking for 45 min. Then, samples were centrifugated from 2 min at 5000 rpm and the pellets were resuspended in 1 mL of RNAlater (25 mM EDTA, 25 mM sodium citrate, 70% w/v ammonium sulphate, pH 5.2) and incubated for 5 min at room temperature. The samples were then centrifugated for 5 min at 5000 rpm and total RNA was extracted using the RNeasy Mini Kit (Qiagen, Hilden, Germany). Supernatants were discarded and pellets were resuspended in 200 µL of TE buffer (10 mM Tris HCl, 1 mM EDTA, pH 8, Qiagen) containing 15 mg/mL of lysozyme (Thermo Scientific™) and 1 mg/mL of

proteinase K (Qiagen), and then the suspensions were incubated at room temperature for 10 min with vortexing every 2 min. Then, 700 µL of RLT buffer were added to the above mixture and the samples were centrifugated for 5 min at 5000 rpm before the addition of 500 µL of absolute ethanol. The lysate was transferred to a RNeasy Mini Spin column and centrifuged for 30 sec at 10000 rpm. The sample was then treated with 80 µL of DNase I solution (Qiagen) and incubated for 15 min at 30 °C. A volume of 350 µL of Buffer RW1 was added to the column which was incubated for 5 min at room temperature. Then, the column was centrifuged for 30 sec at 10000 rpm. The flow-through was discarded and the column was placed in a fresh collection tube. A volume of 500 µL of RPE Buffer was added and then sample was centrifuged for 30 sec at 10000 rpm to wash the column membrane. The flow-through was discarded and the column membrane was washed again with 500 µL of RPE Buffer and centrifuged for 2 min at 10000 rpm. The column was placed in a new Eppendorf tube and 50 µL of RNase/DNase-free water were added to the column. Then the sample was incubated for 3 min at room temperature and centrifuged for 3 min at 10000 rpm to elute the RNA.

2.2.7.3.1. TURBO DNA treatment

A mass of 10 µg of each RNA sample was treated using a TURBO DNA-free™ Kit (Invitrogen™, Waltham, United States) in a final volume of 50 µL. A volume of 0.1 µL of 10X Turbo DNase™ buffer and 1 µL of TURBO DNase™ Enzyme were added and RNase/DNase-free water was added to give a final volume of 50 µL. The mixture was incubated at 37 °C for 30 min. Then, 0.2 volumes of DNase Inactivation Reagent were added. Samples were incubated

for 5 min at room temperature and were then centrifugated for 1.5 min at 10000 rpm. The supernatant was transferred into a fresh tube and stored at -80 °C.

2.2.7.3.2. cDNA synthesis

After TURBO DNase treatment, the RNA samples were used as template to synthesize cDNA using a SuperScript™ VILO™ cDNA Synthesis Kit (Invitrogen™). For each sample, a total of 1 µg of RNA was mixed with 4 µL of 5X VILO™ Reaction Mix (containing random primers, dNTPs and $MgCl_2$), 1 µL of SuperScript™ Enzyme Mix (containing reverse transcriptase and RNase) and DEPC-Treated water (Invitrogen™) up to a final volume of 20 µL. Samples were then incubated in a PCR machine (Bio-Rad T100™, Biorad), for 10 min at 25 °C, 90 min at 42 °C and 5 min at 85 °C. The resulting cDNA samples were stored at -20 °C.

2.2.7.4. Determination of DNA and RNA concentration

DNA (genomic and plasmid) and RNA concentrations were measured using a Denovix DS-11 FX+ system. A volume of 1 µL of each DNA/RNA sample was used to determine concentration in ng/µL. Purity was assessed by measuring the A_{280}/A_{260} and A_{260}/A_{230} ratios. Pure DNA should have an A_{280}/A_{260} ratio of ~1.8 and pure RNA of ~2. The A_{260}/A_{230} ratio is an indicator of organic compound contamination and should be ~2.

2.2.8. Quantitative PCR

Quantitative PCR (qPCR) was used to study the expression of *S*. Enteritidis genes after egg white or OT exposure. qRT-PCR is a very sensitive and specific method detecting the accumulation of fluorescent signals. The first step was to isolate total RNA from relevant strains following growth and reverse

transcribe the RNA into cDNA (RT reaction). Then a fluorescent probe (SYBR®-green) was incorporated into a PCR mix which binds to double-stranded DNA. Thus, at each PCR cycle, the amplification of PCR product (amplicon) was detected by fluorescence. The number of cycles necessary to amplify the target to a detectable level is called Ct (cycle threshold) and was used to determine the fold change in expression. Thus, the initial amount of target is correlated with the Ct values, the lower the Ct value, the higher the level of transcript in the original sample (Arya et al., 2005). Then, relative quantification corresponding to the change of expression of the target with respect to the selected housekeeping genes was determined using the $2^{-\Delta\Delta Ct}$ method (Livak & Schmittgen, 2001).

Firstly, gDNA was used to generate standard curves for each pair of primers and then with cDNA for each test condition. The work area and pipettes were decontaminated with RNase AWAY™ (Thermo Scientific™) and sterile filter tips were used during all experiments. For standard curves, 10-fold series dilutions (until 10^{-6}) of gDNA or cDNA were performed with a starting concentration of 10 ng or 20 ng, respectively. For the Ct value comparisons, a concentration of 2 ng of cDNA was used. In 96-well semi-skirted plates (Alpha Laboratories, Eastleigh, United Kingdom), a volume of 1 µL of gDNA or cDNA was added in 4 µL of reaction mix (0.5 mM of each primer and RNase/DNase free H_2O). Then, 5 µL of PowerTrack™ SYBR Green Master Mix were added to each well and the plate was sealed using an adhesive seal sheet (Thermo Scientific™). The plate was then centrifuged for 2 min at 800 rpm and placed in a StepOne™ Real-Time PCR system (Applied Biosystem™, Waltham, United States). The qPCR was run for ~2.5 h following the program described in Table 2.6.

Table 2.6. qRT-PCR program

Step	Temperature (°C)	Time	Cycle
Enzyme activation	95	5 min	1
Denaturation	95	30 sec	
Annealing	60	1 min	40
Extension	72	90 sec	

Step	Ramp rate	Temperature (°C)	Time
1	1.99°C/sec	95	15 sec
2	1.77°C/sec	60	1 min
3 (dissociation)	0.075°C/sec	95	15 sec

2.2.9. Polymerase Chain Reaction (PCR)

In order to amplify specific DNA regions, PCR was performed using a PCR thermocycler (Bio-Rad T100™, Biorad). All the primers were ordered from Sigma and resuspended with the appropriate volume of RNase/DNase-free water, according to the manufacturer's instructions, to obtain a 100 µM stock solution. Then, the primers were further diluted to 10 µM. In a 0.2 mL Eppendorf tube, 0.5 µL of Phusion™ High-Fidelity DNA Polymerase was mixed with 2.5 µL of each forward and reverse primer (0.5 µM), 10 µL of the 5X Phusion™ HF buffer, 1 µL of dNTP (0.2 mM each), 1 µL of DNA template (~100 ng of genomic DNA) and DNase-free water up to 50 µL. The PCR reaction was performed following the protocol of the manufacturer and as described below (Table 2.7).

Table 2.7. PCR program used with Phusion™ High-Fidelity DNA Polymerase

Step	Temperature (°C)	Time	Cycle
Initial denaturation	98	30 sec	1
Denaturation	98	8 sec	35
Annealing	Tm	20 sec	
Extension	72	15-30 sec/kb	
Final extension	72	5 min	1
Final step	4	Hold	

2.2.10. Agarose gel electrophoresis

DNA and RNA were examined using agarose gel electrophoresis. The percentage of agarose was defined according to the size of the DNA/RNA being analysed. The smaller the molecule the higher the percentage. The gel was prepared by boiling the agarose (Meridian Bioscience®, Cincinnati, United States) in 50 mL solution of 0.5X TBE (40 mM Tris-HCl, 45 mM boric acid, 1 mM EDTA pH 8) using a microwave oven. Once the gel had cooled to ~50 °C, 1X of Gel Red Nucleic Acid gel stain (10,000X in water) was added to allow visualisation of nucleic acids. The DNA samples were diluted in a 6X loading dye and the RNA samples in a 2X loading dye (ThermoScientific™) to give a final concentration of 1X. Due to the structure of the RNA, the preparation of the samples differs from that of the DNA. An additional step was necessary and consisted of heating for 10 min at 70 °C. Then, the electrophoresis was performed for 1 h at 80 V. DNA or RNA bands were visualised and recorded using a G-BOX UV transilluminator (Syngene, Cambridge, United-Kingdom).

2.2.11. Purification of PCR products

After DNA amplification, PCR products were purified using the GeneJET PCR purification kit (Thermo Scientific™). A 1:1 volume of binding buffer was added on the PCR product and mixed by vortexing. An optional step was performed by adding 1:2 volume of absolute isopropanol to the mixture above and mixing by vortexing. This step was included when the size of the DNA fragment amplified by PCR was < 500 bp. The PCR solution was then transferred (up to 800 µL) to the GeneJET purification column which was centrifuged for 1 min at 10000 rpm. The flow-through was discarded and 700 µL of wash buffer were added. Another centrifugation for 1 min at 10000 rpm was performed, and the supernatant was discarded. To remove the residual wash buffer on the column, one more centrifugation for 1 min at 10000 rpm was completed. The column was then transferred into a fresh 1.5 mL Eppendorf tube. A volume of 30 µL of RNase/DNase-free water was added to the column which was incubated for 3 min at room temperature. Then, the purified PCR product was eluted by centrifugation for 1 min at 10000 rpm. The concentration of DNA was measured using a Denovix and then the samples were stored at -20 °C. The purity of the purified PCR product was confirmed by agarose gel electrophoresis.

2.2.12. Double digestion of DNA

One of the cloning steps consisted of digesting DNA and plasmids with restriction enzymes in order to insert the suitably-digested DNA fragment into the plasmid. In this study, a double digestion method using *Eco*RI and *Bam*HI was used. A volume of 2 µL of genomic or plasmid DNA (~ 100 ng/µL) was digested for 1 h at 37 °C, in a 1.5 mL Eppendorf tube containing 2 µL of 10X Green FastDigest buffer, 1 µL of each restriction enzyme, and DNase-free water up to

20 µL. The satisfactory digestion of DNA was verified by performing an agarose gel electrophoresis. Agarose gel bands were then extracted and purified.

2.2.13. Agarose gel extraction and purification

After digestion and agarose gel electrophoresis, PCR-amplified or plasmid DNA was purified using a GeneJET Gel Extraction Kit (Thermo Scientific™). According to the manufacturer, the required band was removed from the gel using a sterile scalpel and placed into a 1.5 mL Eppendorf tube before being weighed. Then, 100 µL of Binding Buffer per 100 mg of gel were added and the mixture was heated at 55 °C to allow melting of the gel. A volume (equivalent to the gel volume) of 100% isopropanol was added if the size of the DNA fragment was lower than 500 bp. After vortexing, up to 800 µL of the mixture was applied to a GeneJET purification column which was then centrifuged for 1 min at 10000 rpm. The flow-through was discarded and the column was washed with 700 µL of Wash Buffer before being centrifuged for 1 min at 10000 rpm. The column was then again centrifuged for 1 min at 10000 rpm to remove residual Wash Buffer. The column was placed onto a fresh 1.5 mL Eppendorf tube for the final step. Thus, 30 µL of DNase-free water were added to the column which was incubated for 3 min at room temperature. DNA was then eluted for 2 min at 10000 rpm. The concentration and purity of the DNA were measured using a Denovix DS-11 FX+.

2.2.14. Ligation of DNA insert into cloning vector

Once digested and purified, PCR products were ligated into the cloning vector. According to the manufacturer, a ratio of 3:1 (insert:vector, with vector at ~100 ng/reaction) was mixed with 4 µL of 5X Ligase Reaction Buffer, 1 µL of T4

DNA Ligase and DNase-free water up to 20 µL. The reaction mixture was incubated for 5 min at room temperature and 5 µL were used for transformation into *E. coli* TOP10 competent cells.

2.2.15. Electroporation

Electroporation was used to introduce plasmids carrying *psp-lacZ* fusions into *S*. Enteritidis electrocompetent cells. A volume of 2 µL of plasmid DNA (~100 ng/µL) was added to 40 µL of *S*. Enteritidis electrocompetent cells, previously thawed. The mixture was transferred to a pre-chilled cuvette (Sigma) and placed in the Micro Pulser II (Biorad). The electroporation took place at 25 µF, 200 Ohms and 1.8 kV for 4 msec pressing the two red bottoms at the same time. A volume of 1 mL of pre-warmed SOC medium was added immediately and the entire reaction was transferred to an Eppendorf tube which was incubated for 1 h at 37 °C and 250 rpm. A 100 µl volume of the electrotransformed-bacterial cells was then spread onto LB agar plates containing ampicillin and X-Gal. The remaining transformation mix was then centrifuged and 700-800 µl of supernatant was removed. The pellet was resuspended in the residual supernatant (100-200 µl) and spread onto a second plate. The plates were incubated for 24 h at 37 °C and the transformants were selected using blue/white screening.

2.2.16. β-Galactosidase assay

A single colony was inoculated into 3 mL of TBS (containing 100 µg/mL of ampicillin) in a 15 mL Falcon tube which was then cultured overnight at 37 °C. A volume of 650 µL of the overnight culture was inoculated into 65 mL of TSB in a 250 mL Erlenmeyer flask which was incubated at 37 °C until an OD_{600} of 0.5 was achieved. The culture was then divided into Falcon tubes which were centrifuged

for 4 min at 4200 rpm at 4 °C. The pellets were washed with the same volume of SM and centrifuged once again for 4 min at 4200 rpm at 4 °C. The pellets were then resuspended the same volume of the required test medium (TSB, TSB with 100 µM carbonyl cyanide m-chlorophenyl hydrazone (CCCP), SM, SM with 10% EW, 13 g/L or 1.3 g/L of OT at various iron-saturation levels) and then incubation was continued at 30 °C for 7 or 45 min, or 6 or 12 h. Following incubation, 1 mL of each culture were immediately centrifuged for 2 min at 10000 rpm, the flow-through was discarded and the pellets were stored at – 80 °C. In the meantime, the growth of S. Enteritidis was measured in a microplate reader Spectra Max 190® (Molecular Devices) at 30 °C and the OD was read every 30 min at 600 nm. The previously frozen pellets were lysed using pre-warmed B-PER™ bacterial protein extraction reagent (Thermo Scientific™). A volume of 50 µL of B-PER™ was used to resuspend the pellets and then the cells were incubated for 15 min at room temperature, 250 rpm. The β-galactosidase assay was conducted according to Miller (1972), in a 96-well plate with 4 µL of lysed bacterial cells, 16 µL of 1X phosphate buffer (PBS, 10 mM Na_2HPO_4, 1.8 mM KH_2PO_4, 2.7 mM HCl, 137 mM NaCl), and 180 µL of Z-buffer (60 mM Na_2HPO_4, 40 mM $NaH_2PO_4.2H_2O$, 10 mM KCl, 1 mM $MgSO_4$, 1.5 mM ONPG, 5 mM DTT) in each well, in triplicate. A control containing PBS and Z-buffer was performed simultaneously. The change in absorbance was measured kinetically at 420 nm every 2 min for 1 h in a Spectra MAX 340 pc (Molecular devices) and the β-galactosidase activities were expressed in nmol ONPG/min/OD_{600} unit using the following formula:

$$Vmax * \frac{Total\ volume\ of\ cells}{Volume\ of\ cells\ used} * \frac{1}{OD600nm\ at\ each\ time\ point} * nmol\ of\ ONPG.$$

2.3. Statistical tests

Average and standard deviations were calculated using Excel software. One-way ANOVA followed by Tukey contrast tests and Student's t-test were performed using R studio (version 1.4.1106).

Chapter 3. Impact of the iron-chelating activity of ovotransferrin on *S.* Enteritidis growth under egg-white conditions

3.1. Introduction

Studies on the antimicrobial properties of EW clearly demonstrate that EW imposes iron restriction on bacteria due to the presence of OT; such an effect is also seen for *S*. Enteritidis despite its considerable capacity for EW resistance. In cases where bacteria manage to persist in EW, subsequent addition of iron enables rapid growth (Baron et al., 1997; Garibaldi, 1960; Lock & Board, 1992). The iron naturally present in EW is likely to be almost entirely bound to OT. Upon exposure to EW, *S*. Enteritidis up-regulates genes encoding ferrous and ferric iron acquisition systems, including the genes specifying siderophore production, secretion, uptake and utilisation (Baron et al., 2017; Huang et al., 2019; Qin et al., 2019). While it is generally accepted that production of siderophores is important for survival in EW (Kang et al., 2006), this production is not sufficient to support growth without addition of iron (Garibaldi, 1970b); this observation raises several questions. Are siderophores produced in EW, and does such production enable acquisition of iron from OT? If siderophores are produced in EW, why do they not allow growth in EW? Is this because they are produced in insufficient quantity? Furthermore, although saturation of OT with iron relieves bacterial growth inhibition, it is unclear what minimal degree of saturation is required for relief of OT-mediated growth inhibition in EW and what impact the availability of carbonate (and other synergist anions required for iron-binding by OT) has upon this. It is also unclear whether the physicochemical parameters of EW (such as pH or temperature) contribute to the production of siderophores and/or to their ability to wrest iron from OT.

In this chapter, the level of iron saturation required for relief of *S*. Enteritidis growth under EW conditions was studied, as well as the impact of the deficiency

of siderophore production. Finally, the ability of siderophores to support the acquisition of iron was also studied on *S*. Enteritidis growth under EW conditions.

3.2. Choice of ovotransferrin

In order to determine which protein is most suitable for this study, two batches of OT were tested. The first was purchased from Sigma and the second was supplied by Liot. It is important to employ OT at high purity and, in particular, exempt from other antimicrobial proteins that might interfere with the results obtained. SDS-PAGE was performed with each batch of OT, at two different amounts (12.5 and 50 µg) (Figure 3.1; section 2.2.5). A major band between 75 and 50 kDa was observed, corresponding to OT (77.77 kDa) in for both batches. Other more minor bands were also present on the gel in both cases. It is difficult to determine with exactitude the identity of the other bands, but it is possible to speculate. The bands around 150 kDa (in both batches) could correspond to ovomucin whose size can vary between 150 and 200 kDa. Ovomucin is responsible for the viscosity of EW and does not have any known antimicrobial activity that may interfere with the results of this study (Robinson & Monsey, 1972). Several EW proteins have a size lower than 50 kDa such as ovalbumin (~45 kDa), but also antimicrobial proteins (ovoinhibitor at ~49.4 kDa, tenp at ~47.4 kDa), and ovalbumin-related protein Y (~43 kDa). One band at around 15 kDa is present only in the Liot batch, corresponding potentially to lysozyme (~14.3 kDa).

Results suggest that OT from Liot may be contaminated with lysozyme whose hydrolysis activity is well-known (Callewaert & Michiels, 2010; Derde et al., 2013). It has been shown that the hen EW lysozyme is also able to

permeabilise the outer and the inner membrane of *E*. coli at 37 °C (Derde et al., 2013).

The OT from Sigma appears to be purer than that from Liot. Indeed, lysozyme is not detectable by SDS-PAGE for the protein from Sigma whereas a band is clearly visible for the protein from Liot. It was therefore decided to use OT supplied by Sigma for all the experiments presented in this study. Moreover, published research on OT routinely use OT from Sigma (Aguilera et al., 2003; Baron et al., 1997; Chart et al., 1986; Chart & Rowe, 1993).

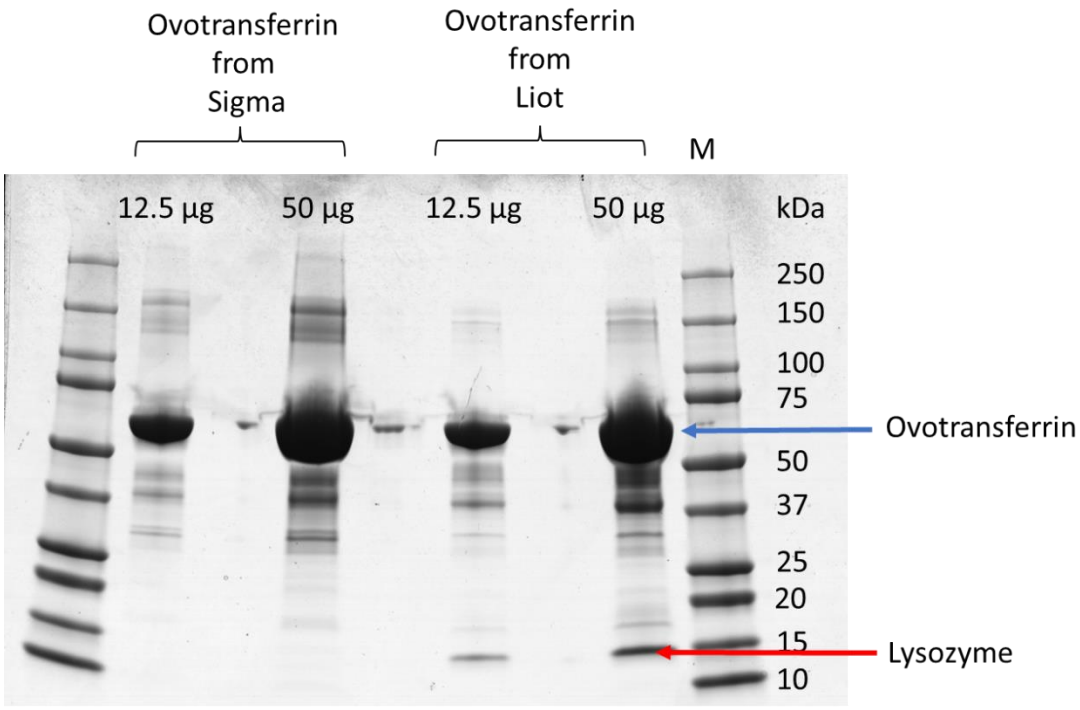

Figure 3.1. Profile of the purity of OT. The protein profiles of two batches of OT (Sigma and Liot) were determined by SDS-PAGE using a 15% acrylamide gel and staining with Coomassie blue. For each protein, two quantities were loaded (12.5 and 50 µg). To determine the size of each band, the Plus Protein™ Biorad 250 kDa (M) ladder was loaded in the outer and inner tracks. The blue and red arrows indicate the bands corresponding to ovotransferrin and lysozyme, respectively**.**

3.3. Ovotransferrin is responsible for the antimicrobial activity of egg white

Due to the presence of two high-affinity iron-binding sites, OT possesses an iron-chelating activity (Baron et al., 1997; Garibaldi, 1960; Lock & Board, 1992). This activity is known to be responsible for the strong antimicrobial activity of EW since all the iron present in EW is bound to the protein (Legros et al., 2021, for a review).

To confirm the involvement of OT in the antimicrobial activity of EW, the growth of *S*. Enteritidis was monitored under different conditions (EWF, EW, EWF with 10% EW, EWF with 1.3 g/L of OT) for 24 h at 30 °C (Figure 3.2; sections 2.2.1 and 2.2.2). In EWF (i.e. EW without <10 kDa molecules), *S*. Enteritidis was able to grow (i.e. cell number increased by 3.47 $\log_{10}$ CFU/mL after 24 h). In EW and in EWF with 10% EW, a significant limitation of bacterial growth was observed (i.e. cell number increased by only 0.25 and 0.57 $\log_{10}$ CFU/mL after 24 h, respectively). Furthermore, no significant difference was observed between growth in EW and in EWF with 10% of EW (p-value >0.05). This result confirms the antimicrobial activity of EW and supports the suggestion that >10 kDa EW proteins are responsible for this activity (Baron et al., 1997; Garibaldi, 1970b; Lock & Board, 1992; Shade & Caroline, 1944). Furthermore, the results show that the same effect is provided by EW or by 10% EW, confirming previous results obtained (Baron et al., 1997) where a similar decrease of *S*. Enteritidis growth at 30 °C was observed after exposure to whole EW or 10% EW (decrease of 3 $\log_{10}$ CFU/mL) .

To confirm the role of OT in the above EW-induced growth limitation, *S*. Enteritidis was propagated in EWF with 1.3 g/L OT (10% of the OT

concentration found in EW) (Figure 3.2). The growth of *S*. Enteritidis in EWF with 1.3 g/L of OT was restricted (i.e. cell number increased by just 1 log_{10} CFU/mL over 24 h), with respect to that in EWF. However, there was a significantly lower growth for *S*. Enteritidis in EW or in EWF with 10% EW, compared with that in EWF with 1.3 g/L of OT (p-value < 0.05). Thus, these results confirm that OT is the main EW factor involved in the antimicrobial activity of EW but also suggest that other EW factors of >10 kDa contribute, although to a lesser degree than OT. These findings are in accordance with those Baron et al. (1997) who demonstrated that OT is the only EW protein affecting *S.* Enteritidis growth in EW at 30 °C. Thus, they observed a decrease of *S*. Enteritidis growth in EWF with 10% EW (i.e. cell number increased by 1.5 log_{10} CFU/mL) and in EWF with 1.3 g/L of OT (i.e. cell number increased by 2.5 log_{10} CFU/mL), but observed no difference in growth between EWF and EWF with other EW proteins (i.e. cell number increased by more than 5 log_{10} CFU/mL).

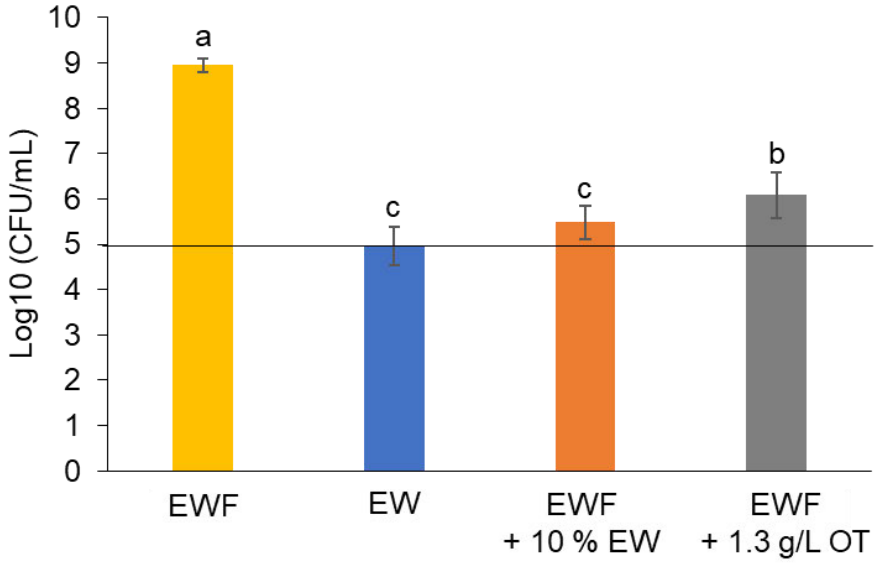

Figure 3.2. Impact of EW and OT on *S*. Enteritidis growth. The growth of *S*. Enteritidis NCTC13349 inoculated at 5 log_{10} CFU/mL (black line) was measured after 24 h incubation at 30 °C in (i) EWF, (ii) EW, (iii) EWF with 10% EW and (iv) EWF with 1.3 g/L OT. Error bars indicate standard deviations from the mean derived from three biological experiments, with three technical

replicates. Significant differences between each condition were assessed using a one-way ANOVA test followed by a Tukey test with R software (version 1.4.1106). Significantly different groups are identified by letters, indicating a p-value <0.05.

3.4. The iron-chelating activity of ovotransferrin mediates the antimicrobial activity of egg white on *S*. Enteritidis growth

Several studies have shown that the addition of iron counteracts the bacterial growth inhibition observed in EW for many microorganisms (Baron et al., 1997; Garibaldi, 1960; Lock & Board, 1992; Shade & Caroline, 1944). However, the level of OT saturation needed to promote bacterial growth remains unclear.

To explore this further, *S*. Enteritidis was incubated in EW, EWF with 10% EW and EWF with 1.3 g/L OT (at 30 °C for 24 h). Under these conditions, OT saturation was achieved by adding an a range of concentrations of iron citrate (section 2.1.5.3). In EW, the level of iron varies between 3.6 to 18 µM (Sauveur, 1988; Nys and Sauveur, 2004; Ciqual, 2021, Stadelman and Cotteril, 2017, Nau et al., 2010), leading to a theoretical OT saturation between 1.07 and 5.4%. The level of saturation tested in these experiments was 0 to 110%, and up to 300% of the theoretical saturation level for OT (Figure 3.3).

For 0 to 75% OT saturation, the growth of *S*. Enteritidis remained limited in EW (Figure 3.3A) (i.e. cell number either remained unchanged or increased by just 0.25 $\log_{10}$ CFU/mL in 24 h). However, a partial but significant relief of *S*. Enteritidis growth inhibition was observed when OT in EW was saturated at 100 or 110% by iron (i.e. cell number increased by 2 $\log_{10}$ CFU/mL after 24 h) (Figure 3.3A). At 24 h of incubation in EWF with 10% EW, the growth of *S*. Enteritidis also remained limited when low levels of iron saturation were applied (i.e. cell number increased by 0.85 and 0.35 $\log_{10}$ CFU/mL for 0 and 25% OT saturation,

respectively) (Figure 3.3B). However, a clear relief of growth inhibition was observed at 50-110% OT saturation by iron, with higher growth achieved as the degree of iron saturation was increased from 50 to 110% (from 1.03 to 2.70 $\log_{10}$ CFU/mL at 50 and 110% OT saturation, respectively) (Figure 3.3B). In EWF with 1.3 g/L of OT, similar results were observed to those observed with EWF with 10% of EW: a limited growth at 0 and 25% iron saturation (i.e. cell number increased by 1.13 and 1.39 $\log_{10}$ CFU/mL in 24 h, respectively) followed by a partial and progressive growth enhancement as saturation levels increased from 50 to 110% (i.e. cell number increased by 1.88, 2.38, 3.04 and 3 $\log_{10}$ CFU/mL at 50-, 75-, 100- and 110%, respectively) (Figure 3.3C).

The reduced growth in iron-saturated EW with respect to EWF with iron-saturated 10% EW or with iron-saturated OT at 1.3 g/L may be related to lower iron availability in EW, due to its high viscosity, or to antimicrobial activity of other EW proteins. To determine if this problem can be overcome by increasing iron availability, the concentration of iron citrate was increased to 300% OT saturation (Figure 3.3D-F). Increasing the iron saturation of OT from 110 to 300% significantly relieved the inhibition of S. Enteritidis growth in EW (Figure 3.3D), EWF with 10% EW (Figure 3.3E) and EWF with 1.3 g/L OT (Figure 3.3F) (enhancement of ~2.5, ~2.5, and of ~3.5 $\log_{10}$ CFU/mL in EW, EWF with 10% EW and EWF with OT 1.3 g/L, respectively). Nevertheless, the iron-saturated growth of *S*. Enteritidis remained lower in EW than in EWF with 10% EW or in EWF with 1.3 g/L OT.

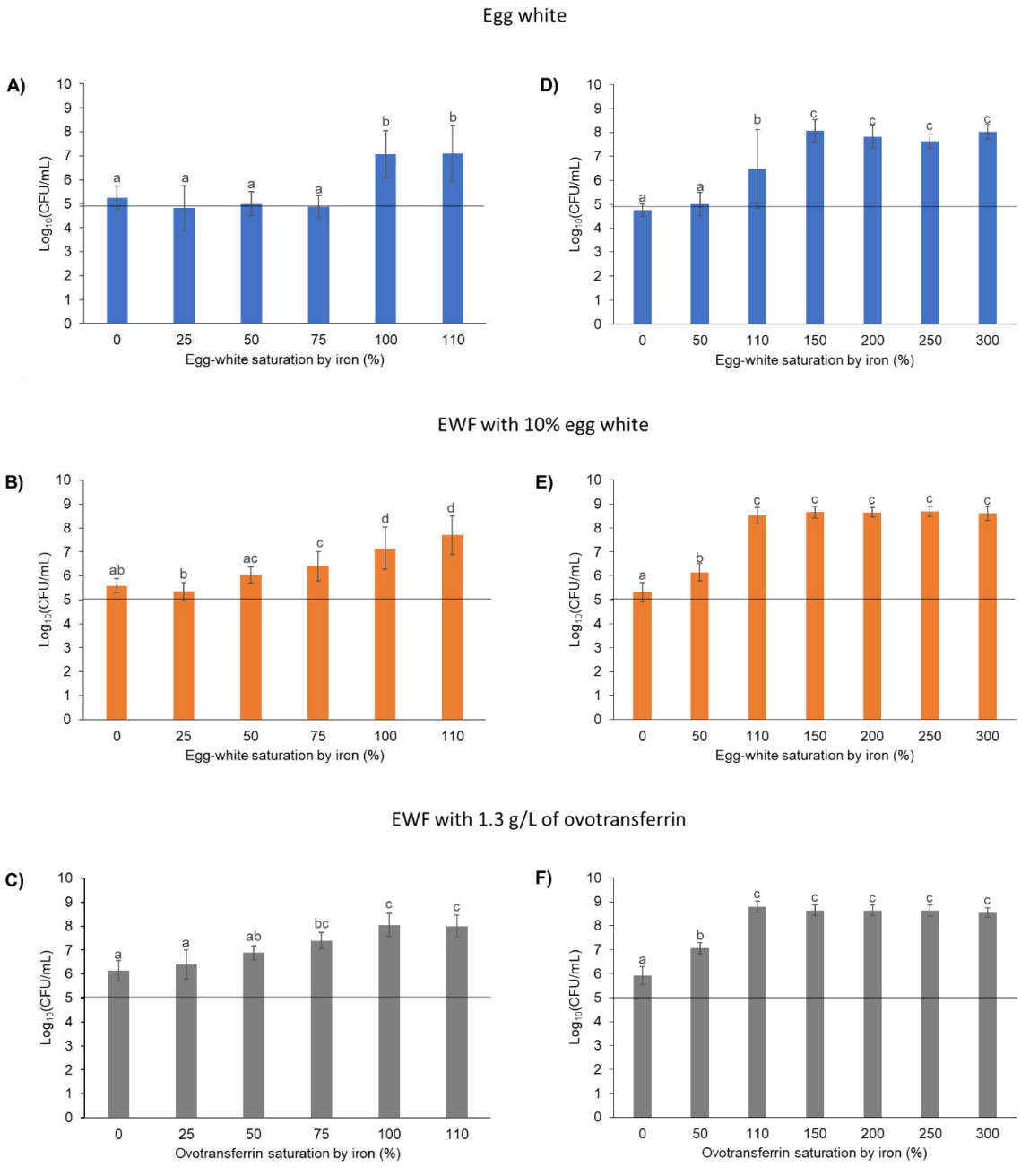

Figure 3.3. Effect of increasing iron saturation levels of OT on the growth of *S.* Enteritidis. The growth of *S*. Enteritidis NCTC13349 inoculated at 5 $\log_{10}$ CFU/mL (black line) was measured after 24 h incubation at 30 °C in EW (A and D), EWF with 10% EW (B and E) and EWF with 1.3 g/L OT (C and F). Iron citrate (33.4 mM) was added to obtain ovotransferrin-iron saturation levels from 0 to 110% (A to C) and up to 300% (D to F). Error bars indicate standard deviations from the mean derived from three biological experiments, with three technical replicates. Significant differences between each condition were assessed using a one-way ANOVA test followed by a Tukey test with R software (version 1.4.1106). Significantly different groups are identified by letters, with a p-value <0.05.

This experiment confirms that the iron-chelating activity of OT is responsible for the antimicrobial properties of EW against *S*. Enteritidis at 30 °C. This result is in accordance with the literature. Indeed, Baron et al. (1997) showed that 110% iron saturation of OT enhanced *S*. Enteritidis growth by 4 log_{10} CFU/mL after 24 h at 30 °C. A similar observation was made by Kang et al. (2006) for *S*. Enteritidis after 24 h growth at 37 °C where 110% OT iron-saturation resulted in a growth enhancement of 5 log_{10} CFU/mL in EW. Additionally, the results indicate a capacity for *S*. Enteritidis to obtain iron directly bound to OT. This observation could be explained by the production of siderophores by *S*. Enteritidis. Indeed, genes involved in siderophore biosynthesis, uptake and utilisation are strongly induced by *S*. Enteritidis after 45 min exposure to EW (1.59 to 7.81-fold) (Baron et al., 2017). However, the growth reduction in EW appears to be only partly reversed by iron since the growth achieved is less than that seen in iron-saturated EWF with 10% EW or with 1.3 g/L OT. This suggests that iron-saturation of 100% EW does not fully reverse the antibacterial effect of EW, possibly due to the high viscosity of EW and/or a lower antimicrobial activity of OT at high concentration, in the presence of other EW molecules, limiting access to Fe-OT.

3.5. Bacterial culture under shaking do not impact *S*. Enteritidis growth in egg white

S. Enteritidis iron restriction appears stronger in EW compared to EWF with 10% EW or EWF with 1.3 g/L OT. Indeed, *S*. Enteritidis growth remains limited once EW is saturated by 0 to 75% (section 3.4). A key property of EW is its viscosity. EW has a viscosity of 5 $mPa.s^{-1}$ at 20 °C and a shear rate of 400 s^{-1}, which corresponds to a highly viscous medium (Lang & Rha, 1982). As described in section 2.1.4.2, EW used in the research described above was

homogenised to decrease its viscosity and facilitate accurate volume dispensing. However, even after homogenisation the viscosity remained higher for EW than for EWF with 10% EW or for EWF with 1.3 g/L OT (Appendix 2). Additionally, during the growth period, no shaking was applied to the bacterial culture. This combination of high viscosity and static incubation would be expected to limit diffusion within the growth medium and the ability of individual bacteria cells to move within the medium. Thus, in an attempt to overcome any lack of mixing caused by the higher viscosity of EW, the impact of the shaking was studied on *S*. Enteritidis growth in EW with increasing concentrations of iron citrate. For this purpose, the 96-well plates were incubated either on a rotary shaker or in a water bath without shaking for 24 h at 30 °C (section 2.2.1 and 2.2.2).

No significant differences were observed with or without shaking (Figure 3.4) whatever the level of EW saturation. Indeed, at 0% of saturation, *S*. Enteritidis growth was limited (i.e. cell number increased by 0.57 and 0.72 $\log_{10}$ CFU/mL in 24 h with and without shaking, respectively). The same result was observed at 25% (i.e. cell number increased by 0.53 and 0.53 $\log_{10}$ CFU/mL in 24 h with and without shaking, respectively) and 50% of saturation (i.e. cell number increased by 0.55 and 0.76 $\log_{10}$ CFU/mL in 24 h with and without shaking, respectively). At 110% saturation, the growth of *S*. Enteritidis was enhanced but remained similar between both culture conditions (i.e. cell number increased by 2.60 and 2.71 $\log_{10}$ CFU/mL in 24 h with and without shaking, respectively).

These results indicate that the agitation of EW during *S*. Enteritidis culture has no impact on growth. They also suggest that if the viscosity of EW is

responsible for the higher relative growth reduction observed under iron saturation then the agitation, as applied here, has failed to reverse this effect.

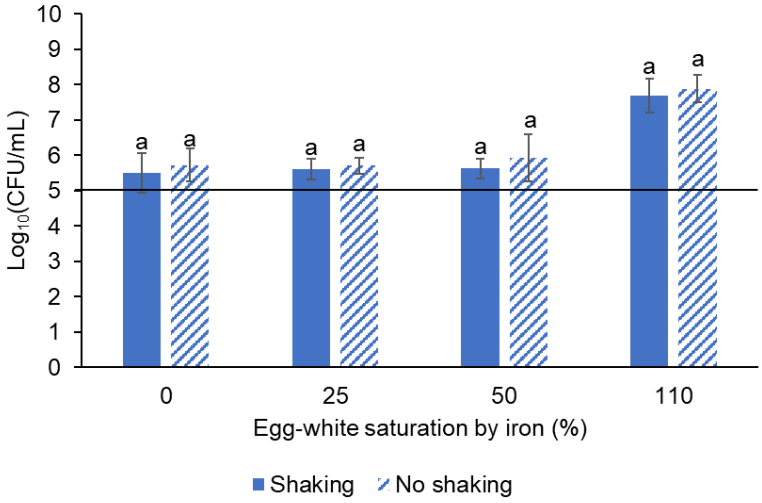

Figure 3.4. Impact of culture shaking on the ability of *S*. Enteritidis to overcome the enhanced growth restriction of EW under iron-saturated conditions. The growth of *S*. Enteritidis NCTC13349 inoculated at a 5 $\log_{10}$ CFU/mL concentration (black line) was measured after 24 h incubation at 30 °C in EW with or without shaking. Iron citrate (33.4 mM) was added to obtain OT-iron saturation levels of 0, 25, 50 and 110%. Error bars indicate standard deviations from the mean derived from three biological experiments, with three technical replicates. Significant differences between each condition were assessed using Student t-test with R software (version 1.4.1106). Significantly different groups are identified by letters, with a p-value <0.05.

3.6. Siderophore production by *S*. Enteritidis counteracts the iron restriction imposed by ovotransferrin, but only under conditions of 100-110% iron-saturation

Due to the presence of OT, EW is known to be an iron-deficient medium for bacterial growth. However, iron is an essential element for bacterial and in the case of iron deficiency, bacteria receive signals via the de-activation of the Fur regulator that leads to the synthesis of molecules called siderophores that can capture ferric iron from the environment (Andrews et al., 2003 for a review). Ent and its glucosylated derivate, Sal, are known to be secreted by *S*. Enteritidis

under iron restriction (Pollack et al., 1970). In the natural context of EW, it remains unclear whether *S*. Enteritidis releases siderophores to counteract the iron deficiency imposed by OT. Thus, in order to explore this questions, an experiment was performed to determine whether *S*. Enteritidis incubated in EW can produce siderophores to obtain either free iron or iron directly bound to OT.

The growth of *S*. Enteritis NCTC13349 (WT) was compared to an isogenic Δ*entB* strain unable to produce Ent, and therefore, its glycosylated derivate Sal (Julien et al., 2020). The growth of each strain was determined by enumeration (section 2.2.2) after incubation for 24 h at 30 °C in EW, EWF with 10% EW or EWF with 1.3 g/L OT, with various levels of iron saturation (from 0 to 110%) achieved using iron citrate (Figure 3.5; section 2.2.1). In EW, a relief of the inhibition of growth of the WT (i.e. cell number increased by 2 $\log_{10}$ CFU/mL in 24 h) was observed when EW was iron-saturated at 100 and 110%. However, under the same conditions (100 and 110% OT saturation in EW), the growth of the Δ*entB* remained limited (i.e. cell number increased by 0.4 $\log_{10}$ CFU/mL in 24 h) (Figure 3.5A). Thus, the ability to produce siderophores enhanced the growth of *S*. Enteritidis in EW saturated for iron.

On the other hand, in the low viscosity medium (EWF with 10% EW), no significant difference between the growth of the WT and the Δ*entB* strain was detected. A partial and progressive lifting of the growth inhibition was observed from 50 to 110% iron saturation (cell number increased by 2.7 and 2.3 $\log_{10}$ CFU/mL in 24 h at 110% for the WT and Δ*entB* mutant, respectively; Figure 3.5B). A similar effect was observed on the growth of both strains in EWF with 1.3 g/L of OT (i.e. cell number increased by 2 and 1.7 $\log_{10}$ CFU/mL in 24 h at 110% for

the WT and Δ*entB* mutant, respectively) (Figure 3.5C). However, a significant difference was noted between the WT and Δ*entB* strain in EWF with 1.3 g/L OT at 100% iron saturation (i.e. cell number increased by 3 and 2.41 log10 CFU/mL, respectively in 24 h; Figure 3.5C), but no such effect was seen at iron-saturation levels at >100% or ≥150-300%; Figure 3.5F). This suggests that (in EWF) there is a narrow Fe:OT ratio (at around 100% Fe saturation) where the levels of iron availability are poised such that iron-restriction can be overcome by siderophore-mediated iron uptake.

It is possible that the lower viscosities of EW with 10% EW or with 1.3 g/L OT explain the difference in the behaviour between the WT and the Δ*entB* mutant strains with respect to that seen in EW. Thus, it may be that iron is less accessible to the bacteria in a viscous environment such as EW and that the release of highly soluble and readily diffusible siderophores enables *S*. Enteritidis to overcome such accessibility issues.

The results indicate that *S*. Enteritidis is able to capture iron directly from OT to enable growth in EWF with either 10% EW or 1.3 g/L OT. This is the case even when *S*. Enteritidis is unable to synthesis siderophores and so strongly suggests that another mechanism is utilized to sequester iron bound to OT during growth in EWF. However, this siderophore-independent mechanism of iron acquisition from OT in EWF is not applicable in EW, as growth remains limited in the absence of siderophore production, even when iron is provided that is much in excess of that needed to saturate OT.

As previously described (section 3.4), the saturation of OT by iron was increased to 300% to study how *S*. Enteritidis manages to use free iron without

siderophore production. In EW, a partial relief of the growth inhibition of the WT strain was observed from 110% to 300% of OT saturation (i.e. cell number increased by 1.5 and 3 $\log_{10}$ CFU/mL in 24 h, respectively). For the Δ*entB* strain, a partial lifting of the growth inhibition was also observed (enhanced by 1.16 to 2.32 $\log_{10}$ CFU/mL in 24 h at 110 and 300%, respectively), but was significantly lower than with the WT strain (Figure 3.5E). In EWF with 10% EW, a partial and progressive relief of growth inhibition was observed when EW was saturated at 50 to 300% (i.e. cell number increased from 1.1 to 3.6 $\log_{10}$ CFU/mL in 24 h, respectively). Similarly, in EWF with 1.3 g/L OT, a partial and progressive relief of *S*. Enteritidis growth was observed when OT was saturated from 50 to 300% (enhanced from 2 to 3.5 $\log_{10}$ CFU/mL in 24 h, respectively). No significant differences were observed between the WT and Δ*entB*; thus, this effect was not siderophore-dependent. In all cases, growth reached a maximum at ≥110-150% OT saturation and was not enhanced further by additional iron supply.

The significantly lower growth of the Δ*entB* mutant (cf. the WT) in iron-saturated EW clearly indicates that *S*. Enteritidis requires siderophores to achieve maximum growth under these conditions. This result supports previous work (Kang et al., 2006) showing that at ≥110% iron saturation there is a 4 $\log_{10}$ CFU/mL reduction in growth in EW after 24 h for an *S*. Enteritidis mutant unable to produce siderophores. However, in this study, even in the presence of excess iron, the growth of *S*. Enteritidis (WT) in EW appears to remain restricted; it is unclear whether this is due to a residual iron restriction. In addition to a possible reduced motility of *S*. Enteritidis, the presence of lipocalins (siderophore-sequestrator) in EW might also affect the capacity of *S*. Enteritidis to use their siderophores. On the other hand, under low-viscosity conditions (EWF with either

10% EW or 1.3 g/L OT), the ability to produce and utilise siderophores seemed to offer only a limited advantage under either condition. Additionally, results show that *S*. Enteritidis possesses a mechanism to capture iron directly bound to OT in a lower viscosity media (EWF with 10% EW or 1.3 g/L OT) even in the absence of siderophore production. Although the identity of this mechanism is unclear, it appears not to function effectively in whole EW.

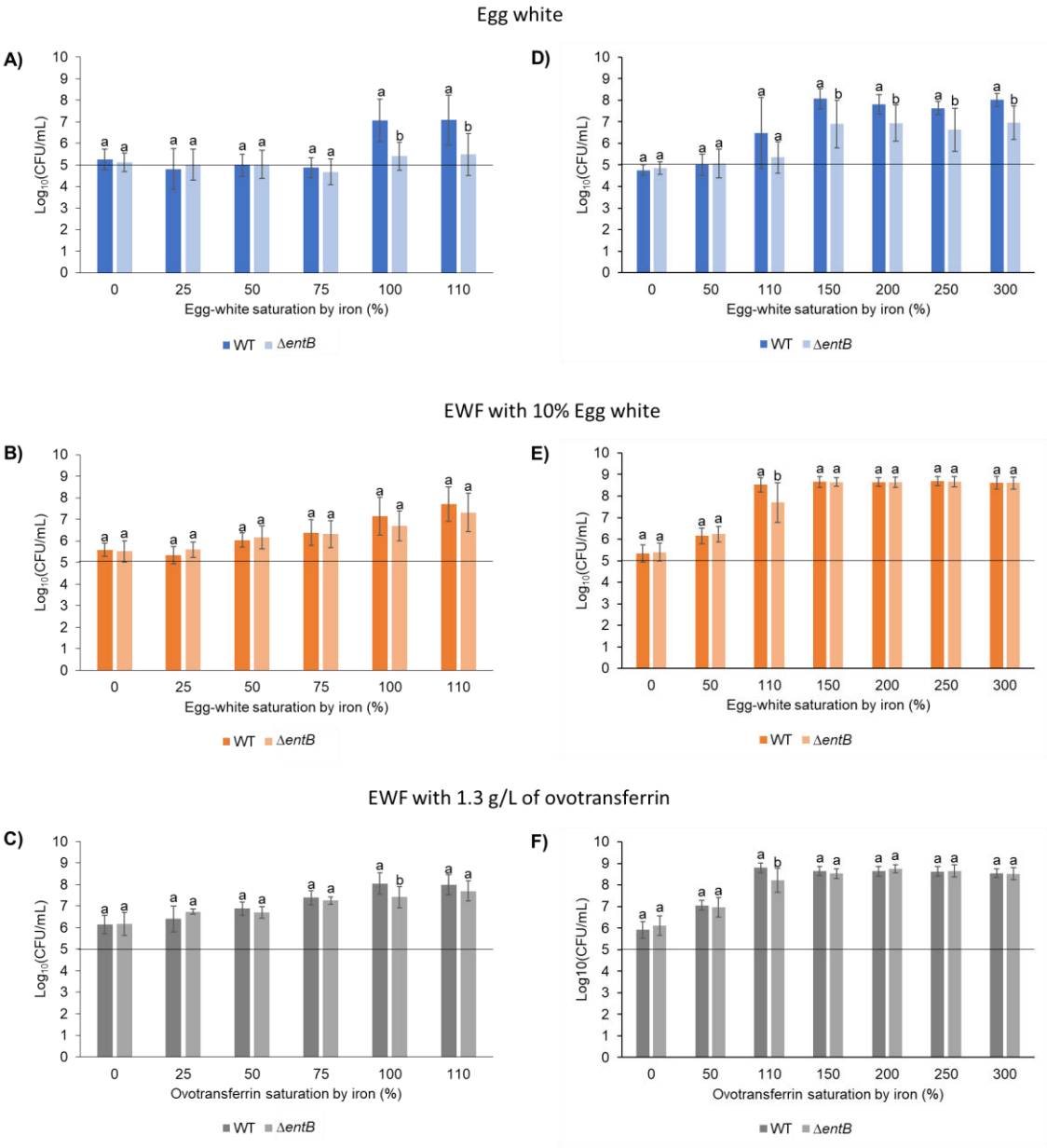

Figure 3.5. Effect of increasing the iron-saturation levels of ovotransferrin on the growth of *S.* Enteritidis NCTC13349 (WT) and the Δ*entB* mutant. The growth of *S*. Enteritidis NCTC13349 and the Δ*entB* mutant inoculated at a 5 $\log_{10}$ CFU/mL (black line) was measured after 24 h incubation at 30 °C in (A and C) EW, (B and D) EWF with 10% EW and (C and E) EWF with 1.3 g/L OT. Iron citrate (33.4 mM) was added to obtain OT-iron saturation levels from 0 to 110% (A to C) and up to 300% (D to F). Error bars indicate standard deviations from the mean derived from three biological experiments, with three technical replicates. Significant differences between each strain were assessed using a student t-test with R software (version 1.4.1106). Significantly different groups are identified by letters, with a p-value <0.05.

3.7. *S*. Enteritidis can use exogenously supplied siderophores to counteract the iron restriction imposed by egg white

Following the observation that siderophore production does not support the growth of *S*. Enteritidis in EWF with 10% EW or 1.3 g/mL OT, further experiments were performed to confirm the ability of siderophores to support the acquisition of iron. Thus, the effect of the addition of Ent to a synthetic EW medium (SM) with 1.3 g/L of OT was tested. SM was used since EW contains Ex-FABP at 5.1 µM, a lipocalin that acts to inhibit the ability of *S*. Enteritidis to use Ent for iron uptake (Julien *et al*., 2020). Thus, if Ent is added directly to the EW, false negative results may be obtained as a result of the sequestration of Ent by Ex-FABP. Additionally, EW and EWF may contain molecules or peptides of less than 10 kDa that display antimicrobial activity (Baron et al., 2016; Cochet et al., 2021). Thus, the use of SM in place of EWF would provide the opportunity to avoid such confounding factors.

3.7.1. Formulation of a synthetic egg-white medium (SM) free of proteins and peptides

Since no suitable EW synthetic medium was available, an important aim was to formulate such a medium that would possess with the same ionic composition and pH as EW. The ionic compositions of EW and EWF have been studied and compared previously (*Ciqual*, 2021; Cochet et al., 2021; Nau et al., 2010b; Nys & Sauveur, 2004; Sauveur, 1988; Stadelman & Cotterill, 1995). The published compositions are summarized in Table 3.1 and the composition of the SM developed in this study is discussed below. The SM was developed according to the ionic composition reported for EW whilst accounting for differences with the

composition of EWF resulting from chemical elements bound to proteins that are removed during the ultrafiltration with a 10 kDa cut-off filter.

Table 3.1. Ionic and glucose composition of EW, EWF and SM

	Minimal concentration in EW (mM)*	Maximal concentration in EW (mM)*	Concentration in EWF (10 kDa cut off) (mM)**	Concentration in SM (mM)
Sodium	67.424	80.908	96.1	59
Sulphur	50.834	56.136	0.69	1
Chloride	-	49	-	44.5
Potassium	35.807	44.247	44.7	40
Phosphorus	4.1971	7.1028	1.7	2
Magnesium	3.7029	4.9372	3.32	2
Calcium	1.2476	2.9942	0.96	0.25
Iron	0.0036	0.0179	<0.00002	-
Zinc	0.0015	0.0185	0.0005	-
Copper	0.0029	0.0058	0.00098	-
Manganese	0.0013	0.0020	0.00002	-
Total N	-	1364	2.3	2
Glucose	-	25	21.5	20

* Ciqual (2021); Sauveur, 1988; Stadelman & Cotterill, 1995; Nys & Sauveur, 2004; Nau et al., 2010
** Cochet et al., 2021

The pH of EW reaches ~9.3 a few days after laying and was, therefore, an important parameter to consider in the elaboration of the SM. Through the addition of 55 mM sodium carbonate/bicarbonate buffer, a pH of 9.3 was obtained. Moreover, this buffer provides a source of sodium and carbonate/bicarbonate ions. This concentration corresponds to the concentration of bicarbonate present in EW, as derived from the hen's blood and transferred during hydration of EW in the hen's uterus (Mongin and Lacassagne, 1966; Brooks and Pace, 1938). In addition, the bicarbonate is also indispensable for the binding of iron to OT.

Sulphur is the second most abundant chemical element found in EW (50.8 to 56.1 mM), but its abundance is closely related to the presence of proteins.

Indeed, almost all the sulphur is bound to proteins in EW, explaining its low concentration in EWF (0.69 mM). Thus, in the SM, sulphur was supplied with a concentration of 1 mM in the form of $(NH_4)_2SO_4$.

Chloride is present in EW at a concentration of 49 mM. Thus, KCl, $MgCl_2$, and $CaCl_2$ were the three forms of chloride included in the SM for achieving the final concentration of 44 mM. These three molecules also provide a source of potassium (40 mM), magnesium (2 mM), and calcium (0.25 mM) in SM, in addition to chloride ions.

In EW, the total nitrogen concentration is very high (1364 mM), but as for sulphur, most of the EW nitrogen is incorporated into proteins. Thus, after ultrafiltration, the concentration of sulphur dropped to 2.3 mM in EWF. For this reason, in the SM, the nitrogen source was provided by ammonium in the form of $(NH_4)_2SO_4$, at the concentration of 2 mM.

The concentration of phosphorus is between 4.2 and 7.1 mM in EW, and is partially bound to the proteins. Thus, a concentration of 2 mM of phosphorus in the form of NaH_2PO_4 was added to the SM, a concentration that matches that of the EWF. In EW and EWF, the concentration of magnesium is almost the same (between 3 and 4 mM). Two millimolars were provided by $MgCl_2$ in the SM. The concentration of calcium in EW is between 1.3 and 3 mM, and is 0.96 mM in EWF. Only a 0.25 mM final concentration of calcium was chosen for the SM since precipitation occurred with higher concentrations. This concentration is slightly higher than that of the M9 minimal medium (i.e. 0.1 mM).

Iron, zinc, copper and manganese are present in trace amounts in EW (between 1.5 and 1.85 µM) and in EWF (between less than 0.02 and 0.98 µM), so these chemical elements were not integrated into the SM considering that they

are present in trace amounts in the others chemicals added. A source of sugar is essential for bacterial growth. In EW like in EWF, glucose is the dominant form of carbohydrate with a concentration of 20 mM. The same quantity was therefore provided in the SM.

The final concentration of each ion and molecule in SM is presented in Table 3.1 and its preparation is detailed in the Materials and Methods section 2.1.4.4. Once the composition of SM was defined, it was tested with 10% EW (section 3.7.2.) and with 0 to 110% iron-saturated OT (section 3.7.3). Finally, it was used to assess the effect of exogenous Ent on *S*. Enteritidis growth (section 2.1.5.4).

3.7.2. Growth of *S*. Enteritidis in SM

S. Enteritidis was incubated for 24 h at 30 °C in SM and SM with 10% EW (section 2.2.1). The egg-based media, EWF and EWF with 10% EW, were used as controls. As shown in Figure 3.6, *S*. Enteritidis growth was similarly strong in EWF and SM (overall increase in cell number of ~4 $\log_{10}$ CFU/mL). However, when 10% EW was applied bacterial growth was greatly limited in both SM and EWF (cell number increased by less than 1 $\log_{10}$ CFU/mL) (Figure 3.6). Additionally, in the presence of OT (1.3 g/L), *S*. Enteritidis growth is slightly but significantly higher in SM than in EWF (i.e. cell number increased by 1.6 and 1.1 $\log_{10}$ CFU/mL, respectively). This slight difference observed for addition of 1.3 g/L OT to SM or EWF can be explained by the presence of antimicrobial peptides in EWF (Cochet et al., 2021). Results are thus consistent with data obtained by Baron et al. (1997) for growth of *S*. Enteritidis at 30 °C for 24 h in: EWF; EWF with 10% EW; and with OT at 1.3 g/L. The use of EWF with 10% EW has already

been shown to allow the same *Salmonella* growth as in EW (Baron et al., 1997, 2017, 2020).

In summary, these results indicate that SM is a suitable medium for studying the impact of EW as well as EW proteins on *S*. Enteritidis without interference from ≥10 kDa EW molecules.

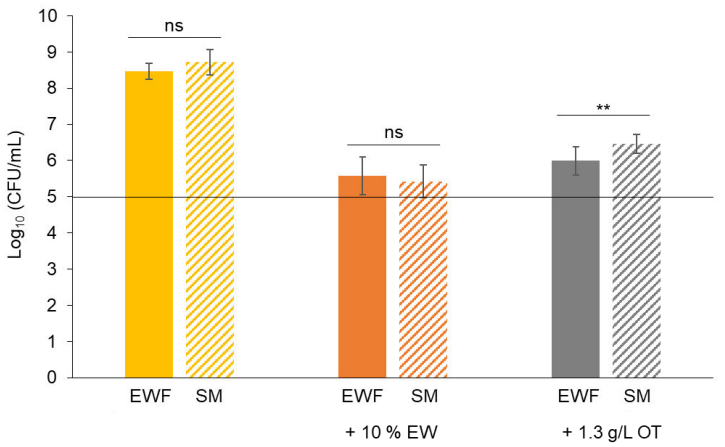

Figure 3.6. Growth of *S.* Enteritidis in SM. *S.* Enteritidis (at an starting cell density of 5 $\log_{10}$ CFU/mL) was incubated at 30 °C for 24 h in SM, EWF, SM with 10% EW, EWF with 10% EW, EWF with 1.3 g/L of OT or SM with 1.3 g/L of OT. Error bars indicate standard deviations from the mean derived from one to three biological experiments, with three technical replicates Significant differences between each condition were assessed using one-way ANOVA followed by a Tukey Contrast test with R software (version 1.4.1106). The 'ns' designation indicates 'no significant difference' with a p-value > 0.05.

3.7.3. Effect of exogenous enterobactin on *S*. Enteritidis growth in SM supplemented with OT at 0-110% iron saturation

Growths were compared in SM with OT (at 1.3 g/L), iron saturated at 0-110%, together with Ent (10 µM) added at 5-10 fold excess of the levels estimated in EW model medium following 4 h growth of *S*. Enteritidis at 37-42 °C (Julien, 2020). It should be noted that the added iron could thus directly associate with the OT and/or the siderophore. As the stock solution of Ent was prepared in 40% DMSO, a control was carried out with SM supplemented with the maximum equivalent volume of 40% DMSO applied. The growth of *S*. Enteritidis was not

affected by the presence of DMSO and was significantly similar to that in EW with 1.3 g/L of OT (data not shown).

As previously described in Figures 3.3 and 3.5, the inhibition of *S*. Enteritidis growth was partially overcome by OT at ≥ 75% iron saturation. In the presence of Ent, the growth inhibition of *S*. Enteritidis was partially and progressively overcome when OT was 10-110% iron-saturated (i.e. cell number increased by between 1.5 $\log_{10}$ and 3.6 $\log_{10}$ CFU/mL at 24 h, whereas in the absence of Ent cell number increased by between 0.5 to 3.5 $\log_{10}$ CFU/mL; Figure 3.8). *S*. Enteritidis should be able to use exogenously supplied Ent to obtain iron and indeed the results indicate that the provision of exogenous Ent at 10 µM enhanced the acquisition of iron from 10-50% iron-saturated OT. Thus, S. Enteritidis is able to remove iron from OT to enhances iron-restricted growth under conditions where OT is partially (10-50%) iron saturated. This finding suggests that, under the iron-restricted conditions tested, *S*. Enteritidis does not produce sufficient Ent to support optimum growth when OT is only partly iron-saturated. However, when OT was 75-110% iron saturated, the addition of Ent had no significant effect on growth; this was presumably because the conditions were no longer iron restricted such that optimal growth was achieved without the need for provision of additional Ent.

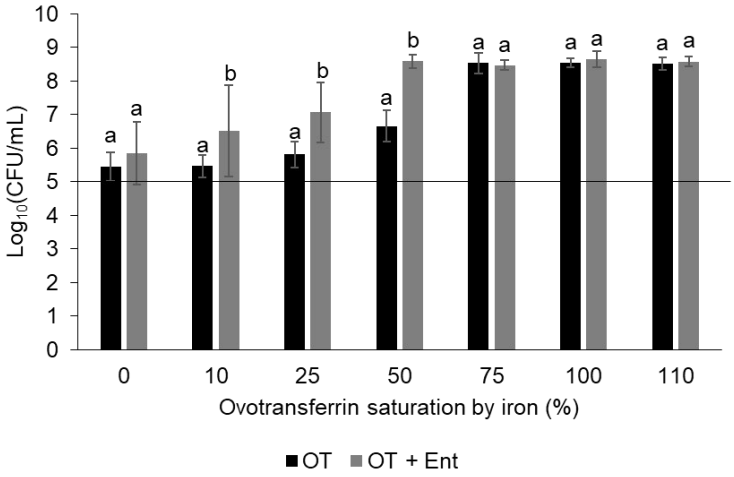

Figure 3.8. Effect of addition of exogenous Ent on *S*. Enteritidis growth as a function of the degree of OT iron saturation. The growth of *S*. Enteritidis NCTC13349 inoculated at a 5 log_{10} CFU/mL concentration (black line) was measured after 24 h incubation at 30 °C in SM with 1.3 g/L of OT in the absence or presence of 10 µM of Ent (+ Ent). Iron citrate (33.4 mM) was added to obtain OT-iron saturation levels from 0 to 110%. Each bar represents the average of three biological experiments with three technical replicates. Error bars indicate standard deviations from the mean derived from four biological experiments, with three technical replicates. Significant differences between each condition were assessed using Student's t-test with R software (version 1.4.1106). Significantly different pairs (+/- Ent) are indicated by two different letters ('a' and 'b'), with a p-value <0.05.

3.8. Discussion and perspectives

The results confirm that the presence of OT is largely responsible for the antimicrobial activity of EW (Figure 3.2). Previous work showed that OT or 10% EW cause an inhibition of *S*. Enteritidis growth at 30 °C, but such an effect is not seen when other EW proteins are provided (Baron et al., 1997). Indeed, Baron et al. (1997) reported that the number of cells increased by just 2.5 and 1.5 log_{10} CFU/mL in EWF with 1.3 g/L of OT and EWF with 10% EW, respectively, whereas in EWF the increase was by 5 log_{10} CFU/mL. In contrast, EW proteins other than OT induced no limitation on growth.

The iron-chelating activity of OT has been reported as being the major factor responsible for EW's antimicrobial activity (Baron et al., 1997; Garibaldi,

1960; Lock & Board, 1992). Garibaldi (1960) was the first to describe this phenomenon on the growth of *Pseudomonas fluorescens*, *Proteus vulgaris, Proteus melanovogenes* and *Aerobacter cloacae* in EW by saturating OT at 105%. Further work showed that *Salmonella* growth is promoted by 4 $\log_{10}$ CFU/mL at 20 and 30 °C when EW was saturated with 40% ferric ammonium citrate (Lock & Board, 1992) or with 110% ferric ammonium citrate at 30 °C (Baron et al., 1997). However, no previous study has directly compared bacterial growth under conditions were both EW and OT are saturated with iron. In the current study, the results indicate that the addition of iron (at a level required to saturate OT at 100%) to EW, EWF with 10% EW or EWF with 1.3 g/L OT resulted in an enhanced *S*. Enteritidis growth (section 3.4). These results thus confirm the role of the metal-chelating activity of OT in the antimicrobial activity of EW.

Despite the lack of iron in EW, *S*. Enteritidis can still survive within this hostile environment. In this chapter, the capacity of *S*. Enteritidis to acquire iron from EW was studied. Bacteria possess the capacity to acquire iron under iron deficiency using different systems. They can directly bind iron from host proteins such as transferrin, utilise iron from exogenous haem or haemoproteins, sequester ferric iron using siderophores or use specific systems for free ferrous or ferric iron binding (Caza & Kronstad, 2013). The result of the current study indicate that *S*. Enteritidis is able to acquire iron from EW but only when OT was fully saturated (section 3.4). However, when *S*. Enteritis was unable to produce siderophores (due to an Δ*entB* mutation), its ability to grow in iron-supplemented EW was inhibited. Thus, in EW with iron supplementation, *S*. Enteritidis did not appear able to acquire iron directly from OT since its growth was dependent on the production of siderophores. However, in a low-viscosity EW-related medium

(EWF with either 10% EW, or OT at 1.3 g/L), *S*. Enteritidis was able to acquire iron from OT which was 50% saturated with iron even in the absence of siderophores. Thus, these results show that, in EWF, *S*. Enteritidis can capture iron directly bound to OT and can use other (non-siderophore) iron-acquisition systems when OT is at least 50% saturated. Under the natural conditions of EW, the level of OT saturation does not exceed 5%, and under these conditions *S*. Enteritidis does not appear to benefit from its ability to produce siderophores. These results suggest that *S*. Enteritidis does not produce enough siderophores to enable it to sequester sufficient iron from OT in EW under natural conditions. Thus, the capacity of *S*. Enteritidis to use exogenous siderophores was tested in SM with 1.3 g/L of OT. Under EW conditions, *S*. Enteritidis appeared to use Ent for its growth when OT was saturated by at least 10%. However, the capacity of *S*. Enteritidis to use Ent was not tested with OT-iron saturation levels lower than 10% and therefore the same experiment might be performed at iron saturation levels closer to those found in EW (1 to 5%). Importantly, the results suggest that siderophore production is insufficient to support *S*. Enteritidis growth in EW. This may be considered that this is caused by the sequestration of Ent by Ex-FABP, as observed in LB with DIP at 37 °C (Julien et al., 2020). However, Julien (2020) failed to observe any such effect for Ex-FABP when applied to EW which suggests that the failure of Ent to support growth in EW, as observed herein, is not Ex-FABP related. In future work, the production of siderophore in EWF by *S*. Enteritidis could be quantified in the presence of 10% EW or EWF 1.3 g/L OT, and with different levels of iron saturation, using the CAS assay (Schwyn & Neilands, 1987). Siderophore production and utilisation might also be affected

by membrane damage caused by other EW molecules such as OT, lysozyme, defensins and BPI.

The difference in the ability of *S*. Enteritidis to grow and thus to acquire iron in EW in comparison to EWF with 10% EW and or 1.3 g/L OT was considered to be possibly due to a reduced capacity to acquire iron in a highly-viscous medium. Indeed, EW is composed of different layers of high and low viscosity due to the presence of ovomucin, resulting in an overall viscosity of 5 $mPa.s^{-1}$ at 20 °C and a shear rate of 400 s^{-1} (Lang & Rha, 1982). This viscosity may cause heterogeneity in the distribution of OT-Fe complex in EW, as has been suggested by some authors (Banks et al., 1986; Li-Chan, 1989). Furthermore, the motility of *S*. Enteritidis in EW could be affected by the high viscosity of EW. Furthermore, several authors have reported that motility affects the survival of *S*. Enteritidis in EW (Cogan et al., 2004; Gantois et al., 2018). In addition, genes involved in flagella biosynthesis were downregulated by *S*. Enteritidis at 45 °C after 7 to 45 min exposure to EWMM (Baron et al., 2017). In future work, whether the motility of *S*. Enteritidis is indeed reduced upon EW exposure could be tested in EW using the semi-solid agar plate method (Tittsler & Sandholzer, 1936) and the absence or presence of flagella could be visualised by transmission electron microscopy (negative staining) (Grossart et al., 2000).

Other experimental conditions could also be considered to further explore the ability of *S*. Enteritidis to acquire iron in EW and on the iron-chelating activity of OT. In this chapter, all the experiments were performed at 30 °C and pH 9.3, and with an inoculum size of 5 $\log_{10}$ CFU/mL Thus, it would be interesting to test conditions reflecting those of the hen oviduct and oviposition (pH of 7.8 and temperature of 42 °C).

According to previous studies, in addition to the ability of OT to chelate metal, it could also have an impact on *S*. Enteritidis membrane integrity which could indirectly dampen the activity of the iron-acquisition systems (Aguilera et al., 2003; Ellison et al., 1988). Thus, Chapter 4 will investigate the capacity of OT to induce *S*. Enteritidis membrane permeabilisation and depolarisation.

Chapter 4.
Impact of ovotransferrin on the *S*. Enteritidis envelope under egg-white conditions

4.1. Introduction

OT, like other transferrin-family members, can chelate divalent ions present on the surface of the outer membrane of Gram-negative bacteria and thus provoke membrane perturbation, probably by direct contact (Aguilera et al., 2003; Ellison et al., 1988, 1990). The bacterial membrane perturbation effects induced by OT include membrane permeabilisation to potassium and dissipation of the pmf (Aguilera et al., 2003; Baron et al., 2014; Ellison et al., 1988; Jan,et al., 2013). In addition, several studies have shown that EW induces the expression of *S.* Enteritidis genes (and/or the production of proteins) involved in the envelope-damage response, maintenance of membrane integrity, and pmf restoration (Baron et al., 2017, 2020; Gantois et al., 2009b; Huang et al., 2019, 2020; Qin et al., 2019). Furthermore, other EW molecules (such as lysozyme, BPI and defensins) can cause bacterial membrane damage and could act in synergy (Derde et al., 2013; Gong et al., 2010; Guérin-Dubiard et al., 2006; Hervé-Grépinet et al., 2010). The mechanism(s) by which OT induces perturbation of bacterial envelopes, under the specific conditions found in EW, remain to be clarified.

In this chapter, the impact of OT on the *S*. Enteritidis envelope was studied. The permeabilisation of inner and outer membranes was examined as well as depolarisation of the inner membrane. A possible synergetic effect between OT and lysozyme on *S*. Enteritidis envelope was also investigated.

4.2. Ovotransferrin induces outer membrane permeabilisation of *S*. Enteritidis under egg-white conditions

The effect of ovotransferrin on the growth of *S.* Enteritidis by its iron chelating activity was well described in literature but not the impact of ovotransferrin on bacterial membranes. For this purpose, the permeabilisation of the outer and inner membranes of *S*. Enteritidis pBBC129, a constructed strain expressing β-lactamase and β-galactosidase in the periplasm and cytoplasm, respectively (Appendix 1), was explored by measuring β-lactamase release from the periplasm and β-galactosidase release from the cytoplasm for *S.* Enteritidis exposed to different factors (section 2.2.3). This method was already successfully used for *E. coli* ML-35 (Derde et al., 2013; Lehrer et al., 1988). When the outer membrane is permeabilised, nitrocefin, a chromogenic cephalosporin and substrate of β-lactamase, is hydrolysed into HP-nitrocefin, a coloured product absorbing at a λmax of 490 nm. When the inner membrane is permeabilized, 2-nitrophenyl-β-D-galactopyranoside (ONPG), the substrate of β-galactosidase, is hydrolyzed into ONP, a coloured product absorbing at a λmax of 405 nm (section 2.2.3). The increase in absorbance at each wavelength highlights the progress of enzymatic conversion of each substrate by the β-lactamase and β-galactosidase, indicating the accessibility of the enzymes to their substrate in response to outer and inner membrane permeabilisation, respectively. To quantify and compare the membrane permeabilisation of *S*. Enteritidis exposed to different factors, the maximal slope (ΔA/30min) representing the enzyme activity of the reaction was calculated (Derde et al., 2013). Because the substrate concentration was fixed, differences in velocity were dictated by the concentration of accessible corresponding enzymes. The higher the accessible enzyme

concentration (and the higher the maximal slope), the stronger the membrane permeabilisation (Derde et al., 2013). For inner membrane permeabilisation, the lag time before the absorbance signal, which represents the delay between the outer and inner membrane was calculated according to Derde et al. (2013) (Section 2.2.3).

Figure 4.1 shows the outer and inner membrane permeabilisation progress of *S.* Enteritidis incubated in different media at 30 °C. Concerning outer membrane permeabilisation (Figure 4.1A and C), polymixin B, an antibiotic peptide, was used as a positive control. Within the first few minutes of exposure to polymyxin B, β-lactamase activity increased rapidly (enzyme activity of 11.2 ± 2.1 milli-A_{490nm}/min), indicating rapid permeabilisation of the outer membrane of *S*. Enteritidis (Figure 4.1A and 4.1C). β-Lactamase activities were also observed upon EW exposure, but significantly differed depending on the medium employed. In SM, the β-lactamase activity was significantly much lower (enzyme activity of 1.4 ± 0.3 milli-A_{490nm}/min) than in EW (enzyme activity of 4.4 ± 0.4 milli-A_{490nm}) or in SM with 13 g/L of OT (enzyme activity of 7.2 ± 0.6 A_{490nm}) (Figures 4.1A and C). These results indicate that the *S*. Enteritidis outer membrane is permeabilised by EW and OT exposure, and that OT (at the concentration employed, corresponding to its theoretical concentration in EW) provokes a more drastic permeabilisation than EW. Furthermore, there was a significant difference between EW and SM with 13 g/L of OT (enzyme activity of 4.4 ± 0.4 and 7.2 ± 0.6 milli-A_{490nm}/min respectively). This result could be explained by the presence of other EW-proteins or peptides that could reduce the impact of OT on the *S*. Enteritidis membrane. The slight permeabilisation of the outer membrane

induced by SM might be explained by the high pH of the medium, however, there was no control with a pH of 7 to confirm this.

Concerning the permeabilisation of the inner membrane, melittin (an amphipathic cytotoxin derived from bee venom), was used as a positive control. β-Galactosidase activity was observed in the presence of melittin, indicating permeabilisation of the inner membrane (enzyme activity of 15.6 ± 4.2 milli-A_{405nm}) (Figure 4.1B and 4.1D). The lag time (section 2.2.3) was 13 ± 6 min (Figure 4.1D). The permeabilisation of the inner membrane of *S*. Enteritidis was observed in EW (enzyme activity of 6.3 ± 0.9 milli-A_{405nm}/min) (Figure 4.1B and 4.1D) with a lag time of 127 ± 6 min (Figure 4.1D). The β-galactosidase activity was significantly higher in EW than in SM (enzyme activity of 3.2 ± 0.6 milli-A_{405nm}/min) or in SM with OT at 13 g/L (enzyme activity of 3.7 ± 0.7 milli-A_{405nm}/min) (Figure 4.1B and D). There was no significant difference in the β-galactosidase activities between SM and SM with OT 13 g/L, with lag times of 122 ± 13 min and 141 ± 20 min, respectively (Figure 4.1). These results indicate that OT does not lead to inner membrane permeabilisation and suggest the implication of other proteins in the weak inner membrane disrupting effect observed in EW.

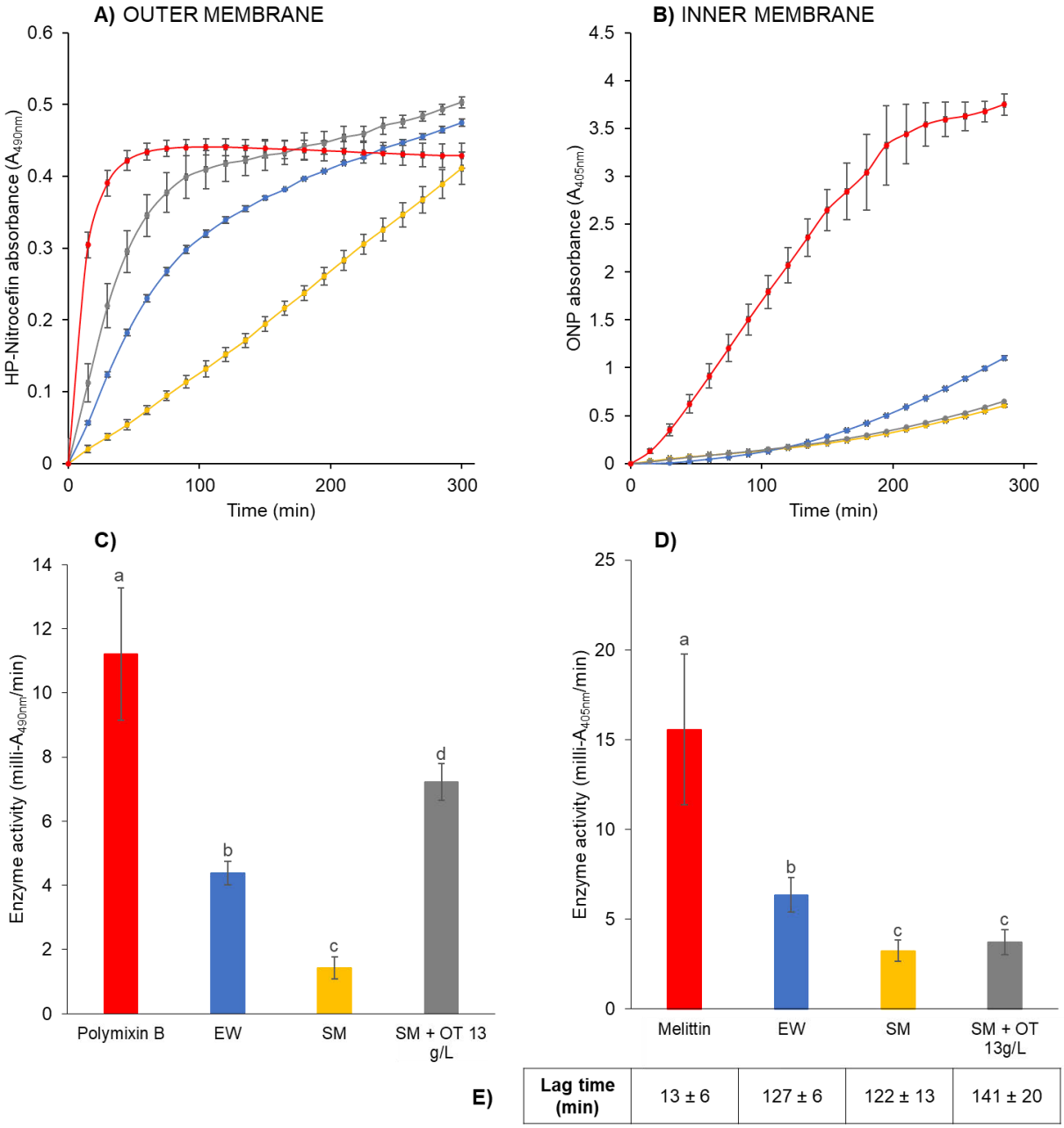

E)

Lag time (min)	13 ± 6	127 ± 6	122 ± 13	141 ± 20

Figure 4.1. *S.* Enteritidis membrane permeabilisation by EW and OT. Monitoring of the permeabilisation of the outer (A) and inner (B) membrane of *S.* Enteritidis (grown to an OD_{600nm} of 0.35) was measured in EW (blue), SM (yellow), SM with 13 g/L of OT (grey) and polymixin B (50 µg/mL) or melittin (15 µg/mL) (red) positive controls, respectively. Comparison of the Vmax for outer (C) and inner (D) membranes with polymixin B or melittin, respectively; EW; SM and SM with 13 g/L of OT (SM + OT 13 g/L). Additionally, (E) the lag time (section 2.2.3, Figure 2.3), corresponding to the delay between the outer and inner membrane permeabilisation, was calculated for each medium. Each error bar represents an average of three biological experiments with three technical replicates. Significant differences between each condition were assessed using a one-way ANOVA test followed by a Tukey test with R software (version 1.4.1106). Several significantly different groups were identified by a letter, with a p-value <0.05.

4.2.1. The concentration of ovotransferrin influences the permeabilisation of *S*. Enteritidis membranes

To confirm the impact of OT on the permeabilisation of *S*. Enteritidis outer membrane and the absence of any effect of OT on the inner membrane, different concentrations of OT were tested, ranging from 0 to 13 g/L in SM (Figure 4.2A and B). The β-lactamase activity progressively increased with OT concentration (Figure 4.2A) while β-galactosidase activity remained unchanged with respect to OT concentration (Figure 4.2B). These results confirm the ability of OT to induce the permeabilisation of the outer membrane of *S*. Enteritidis at 30 °C. The strongest effect was observed at the OT concentration corresponding to its native concentration in EW (13 g/L), which was the highest concentration applied. In contrast, OT was not able to permeabilise the inner membrane to any notable degree.

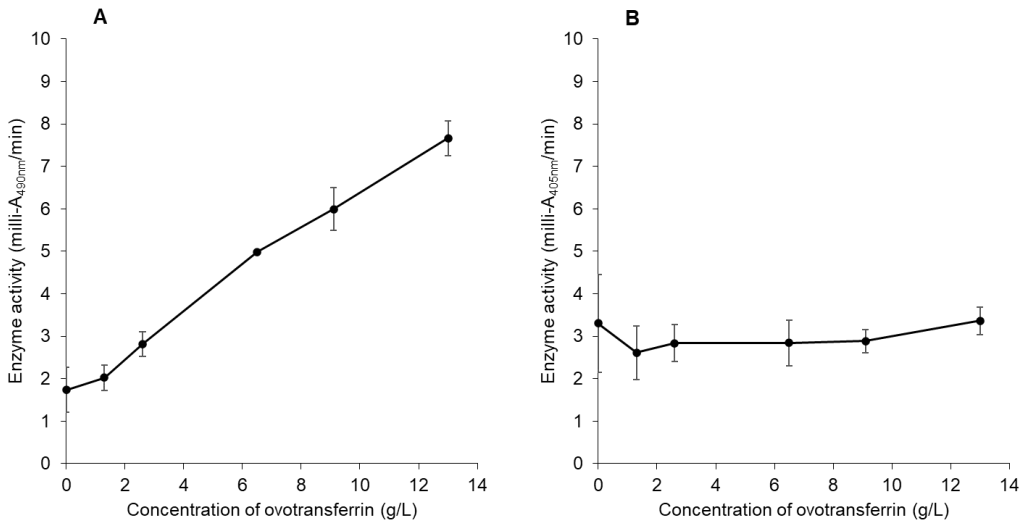

Figure 4.2. Impact of OT concentration on *S*. Enteritidis membrane permeabilisation. Comparison of the enzyme activity for outer (A) and inner membrane (B) permeabilisation of *S*. Enteritidis (grown to an OD_{600nm} of 0.35) exposed to a range of ovotransferrin concentrations in SM (from 0 to 13 g/L). Each error bar represents an average of three biological experiments with three technical replicates.

4.2.2. The iron-chelating activity of ovotransferrin does not have a major impact on the permeabilisation of *S*. Enteritidis membranes

OT and other transferrins are able to bind iron but also other divalent cations (Legros et al., 2021 for a review). The LPS of the outer membrane of Gram-negative bacteria is bridged by divalent cations (Ca^{2+} and Mg^{2+}) that are crucial for the integrity of the outer membrane. Thus, by binding these divalent cations, chelating agents like ethylenediaminetetraacetic acid (EDTA) can disturb the bacterial outer membrane (Bergan et al., 2000). It has been reported that, in a manner comparable to EDTA, lactoferrin and transferrin cause LPS release from the *E. coli* outer membrane (Ellison et al., 1988). Furthermore, the same authors showed that the transferrin and lactoferrin effect on LPS release from *E. coli* is inhibited by the presence of iron (Ellison et al., 1988). For this reason, the impact of the iron-chelating activity of OT was investigated on the outer membrane permeabilisation of *S*. Enteritidis, under EW conditions. According to the metal concentrations ranges detected in EW, OT appears to be only 1.07 to 5.4% iron-saturated, which leaves a considerable residual chelation capacity (Legros et al., 2021). Indeed, iron saturation of OT might limit any chelation of Ca^{2+} and Mg^{2+} from the LPS by OT and thus avoid the outer-membrane permeabilisation that is induced by apo-OT.

Thus, the impact of OT saturation by iron on the permeabilisation of the outer and inner membranes of *S*. Enteritidis was also tested at 30 °C (Figure 4.3). For this purpose, OT (at 13 g/L, concentration found in EW) was saturated from 0 to 110% with iron citrate, in SM. The ability of OT to disrupt the outer membrane was confirmed and was found to be independent of its iron saturation level (enzyme activity of 7.35 ± 0.63 and 7.25 ± 0.86 milli-A_{490nm}/min) at 0 and 110 %

iron saturation of OT, respectively (Figure 4.3A). However, as confirmed in Figure 4.3B, OT induced a slight permeabilisation of the inner membrane when its iron saturation level reached 110% (enzyme activity of 3.71 ± 0.69 and 5.87 ± 1.56 milli-A_{405nm}/min at 0 and 110 % iron saturation of OT, respectively). These results suggest that the iron-chelating activity of OT does not influence its ability to permeabilise the outer membrane of *S*. Enteritidis, but could slightly promote its impact on the inner membrane. However, no control with ferric iron in SM was performed to confirm these findings.

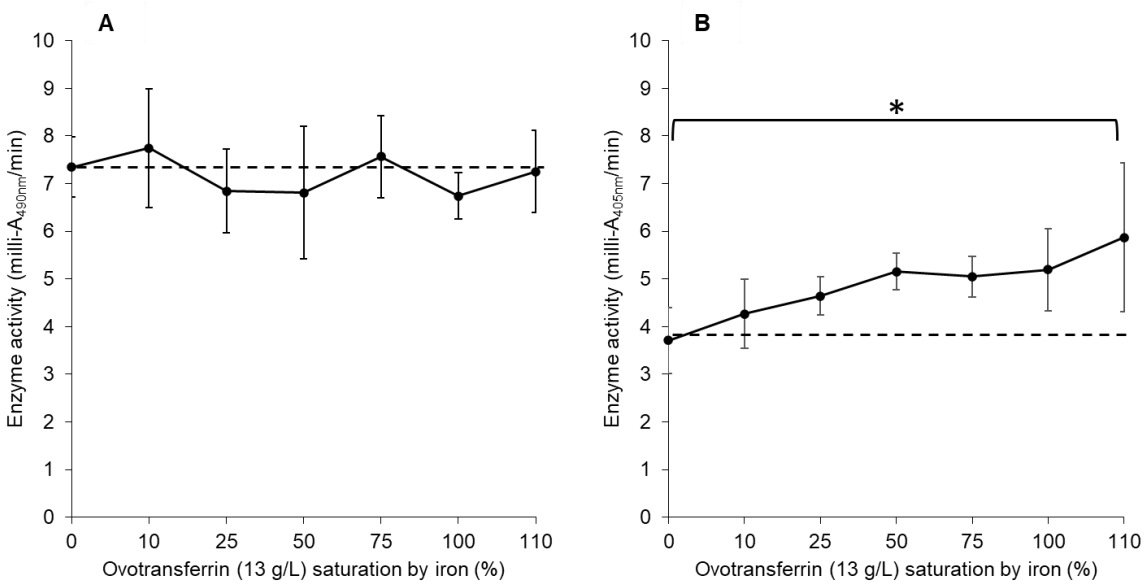

Figure 4.3. Impact of OT iron-saturation on *S*. Enteritidis membrane permeabilisation. Comparison of the enzyme activity for outer (A) and inner membrane (B) permeabilisation of *S*. Enteritidis (grown to an OD_{600nm} of 0.35) exposed to a range of OT (13 g/L in SM) saturation (from 0 to 110 %) with iron citrate. Each error bar represents an average of three biological experiments with three technical replicates.

4.3. Ovotransferrin participates to *S*. Enteritidis inner membrane depolarisation under egg-conditions.

Depolarisation of the *S*. Enteritidis inner membrane was measured using a fluorescent probe ($DiSC_3(5)$) (section 2.2.4). The hydrophobic and cationic nature of the $DiSC_3(5)$ probe allows its penetration into the bacterial cell under the influence of the membrane potential. In the cytoplasm, the probe does not fluoresce due to an autoquenching effect (Waggoner, 1979). When the membrane potential of the bacterium is lowered, the probe, previously internalised by the cell, is released into the medium where it fluoresces.

The depolarisation of the inner membrane of *S*. Enteritidis was first measured after 10 min incubation at 30 °C of *S*. Enteritidis exposed to melittin, used as a positive control (Figure 4.4A). The relative fluorescence unit (RFU) intensity reached 344 ± 76 and was significantly greater than that obtained in response to 5 mM HEPES (pH 7.2), used as negative control (95 ± 8 RFU). After 10 min exposure to EW, the RFU reached a similar level as with melittin (372 ± 117 RFU), indicating the ability of EW to induce membrane depolarisation. Furthermore, no significant difference was observed between EW and 10% EW (372 ± 117 and 344 ± 111 respectively). In SM (i.e. in the absence of EW proteins), the RFU was weak (100 ± 20 RFU), suggesting that EW proteins are involved in the depolarisation effect observed in EW (Figure 4.6A).

S. Enteritidis was then exposed to OT at concentrations ranging from 1.3 to 13 g/L in SM. While a weak depolarisation was detected at 1.3 g/L (99 ± 25 RFU) similar to the value obtained in SM (100 ± 20 RFU), the RFU increased with OT concentration in SM (Figure 4.4A). Indeed, at the concentration found in EW (i.e. 13 g/L), OT caused membrane depolarisation (183 ± 37 RFU) but the effect

was significantly lower than that observed in EW (372 ± 117 RFU). However, it should be noted that OT only gave a significantly raised depolarisation effect with respect to SM when provided at its concentration found in EW (13 g/L). These results suggest that OT is involved in the depolarisation of the inner membrane observed in EW. However, OT seems to not be the only component of EW involved in the EW-induced depolarisation of the *S*. Enteritidis inner membrane.

To confirm this result and to further explore the impact of OT saturation by iron, the depolarisation of the inner membrane of *S*. Enteritidis was investigated by incubating the cells with 0 to 110% iron-saturated OT (13 g/L) (Figure 4.4B). The results show that as the degree of OT iron saturation increased there was a corresponding reduction in the level of OT-induced depolarisation of the *S.* Enteritidis inner membrane. It can be noted that only the value observed for 110% OT saturation (112 ± 8 RFU) was significantly lower than that observed for unsaturated OT (183 ± 37 RFU), and this value was not significantly different from the SM-only control. However, no control with ferric iron in SM was performed, it is therefore difficult to correlate the iron-chelating activity of OT with the membrane depolarisation.

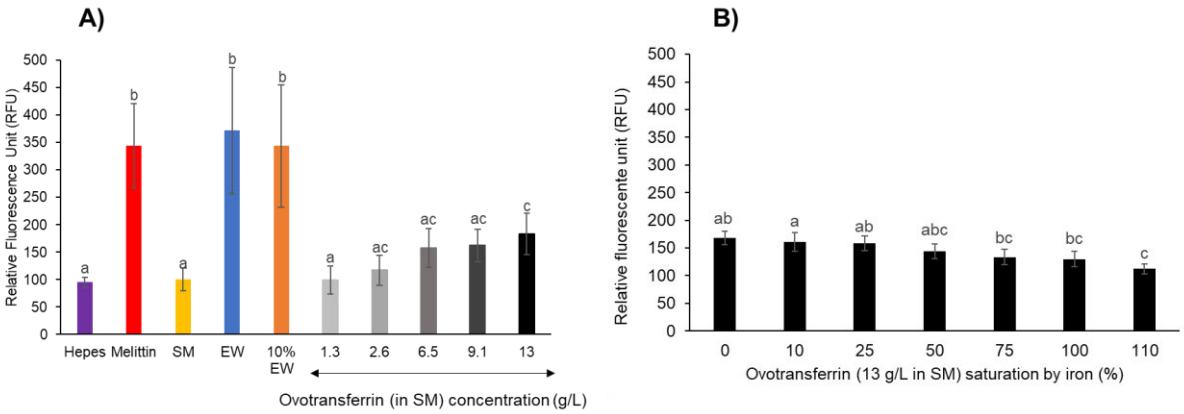

Figure 4.4. *S.* Enteritidis inner membrane depolarisation by OT. Monitoring of inner membrane depolarisation of *S*. Enteritidis at 30 °C after 10 min incubation with (A) melittin (15 µg/mL), SM, EW, SM with 10% EW, SM with OT at different concentrations (from 1.3 to 13 g/L) and (B) in 0 to 110% iron saturated OT in SM (13 g/L). Each bar represents an average of three biological experiments with three technical replicates. Significant differences between each condition were assessed using a one-way ANOVA test followed by a Tukey test with R software (version 1.4.1106). Several significantly different groups were identified by a letter, with a p-value <0.05.

4.4. Membrane damage caused by ovotransferrin do not provoke *S.* Enteritidis lysis.

Membrane damage can directly impact the bacterial cell and their viability. As previously described, OT (at its concentration found in EW) induces the permeabilisation of the outer membrane and the depolarization of the inner membrane of *S*. Enteritidis. Thus, the impact of OT at 13 g/L in SM, as well as its iron-chelating activity on *S*. Enteritidis growth, was studied. *S*. Enteritidis was incubated in SM with 13 g/L of 0 to 110% iron-saturated OT (sections 2.2.1, 2.2.2 and 2.1.5.3). The results showed that after 24 h at 30 °C, *S*. Enteritidis growth was restricted when OT was provided at 0 to 50% saturation (cell number increase by just 0.4-0.7 $\log_{10}$ CFU/mL) (Figure 4.5). However, when OT was provided at an iron saturation above 50%, bacterial growth was significantly enhanced (i.e. cell number increased by 3.5-3.7 $\log_{10}$ CFU/mL over 24 h) (Figure 4.5). These results show that despite its ability to disturb bacterial integrity, OT at

13 g/L does not seem to provoke cell lysis. Indeed, no bactericidal activity was observed in the presence of OT and growth was even observed when OT was >50% iron saturated.

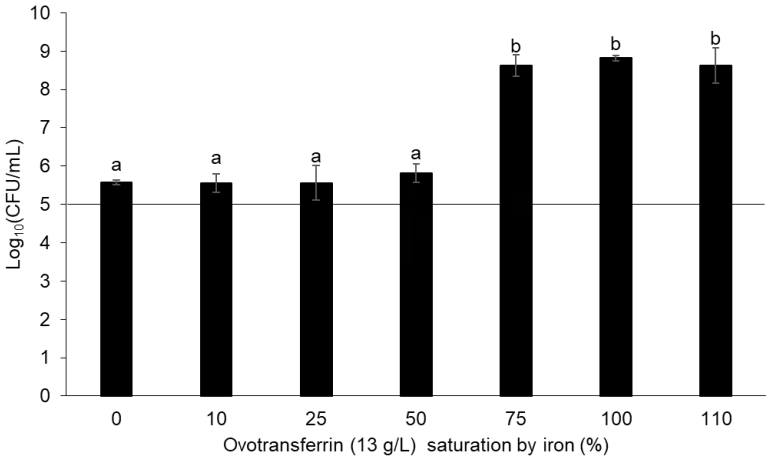

Figure 4.5. Impact of the iron-chelating activity of OT on *S.* Enteritidis growth in SM. *S.* Enteritidis NCTC13349 (5 $\log_{10}$ CFU/mL) was incubated at 30 °C for 24 h in SM with 13 g/L OT +/- saturated with iron citrate (from 0 to 110 %). Error bars indicate standard deviations from the mean derived from one biological experiment, with three technical replicates. Significant differences between each condition were assessed using a one-way ANOVA test followed by a Tukey test with R software (version 1.4.1106). Several significantly different groups were identified by a letter, with a p-value <0.05.

4.5. Ovotransferrin and lysozyme do not act in synergy to induce bacterial membrane damage.

In addition to OT, EW contains several antimicrobial proteins such as lysozyme which is known to induce bacterial lysis by hydrolysis of the β1-4 linkage between the N-acetylglucosamine and N-acetylmuramic residues of the peptidoglycan. Several authors have also described cooperation between lysozyme and transferrin in exerting an antibacterial effect against Gram-negative bacteria (Ellison & Giehl, 1991; Facon & Skura, 1996; Suzuki et al., 1989). Additionally, a synergistic effect between lysozyme and OT against *L. monocytogenes* was reported in presence of bicarbonate at 37 °C but not at

35 °C against *E. coli* (Ko et al., 2008). However, the possible synergy between OT and lysozyme in mediating antibacterial activity remains to be clarified under the natural conditions of EW.

4.5.1. Lysozyme does not affect *S.* Enteritidis growth under egg-white conditions

As described in section 3.3, OT is responsible for the antimicrobial activity of EW against *S*. Enteritidis. However, the effect of lysozyme on *S*. Enteritidis grown at 30 °C in SM remains unknown. Thus, the growth of *S*. Enteritidis was studied at 30 °C in the presence of 3.5 g/L lysozyme diluted in SM. This concentration corresponds to the native lysozyme concentration in EW. Growth was measured after 24 h incubation at 30 °C in SM, in EW, in SM with 13 g/L OT (iron-free) and in SM with 3.5 g/L lysozyme (Figure 4.6). As already described in Chapter 3, no growth of *S*. Enteritidis was observed in EW (section 3.3). A weak bacterial growth was observed in SM (i.e. cell number increased by 2.78 $\log_{10}$ CFU/mL), which was significantly lowered by OT addition at 13 g/L (i.e. cell number increased by only 1.16 $\log_{10}$ CFU/mL). The addition of lysozyme did not affect bacterial growth; i.e. cell number increased by 3.7 $\log_{10}$ CFU/mL which was slightly higher than that seen for SM only (3.5 $\log_{10}$ CFU/mL). Thus surprisingly, inclusion of lysozyme in SM resulted in a slight increase in bacterial growth (Figure 4.6).

The results thus show that lysozyme has no negative impact on *S*. Enteritidis growth at 30 °C under EW conditions. It is consistent with the finding that *ybgC* provided a protection to *S*. Enteritidis against lysozyme in EW (Qin et al., 2020).

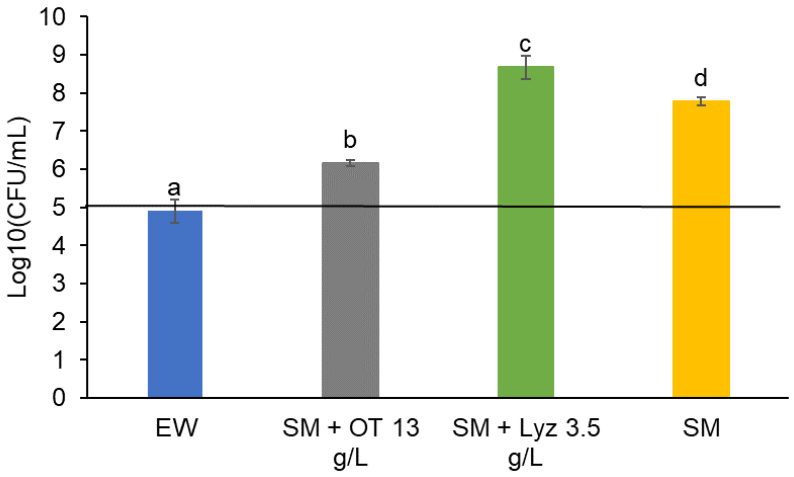

Figure 4.6. Effect of lysozyme on *S.* Enteritidis growth. The growth of *S.* Enteritidis inoculated at 5 $\log_{10}$ CFU/mL was measured after 24 h incubation at 30 °C in (i) egg white (EW), (ii) SM with ovotransferrin at 13 g/L (SM + OT 13 g/L), (iii) SM with lysozyme at 3.5 g/L (SM + Lyz 3.5 g/L), and (iv) synthetic medium (SM). Each bar represents the average of one biological experiment with three technical repeat. Significant differences between each condition were assessed using a one-way ANOVA test followed by a Tukey test with R software (version 1.4.1106). Several significantly different groups were identified by a letter, with a p-value <0.05.

4.5.2. Lysozyme induces the permeabilisation of *S.* Enteritidis inner membrane

The capacity of hen lysozyme to induce membrane permeabilisation was previously studied in *E. coli*, but not in the natural context of EW (Derde et al., 2013). Using the same method as previously described (section 2.2.3), the permeabilisation of the inner and outer membranes of *S.* Enteritidis pBBC129 (Appendix 1) was studied in the presence of lysozyme at 30 °C. The possible synergetic effect between lysozyme and OT was also examined.

Figure 4.7 shows the outer and inner membrane permeabilisation of *S.* Enteritidis after exposure to different factors at 30 °C. As previously described (section 4.3), the exposure to polymyxin B (positive control) leads to a rapid increase β-lactamase activity detection, indicating permeabilisation of the outer

membrane of *S*. Enteritidis (enzyme activity of 10.6 ± 3.3 milli-A_{490nm}/min) (Figure 4.7A and 4.7C).

Although the HP-nitrocefin concentration slightly increased during cell exposure to SM, the β-lactamase activity remained significantly lower (enzyme activity of 1.7 ± 0.4 milli-A_{490nm}/min) than that achieved with EW (enzyme activity of 5 ± 0.6 milli-A_{490nm}/min) and OT at 13 g/L in EW (enzyme activity of 6.8 ± 0.6 milli-A_{490nm}/min) (Figures 4.7A and 4.7C). The presence of 3.5 g/L lysozyme had no additional effect (enzyme activity of 2.3 ± 0.3 mili-A_{490nm}/min) on the weak β-lactamase activity observed in SM. When OT and lysozyme were combined in the SM, the β-lactamase activity was significantly lower (enzyme activity of 5 ± 0.1 milli-A_{490nm}/min) than that with OT alone (enzyme activity of 6.8 ± 0.6 milli-A_{490nm}/min), and significantly higher than that with lysozyme alone (enzyme activity of 2.3 ± 0.3 milli-A_{490nm}/min) (Figure 4.7A and 4.7C). This result suggests that lysozyme may restrict the access of OT to the outer membrane of *S*. Enteritidis.

These results show that lysozyme alone does not induce outer-membrane permeabilisation under the conditions tested, which is consistent with the findings above showing that lysozyme does not cause *S*. Enteritidis growth restriction. Furthermore, there was no synergetic effect between lysozyme and OT on outer-membrane permeabilisation; indeed, lysozyme slightly reduced the effect of OT on outer-membrane permeabilisation.

Concerning the permeabilisation of the inner membrane, β-galactosidase activity was measured in the presence of the melittin positive control (enzyme activity of 11.8 ± 1.5 milli-A_{405nm}/min with a lag time of 11 ± 3 min) (Figure 4.7B

and 4.7D). In EW, permeabilisation was also confirmed with an enzyme activity of 5 ± 0.3 milli-A_{405nm}/min (Figure 4.7B) and a lag time of 113 ± 4 min (Figure 4.7D). As already shown, inner-membrane permeabilisation was higher in EW than in SM alone (enzyme activity of 3.2 ± 1 milli-A_{405nm}/min with a lag time of 118 ± 23 min) or in SM with 13 g/L OT (enzyme activity of 3 ± 0.7 milli-A_{405nm}/min with a lag time of 109 ± 12 min) (Figure 4.7B and 4.7D). However, inner-membrane permeabilisation was stronger in SM with lysozyme and in SM where lysozyme and OT were mixed (enzyme activity of 8 ± 2 and 8 ± 0.5 milli-A_{405nm}/min, respectively, with lag time of 146 ± 8 and 146 ± 6 min, respectively) than in SM, EW and SM with OT 13 g/L (Figure 4.7B and 4.7D).

The results show the ability of lysozyme to induce *S*. Enteritidis inner-membrane permeabilisation under EW condition. The higher inner-membrane permeabilisation observed for lysozyme with respect to EW suggests that unknown factors in EW protect *S*. Enteritidis against the action of lysozyme on the inner membrane.

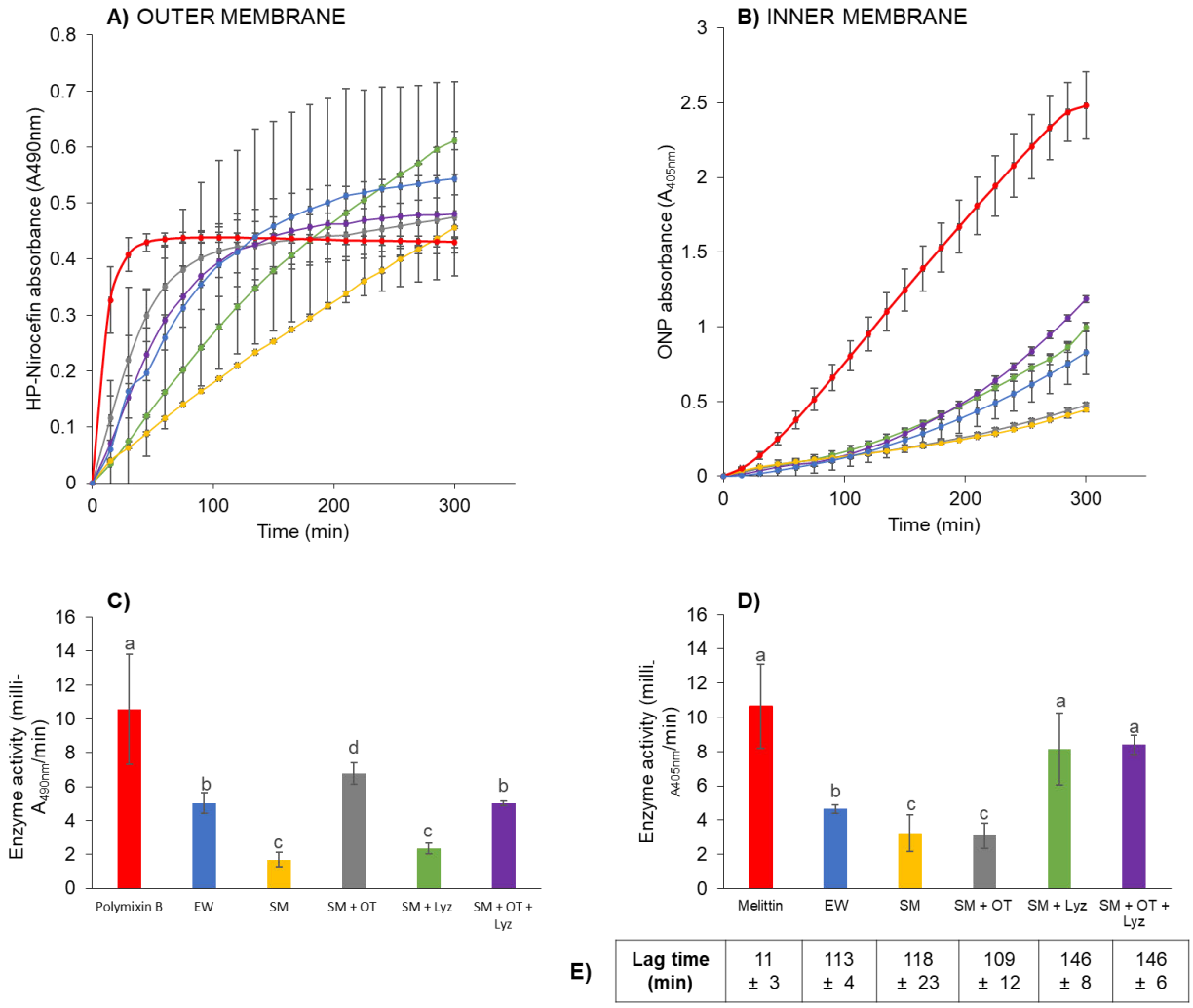

E)

Lag time (min)	11 ± 3	113 ± 4	118 ± 23	109 ± 12	146 ± 8	146 ± 6

Figure 4.7. Impact of lysozyme and OT on *S.* Enteritidis membrane permeabilisation. Monitoring of the permeabilisation of the outer (A) and inner (B) membrane of *S.* Enteritidis (grown to an OD_{600nm} of 0.35) incubated at 30 °C in egg white (blue), synthetic medium (SM) (yellow), SM with ovotransferrin at 13 g/L (grey), SM with lysozyme at 3.5 g/L (green), SM with ovotransferrin at 13 g/L and lysozyme at 3.5 g/L (purple), and polymixin B (50 µg/mL) or melittin (15 µg/mL), respectively (red). Comparison of the Vmax for outer (C) and inner (D) membranes by polymixin B and melittin, respectively, egg white (EW), synthetic medium (SM), SM with ovotransferrin at 13 g/L (SM + OT 13 g/L), SM with lysozyme at 3.5 g/L (SM + Lyz 13 g/L) and SM with ovotransferrin at 13 g/L and lysozyme at 3.5 g/L (SM + OT + Lyz). Additionally, (E) lag time (section 2.2.3, Figure 2.3), corresponding to the delay between the outer and inner membrane permeabilisation was calculated for each medium. Each error bar represents an average of three biological experiments with three technical replicates. Significant differences between each condition were assessed using a one-way ANOVA test followed by a Tukey test with R software (version 1.4.1106). The significantly different groups are identified by letters, with a p-value <0.05.

4.5.3. Lysozyme does not participate in the depolarisation of *S*. Enteritidis inner membrane

No synergetic effect was observed between OT and lysozyme on *S*. Enteritidis membrane permeabilisation. However, it was shown in section 4.3 that EW proteins other than OT should participate in the depolarisation of the *S*. Enteritidis inner membrane. The depolarisation of the inner membrane was measured with *S*. Enteritidis incubated at 30 °C in SM with lysozyme, SM with ovotransferrin or a mix of the two proteins at their concentration in EW (3.5 and 13 g/L, respectively) (Figure 4.8) (section 2.2.4).

Lysozyme had little impact of inner-membrane depolarisation, as indicated by the similar SM and SM plus lysozyme (108 ± 21 and 100 ± 20 RFU, respectively) responses. This suggests that lysozyme is not directly involved in the depolarisation of the *S*. Enteritidis inner membrane at 30 °C by EW. When OT and lysozyme were mixed in SM in the same proportions as in EW (i.e., 13 g/L OT and 3.5 g/L lysozyme), membrane depolarisation was higher than in SM (164 ± 37 RFU). However, this effect was not slightly lower than that obtained with OT (183 ± 38 RFU) alone. The results indicate that there is no synergetic effect between OT and lysozyme in *S*. Enteritidis inner membrane depolarisation.

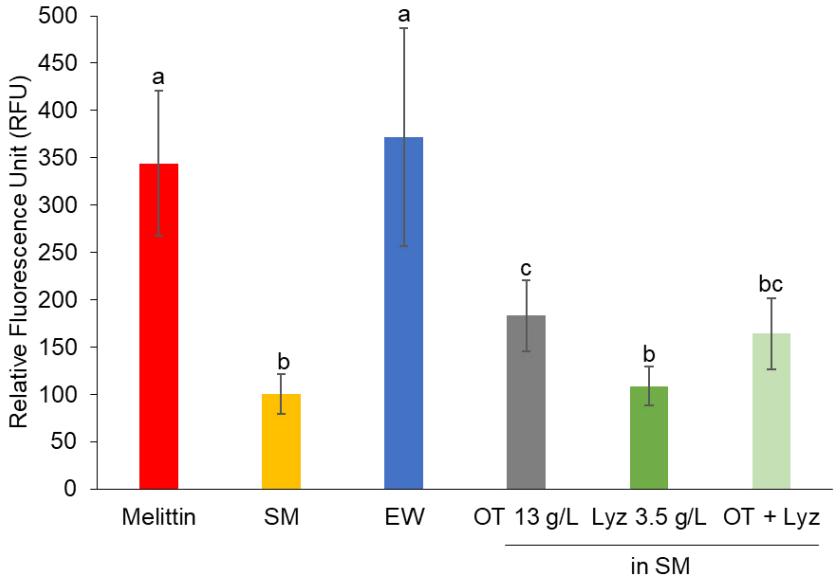

Figure 4.8. Impact of lysozyme and OT on *S*. Enteritidis inner membrane depolarisation. Results show the inner-membrane depolarisation for *S*. Enteritidis at 30 °C after 10 min incubation with melittin (15 µg/mL), synthetic medium (SM), egg white (EW), SM with ovotransferrin at 13 g/L (OT 13 g/L), SM with lysozyme at 3.5 g/L (Lyz 3.5 g/L), and SM with lysozyme or 13 g/L of ovotransferrin and 3.5 g/L of lysozyme (OT + Lyz). Each bar represents an average of four biological experiments with three technical replicates. Significant differences between each condition were assessed using a one-way ANOVA test followed by a Tukey test with R software (version 1.4.1106). Significantly different groups are identified by letters, with a p-value <0.05.

4.6. Discussion and perspectives

4.6.1. Ovotransferrin and *S*. Enteritidis membrane permeabilisation

To study the impact of OT on membrane permeabilisation, the β-lactamase and β-galactosidase activities of *S*. Enteritidis were measured after exposure to SM with OT in comparison to SM alone and EW. Initially, this method was developed by Lehrer et al. (1988) and was successfully used to analyse the impact of hen lysozyme on the permeabilisation of *E. coli* membranes (Derde et al., 2013). Because *S.* Enteritidis lacks a β-galactosidase, strain *S.* Enteritidis pBBC129 was constructed for this study. This strain, producing β-lactamase in the periplasm and β-galactosidase in the cytoplasm, allowed the investigation of outer and inner damage, respectively.

The results presented show that EW, at 30 °C, alters the integrity of *S*. Enteritidis membranes, by inducing permeabilisation of the outer and, to a lesser extent, inner membranes (section 4.1). These results corroborate the findings of the previous work on the antimicrobial activity of EW against *Salmonella* membranes. Indeed, several transcriptional studies have reported the expression of genes involved in the maintenance of the integrity of *S*. Enteritidis membranes in EW (Baron et al., 2017, 2020; Clavijo et al., 2006; Gantois et al., 2008; Huang et al., 2019, 2020; Qin et al., 2019). However, the methods used differed for each study: random mutagenesis (Clavijo et al., 2006), *in vivo* expression technology (Gantois et al., 2008), directed mutagenesis (Gantois et al., 2008; Huang et al., 2020), qualitative proteomics (Qin et al., 2019), global transcriptomic analysis using microarrays (Baron et al., 2017, 2020) and RNAseq (Huang et al., 2019). The experimental conditions employed also differ with gene expression detected after exposure to: EW for 24 h at 27 °C (Clavijo et al., 2006); whole egg for 24 h at 37 °C (Gantois et al., 2008), 80% EW for 0, 6 and 12 h, at 37 °C (Huang et al., 2019, 2020); 50-100% EW for 6 h at 37 °C (Qin et al., 2019); and EWMM (i.e. EWF with 10% EW) or EWF for 7, 25 and 45 min at 45 °C (Baron et al., 2017, 2020). Nevertheless, all the studies agree that most genes/proteins induced after exposure to EW are involved in the membrane damage response and that many are controlled by the CpxAR system which mediates the response to membrane stress and other environmental stress factors such as deleterious pH (Raffa & Raivio, 2002).

Previous studies observed that the *E. coli* outer membrane is permeabilised by human transferrin, lactoferrin (Ellison et al., 1988) and ovotransferrin (Aguilera et al., 2003) at 37 °C. Consistently, the present results

show that at higher OT concentration, an increased outer-membrane permeabilisation occurs (section 4.2.1). At 13 g/L OT (its concentration in EW) in SM (mimicking EW ionic composition and pH), the permeabilisation of the outer membrane was significantly higher than in EW. However, in EW, OT is combined with other EW proteins and its action may therefore be less effective than (as was observed) when provided in the absence of such proteins. Indeed, it may be that the interaction of OT with the outer membrane is competitively limited by the presence of the other EW proteins.

However, no significant differences were observed in outer-membrane permeabilisation of *S*. Enteritidis for apo-OT and iron-loaded OT at 30 °C, whatever the level of iron saturation employed (section 4.2.2). This finding suggests that the metal-chelating activity OT is not involved in outer-membrane permeabilisation. However, this result differs from those of Ellison et al. (1988) in *E. coli.* The reason for this difference is unclear but may relate to differences between the corresponding species, and between OT, and transferrin (e.g. in terms of glycosylation pattern) and lactoferrin (e.g. in terms of metal affinity). Furthermore, these authors reported LPS release in minimal medium at pH 8 without OT, suggesting a role of pH in the membrane instability (Ellison et al., 1988). The present results show a slight increase in HP-nitrocefin concentration after exposure to SM alone at pH 9 (section 4.2) suggesting that outer-membrane instability is induced by SM. Thus, it is possible to conclude that the ability of OT to permeabilise the *S*. Enteritidis outer membrane does not depend on its chelating activity. It should be noted that the ability of lysozyme to penetrate the outer membrane, despite its size, was previously indicated in *E. coli* (Derde et al., 2014; Pellegrini et al., 2000).

However, OT did not provoke permeabilisation of the inner membrane of *S*. Enteritidis (section 4.2) whatever the concentration (section 4.2.1) tested (section 4.2.2). The permeabilisation of the inner membrane after EW exposure should therefore be attributed to other EW proteins. Indeed, the ability of hen lysozyme (present at 3.5 g/L in EW) to permeabilise the *E. coli* outer and inner membrane at 37 °C was shown previously at pH 7.4 (Derde et al., 2013). Furthermore, a slight increase in inner-membrane permeabilisation was observed when OT was saturated with iron (section 4.2.2); however, this result might not be directly correlated with the iron-chelating activity of OT. Indeed, no control consisting of SM plus iron citrate was performed to confirm this finding.

4.6.2. Ovotransferrin and *S*. Enteritidis inner membrane depolarisation

In this study, the change of the potential (i.e. depolarisation) of the inner membrane of *S*. Enteritidis by EW and OT was investigated using a $DiSC_3(5)$ probe with a spectrofluorescence method, developed by Epand et al. (2010). A strong depolarisation of the *S*. Enteritidis inner membrane was observed after exposure to EW in comparison to SM. This is consistent with the literature. Indeed, depolarisation of the inner membrane of *S*. Enteritidis was detected after EWMM exposure but not after EWF exposure (Baron et al., 2020). Furthermore, these authors reported that the *psp* genes were up-regulated by *S*. Enteritidis after 45 min exposure to EW at 45 °C (Baron et al., 2017, 2020) but down-regulated in EWF without EW protein (Baron et al., 2020). The *psp* genes are involved in the maintenance of the proton motive force and participate in the management of membrane stress (Joly et al., 2010 for a review). Taken together, these results support the ability of EW to cause the depolarisation of the *Salmonella* inner membrane.

Concerning OT, the results show that the higher the OT concentration, the greater the extent of inner-membrane depolarisation (section 4.3, Figure 4.4A). However, a significant OT-depolarisation effect was only provoked when OT was provided at the maximum concentration explored (13 g/L). The depolarisation of the cytoplasmic membrane by OT (at 13 g/L) has already been reported for the Gram-positive bacterium, *B. cereus*, in EWF using the same method of measurement (Baron et al., 2014). A dissipation of the *E. coli* electric membrane potential was observed by Aguilera et al. (2003) who showed that ΔΨ dissipation was dependent on OT concentration (a similar effect to that observed here). The depolarisation of the cytoplasmic membrane may be directly associated with the membrane permeabilisation. Indeed, a disruption of the membrane can alter the periplasmic environment, leading to a modification of ion/metabolite import/export to/from the periplasm (Moravej et al., 2018). Furthermore, depolarization can also be caused by the presence of charged molecules in the periplasm resulting in a change in the equilibrium between external and internal charges leading to ion leakage, without necessarily allowing the passage of larger molecules (Epand et al., 2010). This latter depolarisation mechanism is the most likely cause in this case because no inner-membrane permeabilisation by OT was observed (section 4.2). Indeed, at pH 9, OT has a predicted negative charge (Legros et al., 2021), which may modify the electrostatic charge in the periplasm and lead to a disorder in $\Delta\Psi$. Thus, it is possible to hypothesise that at pH 9 the negatively-charged OT is able to accumulate in the periplasm causing a disturbance in membrane potential. This hypothesis is supported by the fact that the depolarisation of the inner membrane was lower when OT was saturated with iron (section 4.3, Figure 4.4B). Such saturation by ferric iron would be expected to lower the overall

negative charge of OT. Thus, Yoshioka et al. (1966) using a polyacrylamide-gel electrophoresis in Tris-EDTA-borate buffer at pH 9.2 showed that diferric-transferrin has a lower mobility than the iron-free protein, suggesting a lower negative charge between the two OT forms at this pH. To test this hypothesis, other experiments are needed to explore the exact mechanism by which iron influences the impact of OT.

However, OT did not fully reiterate the full, strong depolarisation effect induced by exposure to EW (section 4.3, Figure 4.4A). Thus, it is likely that other EW proteins or EW peptides also contribute to the EW-induced membrane depolarisation effect observed for *S*. Enteritidis. Several EW molecules such as lysozyme, defensins and bactericidal permeability-increasing proteins (BPI) or other proteins (Baron et al., 2016 for a review) or unknown peptides may thus also contribute to the observed depolarisation effect of EW.

4.6.3. Cooperation between ovotransferrin and other egg-white proteins

In this study, a hypothetic synergetic effect between lysozyme and OT on *S*. Enteritidis membrane damage was explored. A synergetic effect between transferrin and lysozyme has been reported by several authors. Thus, the addition of lactoferrin and lysozyme showed a reduction of *S*. Typhimurium and *E. coli* O111 growth in peptone medium at 37 °C (Ellison & Giehl, 1991; Suzuki et al., 1989). Additionally, a synergetic effect on *L. monocytogenes* was observed between lysozyme and OT after the addition of 100 mM of bicarbonate in BHI at 37 °C, but not on *E. coli* at 35 °C (Ko et al., 2008, 2009). However, in this study, no growth limitation was observed after the addition of the two EW proteins at their concentrations found in EW (section 4.5.1, Figure 4.6). Opposite to the results obtained for OT, lysozyme showed an ability to permeabilise the

S. Enteritidis inner membrane but not the outer membrane in SM at 30 °C. In contrast, hen lysozyme was previously shown to induce both outer- and inner-membrane permeabilisation in *E. coli* at 37 °C, pH 7 (Derde et al., 2013). The present results suggest a cooperation of the two EW proteins to provoke membrane damage but not a synergetic effect. Thus, the permeabilisation of the outer membrane by OT seems to allow lysozyme to gain access to the peptidoglycan, stimulating the induction of the expression of the lysozyme inhibitor genes in response. Indeed, *ydhA* and *SEN1802* lysozyme inhibitors were up-regulated by *S*. Enteritidis after exposure to EWMN but down-regulated in EWF at 45 °C (Baron et al., 2017, 2020). Nevertheless, even in the absence of OT, lysozyme was able to induce inner membrane perturbation (section 4.5.2). This result confirms the ability of SM at pH 9 to slightly modulate outer-membrane permeability. Additionally, the presence of lysozyme did not influence the ability of OT to provoke the dissipation of the pmf of the inner membrane. These results clearly implicate other EW molecules in this role. Indeed, BPI and defensins were identified in EW and they are known for their ability to disturb the bacterial envelope, even if to date, no attempt has been made to provide evidence for this role in EW (Baron et al., 2016 for a review).

4.6.4. Future work

All the experiments were performed with SM since EWF contains antimicrobial peptides that may induce membrane damage (Cochet et al., 2021). However, SM alone seems to induce slight permeabilisation of the outer membrane. Thus, to confirm if this impact is dependent on the medium or the pH, it would be interesting to investigate membrane permeabilisation (i) by EWF and (ii) at pH 7. To confirm the link between depolarisation and the overall charge of

OT, the same experiment could be performed at pH 7. Finally, further investigations need to be performed on the impact of other EW-molecules such as BPI and defensins on *S*. Enteritidis membrane damage to explain the observed differences between the impact of EW and OT/lysozyme on the *S*. Enteritidis envelope.

4.6.5. Conclusion

In this chapter, the ability of OT to induce bacterial membrane damage was investigated. OT appears to permeabilise the outer membrane of *S*. Enteritidis and cause depolarisation of the inner membrane, at 30 °C, under EW conditions. No synergetic effect was observed between lysozyme and OT, but a possible cooperation was suggested. However, despite the ability of EW to provoke bacterial membrane damage, the survival of *S*. Enteritidis is not affected. Indeed, bacteria can maintain their membrane integrity by deploying different systems. In the next chapter, the regulation of one of these systems (the Psp system) by EW and OT is considered.

Chapter 5.
Regulation of *psp* genes by ovotransferrin

5.1. Introduction

In Chapter 4, the ability of OT to induce *S*. Enteritidis membrane damage was demonstrated. Indeed, the results showed that OT can permeabilise the outer membrane of *S*. Enteritidis and provoke depolarisation of the inner membrane. When bacterial membranes are compromised, several systems (CpxAR, BaeSR, Sigma E factor (σE), Rcs, and Phage Shock Proteins (Psp) are expressed to maintain their integrity (Hews et al., 2019). Such membrane damage also occurs in the natural context of EW. Indeed, several studies have reported the induction of various genes involved in *S*. Enteritidis membrane repair after EW exposure (Baron et al., 2017, 2020; Gantois et al., 2008; Huang et al., 2019, 2020; Qin et al., 2019). Among these genes are those within the *psp* regulon, which are induced by *S*. Enteritidis after EW exposure (but not in absence of ≥10 kDa EW proteins) (Baron et al., 2017, 2020). The *psp* genes are generally expressed when the pmf is dissipated. Thus, the findings of Baron et al. (2017, 2020) implicate EW proteins (>10 kDa) in the observed induction of the *psp* genes. As OT participates in the depolarisation of the inner membrane, resulting in a loss of the pmf, OT could potentially be responsible for this *psp* regulon response.

In this chapter, the transcription of *psp* genes by EW and OT under EW conditions was studied using transcriptional fusions (generated as part of this study) alongside qRT-PCR.

5.2. Generation of *psp-lacZ* transcriptional fusions

The *psp* regulon is composed of seven genes: *pspF*, *pspA*, *pspB*, *pspC*, *pspD, pspE* and *pspG*. Their organisation is represented in Figure 5.1. The *pspF*

and pspABCD are co-located in the genome whereas the *pspG* gene is positioned at a separate locus (Figure 5.1). Membrane stress, such as protein mislocalisation or dissipation of the pmf, acts as a signal for the *psp* response. PspB and C act as membrane-stress sensors that transmit a signal to PspF, initially binding to PspA. In its free form, PspF can activate the transcription of *pspA* and *pspG* (Darwin, 2005 for a review). The role of all *psp* genes is not completely established. PspA, PspG and PspD may be involved in respiration and phospholipid biosynthesis through the modulation of glycerol-3-phosphate metabolism (Jovanovic et al., 2006). Furthermore, PspA is thought to block proton leakage by binding membrane phospholipids (Kobayashi et al., 2007b).

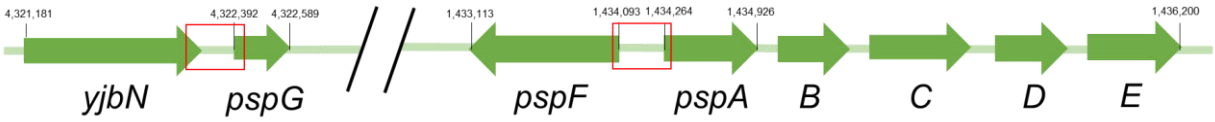

Figure 5.1. Organisation of *psp* genes operon in *S*. Enteritidis NCTC13349 genome. Each gene is represented by the green arrow and the direction indicates the polarity. The promoter regions cloned into pRS1274 are represented by the two red squares. Data were derived using Geneious Prime and the chromosome sequence of accession number AM933172.1.

To study the regulation of *psp* genes, *pspABCDE*, *pspF,* and *pspG*, their predicted promoter regions, were cloned upstream of the promoterless *lacZ* in pRS1274 vector. This vector is a medium copy number plasmid with a size of 10,746 bp. It contains a pBR322 origin of replication and an ampicillin resistance marker. The presence of a promoterless *lac* operon (*lacZYA*) allows the study of transcription by cloning of promoter-regions-of-interest directly upstream into the *Xma*I-*Bam*HI-*Eco*RI (Figure 5.2) multicloning site located just upstream of *lacZ* (Simons et al., 1987). The pRS1274 plasmid was successfully used to study the *yohD* and *yohC* intergenic regions of *S*. Typhimurium and it is therefore

considered suitable for studying the regulation of *psp* genes in *S*. Enteritidis (Kenyon et al., 2007).

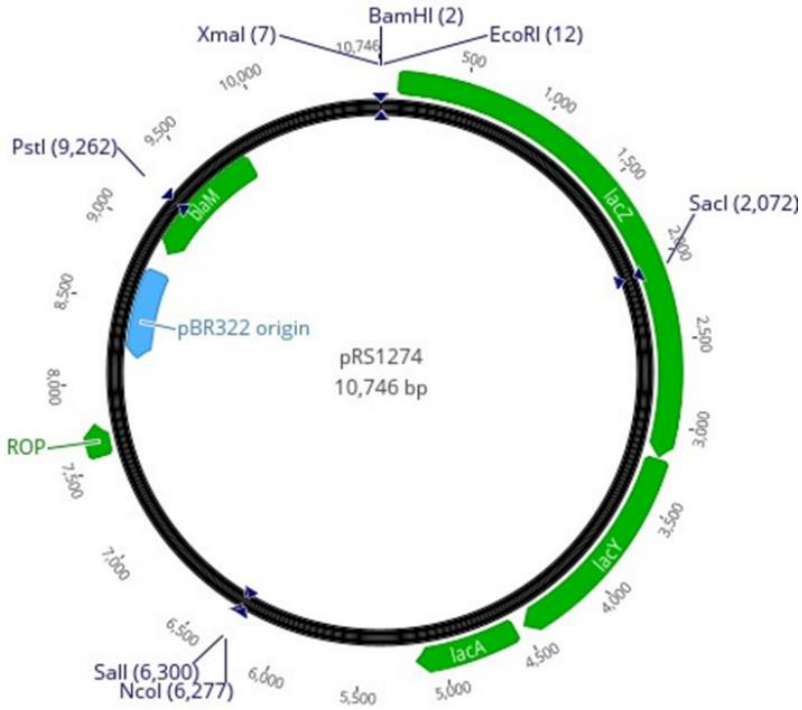

Figure 5.2. Map of expression vector pRS1274. Each gene is represented by a green arrow and the direction indicates the polarity. The blue arrow corresponds to the ColEI origin of replication (*oriV*). Restriction sites and their locations are indicated in black.

For cloning purposes, the putative promoter regions of *pspA*, *pspF* and *pspG* were amplified by PCR (section 2.2.9) and cloned into the cloning vector pJET1.2/blunt (ThermoScientific^{TM}). This vector enhances the cloning efficiency and allows a powerful selection of recombinant plasmids. Indeed, it encodes a lethal restriction enzyme (*Eco*471R) at the ligation site which is disrupted when DNA fragments are inserted at the ligations site. This lethality eliminates non-recombinant transformants. Next, the DNA inserts from pJET1.2/blunt were

cloned into the transcriptional reporter plasmid (pRS1274) to enable the study of *psp*-promoter activity. The cloning steps are summarised in Figure 5.3.

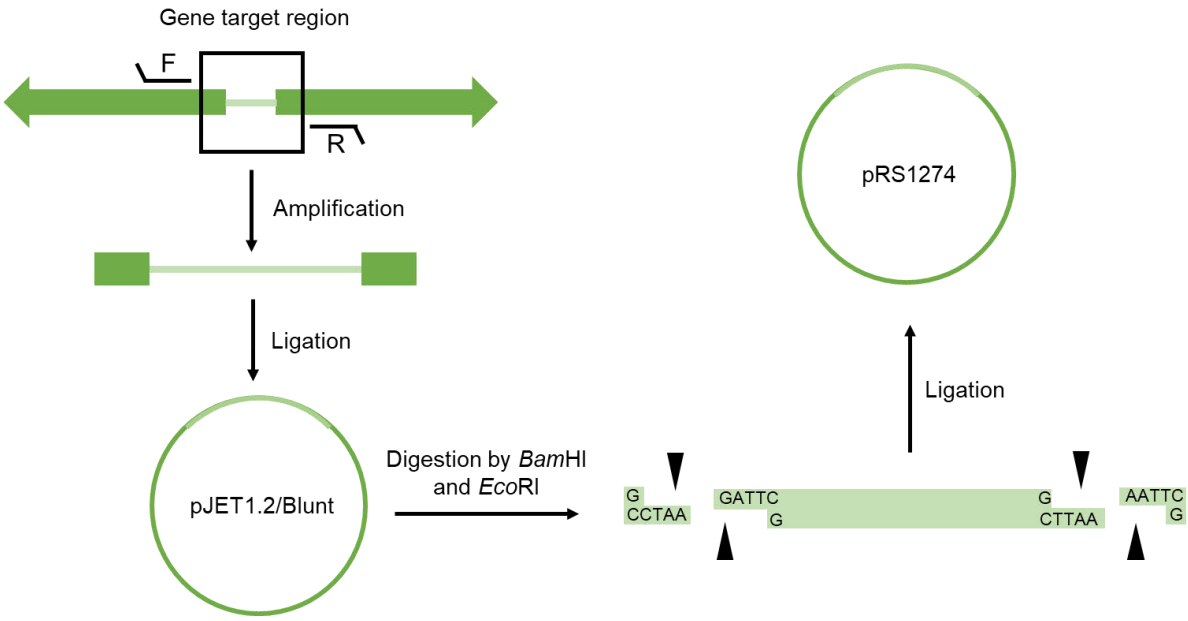

Figure 5.3. Cloning steps. Summary of steps taken to clone putative promoter regions into pRS1274. The putative promoter regions were amplified by PCR and ligated into pJET1.2/Blunt. The resulting plasmid carrying the DNA insert was digested with *Bam*HI and *Eco*RI and then ligated into double-digested pRS1274.

The pRS1274 plasmid DNA was obtained from the lab stock and transformed into *E. coli* TOP10 competent cells (section 2.2.6.1). Transformants were selected on a selective medium containing ampicillin and plasmid DNA was extracted using a GeneJET Plasmid Miniprep Kit (ThermoScientific™) (section 2.2.7.1). The size of the plasmid (10,752 bp) was then checked by agarose gel electrophoresis (section 2.2.10).

S. Enteritidis NCTC13349 DNA was extracted using a GeneJET Genomic DNA Purification Kit (ThermoScientific™) (section 2.2.7.2) and used as a PCR template to amplify the putative promoter region of the selected genes. The concentration and purity (A260/280 and A230/260) of the DNA were measured using a Nanodrop (section 2.2.7.4).

The Geneious Prime program (https://www.geneious.com/) was used to design all the primers necessary to amplify the putative promoter regions of the *psp* genes from *S*. Enteritidis NCTC13349 (AM933172.1). To ensure the amplification of the entire promoter regions, ~100 bp of the upstream gene was included in the PCR amplification (Figure 5.1). The genes *pspA* and *pspF* share the same intergenic region, so identical regions were amplified using primers designed in both orientations. Restriction sites were added at the 5′ end of each primer to match the pRS1274 cloning sites: *Eco*RI (GAATTC) for the downstream site; and *Bam*HI (GGATCC) for the upstream site. The list of primers used in this chapter is summarised in Table 2.3 (section 2.1.3) and the sequences of the amplified promoter regions are shown in Appendix 3.

Before being cloned into pJET1.2/blunt, the putative promoter regions were amplified using High Fidelity Phusion DNA Polymerase (Thermo Scientific^{TM}) (section 2.2.9). The expected sizes of the putative promoter regions were 362 bp for both *pspA* and *pspF* and 457 bp for *pspG.* The target sequences were amplified successfully as confirmed by the band sizes obtained upon agarose gel electrophoresis (section 2.2.10) (Figure 5.4).

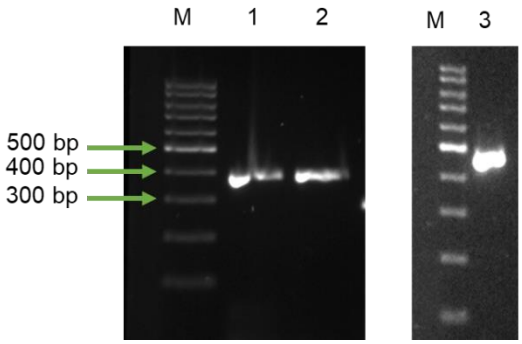

Figure 5.4. Gel electrophoresis of *psp* promoter regions amplified by PCR. Lanes M contain a 100 bp RiboRuler DNA ladder (100-1000 bp) (ThermoScientific™); lanes 1, 2 and 3 correspond to the amplification of the *pspA*, *pspF* and *pspG* promoter regions with expected sizes of 362, 362 and 457 bp, respectively. The electrophoresis was performed for 1 h at 80 V on a 1.7% agarose TBE gel.

To eliminate any excess of dNTP, primers and salts, the PCR products were purified using a GeneJET PCR Purification Kit (section 2.2.11). The successful isolation of the purified PCR products was confirmed by agarose gel electrophoresis (section 2.2.10) (Figure 5.5).

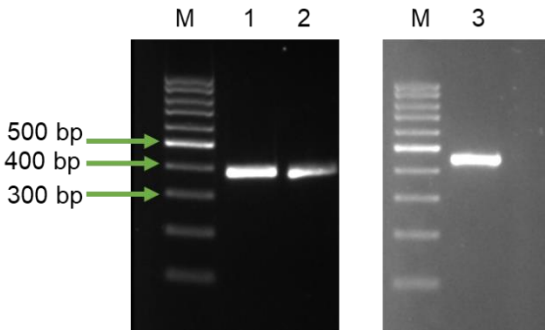

Figure 5.5. Gel electrophoresis of PCR-amplified *psp* promoter regions following purification. Lane M contains a 100 bp RiboRuler DNA ladder (100-1000 bp) (ThermoScientific™); lanes 1, 2 and 3 correspond to the amplification of the *pspA*, *pspF* and *pspG* promoter regions with expected sizes of 362, 362 and 457 bp, respectively. The electrophoresis was performed for 1 h at 80 V on a 1.7% agarose TBE gel.

The putative promoter regions were then ligated into pJET1.2/blunt using the CloneJET PCR cloning site (Thermo Scientific™) (section 2.2.14). The ligation mixtures were transformed into chemically *E. coli* Top10 competent cells (section

2.2.6.1) and transformants were selected on LB agar plates with ampicillin after incubation overnight at 37 °C. Due to the presence of the *blaM* gene in pJET1.2/blunt, only colonies carrying pJET1.2 plasmids were expected to grow on the LB agar plates with ampicillin. The plasmid DNA of 12 transformants (four for each of the three clonings), was extracted using the GeneJET miniprep kit (Thermo Scientific™) (section 2.2.7.1). The size of the extracted plasmids was determined by agarose gel electrophoresis (figure 5.6). The expected size of the circularised plasmid is 2,974 bp whereas the size of the plasmid carrying a putative promoter region should be 3,336 bp for *pspA* and *pspF*, and 3,431 for *pspG*. Figure 5.6 shows that all 12 isolated plasmids had the expected size but could not be readily distinguished from the original vector.

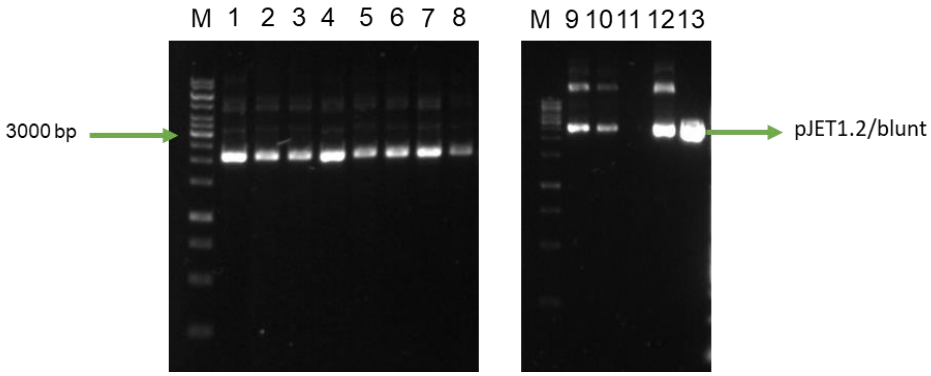

Figure 5.6. Gel electrophoresis of candidate pJET1.2-*psp′* plasmid DNA. Lane M contains the 1000 bp RiboRuler DNA ladder (250-10000 bp) (ThermoScientific™); lanes 1 to 4 correspond to potential pJET1.2 recombinants carrying the *pspA′* insert; lanes 5 to 8 correspond to potential pJET1.2 recombinants carrying the *pspF′* insert; lanes 9 to 12 correspond to potential pJET1.2 recombinants carrying the *pspG′* insert; and lane 13 corresponds to the pJET1.2/blunt vector. The electrophoresis was performed for 1 h at 80 V on a 1.2% agarose TBE gel.

A more precise verification of the isolated plasmids was performed by double digestion with *Bam*HI and *Eco*RI (section 2.2.12) as these sites flank the DNA inserts. Thus, after digestion of the plasmid by these two restriction enzymes, two bands should appear, one corresponding to the vector and another to the *psp*

insert. Agarose gel electrophoresis (section 2.2.19) showed that two bands did indeed appear for each recombinant plasmid with the expected sizes (for the insert, ~350 bp for *pspF* and *pspA*, ~450 bp for *pspG*; Figure 5.7). Sanger sequencing (Eurofins) was used to confirm the presence of the DNA insert and the absence of mutations. Primers used for sequencing are listed in Table 2.4, section 2.1.3. DNA sequences were aligned to the *S*. Enteritidis NTCT13349 genome (accession number: AM933172.1) using Nucleotide BLAST and a match of 100% identity was observed.

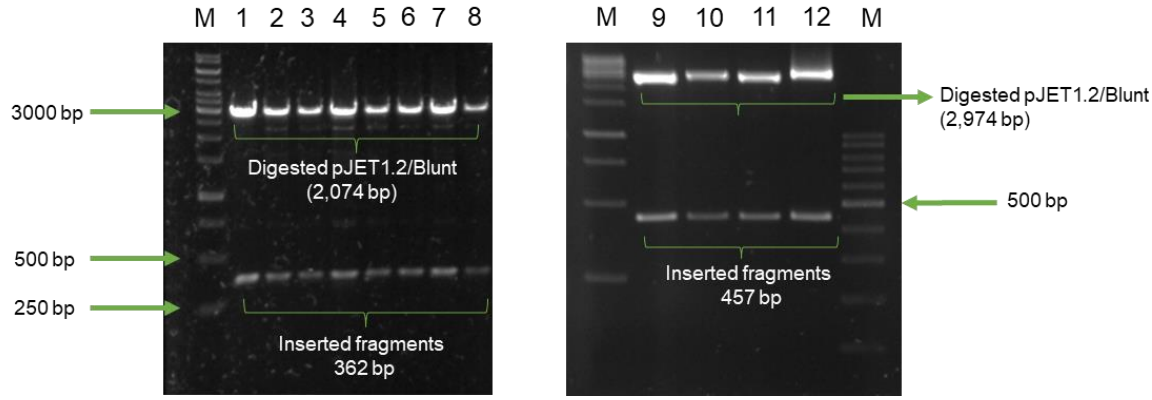

Figure 5.7. Gel electrophoresis of pJET1.2-*psp* recombinant plasmids after double digestion with *Bam*HI and *Eco*RI. Lane M contains the 1 kb RiboRuler DNA ladder (250 – 10,000 bp) or 100 bp RiboRuler DNA ladder (100-1000 bp) (far right) (ThermoScientific™); lanes 1 to 4 correspond to potential pJET1.2 recombinants carrying the *pspA'* insert; lanes 5 to 8 correspond to potential pJET1.2 recombinants carrying the *pspF'* insert; lanes 9 to 12 correspond to potential pJET1.2 recombinants carrying the *pspG'* insert. The electrophoresis was performed for 1 h at 80 V on a 1.2% agarose TBE gel.

Inserts were purified from the agarose gel (section 2.2.13), and after double digestion, the *psp* promoter regions were ligated with double-digested pRS1274, using T4 DNA ligase (section 2.2.14). The ligation mixture was then transformed into competent *E. coli* TOP10 (section 2.2.6.1) and 12 transformants (four for each cloning) were selected on LB agar containing ampicillin and X-Gal. Indeed, recombinant bacteria were selected using the blue/white screening method in LB

agar containing 5-bromo-4-chloro-3-indolyl-beta-D-galacto-pyranoside (X-Gal). Plasmid DNA was extracted from the selected transformants using a GeneJET miniprep kit (ThermoScientific™) (section 2.2.7.1) and the expected sizes (11,108 bp for *pspA'* and *pspF'*, and 11,203 for *pspG'*) were confirmed by agarose gel electrophoresis (section 2.2.11) (Figure 5.8)

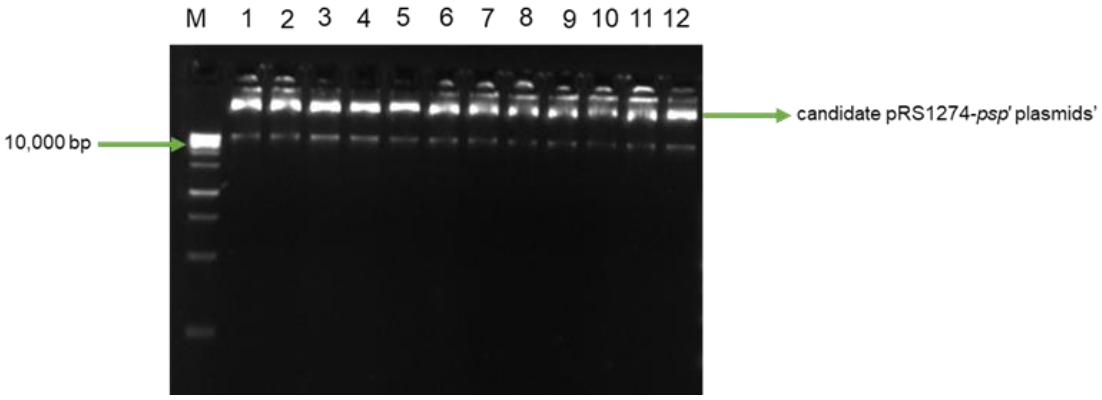

Figure 5.8. Gel electrophoresis of candidate pRS1274-*psp* recombinant plasmids. Lane M contains the 1 kb RiboRuler DNA ladder (250 – 10,000 bp) (ThermoScientific™); lanes 1 to 4 correspond to potential pRS1274 recombinants carrying the *pspA'* insert; lanes 5 to 8 correspond to potential recombinants carrying the *pspF'* insert; lanes 9 to 12 correspond to potential recombinants carrying the *pspG'* insert. The electrophoresis was performed for 1 h at 80 V on a 1.2% agarose TBE gel.

Plasmid DNA of each of the candidate pRS1274-*psp'* plasmids was double digested with *Bam*HI and *Eco*RI to confirm the presence of the putative promoter regions (section 2.2.12). If the plasmid carried the DNA insert, two bands were expected. One corresponding to the empty vector (10,746 bp) and another one corresponding to the insert (362 bp for *pspF'* and *pspA'*, 457 bp for *pspG'*). Bands were visualised on an 1.2% agarose gel (section 2.2.10) and two bands corresponding to pRS1274 and the putative promoter regions were visible in each case (Figure 5.9). Sanger sequencing (Eurofins) was used to confirm the presence of the DNA insert and the absence of mutations. Primers used for sequencing are listed in Table 2.3, section 2.1.3. DNA sequences were aligned

to *S*. Enteritidis NTCT13349 genome (Accession number: AM933172.1) using Nucleotide BLAST and a match of 100% identity was observed in each case. The resulting plasmids (one of each) were thus designated pRS1274-*pspA-lacZ*, pRS1274-*pspF-lacZ* and pRS1274-*pspG-lacZ.*

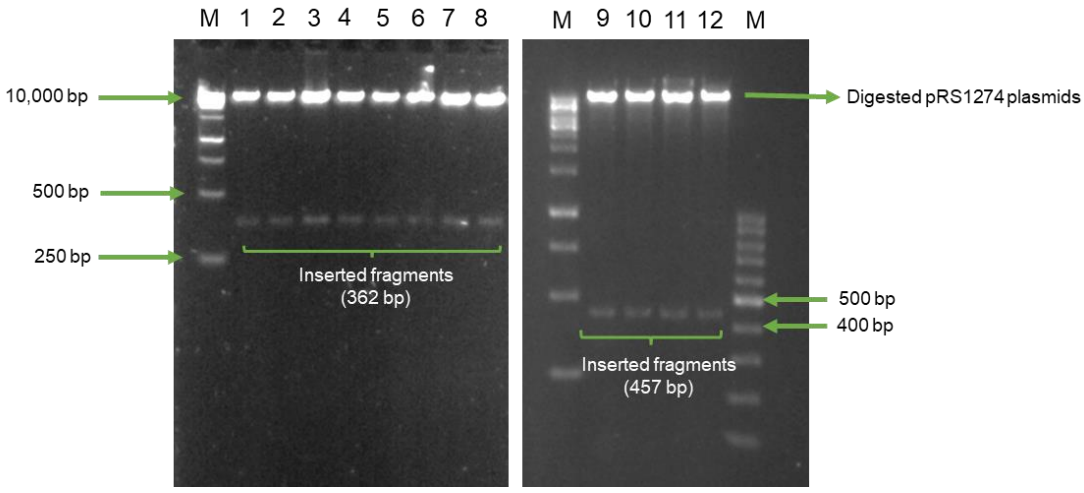

Figure 5.9. Gel electrophoresis of double-digested candidate pRS1274-*psp* recombinant plasmids. Lanes M contain a 1 kb RiboRuler DNA ladder (250 – 10,000 bp) or 100 bp RiboRuler DNA ladder (100-1000 bp) (far right) (ThermoScientific™); lanes 1 to 4 correspond to pRS1274 recombinants carrying the *pspA'* insert; lanes 5 to 8 correspond to recombinants carrying the *pspF'* insert; lanes 9 to 12 correspond to recombinants carrying the *pspG'* insert. The electrophoresis was performed for 1 h at 80 V on a 1.2% agarose TBE gel.

Each *psp-lacZ* plasmid was transformed into *S*. Enteritidis for the study of the *psp* expression response. Thus, four isolates for each *psp-lacZ* plasmid were transformed into *S*. Enteritidis electro-competent cells by electroporation (sections 2.2.6.2 and 2.2.15) and transformants were selected on LB agar containing ampicillin and X-Gal. The presence of the plasmid (11,108 bp for *pspA* and *pspF*, 11,203 for *pspG*) was confirmed by agarose gel electrophoresis (section 2.2.11) of the plasmid DNA isolated from the *S*. Enteritidis transformants (Figure 5.10). To confirm the identities of the plasmids, double digestion (*Bam*HI and *Eco*RI) of the plasmid DNA was performed (section 2.2.12). However,

S. Enteritidis possesses several host restriction systems, and the plasmid DNA was degraded in the presence of restriction enzymes (Roer et al., 2016). Thus, the presence of the putative promoter region was analysed by Nanopore 30 sequencing (service provided by Source Bioscience).

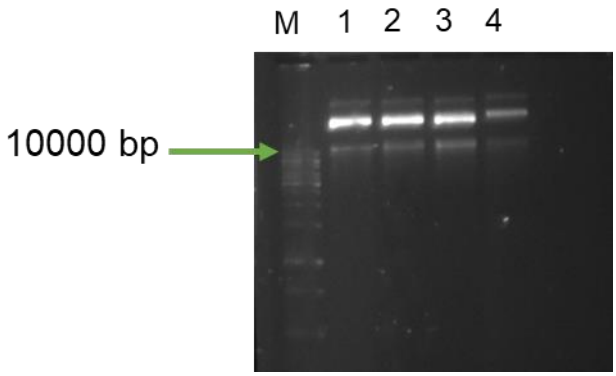

Figure 5.10. Gel electrophoresis of pRS1274-*psp-lacZ* plasmid DNA isolated from *S.* Enteritidis. Lane M contains the 1 kb RiboRuler DNA ladder (250 – 10,000 bp) (ThermoScientific™); lane 1 contains pRS1274-*pspA-lacZ*; lane 2, pRS1274-*pspF-lacZ*; lane 3, pRS1274-*pspG-lacZ*; and lane 4, pRS1274. The electrophoresis was performed for 1 h at 80 V on a 1.2% agarose TBE gel.

5.3. Prediction of the promoter regions using bioinformatic tools

The promoter regions (-10 and -35 sites) of *pspF*, *pspA* and *pspG* were predicted bioinformatically using BPROM (http://www.softberry.com/). This tool recognises promoters regulated by σ70 factor with around 80% accuracy and efficiency for *E. coli* (Solovyev & Salamov). Thus, each amplified DNA sequence was analysed, and putative promoter regions were predicted using this specific program (Figure 5.11; Table 5.1). The promoter is an essential element for gene transcription and regulation. Two upstream conservative sequences, located near to the transcription start site (TSS), constitute the prokaryotic promoter: -10 and -35 sequence elements. These latter are relatively conserved, with

consensus sequence TATAAT at -10 and TTGACA at -35 site, optimally separated by 17 bp. For *pspF*, BPROM predicted a -10 motif of (aATaAT) with 4/6 matches and a -35 motif (TTtAtA) with 4/6 matches. However, the -10 and -35 sites are spaced a 16 bp (38 GC%) which is close to the optimum for a functional promoter (Klein et al., 2021) (Figure 5.11A, Table 5.1). For *pspA*, the TAaAAc -10 (4/6 matches) and TTtAtt -35 sequence (3/6 matches) were predicted, with a spacer of 17 bp, which is optimal (50% GC) (Figure 5.11B, Table 5.1). Finally, the program indicated a -10 site (cATgAT; 4/6 match) and a -35 site (TTtAtA; 4/6 match) with a spacer of 21 bp (11% GC) (Figure 5.11C, Table 5.1) for *pspG*. As indicated above, the optimal spacer length is 17 bp for a σ70 promoter, which suggests that the predicted *pspG* promoter is unlikely to be valid. Also, a GC-rich spacer induces a reduction of promoter activity and thus the moderate to low GC contents of the 3 spacers indicated above should support expression (Hook-Barnard & Hinton, 2009). However, it should be noted that in *E. coli*, *pspA* and *pspG* are under the control of σ54 whilst only *pspF* is dependent on σ70 (Jovanovic et al., 1996; Weiner et al., 1991). Sigma 54 promoters consist of a -12 (GC) and -24 (GG) element: tGGcacgnntntTGCa (Bonocora et al., 2015). Based on this consensus, the σ54 promoter sequences were predicted for all *pspF, pspA* and *pspG*. Indeed, even if the transcription of *pspF* is dependent of σ70, it shares the same intergenic region as *pspA* and thus its expression may be influenced by σ54-dependent transcription of *pspA*. Furthermore, a σ54 promoter was identified in this intergenic region in *E. coli*, controlling the transcription of the *pspABCDE* operon (Jovanovic et al., 1996). Thus, a sequence that may correspond to a σ54 promoter was found in the intergenic region between *pspF* and *pspA* (Figure 5.11A and 5.11B). This sequence

(tGGttaatacaattTGCg) matches with the consensus defined previously, as the two motifs GG and TGC are conserved, separated by 11 bp. A σ54 promoter was also predicted for *pspG* (tGGggagcgactaTGCt) and seems to correspond to the consensus sequence. However, the exact location of the *psp* promoter in *S.* Enteritidis requires further investigation.

A

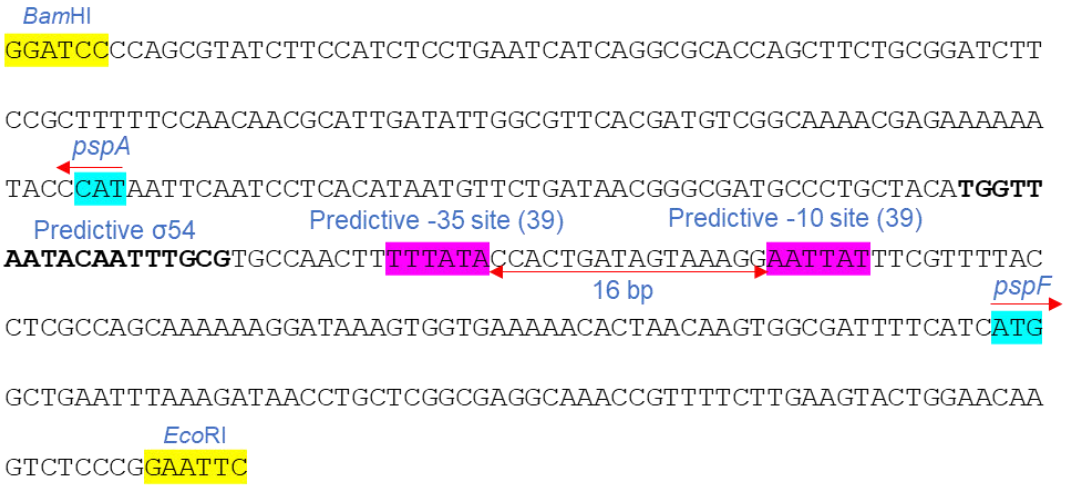

B

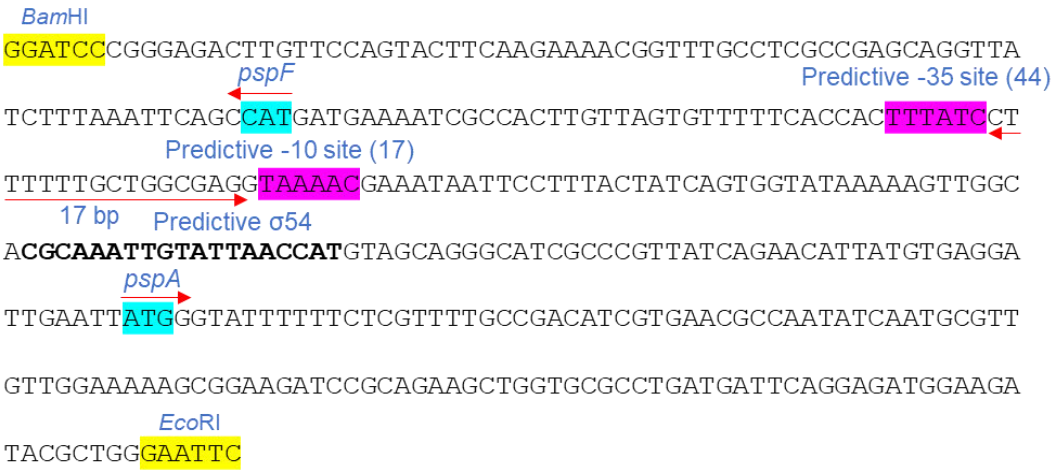

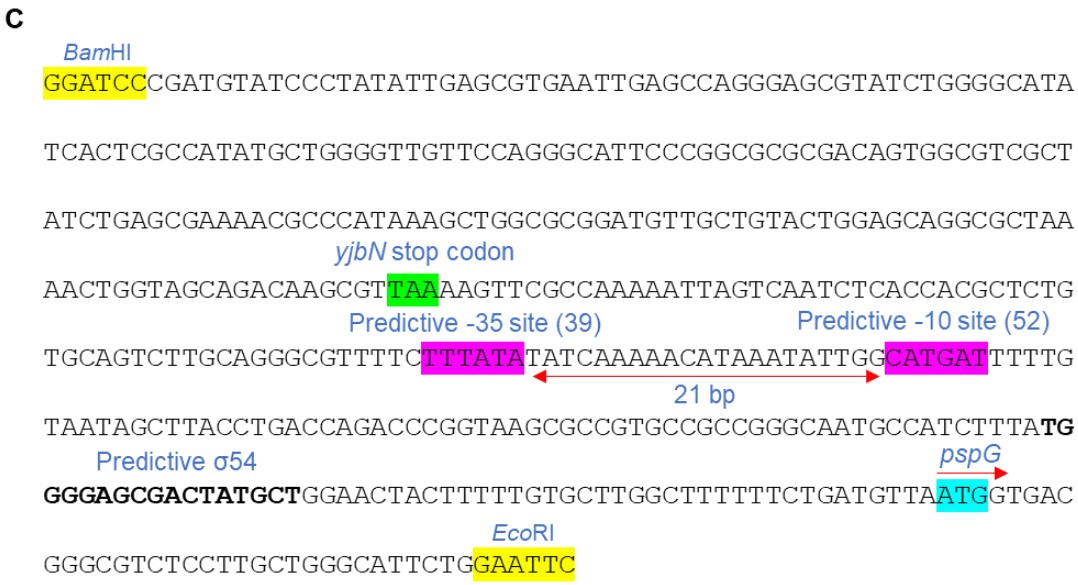

Figure 5.11. Bioinformatic predictions of the putative *psp* promoter regions using BPROM. Putative promoter regions of (A) *pspF*, (B) *pspA* and (C) *pspG*. Restriction cloning sites are in yellow, stop codons are in green, start codon are in turquoise, and the -10 and -35 predicted sites are in pink. Spacing between predicted -10 and -35 elements is indicated and the BPROM prediction scores are in parentheses. Predictions of σ54 according to the consensus find by Bonocora et al. (2015) were indicated in bold.

Table 5.1. Summary of predicted *psp* σ70 promoters using BPROM

Genes	TATAAT-10		TTGACA -35		Distance between -10 and -35 (bp)
	Sequence	Score	Sequence	Score	
pspF	AATTAT	39	TTTATA	39	16
pspA	TAAAAC	44	TTTATC	17	17
pspG	CATGAT	52	TTTATA	39	21

5.4. Study of *psp* gene regulation by egg white and ovotransferrin

Using transcriptional fusions previously constructed (section 5.2), the regulation of *pspA*, *pspF* and *pspG* was analysed. The β-galactosidase activity was measured after 7 and 45 min, and 6 and 12 h at 30 °C, in different media (TSB or SM, with/without 100 µM CCCP, 10% EW, and OT at 1.3 or 13 g/L) (section 2.2.17). The iron-chelating activity of OT was also tested by addition of iron citrate to reach 100% OT iron saturation (section 2.1.5.3).

5.4.1. Measurement of β-galactosidase activity

The putative promoter regions of the *psp* genes were fused with a promoterless *lacZ* operon in the transcriptional-fusion vector, pRS1274. Thus, the relative activity of the promoter and expression level of the corresponding gene) can be quantified by measuring the β-galactosidase activity. Indeed, when the promoter of the target gene is activated, the promoterless *lacZ* is transcribed and translated into β-galactosidase. The enzymatic reaction occurs after addition of β-galactosidase substrate (ortho-Nitrophenyl-β-galactoside, ONPG) to corresponding cell extracts. The enzyme hydrolyses the colourless ONPG into the yellow ONP product which is detectable at 420 nm (section 2.2.17). The amount of enzyme directly correlates with the rate of enzyme activity and, therefore, the relative activity of the studied promoter.

5.4.1.1. Controls

The empty expression vector, pRS1274, was used as negative control and the β-galactosidase activity was measured for each condition and converted in nmoles/ONPG/min/OD unit cells (section 2.2.16). For each growth condition and each incubation time, the β-galactosidase activity of pRS1274 was less than 6 nmoles/ONPG/min/OD unit cells (Figure 5.12). This result corresponds to the basal activity of te promoterless *lacZ* and can be used to compare the expression of active promoters. Thus, an activity higher than the promoterless lacZ pRS1274 indicates activation of the studied putative promoter.

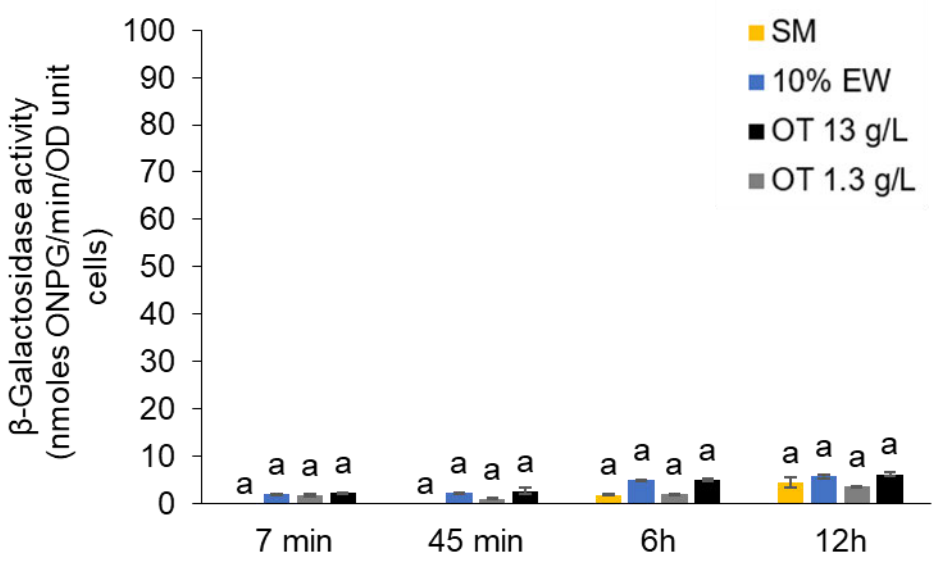

Figure 5.12. β-galactosidase activity of empty expression vector pRS1274. The β-galactosidase activity of pRS1274 was measured after 7 and 45 min, and 6 and 12 h exposure to (i) SM, (ii) SM with 10% egg white (10% EW), (iii) SM with ovotransferrin at 1.3 g/L (OT 1.3 g/L) and (IV) SM with ovotransferrin at 13 g/L (OT 13 g/L). Error bars indicate standard deviations from the mean derived from one biological experiment, with three technical replicates. Significant differences between each condition were assessed using a one-way ANOVA test followed by a Tukey test with R software (version 1.4.1106). Several significantly different groups were identified by a letter, with a p-value ≤ 0.05.

It was shown that the *psp* genes are induced by different factors such as filamentous phage infection, ethanol (5, 10%), methanol (5, 10%), extreme heat shock (48 and 50 °C), ionophores and protonophores (Joly et al., 2010, for a review). Thus, in this study, CCCP was used as a positive control for *psp* induction. Indeed, it was shown that *pspA* is induced in *S*. Typhimurium after 1 h exposure to 40 µM CCCP (Becker et al., 2005), and in *E. coli* after 15 min exposure to 40 and 60 µM CCCP (Weiner & Model, 1994). To recap, CCCP causes a dissipation of the pmf by mediating the unregulated influx of H^+ through the inner membrane. In this study, *S*. Enteritidis was incubated with 100 µM CCCP, in TSB. The impact of CCCP in SM was not considered as preliminary results showed no difference in activity between SM with and without CCCP.

The *psp-lacZ* activity after exposure to TSB and CCCP is presented in Figure 5.13. After 7 min, a high activity of *pspF-lacZ* was observed in TSB and CCCP (~2000 fold higher than the negative control) (Figure 5.13A). After 45 min, this activity dropped in TSB but remained higher than the promoterless *lacZ* (~1100-fold greater). In the presence of CCCP, *pspA-lacZ* activity increased (1.66-fold higher than TSB). After longer incubation times (6 and 12 h), the β-galactosidase activity decreased below 1000 nmoles/ONPG/min/OD unit cells. A similar result was observed for *pspA* and *pspG*. Thus after addition of CCCP, the promoter activity increased after 45 min (1.79- and 1.70-fold higher than in TSB, for *pspA* and *pspG* respectively). After long-time exposure, the activity also dropped between 500 and 1000 nmoles/ONPG/min/OD unit cells. The results confirm that the three putative promoters are active and show that CCCP induces overexpression of *psp genes* at 45 min, but not at the other three time points considered, probably due to the antimicrobial activity of CCCP.

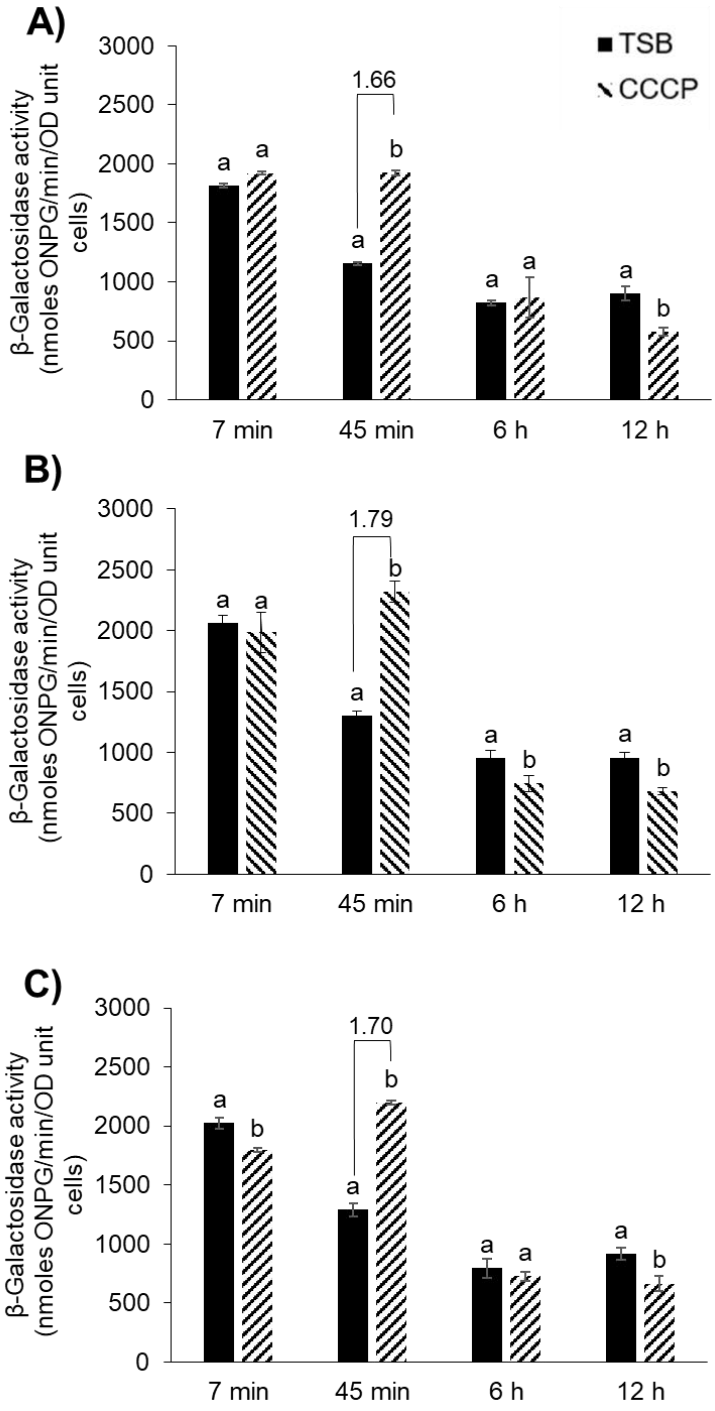

Figure 5.13. Expression *psp-lacZ* over time and response to CCCP. The β-galactosidase activity of (A) pRS1274-*pspF-lacZ*, (B) pRS1274-*pspA-lacZ and* (C) pRS1274-*pspG-lacZ* was measured after 7 and 45 min, and 6 and 12 h in TSB with/without 100 µM CCCP. Error bars indicate standard deviations from the mean derived from two biological experiments, with three technical replicates. Significant differences between each condition were assessed using the Student's t-test with R software (version 1.4.1106). Significantly different (p-value ≤ 0.05) groups are indicated by distinct lowercase letters (a or b).

5.4.1.2. Regulation of *pspF*

After exposure to SM (which mimics the conditions of EW), *pspF* expression was evident at all four incubation times (1604 ± 53, 1715 ± 44 and 1876 ± 109 nmoles ONPG/min/OD unit after 7 and 45 min, and 12 h, respectively) with a lower expression after 6 h (1137 ± 130 nmoles ONPG/min/OD unit) (Figure 5.14A). Thus, exposure to SM alone supported *pspF* expression. After addition of 10% EW in SM, *pspF-lacZ* activity was significantly higher (1.35-fold) than in SM, but only after 6 h (Figure 5.14A and B). This result indicates that EW proteins induce expression of *pspF* after 6 h exposure.

As demonstrated previously, OT causes the depolarisation of the *S*. Enteritidis inner membrane (Chapter 4, section 4.3). Thus, the expression of *pspF* was also measured after OT exposure at 1.3 g/L (10% of its concentration found in EW) and at 13 g/L (its concentration found in EW). After OT 1.3 g/L exposure, *pspF-lacZ* was expressed well but its expression was not significantly higher than in SM alone (Figure 5.14A and B). Indeed, after 12 h, β-galactosidase activity dropped (-1.19-fold lower than in SM). However, for the higher concentration of OT, the activity of *pspF-lacZ* was significantly increased with respect to SM alone, at all four-time points (1.14-, 1.07-, 1.45- and 1.20-fold after 7 and 45 min, and 6 and 12 h, respectively) (Figure 5.14A and B). Thus, at the concentration found in EW, OT induces *pspF* overexpression at 30 °C, under EW conditions, whatever the time point. It can also be noticed that after 6 h exposure, the expression of *pspF* was lower in all conditions.

A)

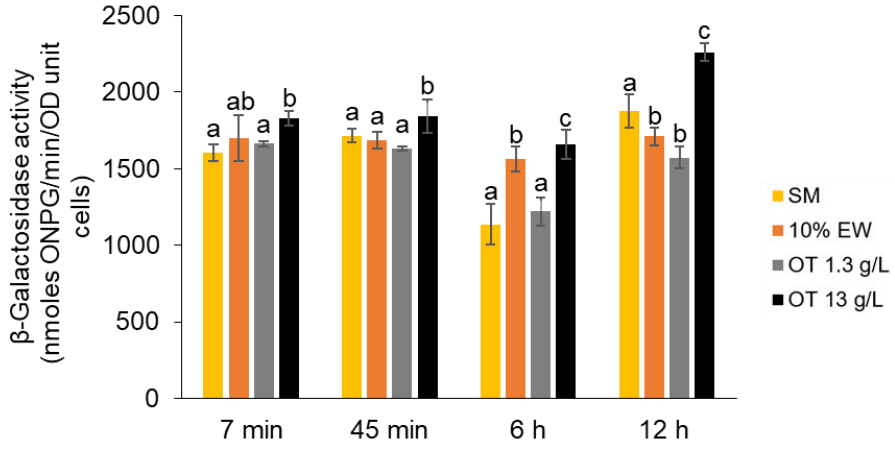

B)

	Fold change			
	7 min	45 min	6 h	12 h
10% EW	1.06	0.98	1.35	0.91
OT 1.3 g/L	1.04	0.95	1.06	0.83
OT 13 g/L	1.14	1.07	1.45	1.20

Figure 5.14. Expression of *pspF-lacZ* in SM in response to 10% EW and OT. (A) The β-galactosidase activity of pRS1274-*pspF-lacZ* was measured after 7 and 45 min, and 6 and 12 h exposure to (i) synthetic medium (SM), (ii) SM with 10% egg white (10% EW), (iii) SM with ovotransferrin at 1.3 g/L (OT 1.3 g/L) and (IV) SM with ovotransferrin at 13 g/L (OT 13 g/L). Error bars indicate standard deviations from the mean derived from two biological experiments, with three technical replicates. Significant differences between each condition were assessed using a one-way ANOVA test followed by a Tuckey test with R software (version 1.4.1106). Significantly different (p-value ≤ 0.05) groups are indicated by distinct lowercase letters (a-c). (B) Table showing the fold changes corresponding to up-regulation of *pspF* in response to EW or OT (compared to SM only); significant changes (p-values ≤ 0.05) are indicated by grey highlights.

5.4.1.3. Regulation of *pspA*

As for *pspF*, *pspA* was well expressed in SM (Figure 5.15A). The activity was higher after short-time exposure (1792 ± 53 and 1920 ± 48 nmoles ONPG/min/OD unit cells, after 7- and 45 min exposure, respectively) than after long-term exposure (6 and 12 h; 1344 ± 28 and 1463 ± 116 nmoles ONPG/min/OD unit cells, respectively). After addition of 10% EW to SM, the β-galactosidase activity was significantly greater at 6 and 12 h (1.52- and 1.33-fold)

than in SM alone (Figure 5.15A and B). Thus, EW proteins appear to induce *pspA* expression at 6 and 12 h. After addition of 1.3 g/L of OT, *pspA-lacZ* activity was significantly higher at 7 min and 12 h (1.07- and 1.08-fold, respectively), than in absence of EW proteins (Figure 5.15A and B). This result indicates that OT weakly induces *pspA* after 7 min and 12 h exposure. When the concentration of OT increased to 13 g/L (as found in EW), the activity of *pspA-lacZ* was raised at 7 min, and 6 and 12 h (1.13-, 2.01- and 1.62-fold, respectively) with respect to SM only (Figure 5.15A and B). Thus, OT concentration influences the expression of *pspA* under EW conditions, with higher concentrations having a greater effect.

In summary, these results indicate that EW induces raised expression of *pspA* after 6 and 12 h, and OT seems to play a major role in this expression given the higher induction seen for 10% EW with respect to 1.3 g/L OT.

A)

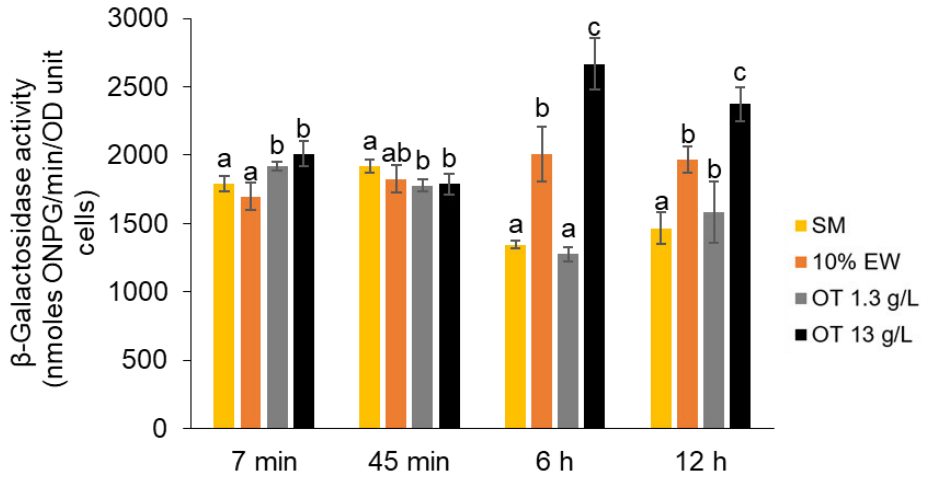

B)

	Fold change			
	7 min	45 min	6 h	12 h
10% EW	0.95	0.94	1.52	1.33
OT 1.3 g/L	1.07	0.93	0.95	1.09
OT 13 g/L	1.13	0.94	2.01	1.62

Figure 5.15. Expression of *pspA-lacZ* in SM in response to 10%EW and OT. (A) The β-galactosidase activity of pRS1274-*pspA-lacZ* was measured after 7 and 45 min, and 6 and 12 h exposure to (i) synthetic medium (SM), (ii) SM with 10% egg white (10% EW), (iii) SM with ovotransferrin at 1.3 g/L (OT 1.3 g/L) and (IV) SM with ovotransferrin at 13 g/L (OT 13 g/L). Error bars indicate standard deviations from the mean derived from two biological experiments, with three technical replicates. Significant differences between each condition were assessed using a one-way ANOVA test followed by a Tuckey test with R software (version 1.4.1106). Significantly different (p-value ≤ 0.05) groups are indicated by distinct lowercase letters (a-c). (B) Table showing the fold changes corresponding to up-regulation of *pspA* in response to EW or OT (compared to SM only); significant changes (p-values ≤ 0.05) are indicated by grey highlights.

5.4.1.4. Regulation of *pspG*

As for *pspF* and *pspA*, *pspG* was also well expressed in SM, and its expression was also generally lower after 6 h (1242 ± 100 nmoles ONPG/min/OD unit cells) compared with the other time points (1803 ± 118, 1569 ± 163 and 1588 ± 131 nmoles ONPG/min/OD unit cells, respectively) (Figure 5.16A and B). After addition of 10% EW, the β-galactosidase activity was increased significantly at 45 min (1.19-fold) (Figure 5.16A and B) indicating that EW proteins induce

expression of *pspG* at this time point. In addition, there was a the significantly higher expression after exposure to 1.3 g/L OT for 45 min (1.14-fold higher than in SM). Additionally, when the concentration of OT was increased to its concentration found in EW, the expression of *pspG-lacZ* was further induced in a significant fashion (1.10-, 1.46- and 1.26-fold higher than in SM at 45 min, and 6 and 12 h, respectively) (Figure 5.16A and B). Results thus show that *pspG* expression was greater in 13 g/L OT at the longer time points.

A)

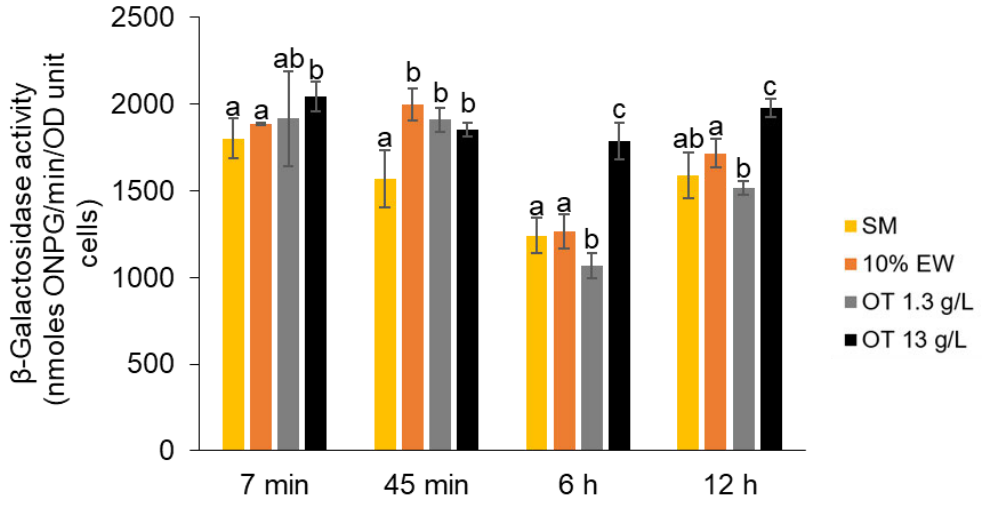

B)

	Fold change			
	7 min	45 min	6 h	12 h
10% EW	1.05	1.19	1.03	1.10
OT 1.3 g/L	1.09	1.14	0.88	0.96
OT 13 g/L	1.13	1.10	1.46	1.26

Figure 5.16. Expression of *pspG-lacZ* in SM in response to EW and OT. (A) The β-galactosidase activity of pRS1274-*pspG-lacZ* was measured after 7 and 45 min, and 6 and 12 h exposure to (i) synthetic medium (SM), (ii) SM with 10% egg white (10% EW), (iii) SM with ovotransferrin at 1.3 g/L (OT 1.3 g/L) and (IV) SM with ovotransferrin at 13 g/L (OT 13 g/L). Error bars indicate standard deviations from the mean derived from two biological experiments, with three technical replicates. Significant differences between each condition were assessed using a one-way ANOVA test followed by a Tuckey test with R software (version 1.4.1106). Significantly different (p-value ≤ 0.05) groups are indicated by distinct lowercase letters (a-c). (B) Table showing the fold changes corresponding to up-regulation of *pspG* in response to EW or OT (compared to SM only); significant changes (p-values ≤ 0.05) are indicated by grey highlights.

5.4.1.5. An uncertain role of the iron-chelating activity of ovotransferrin on the regulation of *psp* genes

As described in the literature and confirmed in this study, due to its metal-chelating activity, OT is responsible for antimicrobial activity of EW against *S*. Enteritidis growth at 30 °C (Chapter 3). The *S*. Enteritidis membrane permeabilisation activity of OT was slightly affected by the iron-saturation level of OT, although the inner-membrane depolarisation was lowered when OT was iron-saturated (chapter 4, section 4.2.2 and 4.3). However, results presented above indicate that the OT-induced membrane damage is dependent (in part at least) on the metal-chelating activity of OT. Thus, the impact of saturation of the metal-chelating activity of OT was tested on *psp* genes expression. Iron citrate was added to achieve theoretical 100% OT iron-saturation in SM with/without 10% EW, or 1.3 or 13 g/L OT.

5.4.1.5.1. Regulation of *pspF*

After 7 min, the activity of *pspF-lacZ* was slightly higher only in SM supplemented with iron (1.09-fold) but was not significantly different in the other conditions (Figure 5.17A). After 45 min, the β-galactosidase activity was significantly lower in SM with iron (1.11-fold) but greater in 1.3 g/L OT with iron (1.08-fold) (Figure 5.17B). After 6 h, the expression of *pspF-lacZ* was increased in SM with iron (1.43-fold) whereas it was decreased in the other conditions (-1.36, -1.37 and -1.42-fold lower in 10% EW, and OT at 1.3 g/L and 13 g/L, respectively) (Figure 5.17C). However, after 12 h, the enzymatic activity dropped in all cases (Figure 5.17D). When OT 13 g/L was iron-saturated, *pspF* (which was induced at 6 and 12 h by apo-OT at 13 g/L), was repressed (Figure 5.17C and D).

Thus, after 6 and 12 h, the saturation of OT with iron reversed the induction effect of apo-OT and instead resulted in a reduction of *pspF* expression. Globally, the expression of *pspF* was lower after 6 and 12 h in all of the conditions where iron was added except for the SM condition where the added iron would remain free (i.e. unchelated by OT).

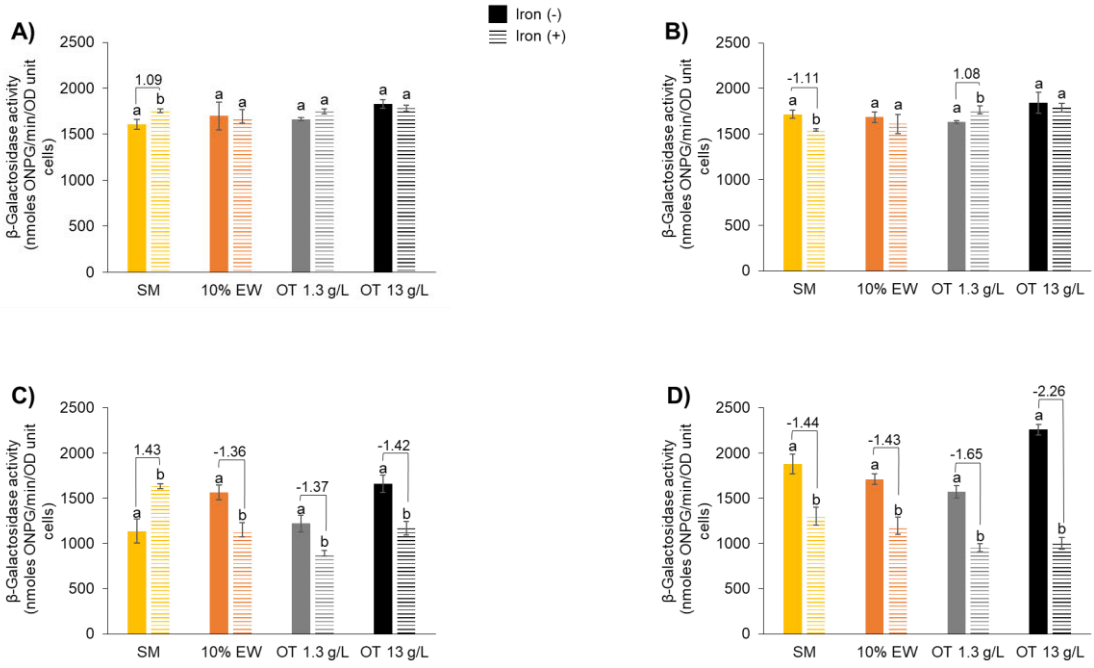

Figure 5.17. Effect of iron on the EW- and OT-dependent regulation of *pspF-lacZ* expression. The β-galactosidase activity of pRS1274-*pspF-lacZ* was measured after (A) 7 min, (B), 45 min, (C), 6 h and (D), 12 h exposure to (i) synthetic medium (SM), (ii) SM with 10% egg white (10% EW), (iii) SM with ovotransferrin at 1.3 g/L (OT 1.3 g/L) and (IV) SM with ovotransferrin at 13 g/L (OT 13 g/L), with or without addition of iron citrate (corresponding to 100% OT iron saturation). For the 'SM only' conditions, iron citrate was added at 334 µM, same level as used for saturation of OT at 13g/L. Error bars indicate standard deviations from the mean derived from two biological experiments, with three technical replicates. Significant differences between the +/- Fe conditions were assessed using Student's t-test with R software (version 1.4.1106) and significant differences (p-value ≤ 0.05) are identified by the letters a and b. Where a significant difference was identified, the fold change is indicated.

5.4.1.5.2. Regulation of *pspA*

At 7 min, the β-galactosidase activity for *pspA-lacZ* was not affected by any of the additions except for the addition of iron to SM-only, where a

significantly higher level (1.12-fold) (Figure 5.18A) was observed, as for *pspF*. At 45 min, activity was slightly greater with the addition of iron in SM, and 1.3 and 13 g/L OT (1.06-, 1.06- and 1.08-fold than the corresponding iron-free condition) (Figure 5.18B). However, at 6 h, *pspA-lacZ* activity was significantly higher (1.11-fold) in SM with addition of iron. In contrast, expression was significantly lower for iron-saturated OT at 13 g/L than for the corresponding condition without iron saturation (-1.80-fold than OT 1.3 g/L). However, no such effect was seen with OT at 1.3 g/L presumably due to the lack of induction caused by this concentration of OT. Similarly, there was no iron effect in the 10% EW condition. At 12 h, the expression of *pspA-lacZ* was not affected by iron for the SM and OT at 1.3 g/L conditions. However, in 10% EW and OT at 13 g/L, the β-galactosidase activity was reduced by 1.23-, and 1.77-fold, respectively, by the inclusion of iron (Figure 5.18D).

Thus, in summary, saturation of OT reverses the ability of OT (at its concentration found in EW) to induce *pspA* expression at 6 and 12 h.

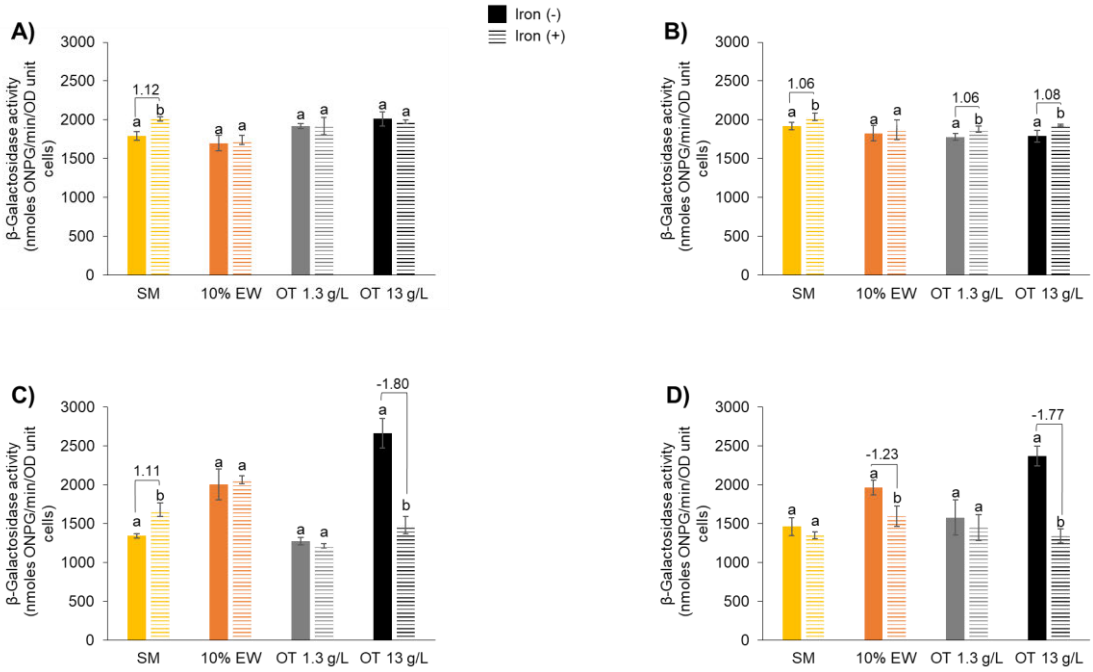

Figure 5.18. Effect of iron on the EW- and OT-dependent regulation of *pspA-lacZ* expression. The β-galactosidase activity of pRS1274-*pspA-lacZ* was measured after (A) 7 min, (B), 45 min, (C), 6 h and (D), 12 h exposure to (i) synthetic medium (SM), (ii) SM with 10% egg white (10% EW), (iii) SM with ovotransferrin at 1.3 g/L (OT 1.3 g/L) and (IV) SM with ovotransferrin at 13 g/L (OT 13 g/L), with or without addition of iron citrate (corresponding to 100% OT iron saturation). For the 'SM only' conditions, iron citrate was added at 334 µM, the same level as used for saturation of OT at 13g/L. Error bars indicate standard deviations from the mean derived from two biological experiments, with three technical replicates. Significant differences between the +/-Fe conditions were assessed using Student's t-test with R software (version 1.4.1106) and significant differences (p-value ≤ 0.05) are identified by the letters a and b. Where a significant difference was identified, the fold change is indicated.

5.4.1.5.3. Regulation of *pspG*

At 7 min, *pspG-lacZ* activity was significantly higher (1.17-fold) in SM with iron compared to SM alone, similar to the findings for *pspA* and *pspG*. No other difference was found after exposure to the other conditions (Figure 5.19A), as was the case with *pspA* and *pspF*. At 45 min, significantly greater activity was observed after exposure to iron-saturated OT at 13 g/L (1.56-fold higher than for OT at 13 g/L without iron) (Figure 5.19B). The activity was significantly reduced at 6 h for the iron-saturated OT at 13 g/L condition (-1.18-fold than OT 13 g/L)

(Figure 5.19C) while the addition of iron in SM did not induce any *pspG* expression changes. Thus, the iron saturation of OT at 13 g/L reveres the induction caused by OT at 13 g/L in the absence of iron. This result indicates that the induction of *pspG* by OT is attributable to its metal-chelating activity. At 12 h, similar iron-induced reductions in *pspG-lacZ* activity were observed in all four conditions: SM, 10% EW, and OT at 1.3 and 13 g/L; -1.43-, -1.39, -1.36 and -1.87-fold, respectively) (Figure 5.19D). Thus, the effects cannot be entirely attributed to the chelating activity of OT, although this may be the case for the 13 g/L OT condition given the much higher iron-induced repression effect observed. Furthermore, it should be noted that after addition of iron, the *pspG-lacZ* activity was globally lower after long-time exposure than 7 and 45 min incubation times.

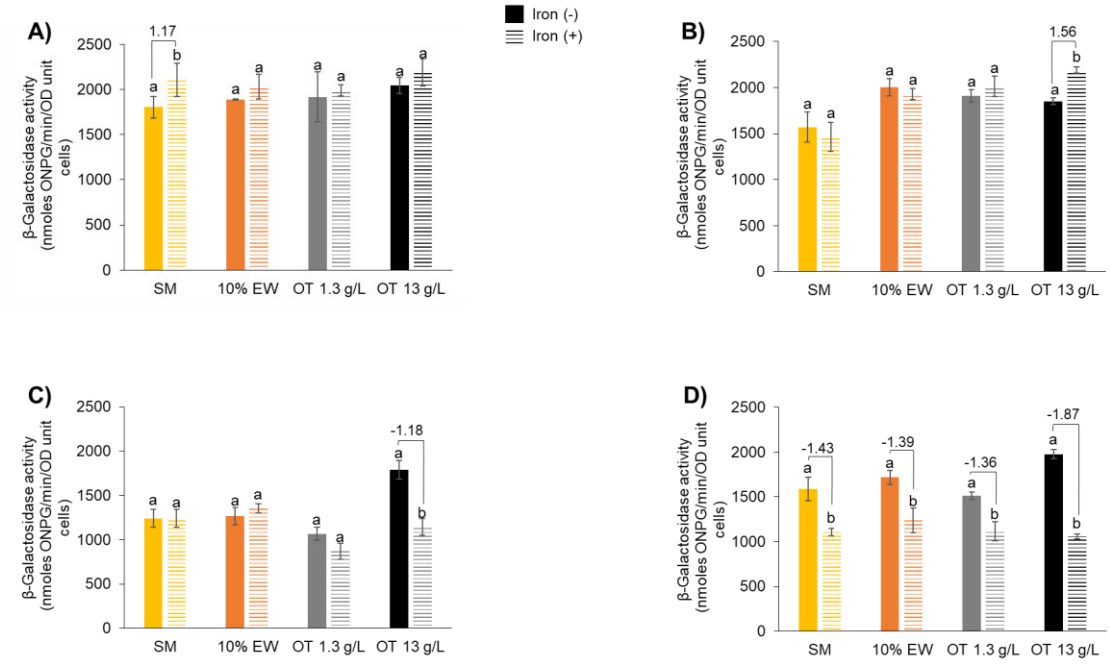

Figure 5.19. Effect of iron on the EW- and OT-dependent regulation of *pspG-lacZ* expression. The β-galactosidase activity of pRS1274-*pspG-lacZ* was measured after (A) 7 min, (B), 45 min, (C), 6 h and (D), 12 h exposure to (i) synthetic medium (SM), (ii) SM with 10% egg white (10% EW), (iii) SM with ovotransferrin at 1.3 g/L (OT 1.3 g/L) and (IV) SM with ovotransferrin at 13 g/L (OT 13 g/L), with or without addition of iron citrate (corresponding to 100% OT iron saturation). For the 'SM only' conditions, iron citrate was added at 334 µM, the same level as used for saturation of OT at 13g/L Error bars indicate standard deviations from the mean derived from two biological experiments, with three technical replicates. Significant differences between the +/-Fe conditions were assessed using Student's t-test with R software (version 1.4.1106) and significant differences (p-value ≤ 0.05) are identified by the letters a and b. Where a significant difference was identified, the fold change is indicated.

5.4.2. Analysis of *psp* genes expression by qRT-PCR

Other methods can be used to study gene expression and have been successfully applied to analyse the *S*. Enteritidis response to EW: *in vivo* expression technology (IVET) (Gantois et al., 2008), qualitative proteomics (Qin et al., 2019), RNAseq (Huang et al., 2019, 2020) and global transcriptomic analysis using microarrays (Baron et al., 2017, 2020). Additionally, the *psp* response has been studied after 7-, 25- and 45-min EW exposure of *S*. Enteritidis

by global transcriptomic analysis using microarrays (Baron et al., 2017, 2020) and after 45 min by qRT-PCR (Baron et al., 2020), both at 45 °C in EWMM (EWF with 10% EW). This latter technique was used in the present work to study and compare the expression of *pspA* and *pspG* at 30 °C, after 45 min exposure to SM, SM with 10% EW, SM with OT at 1.3 and 13 g/L (section 2.2.8).

5.4.2.1. Quality control of RNA and primers

S. Enteritidis total RNA was extracted (section 2.2.7.3), and the concentration and purity were verified using a Nanodrop (section 2.2.7.4) and agarose gel electrophoresis (section 2.2.11, Figure 5.20). Figure 5.20 shows four RNA samples representing the four tested conditions. Two bands, corresponding to 23S and 16S rRNA, are apparent for each sample (at around 3000 and 1500 nt, respectively). However, the 5S rRNA species was not visible. The isolated RNA was also tested by traditional PCR for one of the genes (*asmA*), to confirm the absence of gDNA contamination (Appendix 4). No amplification was observed, although a product was obtained with gDNA, confirming the absence of gDNA in the isolated RNA. From the pure total RNA samples, cDNA was synthesised and used as a template for qPCR reaction (section 2.2.7.3.2).

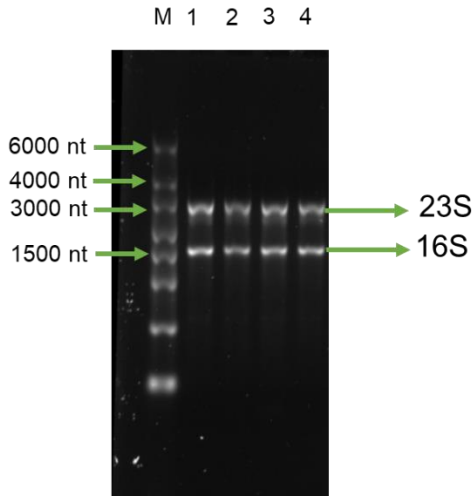

Figure 5.20. Verification of RNA purity by agarose gel electrophoresis. Lane M contains the high-range RNA ladder (200 – 6000 nucleotides) (ThermoScientific™). Lanes 1, 2, 3 and 4 contain RNA extracted from *S*. Enteritidis grown for 45 min SM, SM with 10% EW, SM with OT at 1.3 g/L or SM with OT at 13 g/L, respectively (for the first biological replicate). For each RNA sample, the 16S and 23S rRNA bands are indicated on the right. The electrophoresis was performed for 1 h at 80 V on a 1.2% agarose TBE gel.

For each gene (housekeeping and target genes), a specific pair of primers (Table 2.5, section 2.1.3) was designed using Geneious Prime software. During the design, a set of key criteria were considered to ensure the quality and reliability of the PCR: an ideal amplicon size between 70 and 200 bp; a melting temperature of 60 °C (63 °C maximum): a GC% around 40-60 °C; and the presence of C/G residues in 3' end of the primers. Amplification with each primer pair was tested by PCR using *S*. Enteritidis gDNA (Figure 5.21) (section 2.2.9). The size of each amplicon corresponded to those expected (109, 172, 150 and 105 bp for *asmA*, *emrA, pspA* and *pspG,* respectively). The expression of *pspF* was not considered by qRT-PCR as the bacterial physiological response resulted in the expression of *pspA and pspG* only (Joly et al., 2010).

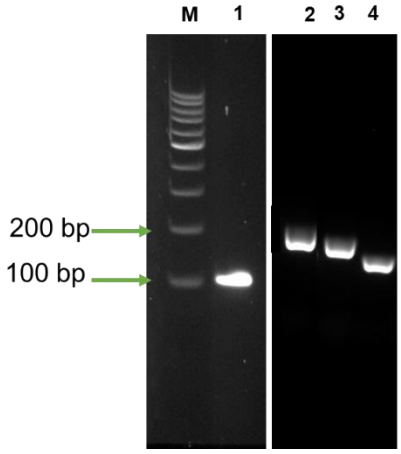

Figure 5.21. PCR amplification of gDNA with qRT-PCR primers. Each pair of primers was used to amplify the corresponding target by PCR using *S*. Enteritidis NCTC13349 gDNA as a template. Lane M contains the 100 bp RiboRuler DNA ladder (100-1000 bp) (ThermoScientific™); lanes 1, 2, 3 and 4 correspond to the amplification of *asmA*, *emrA, pspA* and *pspG* with expected sizes of 109, 172, 150 and 105 bp, respectively. The electrophoresis was performed for 1 h at 80 V on a 1.7% agarose TBE gel.

To test the efficiency of each pair of primer, standard curves were performed, first with gDNA (Figure 5.22) and then cDNA (Figure 5.23) (section 2.2.8). Thus, tenfold serial dilutions of 10 ng/µl of gDNA and 20 ng/µl of cDNA were prepared, up to dilutions of 10^{-6} (section 2.2.8). A good efficiency of amplification should be between 90 and 110% (Wittwer, 2001). The PCR efficiency was higher than 90% for all the primer pairs tested with gDNA and in all conditions with cDNA. A fixed concentration of 2 ng/µl of cDNA was selected for Ct values determination and comparison (section 2.2.8).

A

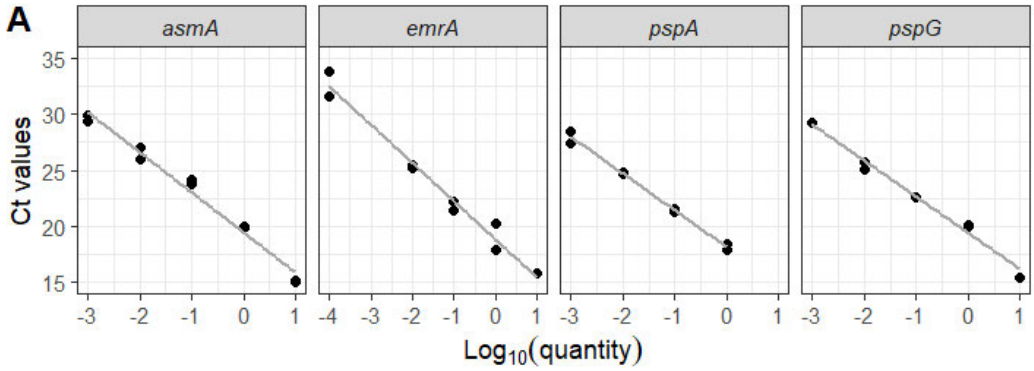

B

Gene	Slope	Efficiency (%)
emrA	-3.5628	91
asmA	-3.5694	91
pspA	-3.4205	96
pspG	-3.3465	99

Figure 5.22. Determination of primer efficiency using the gDNA standard curve method. (A) Standard curves of each pair of primers were tested in duplicate using *S*. Enteritidis NCTC13349 gDNA as a template. (B) The efficiency of each pair of primers as determined using StepOne™ Real -Time PCR system (Applied Biosystem™) software.

A

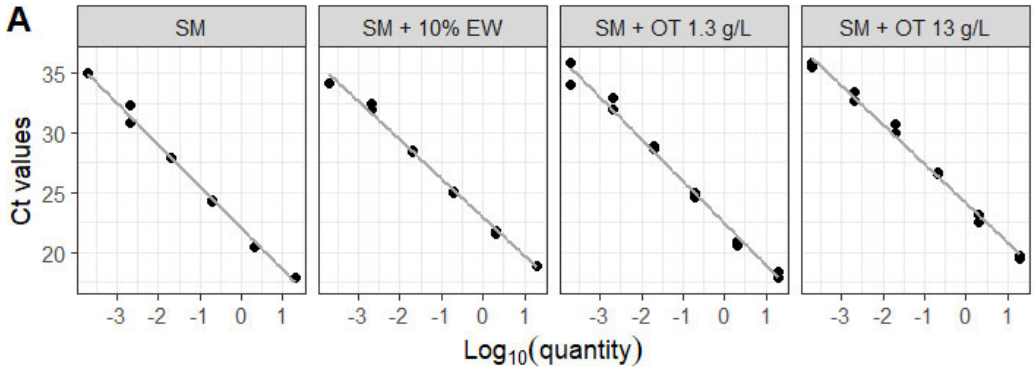

B

Conditions	Slope	Efficiency (%)
SM	-3.4954	93
SM + 10% EW	-3.1881	106
SM + OT 1.3 g/L	-3.5147	93
SM + OT 13 g/L	-3.2849	102

Figure 5.23. Determination of *pspA* primer efficiency using the cDNA standard curve method. (A) Standard curves with the *pspA* primers were tested in triplicate using the indicated cDNA templates. (B) Efficiency of the *pspA* primers for each condition (one biological replicate). Efficiency of each pair of primers as determined using StepOne™ Real -Time PCR system (Applied Biosystem™) software.

5.4.2.2. Analysis of the fold change expression of *psp* genes

The $2^{-\Delta\Delta Ct}$ method was used to analyse the qRT-PCR results (Livak & Schmittgen, 2001). The relative fold-change expression of *pspA* and *pspG* was determined after 45 min exposure of *S.* Enteritidis to SM with/without 10% EW or OT at 1.3 or 13 g/L, and was compared to the relative fold-change expression after 0 min (Figure 5.24). Data were normalised using two housekeeping genes (*asmA* and *emrA*). These genes were two of three previously used as internal controls by Baron et al. (2020) with the same strain at 45 min exposure to EW and EWF.

After exposure to SM, *pspA* was induced eightfold with respect to levels at 0 min (Figure 5.24A). After addition of 10% EW, *pspA* expression was increased by 2.5-fold (with respect to SM only) and 20-fold with respect to 0 min, indicating that EW proteins induce *pspA* at the transcriptional level. The exposure to OT at 1.3 or 13 g/L resulted in a 5 and 8-fold induction, respectively, with respect to levels at 0 min, but the induction was slightly lower than that achieved with SM alone (and not significantly different). Similar results were obtained for *pspG* (Figure 5.24B). Indeed, *pspG* was induced after 45 min exposure to SM (~3-fold greater than at 0 min). Upon addition of 10% EW, the expression of *pspG* increased significantly by 2.6-fold with respect to SM only, again suggesting a role for EW proteins in the induction of *pspG*. However, after exposure to OT at 1.3 or 13 g/L, the expression of *pspG* was not higher different to that seen for SM alone (3- and 4-fold higher than at 0 min).

Thus, the results show that *pspA* and *pspG* are induced 8- and 3-fold by 45 min exposure to SM, respectively, but are further induced (2.5- and 2.6-fold, respectively) by the presence of 10% EW. However, OT was not involved in the regulation of the two *psp* genes under EW conditions following a 45 min exposure. These results are in accordance with the findings that *pspA* and *pspG* were expressed in EWMM at 45 °C for 45 min. In fact, after 45 min, the two genes were up-regulated (2.42- and 2.38- fold for *pspA* and *pspG* respectively) using microarray analysis (Baron et al., 2017). Additionally, the expression of *pspG* was confirmed by qRT-PCR, showing a fold change of 6.47 ± 2.81 at 45 °C for 45 min (Baron et al., 2020). It can be noticed that in this study results indicate a higher expression of *pspA* than *pspG* in all conditions that is not the case for the

observations of Baron et al. (2017) who did not highlight any difference at 45°C in both gene expression levels.

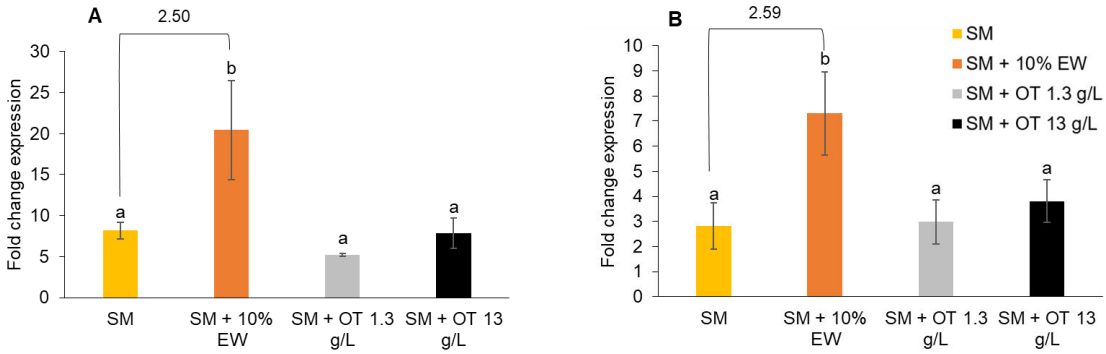

Figure 5.24. qRT-PCR analysis. Fold change in expression of (A) *pspA* and (B) *pspG* (controls were determined using $2^{-\Delta\Delta Ct}$ method; Livak & Schmittgen, 2001) after 45 min exposure to SM with/without 10% EW, OT at 1.3 g/ or OT at 13 g/L compared to 0 min in TSB. Data were normalised using two internal controls (*asmA* and *emrA*). Fold change is indicated between SM with and without 10% EW, since this difference was significant. Error bars indicate standard deviations from the mean derived from three biological experiments, with three technical replicates. Significant differences between each condition were assessed using an ANOVA test followed by a Tukey test using R software (version 1.4.1106). Significantly different groups (p-value ≤ 0.05) are indicated by letters (a and b).

5.4.2.3. Comparison *psp-lacZ* fusion and qRT-PCR results

The two techniques both showed that *pspA* and *pspG* are well expressed after 45 min exposure to SM with/without 10% EW, or 1.3 or 13 g/L OT. However, while an induction of *pspA* was observed with qRT-PCR after exposure to 10% EW (Figure 5.24A), no significant differences were observed using the transcriptional fusions (Figure 5.14). For *pspG*, induction was observed in presence of 10% EW with both methods (Figure 5.24B and 5.16). However, the fusion showed induction of *pspG* after 45 min exposure to OT at 1.3 and 13 g/L (Figure 5.16) whereas such an effect was not seen with qRT-PCR. Furthermore, it is difficult to compare these results with the literature since *psp* genes expression seems to be influenced by the strain, the percentage of EW, the

medium used to dilute EW, the temperature and the technique used. However, qRT-PCR directly quantifies mRNA levels whereas the *lac* transcriptional fusions measure promoter activity based upon the activity of the *lacZ* gene product (β-galactosidase). According to Bremer & Yuan (1968), RNA polymerase progresses at around 55 nt/sec at 37°C in *E. coli*. Taking this rate and the position of the primers used for the qRT-PCR, into consideration, an increase in *pspA* and *pspG* transcripts should be detectable by qRT-PCR by around 6 and 0.2 sec after induction, respectively. However, for the *lacZ* fusion, the time taken for appearance of a complete translation product (1025 amino acids) would be at least 1 min. Thus, both methods employed would detect increases in expression soon after they were initiated, although qRT-PCR would be expected to detect any induction earlier. In addition, it should be noted that the half-live of mRNA is shorter (from 40 sec to 1 h) than that of proteins which are more stable (from min to a few days) (Belasco & Brawerman, 2012; Nagar et al., 2021). Indeed, β-galactosidase is considered to be a highly stable protein but the *lacZ* transcript has a short half-life (~3 min). Thus, qRT-PCR should readily detect any cases where induction is transient unlike the *lacZ*-fusion approach where LacZ levels would decline far more slowly (as a consequence of growth).

5.5. Discussion and perspectives

In Chapter 4, the membrane damage caused to *S*. Enteritidis by EW and OT was demonstrated. Despite the ability of EW and OT to induce *S*. Enteritidis membrane damage, bacterial survival was not affected. Indeed, bacteria have the capacity to deploy systems that restore the membrane and maintain its

integrity. Several key regulatory systems are involved in such functions: RpoE, CpxAR, BaeSR, Rcs and Psp (Darwin, 2005; Duguay & Silhavy, 2004; Humphreys et al., 2004). Although the critical role of the CpxAR system in the response of *S*. Enteritidis to EW was reported by Huang et al. (2019), it was considered possible that the *psp* genes could also be regulated in response to membrane damage by EW proteins. In fact, *psp* genes are known to be induced after 7-, 25- and 45-min exposure to EWMM at 45 °C but not after exposure to EWF, implicating EW proteins of >10 kDa in the *psp* response (Baron et al., 2017, 2020). It is generally accepted that the dissipation of the pmf induces a signal for the activation of the *psp* response (Darwin, 2005). By their capacity to provoke *S*. Enteritidis inner-membrane damage, and therefore pmf dissipation, EW and/or OT might participate in the regulation of *psp* genes. In this study, the regulation of the *psp* genes (*pspF*, *pspA* and *pspG*) by EW and OT was studied using transcriptional fusions and qRT-PCR.

5.5.1. Prediction of *psp* gene promoters

In this study, the *psp* promoters were predicted using bioinformatic tools for σ70-dependent promoters and σ54-dependent promoter were predicted using the consensus sequence previously described (Bonocora et al., 2015). However, these approaches have limitations and thus the predictions may not be accurate. Indeed, one σ70-dependent promoter was predicted for each gene (Figure 5.11, Table 5.1) while in *E. coli* three σ70-dependent promoter were identified for *pspF* (one major and two minors), whereas the transcription of *pspA* and *pspG* is driven by σ54 (Jovanovic et al., 1996; Lloyd et al., 2004; Weiner et al., 1991). Thus, -24 (GG) and -12 (GC) motifs corresponding to the σ54-promoter consensus were

predicted for each gene (Figure 5.11). However, it is important to characterise with accuracy the promoter of these three genes. For this purpose, different techniques can be used such as chromatin immunoprecipitation to investigate the interaction between RNA polymerase and sigma factor, RNAseq or primer extension analysis (Bonocora et al., 2015; Jovanovic et al., 1996).

5.5.2. Expression of *psp* genes in egg white

Only a few publications aimed at studying the expression of *psp* genes by *S*. Enteritidis in EW. After 7-, 25- and 45 min exposure to EWMM, *pspA* and *pspG* were up-regulated (2.38- to 4.08-fold) with higher expression after 7 min (4.08-fold) (Baron et al., 2017). This induction of *pspG* was confirmed after 45 min by qRT-PCR (6.47-fold). However, Huang et al. (2019) did not observe expression change of *psp* genes after 6-, 12- and 24 h in 80% EW. In the present study, *pspG* was induced after 45 min exposure to EW as determined using a *pspG-lacZ* transcriptional fusion (Figure 5.16) and qRT-PCR (Figure 5.24). Concerning *pspA*, induction was noted after 45 min (transcriptional fusion and qRT-PCR) and after 6- and 12 h (transcriptional fusion). The results suggest that the up-regulation of these *psp* genes may be stimulated by a factor other than high alkaline pH. Indeed, in the absence of EW proteins of >10 kDa (EWF), no change of *pspA* and *pspG* expression was observed, supporting a role for EW proteins in the induction of these genes (Baron et al., 2020). At its concentration found in EW, OT appeared to be involved in the *psp* response as induction of *psp* genes was generally observed (Figures 5.14, 5.15 and 5.16). However, qRT-PCR analysis did not show up-regulation of *psp* genes by OT (Figure 5.17). These results show that the expression of *psp* genes may be multifactorial (alkaline pH,

dissipation of the pmf, envelope stress) and may therefore affect, and be affected by, other bacterial functions (motility, metabolism).

5.5.3. Expression of *psp* genes in alkaline condition

In this study, *pspF*, *pspA* and *pspG* were induced after exposure to SM (synthetic medium mimicking EW conditions: ionic composition, alkaline pH) (Figures 5.14, 5.15 and 5.16) although SM (alone) did not induce a loss of the pmf (Chapter 4, Figure 4.4). This is in accordance with a previous study showing an increase of *pspA* expression after alkaline shock. Indeed, *pspA* was induced (11.9-fold) in *Bacillus subtilis* after addition of 24 mM NaOH (Wiegert et al., 2001). A similar result was observed in *Streptomyces lividans* with the activation of the *pspA* promoter by 20 mM NaOH (Vrancken et al., 2008). The activity of *pspA* in *S*. Typhimurium was also higher in M9 at pH 9 than pH 7 (2.6-fold) (Becker et al., 2005). These results suggest that the alkaline pH of EW could influence the expression of *psp* genes. However, *psp* genes were not expressed at 45 °C after 7, 25 and 45 min exposure in EWF as assessed by transcriptome analysis using microarrays analysis (Baron et al., 2020).

5.5.4. Expression of *psp* genes and energy production

The depolarisation of the *S*. Enteritidis membrane by EW and OT, and the up-regulation of the *psp* genes in the presence of EW and OT, confirm the role of pmf dissipation on *psp* genes expression. Indeed, several authors have reported this fact. In *S*. Typhimurium, the expression of *pspA* increased (5-fold) when the strain was mutated for one of the F_1F_0ATPase subunits involved in the maintenance of the pmf) (Becker et al., 2005). A mutation of the same subunit in

Yersinia enterocolitica also induced expression of *pspA* at pH 8 after 8 h (8-fold) and 24 h (22-fold). Additionally, the overexpression of F_1F_0ATPase led to the induction of *pspA* in *E. coli* (Kobayashi et al., 2007a). These results were confirmed by the induction of *pspA* by numerous molecules (e.g. CCCP and antibiotics such as vancomycin and bacitracin) resulting in a dissipation of the pmf (Joly et al., 2010, for a review). Interestingly, it has been shown that *S*. Typhimurium *rpoE* and *pspA* mutants exhibit increased sensitivity to BPI (Becker et al., 2005).

5.5.5. Expression of psp genes and iron metabolism

In this study, the impact of OT metal-chelating activity on the *psp* response was investigated by addition of iron to give a 100% OT saturation level. The metal-chelating activity of OT seemed to impact the *psp* response (down-regulation of *pspF* after 6 and 12 h exposure). A decrease in *pspA* and *pspG* expression was also observed but did not seem corelated with the metal-chelating activity of OT. This lower expression of the *psp* genes was observed only after a relatively long exposure time (stationary phase), which may arise from an ability of *S*. Enteritidis to use iron directly bound to OT for supporting its respiration apparatus. The reasons for these findings remain unclear and require further investigation. However, the role of PspG in the control of iron usage has been established in *E. coli* (Jovanovic et al., 2006). Thus, overexpression of PspG induced a down-regulation of genes involved in iron transport and uptake, and an up-regulation of Fe-S cluster genes. Interestingly, the authors suggested that modulation of intracellular iron concentration occurs as part of the *psp* response (Jovanovic et al., 2006).

5.5.6. Future work

The analysis of *psp* promoter activity was complex. The expression of the *psp* genes seem to be influenced by several factors and further investigations are required to better understand the importance of the *psp* response in EW. It was clear that 10% EW influences *pspF*, *pspA* and *pspG* expression at 30 °C. Induction of the *psp* genes was also observed after OT exposure, indicating a major role of this EW protein in the response of the *S*. Enteritidis *psp* genes to EW. However, the *psp* response fluctuated according to the concentration of OT, the time of exposure and the addition of iron. To better understand the *psp* response of *S*. Enteritidis, different temperatures could also be tested (4, 10, 20, 37 or 42 °C; the latter corresponds to the hen's body temperature). To confirm the influence of OT concentration, it would be interesting to test the expression of *psp* genes using different EW percentages. Furthermore, the method used to analyse gene expression seems to have an impact on the results, indeed, no induction of the *psp* genes was found after OT exposure for 45 min using qRT-PCR. The qRT-PCR analysis was performed only after 45 min and it would be interesting to repeat the experiment with longer time exposure (6 and 12h) as was performed with the transcriptional fusions. Utilisation of reporter gene to quantify the promoter activity has the advantage of being cheap, sensitive and easy to set up allowing numerous experimental conditions. However, the plasmid copy number can influence the gene expression due to regulator titration effects. Other more sensitive methods to study genes expression, such as qRT-PCR, can thus be utilised. Even if the cost of this method is not negligible, it does not require any cloning step and allows the direct quantification of the gene.

In this study, SM was used to dilute EW and OT; however *psp* gene expression could be influenced by this medium and it would be interesting to compare *psp* expression in SM and EWF (as used by Baron et al., 2017, 2020). As suggested in the previous chapter, other EW molecules might participate in the dissipation of the pmf of *S*. Enteritidis in EW. Among these molecules, BPIs are likely involved in this role. Thus, if these proteins appear to participate in the depolarisation of *S*. Enteritidis membranes, their role in the regulation of *psp* response should be investigated.

5.5.7. Conclusion

The *psp* response in EW is complex and seems to be subject to several factors. In this study, alkaline pH appears to be the major factor responsible for the *psp* gene expression in EW and this has been corroborated by several studies. The maintenance of the pmf seems to have a consequence on down-regulation of ATP-dependent genes involved in bacterial motility and metabolism (iron transport and uptake). Even if OT at its concentration found in EW seems to be able to induce *psp* genes expression, the influence of other proteins such as BPI could also play an important role.

Chapter 6.
General discussion

6.1. Introduction

Antimicrobial molecules possess several mechanisms to inhibit bacterial growth, targeting protein, DNA, RNA synthesis and bacterial membranes. Some of these molecules are naturally present in food. Phenolic compounds (polyphenols, tannins, flavonoids and other bioactive components) from fruits and vegetables have antimicrobial activity against both Gram-negative and -positive bacteria (Gyawali and Ibrahim, 2014 for a review). Dietary antimicrobial molecules can also come from animals sources, e.g. lactoferrin (milk), chitosan (exoskeletons of crustaceans and arthropods) and protamine (salmon) (Gyawali and Ibrahim, 2014 for a review). EW also contains numerous antimicrobial proteins such as OT, lysozyme, avidin and ovostatin (Baron et al., 2016 for review). However, eggs are often involved in food poisoning which is generally caused by *S*. Enteritidis contamination (EFSA, 2020). The frequency of salmonellosis, despite the natural defences of EW against bacteria, led to the study of the mechanism of action of EW-proteins toward *S*. Enteritidis. Among the antimicrobial EW proteins, OT has the major responsibility for the anti-*Salmonella* activity of EW which is due to its metal-chelating activity (Baron et al., 2016 for a review). In addition to their capacity to chelate iron, transferrins are also known to induce bacterial membrane damage (Aguilera et al., 2003; Baron et al., 2014; Ellison et al., 1988). Furthermore, the capacity of *S*. Enteritidis to acquire iron in EW remains theoretical. On the other hand, the impact of OT against *S*. Enteritidis membranes under EW conditions had not been previously investigated.

This study aimed to better understand the role of the metal-chelating activity of OT on *S*. Enteritidis growth and the capacity of *S*. Enteritidis to counteract the antimicrobial activity imposed by EW. Furthermore, this study determined the

impact of OT on *S*. Enteritidis membrane damage and the role of OT in the regulation of genes involved in the maintenance of membrane integrity.

6.2. *S*. Enteritidis and iron acquisition in egg white

This study determined that *S*. Enteritidis needs to synthesise and use siderophores to promote its growth in EW. The viscosity and the restricted motility of *S*. Enteritidis in EW might be a limiting factor in the diffusion of, and access to, free iron, and therefore in the growth of *S*. Enteritidis; this appears to be overcome by siderophore production. In low viscosity conditions (10% EW, 1.3 g/L OT), *S*. Enteritidis appears able to use systems other than siderophores to capture iron from its environment as no difference in growth was observed between the WT and Δ*entB* mutant. Finally, results showed that under EW conditions, the concentration of Ent (1 to 2 µM equivalent Desferal; Julien, 2020) produced by *S*. Enteritidis may not be sufficient to support bacterial growth. These results suggested: (i) low *S*. Enteritidis motility and therefore poor accessibility to iron in EW, directly caused by the high viscosity of EW; (ii) the capacity of *S*. Enteritidis to capture the iron directly bound to OT; (iii) the importance of siderophores to support *S*. Enteritidis growth in EW; (iv) the ability of *S*. Enteritidis to use other iron-system acquisition; and (v) an insufficient production of Ent in EW.

6.2.1. Egg-white viscosity and its impact on bacterial motility

The difficulty faced by *S*. Enteritidis in acquiring iron in EW could be explained by the high viscosity of EW and the consequent reduction in accessibility to nutrients. In fact, EW viscosity (5 mPa.s^{-1} at 20 °C and a shear rate of 400 s^{-1}; Lang & Rha, 1982) can directly influence bacterial motility. Indeed, authors using the same *S*. Enteritidis strain observed a down-regulation of many

genes involved in flagella biosynthesis after exposure to 10% EW for 7, 25 and 45 min (Baron et al., 2017). This result supports the notion that the difficulty faced by *S*. Enteritidis in acquiring iron in EW might be due lack of flagella associated with the high viscosity of this medium. Furthermore, several authors have reported the importance of flagella in *Salmonella* survival in EW. Gantois et al. (2008) observed expression of the flagellar basal body rod protein-G (*flgG)* (flagellar basal body rod protein) after 7 days in the oviduct but not in contaminated eggs, confirming a lack of flagella in EW. All relevant studies agree that lack of flagella affects the survival of *S*. Enteritidis in EW. A reduction in EW survival was observed for a non-motile *S*. Enteritidis mutant at 42 °C (hen body temperature) (Gantois et al., 2008). A similar observation was made by others (Cogan et al., 2004) as *S*. Enteritidis non-motile mutants (Δ*fliC* and Δ*motAB*) were unable to grow in EW compared to the WT. However, these authors reported the expression of *S*. Enteritidis flagella at high pH and iron-restricted conditions (colonization factor antigen broth (CFA) containing 0.5 g/L of OT). Additionally, the same authors reported that *S*. Enteritidis PT4 is motile in EW whereas motility mutants were not.

6.2.2. The effect of addition of iron to bacterial growth in egg white

The principal function of transferrin is to chelate iron and other metals. The iron-chelating activity of OT was described several times as responsible for EW's antimicrobial activity (Baron et al., 1997; Garibaldi, 1960; Lock & Board, 1992). Garibaldi (1960) was the first to describe this phenomenon on the growth of *Pseudomonas fluorescens*, *Proteus vulgaris*, *Proteus melanovogenes* and *Aerobacter cloacae* in EW by saturating OT at 105%. *Salmonella* growth was promoted by 4 $\log_{10}$ CFU/mL at 20 and 30 °C in EW saturated with 40% ferric

ammonium citrate (Lock & Board, 1992) and at 30 °C in EW saturated with 110% ferric ammonium citrate (Baron et al., 1997). These observations confirm the major role played by the iron-chelating activity of OT in EW.

6.2.3. Importance of siderophores for *S*. Enteritidis growth in egg white

The survival of *S*. Enteritidis in EW is often attributed to the production of siderophores. Thus, Kang et al. (2006) observed a delay of *S*. Enteritidis growth in EW after addition of iron (110% theorical OT iron saturation) when the bacteria were unable to produce siderophores (Δ*entF* and Δ*entF/feoAB*) (reduction of 3 $\log_{10}$ CFU/mL cf. the WT). These findings confirm the importance of siderophore production for *S*. Enteritidis survival in EW. Indeed, in the present study, while OT was fully saturated in EW, the presence of siderophores was important to support *S*. Enteritidis growth (section 3.6). Furthermore, systems involved in the biosynthesis, uptake, utilisation and export of siderophores were expressed by *S*. Enteritidis after EW exposure (Baron et al., 2017; Huang et al., 2019).

Siderophores synthesis, uptake and export pathways

Using microarrays, *S*. Enteritidis global gene expression was studied after 7, 25 and 45 min exposure to EWMM at 45 °C by Baron et al. (2017). The authors observed a strong expression of *ent* genes, involved in the biosynthesis and export of Ent (4.13- to 7.81-fold at 45 min), and of *iro* genes, essential for the conversion of Ent to Sal and for Sal utilisation (1.59- to 4.11-fold at 45 min). These genes were also induced in EWF (proteins free EW), suggesting that the expression of siderophores is not directly correlated with the presence of OT. Huang et al. (2019) used RNAseq to study *S*. Enteritidis gene expressions after 6, 12 and 24 h exposure to 80% EW. Interestingly, *iro* genes were up-regulated

after 6, 12 and 24 h (0.7- to 2.4- fold at 24 h) whereas *ent* genes were down-regulated (-1.9- to -2.6-fold at 24 h) (Huang et al., 2019). Once synthesised in the cytoplasm, siderophores are secreted into the environment via EntS (Ent export) or IroC (Sal export). Despite the loss of the pmf caused by EW, which may affect ATP-dependent gene expression, both siderophore systems are up-regulated by *S*. Enteritidis after 45 min exposure to EWMM (2.75-fold for *iroC* and 4.13-fold for *entS*) (Baron et al., 2017, 2020). A two-fold expression of *iroC* was also reported after 6, 12 and 24 h exposure to 80% EW by Huang et al. (2019). Expression of systems used to uptake siderophore-iron complexes seems to be unaffected by outer-membrane permeabilisation as induced by OT. Thus, genes coding the specific receptors Ent, CirA and FepA were expressed after 45 min in EWMM (4-fold and 7.18-fold, respectively) as was the gene encoding IroN, which is specific for Sal (2.47-fold) (Baron et al., 2017). These genes were also up-regulated after 6, 12 and 24 h exposure to 80% EW (1.66-fold and 2.47-fold at 24 h for *cirA* and *iroN*, respectively) (Huang et al., 2019). Additionally, all these genes were also expressed after EWF exposure, confirming that membrane damaged cause by EW and OT does not influence the expression of genes involved in siderophore import/export, in EW. Although the genes involved in the acquisition of iron via siderophores were induced in EW conditions, those responsible for iron storage (ferritin, *ftn*) were repressed (0.19-fold at 45 min) in EWMM and in EWF (Baron et al., 2017, 2020). However, despite the expression of the siderophore pathways by *S*. Enteritidis in EW, insufficient production of Ent for the support of bacterial growth is suggested by this study (section 3.7).

This may be related to the presence of lipocalins (i.e. proteins with siderophore-sequestering activity). Indeed, these proteins were identified in EW

(D'Ambrosio et al., 2008; Desert et al., 2001; Guérin-Dubiard et al., 2006; Mann, 2007; Mann & Mann, 2011) and, among these proteins, Ex-FABP, at its concentration found in EW (i.e. ~5 µM), was shown to limit Ent activity. Indeed, *S*. Enteritidis Δ*entB* growth was reduced 4 $\log^{10}$ CFU/mL in the presence of Ex-FABP and DIP (strong iron chelator) (Julien et al., 2020). Thus, Ex-FABP may have a significant impact on the ability of Ent to support *S*. Enteritidis growth in EW. Furthermore, in the absence of lipocalins (EWF with 1.3 g/L of OT) or at lower concentration (0.5 µM; EWF with 10% of EW), siderophores appear not to be essential for bacterial survival (section 3.6) suggesting (i) the inefficiency of lipocalins at low concentration and (ii) the ability of *S*. Enteritidis in absence of siderophores to use other iron-acquisition systems.

6.2.4. Other iron acquisition systems

6.2.4.1. Iron uptake from transferrins

S. Enteritidis seems able to use iron directly bound from the fully-saturated OT in EW and from 50%-saturated OT in EWF with 10% EW and EWF with 1.3 g/L OT (section 3.5 and 3.6). This is in accordance with the finding that *S*. Typhimurium was able to use iron directly bound to human transferrin in M9 medium (Choe et al., 2017). Indeed, this capacity to bind iron directly from transferrin seems to be mediated by the presence of outer membrane receptors. In fact, transferrin and lactoferrin receptors were identified (TbpAB and LbpAB respectively) in *Neisseria meningitidis* and *Neisseria gonorrhoeae* (Biswas & Sparling, 1995; Cornelissen & Sparling, 1994). Furthermore, the porin OmpC was identified as a potential candidate for the binding between transferrin and *S*. Typhimurium (Sandrini et al., 2013). However, to date, no OT receptor has been discovered in *Salmonella*. Nevertheless, in EW, OT is not fully saturated (1.07 to

5.4%) and *S*. Enteritidis was not able to acquire iron from OT for growth, unlike in absence of OT (EWF) (section 3.3). This result suggests that *S*. Enteritidis can use other iron-acquisition systems to survive in EW.

6.2.4.2. Iron uptake from haem

One gene related to haem acquisition (*ydiE*) was up regulated by *S*. Enteritidis after EWMM exposure for 7, 25 and 45 min at 45 °C (Baron et al., 2017). However, the function of this gene in *Salmonella* remains unclear. Furthermore, free non-haem iron and haem-containing proteins are not present in EW. Thus, this gene, even expressed, is probably not effective in supporting iron uptake in EW.

6.2.4.3. Acquisition of ferrous iron

The second common form of iron available on Earth is ferrous iron (Fe^{2+}). The major transporter of Fe^{2+} is the FeoABC system (Cartron et al., 2006). No change in *feoABC* expression was observed after 45 min exposure to EWMM at 45 °C (Baron et al., 2017). Additionally, these genes were down-regulated after 6, 12 and 24 h exposure to 80% EW at 37 °C (Huang et al., 2019). However, both the *ent* and *feo* systems appeared important for *S*. Enteritidis survival in EW. Indeed, growth of *S*. Enteritidis Δ*entF* and Δ*feoAB* mutants was lower than the WT in EW at 37 °C (Kang et al., 2006). These findings highlight the variability of results depending on the strains and techniques employed. Thus, the role of the Feo system in EW remains unclear. Nevertheless, if ferrous iron is present in EW, alternative systems expressed by *S*. Enteritidis in EW may be used instead of *feo* (MntH, SitABCD, ZypT and YiipP). However, the primary function of these alternative systems is in the transport other metals (Mn^{2+} or Zn^{2+}) (Cunrath & Palmer, 2021).

6.2.4.4. Other metal acquisition pathways

Induction of the alternative Fe-S cluster biosynthesis pathway. Fe-S clusters are important cofactors composed of iron and sulphur, playing a role in cellular respiration and metabolism. In *S*. Enteritidis, the *sufABCDS* operon was induced in EWMM at 45 °C (3.77- to 9.35-fold at 45 min) (Baron et al., 2017). A similar result was observed after *S*. Enteritidis exposure to 80% EW for 6, 12 and 24 h at 37 °C (1.80- to 3.19-fold at 24 h) (Huang et al., 2019). These results are consistent with the finding that in *E. coli*, the *suf* operon is important in Fe-S construction when iron is scarce in the environment. Indeed, a second pathway (*isc*) is generally used for the biosynthesis of Fe-S clusters. However, even if both *suf* and *isc* operons were induced by iron starvation, a decrease of *E. coli* growth was observed in a Δ*sufABCDSE* mutant compared to the WT and *iscS* mutant (Outten et al., 2004). Thus, it is likely that in EW, *S*. Enteritidis might use this pathway to deal with its restricted iron environment.

Manganese-dependent pathway. Two transporters of Mn^{2+} with low Fe^{2+} affinity can be synthetised and used by *Salmonella* serovars under alkaline (SitABCD) or acidic conditions (MntH) (Wellawa et al., 2020). These two transporters were induced by *S*. Enteritidis after EWMM exposure (4.71- to 9.54-fold and 2.21-fold at 45 min for *sitABCD* and *mntH*, respectively) (Baron et al., 2017). After lengthy exposure to 80% EW, the expression of these transporters was also observed (3.84- to 4.68-fold and 3-fold at 24 h for *sitABCD* and *mntH*, respectively) (Huang et al., 2019). Furthermore, it has been shown that in a poor iron environment, both systems are induced by *S*. Typhimurium in minimal medium, after 24 h at 37 °C (Ikeda et al., 2005). However, the induction of

sitABCD in EWMM was greater than MntH and this might be explained by the fact that the latter has preference for acidic conditions.

6.2.5. Conclusion

All the genes involved in the different iron-acquisition pathways are under the control of Fur (Ferric Uptake Regulator) (Hantke, 1990). In its active form, Fur is a homodimer with each monomers carrying one structural zinc site which controls dimerization, and one regulatory iron-binding site. When iron is abundant in the bacterial niche, Fe-Fur binds specific sequences in the DNA (Fur boxes) which generally acts to block the transcription of iron transporters to prevent the uptake of excess iron that could result in toxicity. However, in the case of iron restriction, Fur cannot bind iron and therefore the Fur boxes are not occupied by Fur. Consequently, the transcription of genes controlling iron acquisition systems is turned on (derepressed). Thus, in EW, all such genes are expressed but do not seem effective in supporting growth. Indeed, membrane damaged caused by EW could potentially affect the proper functioning of the iron-acquisition systems.

6.3. *S*. Enteritidis envelope integrity in egg white

The second main objective of this study was to investigate the capacity of EW and OT to induce bacterial membrane damage. The hypothetical action of EW and OT on *S*. Enteritidis membranes is summarised in figure 6.1. Indeed, the results reported in this study prove the role of OT in inducing *S*. Enteritidis membrane damage, under EW conditions (same ionic environment and pH of 9.3), at 30 °C. EW can permeabilise the outer membrane and OT plays a major role in this permeabilisation. EW can also provoke, to a lesser extent, inner-membrane permeabilisation, whilst OT cannot. EW and OT, to a lesser extent,

provoke depolarisation of the inner membrane. Iron saturation of OT causes a slight inhibition of the capacity to depolarise the inner membrane but iron has no effect on outer membrane permeability although it has a modest impact on the inner membrane.

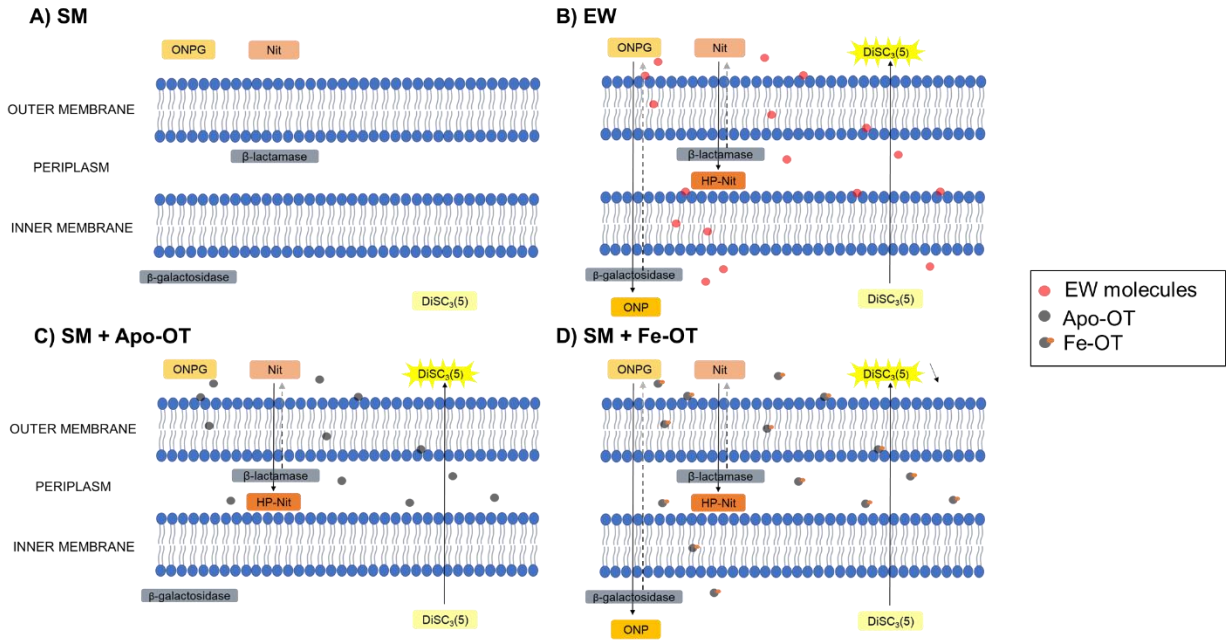

Figure 6.1. Hypothetical action of EW and OT on the membranes of *S*. Enteritidis. Abbreviations are as follow: Nit (nitrocefin) and HP-Nit (HP-nitrocefin) are the substrate and product of β-lactamase, respectively); ONPG and ONP are the substrate and product of β-galactosidase, respectively; $DiSC_3(5)$ is the potentiometric probe. After exposure to (A) SM, no change in membrane permeabilisation or depolarisation were observed. After exposure to (B) EW, Nit was internalised into the periplasm and hydrolysed into HP-Nit by the β-lactamase, indicating a permeabilisation of the outer membrane of *S*. Enteritidis. In the same manner, ONPG was internalised into the cytoplasm and hydrolysed into ONP by the β-galactosidase, indicating a slight permeabilisation of the inner membrane. Furthermore, the depolarisation of the inner membrane was also indicated by the extracellular release of the fluorescence probe $DiSC_3(5)$. After exposure to (C) SM with OT, Nit was internalised into the periplasm and hydrolysed into HP-Nit, indicating a permeabilisation of the outer membrane, however, ONPG was not internalised into the cytoplasm. Independently of the permeabilisation of the inner membrane, $DiSC_3(5)$ was released, showing the ability of OT to induce inner-membrane depolarisation. For (D) OT saturated with iron, a similar result was observed as in (C) with unsaturated OT concerning the permeabilisation of *S*. Enteritidis membranes, although Fe-OT caused a modest increase in inner-membrane permeability. However, the depolarisation of the inner membrane by OT was inhibited by saturation with iron. The dashed lines represent the possibility of enzyme release from the cell. Both periplasmic and released / cytoplasmic and released enzyme would be quantitated in this assay.

It is important to note that despite the membrane perturbations observed, *S*. Enteritidis is able to survive in EW or in SM with OT at 30 °C (i.e. cell number increased by 0.3 and 0.4 log_{10} CFU/mL, respectively). Thus, OT does not provoke bacterial lysis and at 30 °C, *S.* Enteritidis is able to deal with these membranes stresses to generate an appropriate response that many authors have highlighted through the observation of induction of genes involved in the maintenance of *S*. Enteritidis membrane integrity in EW (Baron et al., 2017; Clavijo et al., 2006; Gantois et al., 2008; Huang et al., 2019, 2020; Qin et al., 2019). Indeed, many genes involved in the envelope stress response were induced after exposure to EWMM and EWF at 45 °C (Baron et al., 2017, 2020). However, *psp* genes were not induced after EWF exposure suggesting a role for EW proteins in the regulation of these genes (Baron et al., 2020). In this study, the ability of EW and OT (at its concentration found in EW) to promote *psp* gene expression was observed, confirming these previous findings. Indeed, these genes are known to be expressed following a dissipation of the pmf (section 5.5.4) (Becker et al., 2005; Kobayashi et al., 2007a). Furthermore, alkaline pH might also induce *psp* gene expression since several authors have reported this (section 5.5.3) (Becker et al., 2005; Vrancken et al., 2008; Wiegert et al., 2001). This is in accordance with the present results showing expression of *psp* genes after SM exposure (pH 9.2). However no change of expression was observed by Baron et al., (2020) in *S*. Enteritidis after EWF exposure. Thus, the impact of alkaline pH on *psp* response in EW requires further investigation. Furthermore, expression of *psp* genes can impact bacterial motility. Indeed, the motility of *E. coli* decreased when *pspG* was over-expressed (Lloyd et al., 2004). Furthermore, it has been confirmed that overproduction of PspG (independently of other proteins) resulted

in a down-regulation of genes involved in *E. coli* motility after exposure to minimal medium supplemented with 0.4% of glucose and 10 mM of NH_4Cl, at 37 °C (Jovanovic et al., 2006). Interestingly, a down-regulation of *S*. Enteritidis motility genes combined with an up-regulation of *pspG* in EWMM were observed (Baron et al., 2017). This observation might be linked with the loss of the pmf caused by EW as this latter drives flagella motility (Manson et al., 1977).

Furthermore, other EW molecules seem also to be involved in the membrane stress observed in EW. Indeed, in this study a possible cooperation between OT and lysozyme was suggested as lysozyme was able to induce inner membrane permeabilisation (section 4.5.2). Nevertheless, lysozyme does not induce membrane depolarisation, suggesting the implication of other EW molecules such as defensins and BPI. Two defensins (AvBD11 and Gallin) have been identified in EW (Mann, 2007). AvBD11 shows an antimicrobial activity against *S*. Enteritidis in TBS and BHI at 37 °C (Hervé-Grépinet et al., 2010). A drastic effect of Gallin on *E. coli* survival was also observed (95% inhibition at 1 µM) (Gong et al., 2010). As suggested by van Dijk et al. (2008), these defensins could interact with outer membrane components and destabilise membrane integrity. Three BPI proteins (Tenp, BPIL2 and Similar to BPI) have also been identified in EW (Guérin-Dubiard et al., 2006; Mann, 2007). The role of these proteins in EW remains unknown. However, they could act by binding to LPS resulting in bacterial growth arrest followed by a bactericidal effect as a result of inner membrane damage (Elsbach & Weiss, 1998). Furthermore, it has been shown that BPI causes dissipation of the pmf, reinforcing the hypothesis that these proteins participate in *S*. Enteritidis inner membrane depolarisation in EW

(Barker et al., 2000). However, to date, no study has demonstrated the implication of BPI or defensins in *S*. Enteritidis membranes damage in EW.

6.4. Future work

This study focused on three main points: (1) the impact of the iron-chelating activity of OT in EW on *S*. Enteritidis; (2) the membrane damage caused by OT in EW; and (3) the response of *S*. Enteritidis to maintain membrane integrity. The impact of EW on the *S*. Enteritidis membrane might be directly correlated with the capacity of the bacteria to acquire iron. Indeed, many iron-acquisition systems are located in the outer membrane and are pmf- as well as ATP-dependent, and could therefore be affected by membrane damage. Thus, further experiments should be performed to study the effectiveness of such transporters in EW. Indeed, as previously described (section 6.2.3), genes encoding iron-acquisition systems are induced by *S*. Enteritidis in EWMM but might be not functional. The present results have reported the ability of OT to depolarise the *S*. Enteritidis inner membrane. In response to this stress, results showed that *psp* genes were induced. It has been suggested using liposomes that PspA, by forming a scaffold on the inner membrane and by binding both phosphatidylglycerol and phosphatidylserine, could modify the rigidity of the membrane to facilitate pmf restoration (Kobayashi et al., 2007). However, the physiological response of *psp* genes in EW is unknown and could be investigated. Additionally, it would be interesting to consider the impact of EW viscosity and *psp* gene expression on *S*. Enteritidis motility, and the consequent ability of bacteria to acquire iron. For these future experiments, *S*. Enteritidis single and double mutants for *pspA* and *pspG* should be constructed and employed.

The permeabilisation of the outer membrane requires a specific mechanism which is remains unknown. The location of fluorescently-labelled proteins can be visualised by confocal microscopy (Farkas et al., 2017). It is possible that OT can interact with and interfere with membrane proteins; such an interaction could be explored by crosslinking and co-precipitation combined with mass spectrometry or proteome microarray (Mücke et al., 2020; Shah et al., 2016). It could be possible to consider more direct method to monitor membrane perturbation using fluorescent probes (phase contrast and fluorescence microscopy) (Buttress et al., 2022). The cooperation of different EW proteins, especially those inducing bacterial membrane damage, might also be explored. Indeed, it is likely that BPI proteins also play a major role in *S*. Enteritidis membrane damage and, therefore, the *psp* response. Future studies exploring this possibility could involve purification of BPIs (Tenp, BPI-2 and Similar-to-BPI) from EW (or from overexpressing strains) which would allow their structural characterisation. Then, the ability of these proteins to induce *S*. Enteritidis inner-membrane depolarisation and *psp* response could be explored.

References

Aasa, R., Malmström, B. G., Saltman, P., & Vänngård, T. (1963). The specific binding of iron(III) and copper(II) to transferrin and conalbumin. *Biochimica et Biophysica Acta*, *75*, 203-222.

Achtman, M., Wain, J., Weill, F.-X., Nair, S., Zhou, Z., Sangal, V., Krauland, M. G., Hale, J. L., Harbottle, H., Uesbeck, A., Dougan, G., Harrison, L. H., Brisse, S., & Group, the S. enterica M. study. (2012). Multilocus sequence typing as a replacement for serotyping in *Salmonella enterica*. *PLOS Pathogens*, *8*(6), e1002776.

Ades, S. E., Connolly, L. E., Alba, B. M., & Gross, C. A. (1999). The *Escherichia coli* ςE-dependent extracytoplasmic stress response is controlled by the regulated proteolysis of an anti-ς factor. *Genes & Development*, *13*(18), 2449-2461.

Aguilera, O., Quiros, L. M., & Fierro, F. (2003). Transferrins selectively cause ion efflux through bacterial and artificial membranes. *FEBS Letters*, *548*(1-3), 5-10.

Akiyama, Y., Kanehara, K., & Ito, K. (2004). RseP (YaeL), an Escherichia coli RIP protease, cleaves transmembrane sequences. *The EMBO journal*, 23(22), 4434-4442.

Alabdeh, M., Lechevalier, V., Nau, F., Gautier, M., Cochet, M.-F., Gonnet, F., Jan, S., & Baron, F. (2011). Role of incubation conditions and protein fraction on the antimicrobial activity of egg white against *Salmonella* Enteritidis and *Escherichia coli* . *Journal of Food Protection*, *74*(1), 24-31.

Alderton, G., Ward, W. H., & Fevold, H. L. (1946). Identification of the bacteria-inhibiting, iron binding protein of egg white as conalbumin. *Archives of Biochemistry and Biophysics*, *11*, 9-13.

Anderson, B. F., Baker, H. M., Morris, G. E., Rumball, S. V., & Baker, E. N. (1990). Apolactoferrin structure demonstrates ligand-induced conformational change in transferrins. *Nature*, *344*(6268), 784-787.

Andrews, S. C., Robinson, A. K., & Rodriguez-Quinones, F. (2003). Bacterial iron homeostasis. *FEMS Microbiology Reviews*, *27*(2-3), 215-237.

Arya, M., Shergill, I. S., Williamson, M., Gommersall, L., Arya, N., & Patel, H. R. (2005). Basic principles of real-time quantitative PCR. *Expert Review of Molecular Diagnostics*, *5*(2), 209-219.

Azari, P. R., & Feeney, R. E. (1958). Resistance of metal complexes of conalbumin and transferrin to proteolysis and to thermal denaturation. *Journal of Biological Chemistry*, *232*(1), 293-302.

Banks, J., Board, R., & Sparks, N. (1986). Natural antimicrobial systems and their potential in food preservation of the future. *Biotechnology and Applied Biochemistry*, *8*(2-3), 103-147.

Barker, H. C., Kinsella, N., Jaspe, A., Friedrich, T., & O'Connor, C. D. (2000). Formate protects stationary-phase *Escherichia coli* and *Salmonella* cells from killing by a cationic antimicrobial peptide. *Molecular Microbiology*, *35*(6), 1518-1529.

Baron, F., Bonnassie, S., Alabdeh, M., Cochet, M.-F., Nau, F., Guérin-Dubiard, C., Gautier, M., Andrews, S. C., & Jan, S. (2017). Global gene-expression analysis of the response of *Salmonella* Enteritidis to egg white exposure reveals multiple egg white-imposed stress responses. *Frontiers in Microbiology*, *8*, 829.

Baron, F., Cochet, M.-F., Alabdeh, M., Guérin-Dubiard, C., Gautier, M., Nau, F., Andrews, S. C., Bonnassie, S., & Jan, S. (2020). Egg-White proteins have a minor impact on the bactericidal action of egg white toward *Salmonella* Enteritidis at 45°C. *Frontiers in Microbiology*, *11*, 584986.

Baron, F., Gautier, M., & Brule, G. (1997). Factors involved in the inhibition of growth of *Salmonella* enteritidis in liquid egg white. *Journal of Food Protection*, *60*(11), 1318-1323.

Baron, F., Gautier, M., & Brule, G. (1999). Rapid growth of *Salmonella* Enteritidis in egg white reconstituted from industrial egg white powder. *Journal of Food Protection*, *62*(6), 585-591.

Baron, F., & Jan, S. (2011). Egg and egg product microbiology. In Y. Nys, M. Bain, & F. Van Immerseel, *Improving the safety and quality of eggs and egg products. Vol. 1 : Egg chemistry, production and consumption* (Woodhead Publishing Limited, Vol. 1, p. 330-350). Woodhead Publishing Limited.

Baron, F., & Jan, S. (2017). Mechanisms for transmission of pathogens into eggs. In *Achieving sustainable production of eggs Volume 1* (p. 131-160). Burleigh Dodds Science Publishing.

Baron, F., Jan, S., Gonnet, F., Pasco, M., & Jardin, J. (2014). Ovotransferrin plays a major role in the strong bactericidal effect of egg white against the *Bacillus cereus* group. *Journal of Food Protection*, *77*(6), 955-962.

Baron, F., Jan, S., Techer, C. (2023). Microbiology of egg and egg products. In *Handbook of Egg Science and Technology* (p. 355-396). CRC Press.

Baron, F., Nau, F., Guérin-Dubiard, C., Bonnassie, S., Gautier, M., Andrews, S. C., & Jan, S. (2016). Egg white versus *Salmonella* Enteritidis ! A harsh medium meets a resilient pathogen. *Food Microbiology*, *53*, 82-93.

Baron, F., Nau, F., Guérin-Dubiard, C., Gonnet, F., Dubois, J.-J., & Gautier, M. (2003). Effect of dry heating on the microbiological quality, functional properties, and natural bacteriostatic ability of egg white after reconstitution. *Journal of Food Protection*, *66*(5), 825-832.

Barrow, P. A., Jones, M. A., Smith, A. L., & Wigley, P. (2012). The long view : *Salmonella* – the last forty years. *Avian Pathology*, *41*(5), 413-420.

Barrow, P. A., & Lovell, M. A. (1991). Experimental infection of egg-laying hens with *Salmonella* enteritidis phage type 4. *Avian Pathology*, *20*(2), 335-348.

Bäumler, A. J., Norris, T. L., Lasco, T., Voigt, W., Reissbrodt, R., Rabsch, W., & Heffron, F. (1998). IroN, a novel outer membrane siderophore receptor characteristic of *Salmonella enterica* . *Journal of Bacteriology*, *180*(6), 1446-1453.

Becker, L. A., Bang, I.-S., Crouch, M.-L., & Fang, F. C. (2005). Compensatory role of PspA, a member of the phage shock protein operon, in rpoE mutant *Salmonella enterica* serovar Typhimurium. *Molecular Microbiology*, *56*(4), 1004-1016.

Beckett, D. (2007). Biotin sensing : Universal influence of biotin status on transcription. *Annual Review of Genetics*, *41*(1), 443-464.

Belasco, J. G., & Brawerman, G. (2012). *Control of Messenger RNA Stability*. Elsevier.

Bergan, T., Bergan, T., Klaveness, J., Klaveness, J., Aasen, A. J., & Aasen, A. J. (2000). Chelating agents. *Chemotherapy*, *47*(1), 10-14.

Bichler, L. A., Nagaraja, K. V., & Halvorson, D. A. (1996). *Salmonella* enteritidis in eggs, cloacal swab specimens, and internal organs of experimentally infected White Leghorn chickens. *American Journal of Veterinary Research*, *57*(4), 489-495.

Bingle, C. D., & Craven, C. J. (2004). Meet the relatives : A family of BPI- and LBP-related proteins. *Trends in Immunology*, *25*(2), 53-55.

Biswas, G. D., & Sparling, P. F. (1995). Characterization of lbpA, the structural gene for a lactoferrin receptor in *Neisseria gonorrhoeae* . *Infection and Immunity*, *63*(8), 2958-2967.

Blattner, F. R., Plunkett, G., Bloch, C. A., Perna, N. T., Burland, V., Riley, M., Collado-Vides, J., Glasner, J. D., Rode, C. K., Mayhew, G. F., Gregor, J., Davis, N. W., Kirkpatrick, H. A., Goeden, M. A., Rose, D. J., Mau, B., & Shao, Y. (1997). The complete genome sequence of *Escherichia coli* K-12. *Science*, *277*(5331), 1453-1462.

Bolivar, F., Rodriguez, R. L., Greene, P. J., Betlach, M. C., Heyneker, H. L., Boyer, H. W., Crosa, J. H., & Falkow, S. (1977). Construction and characterization of new cloning vehicles. II. A multipurpose cloning system. *Gene*, *2*(2), 95-113.

Bonocora, R. P., Smith, C., Lapierre, P., & Wade, J. T. (2015). Genome-scale mapping of *Escherichia coli* σ54 reveals widespread, conserved intragenic binding. *PLOS Genetics*, *11*(10), e1005552.

Booth, I. R. (1985). Regulation of cytoplasmic pH in bacteria. *Microbiological Reviews*, *49*(4), 359-378.

Branen, J. K., & Davidson, P. M. (2004). Enhancement of nisin, lysozyme, and monolaurin antimicrobial activities by ethylenediaminetetraacetic acid and lactoferrin. *International Journal of Food Microbiology*, *90*(1), 63-74.

Braun, V. (1975). Covalent lipoprotein from the outer membrane of *Escherichia coli* . *Biochimica et Biophysica Acta (BBA) - Biomembranes*, *415*(3), 335-377.

Bremer, H., & Yuan, D. (1968). RNA chain growth-rate in *Escherichia coli*. *Journal of Molecular Biology*, *38*(2), 163-180.

Brooks, J., & Hale, H. P. (1959). The mechanical properties of the thick white of the hen's egg. *Biochimica et Biophysica Acta*, *32*, 237-250.

Brooks, J., & Pace, J. (1938). The distribution of carbon dioxide in the hen's egg. *Proceedings of the Royal Society of London. Series B-Biological Sciences*, *126*(843), 15.

Bullis, K. L. (1977). The history of avian medicine in the U.S. II. Pullorum disease and fowl typhoid. *Avian Diseases*, *21*(3), 422-429.

Burley, R. W., & Vadehra, D. V. (1989). *The avian egg : Chemistry and biology*. Wiley-Blackwell.

Buttress, J. A., Halte, M., Te Winkel, J. D., Erhardt, M., Popp, P. F., & Strahl, H (2022). A guide for membrane potential measurements in Gram-negative bacteria using voltage-sensitive dyes. *bioRxiv*. 2022-04.

Callewaert, L., & Michiels, C. W. (2010). Lysozymes in the animal kingdom. *Journal of Biosciences*, *35*(1), 127-160.

Carbonetti, N. H., & Williams, P. H. (1984). A cluster of five genes specifying the aerobactin iron uptake system of plasmid ColV-K30. *Infection and Immunity*, *46*(1), 7-12.

Cartron, M. L., Maddocks, S., Gillingham, P., Craven, C. J., & Andrews, S. C. (2006). Feo – Transport of ferrous iron into bacteria. *BioMetals*, *19*(2), 143-157.

Caza, M., Garénaux, A., Lépine, F., & Dozois, C. M. (2015). Catecholate siderophore esterases Fes, IroD and IroE are required for salmochelins secretion following utilization, but only IroD contributes to virulence of extra-intestinal pathogenic Escherichia coli. *Molecular Microbiology*, *97*(4), 717-732.

Caza, M., & Kronstad, J. (2013). Shared and distinct mechanisms of iron acquisition by bacterial and fungal pathogens of humans. *Frontiers in Cellular and Infection Microbiology*, *3*.

Chart, H., Buck, M., Stevenson, P., & Griffiths, E. (1986). Iron regulated outer membrane proteins of *Escherichia coli* : Variations in expression due to the chelator used

to restrict the availability of iron. *Journal of General Microbiology*, *132*(5), 1373-1378.

Chart, H., & Rowe, B. (1993). Iron restriction and the growth of *Salmonella enteritidis*. *Epidemiology and Infection*, *110*(1), 41-47.

Choe, Y., Yoo, A. Y., Kim, S. W., Hwang, J., & Kang, H. Y. (2017). *Salmonella* Typhimurium SL1344 utilizing human transferrin-bound iron as an iron source regardless of siderophore-mediated uptake. *Journal of Life Science*, *27*(1), 72-77.

Ciqual. (2021). https://ciqual.anses.fr/

Clavijo, R. I., Loui, C., Andersen, G. L., Riley, L. W., & Lu, S. (2006). Identification of genes associated with survival of *Salmonella enterica* Serovar Enteritidis in chicken egg albumen. *Applied and Environmental Microbiology*, *72*(2), 1055-1064.

Cochet, M.-F., Baron, F., Bonnassie, S., Jan, S., Leconte, N., Jardin, J., Briard-Bion, V., Gautier, M., Andrews, S. C., Guérin-Dubiard, C., & Nau, F. (2021). Identification of new antimicrobial peptides that contribute to the bactericidal activity of egg white against *Salmonella enterica* serovar Enteritidis at 45 °C. *Journal of Agricultural and Food Chemistry*, *69*(7), 2118-2128.

Cogan, T. A., Jørgensen, F., Lappin-Scott, H. M., Benson, C. E., Woodward, M. J., & Humphrey, T. J. (2004). Flagella and curli fimbriae are important for the growth of *Salmonella* enterica serovars in hen eggs. *Microbiology*, *150*(4), 1063-1071.

Collinet, B., Yuzawa, H., Chen, T., Herrera, C., & Missiakas, D. (2000). RseB binding to the periplasmic domain of RseA modulates the RseA:ςE interaction in the cytoplasm and the availability of ςE·RNA polymerase. *Journal of Biological Chemistry*, *275*(43), 33898-33904.

Cornelissen, C. N., & Sparling, P. F. (1994). Iron piracy : Acquisition of transferrin-bound iron by bacterial pathogens. *Molecular Microbiology*, *14*(5), 843-850.

Correnti, C., Clifton, M. C., Abergel, R. J., Allred, B., Hoette, T. M., Ruiz, M., Cancedda, R., Raymond, K. N., Descalzi, F., & Strong, R. K. (2011). Galline Ex-FABP is an antibacterial siderocalin and a lysophosphatidic acid sensor functioning through dual ligand specificities. *Structure*, *19*(12), 1796-1806.

Cotterill, O. J., & Winter, A. R. (1955). Egg White lysozyme : 3. The effect of pH on the lysozyme-ovomucin interaction. *Poultry Science*, *34*(3), 679-686.

Crichton, R. R. (1990). Proteins of iron storage and transport. In C. B. Anfinsen, J. T. Edsall, F. M. Richards, & D. S. Eisenberg (Éds.), *Advances in Protein Chemistry* (Vol. 40, p. 281-363). Academic Press.

Cunrath, O., & Palmer, J. D. (2021). An overview of *Salmonella enterica* metal homeostasis pathways during infection. *Microlife*, *2*, uqab001.

D'Ambrosio, C., Arena, S., Scaloni, A., Guerrier, L., Boschetti, E., Mendieta, M. E., Citterio, A., & Righetti, P. G. (2008). Exploring the chicken egg white proteome with combinatorial peptide ligand libraries. *Journal of Proteome Research*, *7*(8), 3461-3474.

D'Aoust, J., & Maurer, J. (2007). Salmonella *Species* (Doyle M, Beuchat L). ASM Press.

Darwin, A. J. (2005). The phage-shock-protein response. *Molecular Microbiology*, *57*(3), 661-628.

Derde, M., Guérin-Dubiard, C., Lechevalier, V., Cochet, M.-F., Jan, S., Baron, F., Gautier, M., Vié, V., & Nau, F. (2014). Dry-heating of lysozyme increases its activity against *Escherichia coli* membranes. *Journal of Agricultural and Food Chemistry*, *62*(7), 1692-1700.

Derde, M., Lechevalier, V., Guérin-Dubiard, C., Cochet, M.-F., Jan, S., Baron, F., Gautier, M., Vié, V., & Nau, F. (2013). Hen egg white lysozyme permeabilizes *Escherichia coli* outer and inner membranes. *Journal of Agricultural and Food Chemistry*, *61*(41), 9922-9929.

Desert, C., Guérin-Dubiard, C., Nau, F., Jan, G., Val, F., & Mallard, J. (2001). Comparison of different electrophoretic separations of hen egg white proteins. *Journal of Agricultural and Food Chemistry*, *49*(10), 4553-4561.

Devireddy, L. R., Gazin, C., Zhu, X., & Green, M. R. (2005). A cell-surface receptor for lipocalin 24p3 selectively mediates apoptosis and iron uptake. *Cell*, *123*(7), 1293-1305.

Du, H., Sheng, X., Zhang, H., Zou, X., Ni, B., Xu, S., Zhu, X., Xu, H., & Huang, X. (2011). RpoE may promote flagellar gene expression in *Salmonella enterica* serovar Typhi under hyperosmotic stress. *Current Microbiology*, *62*(2), 492-500.

Duguay, A. R., & Silhavy, T. J. (2004). Quality control in the bacterial periplasm. *Biochimica et Biophysica Acta (BBA) - Molecular Cell Research*, *1694*(1-3), 121-134.

EFSA, & ECDC. (2022). The European Union One Health 2021 Zoonoses Report. *EFSA Journal*, *20*(12), e07666.

Ellison, R. T., & Giehl, T. J. (1991). Killing of Gram-negative bacteria by lactofernn and lysozyme. *The Journal of Clinical Investigation*, *88*(4), 1080-1091.

Ellison, R. T., Giehl, T. J., & Laforce, F. M. (1988). Damage of the outer membrane of enteric Gram-negative bacteria by lactoferrin and transferrin. *Infection and Immunity*, *56*(11), 2774-2781.

Ellison, R. T., LaForce, F. M., Giehl, T. J., Boose, D. S., & Dunn, B. E. (1990). Lactoferrin and transferrin damage of the Gram-negative outer membrane is modulated by Ca2+ and Mg2+. *Journal of General Microbiology*, *136*(7), 1437-1446.

Elsbach, P., & Weiss, J. (1998). Role of the bactericidal/permeability-increasing protein in host defence. *Current Opinion in Immunology*, *10*(1), 45-49.

Epand, R. F., Pollard, J. E., Wright, J. O., Savage, P. B., & Epand, R. M. (2010). Depolarization, bacterial membrane composition, and the antimicrobial action of ceragenins. *Antimicrobial Agents and Chemotherapy*, *54*(9), 3708-3713.

Evans, R. W., Donovan, J. W., & Williams, J. (1977). Calorimetric studies on the binding of iron and aluminium to the amino- and carboxyl-terminal fragments of hen ovotransferrin. *FEBS Letters*, *83*(1), 19-22.

Facon, M. J., & Skura, B. J. (1996). Antibacterial activity of lactoferricin, lysozyme and EDTA against *Salmonella* Enteritidis. *International Dairy Journal*, *6*(3), 303-313.

Farkas, A., Maróti, G., Kereszt, A., & Kondorosi, É. (2017). Comparative analysis of the bacterial membrane disruption effect of two natural plant antimicrobial peptides. *Frontiers in Microbiology*, *8*.

Ferrières, Lionel., Aslam, S. N., Cooper, R. M., & Clarke, D. J. (2007). The yjbEFGH locus in *Escherichia coli* K-12 is an operon encoding proteins involved in exopolysaccharide production. *Microbiology*, *153*(4), 1070-1080.

Francez-Charlot, A., Laugel, B., Van Gemert, A., Dubarry, N., Wiorowski, F., Castanié-Cornet, M.-P., Gutierrez, C., & Cam, K. (2003). RcsCDB His-Asp phosphorelay system negatively regulates the flhDC operon in *Escherichia coli*. *Molecular Microbiology*, *49*(3), 823-832.

Gantois, I., Ducatelle, R., Pasmans, F., Haesebrouck, F., Gast, R., Humphrey, T. J., & Van Immerseel, F. (2009a). Mechanisms of egg contamination by *Salmonella Enteritidis* . *FEMS Microbiology Reviews*, *33*(4), 718-738.

Gantois, I., Ducatelle, R., Pasmans, F., Haesebrouck, F., & Immerseel, F. V. (2008). *Salmonella enterica* serovar Enteritidis genes induced during oviduct colonization and egg contamination in laying hens. *Applied and Environmental Microbiology*, *74*(21), 6616-6622.

Gantois, I., Ducatelle, R., Pasmans, F., Haesebrouck, F., & Van Immerseel, F. (2009b). The *Salmonella* Enteritidis lipopolysaccharide biosynthesis gene rfbH is required for survival in egg albumen. *Zoonoses and Public Health*, *56*(3), 145-149.

Garénaux, A., Houle, S., Folch, B., Dallaire, G., Truesdell, M., Lépine, F., Doucet, N., & Dozois, C. M. (2013). Avian lipocalin expression in chickens following *Escherichia coli* infection and inhibition of avian pathogenic *Escherichia coli*

growth by Ex-FABP. *Veterinary Immunology and Immunopathology*, *152*(1-2), 156-167.

Garibaldi, J. A. (1960). Factors in egg white which control growth of bacteria. *Journal of Food Science*, *25*(3), 337-344.

Garibaldi, J. A. (1970). Role of microbial iron transport compounds in the bacterial spoilage of eggs. *Applied Microbiology*, *20*(4), 558-560.

Gast, R. K., & Beard, C. W. (1990). Production of *Salmonella* Enteritidis-contaminated eggs by experimentally infected hens. *Avian Diseases*, *34*(2), 438-446.

Gehring, A. M., Mori, I., & Walsh, C. T. (1998). Reconstitution and characterization of the *Escherichia coli* enterobactin synthetase from EntB, EntE, and EntF. *Biochemistry*, *37*(8), 2648-2659.

Goetz, D. H., Holmes, M. A., Borregaard, N., Bluhm, M. E., Raymond, K. N., & Strong, R. K. (2002). The neutrophil lipocalin NGAL is a bacteriostatic agent that interferes with siderophore-mediated iron acquisition. *Molecular Cell*, *10*(5), 1033-1043.

Gong, D., Wilson, P. W., Bain, M. M., McDade, K., Kalina, J., Hervé-Grépinet, V., Nys, Y., & Dunn, I. C. (2010). Gallin; an antimicrobial peptide member of a new avian defensin family, the ovodefensins, has been subject to recent gene duplication. *BMC Immunology*, *11*(1), 12.

Gray, J. T., & Fedorka-Cray, P. J. (2002). *Salmonella* (In Cliver, D. O. and Riemann, H. P.). Academic Press.

Griffiths, E. L. W. Y. N. (1983). Availability of iron and survival of bacteria in infection. *Medical microbiology*, *3*, 153-177.

Grimont, P. A., & Weill, F.-X. (2007). Antigenic formulae of the *Salmonella serovars* . *WHO collaborating centre for reference and research on Salmonella*, *9*, 1-166.

Grittins, J. E., & Overfield, N. D. (1991). The nutrient content of eggs in Great Britain. *4th European Symposium on the Quality of eggs and eggs products*, 113-116.

Grossart, H.-P., Steward, G. F., Martinez, J., & Azam, F. (2000). A simple, rapid method for demonstrating bacterial flagella. *Applied and Environmental Microbiology*, *66*(8), 3632-3636.

Grossmann, J. G., Neu, M., Pantos, E., Schwab, F. J., Evans, R. W., Townes-Andrews, E., Lindley, P. F., Appel, H., Thies, W.-G., & Hasnain, S. S. (1992). X-ray solution scattering reveals conformational changes upon iron uptake in lactoferrin, serum and ovo-transferrins. *Journal of Molecular Biology*, *225*(3), 811-819.

Guérin-Dubiard, C., Pasco, M., Mollé, D., Désert, C., Croguennec, T., & Nau, F. (2006). Proteomic analysis of hen egg white. *Journal of Agricultural and Food Chemistry*, *54*(11), 3901-3910.

Guha Thakurta, P., Choudhury, D., Dasgupta, R., & Dattagupta, J. K. (2003). Structure of diferric hen serum transferrin at 2.8 Å resolution. *Acta Crystallographica Section D Biological Crystallography*, *59*(10), 1773-1781.

Gyawali, R., & Ibrahim, S. A. (2014). Natural products as antimicrobial agents. *Food Control*, *46*, 412-429.

Hantke, K. (1990). Iron and metal regulation in bacteria. *FEMS Microbiology Letters*, *67*(1-2), 5-8.

Hantke, K. (2001). Iron and metal regulation in bacteria. *Current Opinion in Microbiology*, *4*(2), 172-177.

Hellman, L. M., & Fried, M. G. (2007). Electrophoretic mobility shift assay (EMSA) for detecting protein–nucleic acid interactions. *Nature Protocols*, *2*(8), 8.

Hervé-Grépinet, V., Réhault-Godbert, S., Labas, V., Magallon, T., Derache, C., Lavergne, M., Gautron, J., Lalmanach, A.-C., & Nys, Y. (2010). Purification and characterization of avian β-Defensin 11, an antimicrobial peptide of the hen egg. *Antimicrobial Agents and Chemotherapy*, *54*(10), 4401-4409.

Hews, C. L., Cho, T., Rowley, G., & Raivio, T. L. (2019). Maintaining integrity under stress : Envelope stress response regulation of pathogenesis in Gram-negative bacteria. *Frontiers in Cellular and Infection Microbiology*, *9*, 313.

Hincke, M. T., Gautron, J., Panheleux, M., Garcia-Ruiz, J., McKee, M. D., & Nys, Y. (2000). Identification and localization of lysozyme as a component of eggshell membranes and eggshell matrix. *Matrix Biology: Journal of the International Society for Matrix Biology*, *19*(5), 443-453.

Hirose, J., Fujiwara, H., Magarifuchi, T., Iguti, Y., Iwamoto, H., Kominami, S., & Hiromi, K. (1996). Copper binding selectivity of N- and C-sites in serum (human)- and ovo-transferrin. *Biochimica et Biophysica Acta (BBA) - Protein Structure and Molecular Enzymology*, *1296*(1), 103-111.

Hook-Barnard, I. G., & Hinton, D. M. (2009). The promoter spacer influences transcription initiation via σ70 region 1.1 of *Escherichia coli* RNA polymerase. *Proceedings of the National Academy of Sciences*, *106*(3), 737-742.

Huang, X., Hu, M., Zhou, X., Liu, Y., Shi, C., & Shi, X. (2020). Role of yoaE gene regulated by CpxR in the survival of *Salmonella enterica* Serovar Enteritidis in antibacterial egg white. *MSphere*, *5*(1), 10-1128.

Huang, X., Zhou, X., Jia, B., Li, N., Jia, J., He, M., He, Y., Qin, X., Cui, Y., Shi, C., Liu, Y., & Shi, X. (2019). Transcriptional sequencing uncovers survival mechanisms

of *Salmonella enterica* Serovar Enteritidis in antibacterial egg white. *MSphere*, *4*(1).

Humphreys, S., Rowley, G., Stevenson, A., Anjum, M. F., Woodward, M. J., Gilbert, S., Kormanec, J., & Roberts, M. (2004). Role of the two-component regulator CpxAR in the virulence of *Salmonella enterica* Serotype Typhimurium. *Infection and Immunity*, *72*(8), 4654-4661.

Ibrahim, H. R., Sugimoto, Y., & Aoki, T. (2000). Ovotransferrin antimicrobial peptide (OTAP-92) kills bacteria through a membrane damage mechanism. *Biochimica et Biophysica Acta (BBA) - General Subjects*, *1523*(2), 196-205.

Ikeda, J. S., Janakiraman, A., Kehres, D. G., Maguire, M. E., & Slauch, J. M. (2005). Transcriptional Regulation of sitABCD of *Salmonella* enterica Serovar Typhimurium by MntR and Fur. *Molecular Biology of Pathogens*, *187*(3), 912-922.

Jan, S., Baron, F., Alabdeh, M., Chaari, W., Grosset, N. L., Cochet, M.-F. O., & Gautier, M. (2013). Biochemical and micrographic evidence of *Escherichia coli* membrane damage during incubation in egg white under bactericidal conditions. *Journal of Food Protection*, *76*(9), 1523-1529.

Jeltsch, J.-M., & Chambon, P. (1982). The complete nucleotide sequence of the chicken ovotransferrin mRNA. *European Journal of Biochemistry*, *122*(2), 291-295.

Jin, Q., & Kirk, M. F. (2018). pH as a primary control in environmental microbiology : 1. thermodynamic perspective. *Frontiers in Environmental Science*, *6*, 21.

Joly, N., Burrows, P. C., Engl, C., Jovanovic, G., & Buck, M. (2009). A lower-order oligomer form of phage shock protein A (PspA) stably associates with the hexameric AAA+ transcription activator protein PspF for negative regulation. *Journal of Molecular Biology*, *394*(4), 764-775.

Joly, N., Engl, C., Jovanovic, G., Huvet, M., Toni, T., Sheng, X., Stumpf, M. P. H., & Buck, M. (2010). Managing membrane stress : The phage shock protein (Psp) response, from molecular mechanisms to physiology. *FEMS Microbiology Reviews*, *34*(5), 797-827.

Jovanovic, G., Lloyd, L. J., Stumpf, M. P. H., Mayhew, A. J., & Buck, M. (2006). Induction and function of the phage shock protein extracytoplasmic stress response in *Escherichia coli* . *Journal of Biological Chemistry*, *281*(30), 21147-21161.

Jovanovic, G., Weiner, L., & Model, P. (1996). Identification, nucleotide sequence, and characterization of PspF, the transcriptional activator of the Escherichia coli stress-induced psp operon. *Journal of Bacteriology*, *178*(7), 1936-1945.

Julien, L. A. (2020). *Understanding the relationship between antibacterial activity and iron-restriction mechanisms in egg-white* [Thèse de doctorat, Institut Agro Rennes Angers ; University of Reading].

Julien, L. A., Fau, C., Baron, F., Guérin-Dubiard, C., Nau, F., Gautier, M., Karatzas, K. A., Jan, S., & Andrews, S. C. (2020). The three lipocalins of egg-white : Only Ex-FABP inhibits siderophore-dependent iron sequestration by *Salmonella* Enteritidis. *Frontiers in Microbiology*, *11*, 913.

Kang, H., Loui, C., Clavijo, R. I., Riley, L. W., & Lu, S. (2006). Survival characteristics of *Salmonella enterica* serovar Enteritidis in chicken egg albumen. *Epidemiology & Infection*, *134*(5), 967-976.

Kato, A., Ogato, S., Matsudomi, N., & Kobayashi, K. (1981). Comparative study of aggregated and disaggregated ovomucin during egg white thinning. *Journal of Agricultural and Food Chemistry*, *29*(4), 821-823.

Kato, A., Ogino, K., Kuramoto, Y., & Kobayashi, K. (1979). Degradation of the p-glycosidally linked carbohydrate units of ovomucin during egg white thinning. *Journal of Food Science*, *44*(5), 1341-1344.

Kenyon, W. J., Nicholson, K. L., Rezuchova, B., Homerova, D., Garcia-del Portillo, F., Finlay, B. B., Pallen, M. J., Kormanec, J., & Spector, M. P. (2007). σ s-Dependent carbon-starvation induction of pbpG (PBP 7) is required for the starvation-stress response in *Salmonella enterica* serovar Typhimurium. *Microbiology*, *153*(7), 2148-2158.

Kleerebezem, M., Crielaard, W., & Tommassen, J. (1996). Involvement of stress protein PspA (phage shock protein A) of *Escherichia coli* in maintenance of the protonmotive force under stress conditions. *The EMBO Journal*, *15*(1), 162-171.

Klein, C. A., Teufel, M., Weile, C. J., & Sobetzko, P. (2021). The bacterial promoter spacer modulates promoter strength and timing by length, TG-motifs and DNA supercoiling sensitivity. *Scientific Reports*, *11*(1), 1.

Ko, K. Y., & Ahn, D. U. (2008). An economic and simple purification procedure for the large-scale production of ovotransferrin from egg white. *Poultry Science*, *87*(7), 1441-1450.

Ko, K. Y., Mendonca, A. F., & Ahn, D. U. (2008). Effect of ethylenediaminetetraacetate and lysozyme on the antimicrobial activity of ovotransferrin against *Listeria monocytogenes* . *Poultry Science*, *87*(8), 1649-1658.

Ko, K. Y., Mendoncam, A. F., Ismail, H., & Ahn, D. U. (2009). Ethylenediaminetetraacetate and lysozyme improves antimicrobial activities of ovotransferrin against *Escherichia coli* O157:H7. *Poultry Science*, *88*(2), 9.

Kobayashi, R., Suzuki, T., & Yoshida, M. (2007). Escherichia coli phage-shock protein A (PspA) binds to membrane phospholipids and repairs proton leakage of the damaged membranes. *Molecular Microbiology*, *66*(1), 100-109.

Kurokawa, H., Dewan, J. C., Mikami, B., Sacchettini, J. C., & Hirose, M. (1999). Crystal structure of hen apo-ovotransferrin : Both lobes adopt an open conformation upon loss of iron. *Journal of Biological Chemistry*, *274*(40), 28445-28452.

Kurokawa, H., Mikami, B., & Hirose, M. (1995). Crystal structure of diferric hen ovotransferrin at 2.4 Å resolution. *Journal of Molecular Biology*, *254*(2), 196-207.

Lang, E. R., & Rha, C. (1982). Apparent shear viscosity of native egg white. *Journal of Food Science & Technology*, *17*(5), 595-606.

Legros, J., Jan, S., Bonnassie, S., Gautier, M., Croguennec, T., Pezennec, S., Cochet, M.-F., Nau, F., Andrews, S. C., & Baron, F. (2021). The role of ovotransferrin in egg-white antimicrobial activity : A review. *Foods*, *10*(4), 4.

Lehrer, R. I., Barton, A., & Ganz, T. (1988). Concurrent assessment of inner and outer membrane permeabilization and bacteriolysis in *E. coli* by multiple-wavelength spectrophotometry. *Journal of Immunological Methods*, *108*(1), 153-158.

Lehrer, R. I., Bevins, C. L., & Ganz, T. (2005). Defensins and other antimicrobial peptides and proteins. *Mucosal Immunology*, 95-110.

Leive, L. (1974). The barrier function of the Gram-negative envelope. *Annals of the New York Academy of Sciences*, *235*(1), 109-129.

Li-Chan, E. (1989). Biochemical basis for the properties of egg white. *Critical reviews in poultry biology*, *2*, 21-58.

Lignieres, J. (1900). *Maladies du porc*. *18*, 389-431.

Lin, H., Fischbach, M. A., Liu, D. R., & Walsh, C. T. (2005). In vitro characterization of salmochelin and enterobactin trilactone hydrolases IroD, IroE, and Fes. *Journal of the American Chemical Society*, *127*(31), 11075-11084.

Lin, L. N., Mason, A. B., Woodworth, R. C., & Brandts, J. F. (1994). Calorimetric studies of serum transferrin and ovotransferrin. Estimates of domain interactions, and study of the kinetic complexities of ferric ion binding. *Biochemistry*, *33*(7), 1881-1888.

Liu, M., Yu, W., Ren, F., & Wu, J. (2018). Formation and characterization of peptides in egg white during storage at ambient temperature. *Food Chemistry*, *263*, 135-141.

Livak, K. J., & Schmittgen, T. D. (2001). Analysis of Relative Gene Expression Data Using Real-Time Quantitative PCR and the 2−ΔΔCT Method. *Methods*, *25*(4), 402-408.

Lloyd, L. J., Jones, S. E., Jovanovic, G., Gyaneshwar, P., Rolfe, M. D., Thompson, A., Hinton, J. C., & Buck, M. (2004). Identification of a new member of the phage shock protein response in *Escherichia coli* , the phage shock protein G (PspG). *Journal of Biological Chemistry*, *279*(53), 55707-55714.

Lock, J. L., & Board, R. G. (1992). Persistence of contamination of hens' egg albumen in vitro with *Salmonella* serotypes. *Epidemiology & Infection*, *108*(3), 389-396.

Luckey, M., Pollack, J. R., Wayne, I. R., Ames, B. N., & Neilands, J. B. (1972). Iron uptake in *Salmonella* Typhimurium : Utilization of exogenous siderochromes as iron carriers. *Journal of Bacteriology*, *111*(3), 731-738.

Ma, B., Guo, Y., Fu, X., & Jin, Y. (2020). Identification and antimicrobial mechanisms of a novel peptide derived from egg white ovotransferrin hydrolysates. *LWT*, *131*, 109720.

Mann, K. (2007). The chicken egg white proteome. *Proteomics*, *7*(19), 3558-3568.

Mann, K., & Mann, M. (2011). In-depth analysis of the chicken egg white proteome using an LTQ Orbitrap Velos. *Proteome Science*, *9*(1), 7.

Manson, M. D., Tedesco, P., Berg, H. C., Harold, F. M., & Van der Drift, C. (1977). A protonmotive force drives bacterial flagella. *Proceedings of the National Academy of Sciences*, *74*(7), 3060-3064. 0

Masse, E., & Gottesman, S. (2002). A small RNA regulates the expression of genes involved in iron metabolism in *Escherichia coli* . *Proceedings of the National Academy of Sciences*, *99*(7), 4620-4625.

Meselson, M., & Yuan, R. (1968). DNA restriction enzyme from *E. coli* . *Nature*, *217*(5134), 1110-1114.

Messens, W., Duboccage, L., Grijspeerdt, K., Heyndrickx, M., & Herman, L. (2004). Growth of *Salmonella* serovars in hens' egg albumen as affected by storage prior to inoculation. *Food Microbiology*, *21*(1), 25-32.

Miller, J. H. (1972). *Experiments in molecular genetics*. Cold Spring Harbor Laboratory.

Minamino, T., Morimoto, Y. V., Kawamoto, A., Terashima, H., Imada, K., Minamino, T., Morimoto, Y. V., Kawamoto, A., Terashima, H., & Imada, K. (2018). *Salmonella* Flagellum. In *Salmonella—A Re-emerging Pathogen*. IntechOpen.

Mitchell, A. M., & Silhavy, T. J. (2019). Envelope stress responses : Balancing damage repair and toxicity. *Nature Reviews Microbiology*, *17*(7), 7.

Mitchell, P. (1966). Chemiosmotic coupling in oxidative and photosynthetic phosphorylation. *Biochimica et Biophysica Acta (BBA) - Bioenergetics*, *1807*(12), 445-502.

Miyamoto, T., Baba, E., Tanaka, T., Sasai, K., Fukata, T., & Arakawa, A. (1997). *Salmonella* Enteritidis contamination of eggs from hens inoculated by vaginal, cloacal, and intravenous routes. *Avian Diseases*, *41*(2), 296-303.

Mizutani, K. (1999). Alternative structural state of transferrin. *The Journal of Biological Chemistry*, *274*(15), 10190-10194.

Molla, A., Matsumura, Y., Yamamoto, T., Okamura, R., & Maeda, H. (1987). Pathogenic capacity of proteases from *Serratia marcescens* and *Pseudomonas aeruginosa* and their suppression by chicken egg white ovomacroglobulin. *Infection and Immunity*, *55*(10), 2509-2517.

Mongin, P., & Lacassagne, L. (1966). Equilibre acido-basique du sang et formation de la coquille de l'oeuf. *Annales de Biologie Animale Biochimie Biophysique*, *6*(1), 93-100.

Moravej, H., Moravej, Z., Yazdanparast, M., Heiat, M., Mirhosseini, A., Moosazadeh Moghaddam, M., & Mirnejad, R. (2018). Antimicrobial Peptides : Features, Action, and Their Resistance Mechanisms in Bacteria. *Microbial Drug Resistance*, *24*(6), 747-767.

Mücke, P.-A., Maaß, S., Kohler, T. P., Hammerschmidt, S., & Becher, D. (2020). Proteomic Adaptation of *Streptococcus pneumoniae* to the Human Antimicrobial Peptide LL-37. *Microorganisms*, *8*(3), 3.

Muniyappa, K., & Adiga, P. R. (1979). Isolation and characterization of thiamin-binding protein from chicken egg white. *Biochemical Journal*, *177*(3), 887-894.

Nagakubo, S., Nishino, K., Hirata, T., & Yamaguchi, A. (2002). The putative response regulator BaeR stimulates multidrug resistance of *Escherichia coli* via a novel multidrug exporter system, MdtABC. *Journal of Bacteriology*, *184*(15), 4161-4167.

Nagar, N., Ecker, N., Loewenthal, G., Avram, O., Ben-Meir, D., Biran, D., Ron, E., & Pupko, T. (2021). Harnessing Machine Learning To Unravel Protein Degradation in Escherichia coli. *MSystems*, *6*(1), e01296-20.

Nagasawa, S., Ishige, K., & Mizuno, T. (1993). Novel members of the two-component signal transduction genes in *Escherichia coli*. *The Journal of Biochemistry*, *114*(3), 350-357.

Nau, F., Guérin-Dubiard, C., Baron, F., & Thapon, J.-L. (2010a). *Science et technologie de l'oeuf, volume 1 : Production et qualité* (Tec&Doc, Vol. 1). Lavoisier.

Nau, F., Guérin-Dubiard, C., Baron, F., & Thapon, J.-L. (2010b). *Science et technologie de l'oeuf, volume 2 : De l'oeuf aux ovoproduits* (Tec&Doc, Vol. 2). Lavoisier.

Nikaidoi, H., & Vaara, M. (1985). Molecular basis of bacterial outer membrane permeability. *Microbiological Reviews*, *49*(1), 1-32.

Nishino, K., Honda, T., & Yamaguchi, A. (2005). Genome-wide analyses of Escherichia coli gene expression responsive to BaeSR two-component regulatory system. *Journal of Bacteriology*, *187*(5), 1763-1772.

Nys, Y., & Sauveur, B. (2004). Valeur nutritionnelle des oeufs. *INRAE Productions Animales*, *17*(5), 385-393.

Okamoto, I., Mizutani, K., & Hirose, M. (2004). Iron-binding process in the amino- and carboxyl-terminal lobes of ovotransferrin : Quantitative studies utilizing single Fe $^{3+}$ -binding Mutants. *Biochemistry*, *43*(34), 11118-11125.

Outten, F. W., Djaman, O., & Storz, G. (2004). A suf operon requirement for Fe–S cluster assembly during iron starvation in *Escherichia coli* . *Molecular Microbiology*, *52*(3), 861-872.

Padan, E., Zilberstein, D., & Rottenberg, H. (1976). The Proton electrochemical gradient in *Escherichia coli* cells. *European Journal of Biochemistry*, *63*(2), 533-541.

Padan, E., Zilberstein, D., & Schuldiner, S. (1981). PH homesstasis in bacteria. *Biochimica et Biophysica Acta (BBA) - Reviews on Biomembranes*, *650*(2), 151-166.

Palmiter, R. D., Mulvihill, E. R., McKnight, G. S., & Senear, A. W. (1978). Regulation of gene expression in the chick oviduct by steroid hormones. *Cold Spring Harbor Symposia on Quantitative Biology*, *42*(0), 639-647.

Pan, Z., Carter, B., Núñez-García, J., AbuOun, M., Fookes, M., Ivens, A., Woodward, M. J., & Anjum, M. F. (2009). Identification of genetic and phenotypic differences associated with prevalent and non-prevalent *Salmonella* Enteritidis phage types : Analysis of variation in amino acid transport. *Microbiology*, *155*(10), 3200-3213.

Parsons, A. H. (1982). Structure of the eggshell. *Poultry Science*, *61*(10), 2013-2021.

Pellegrini, A., Thomas, U., von Fellenberg, R., & Wild, P. (1992). Bactericidal activities of lysozyme and aprotinin against Gram-negative and Gram-positive bacteria related to their basic character. *Journal of Applied Bacteriology*, *72*(3), 180-187.

Pellegrini, A., Thomas, U., Wild, P., Schraner, E., & Von Fellenberg, R. (2000). Effect of lysozyme or modified lysozyme fragments on DNA and RNA synthesis and membrane permeability of *Escherichia coli* . *Microbiological Research*, *155*(2), 69-77.

Penner, J. L. (1988). International committee on systematic bacteriology taxonomic subcommittee on Enterobacteriaceae. *International Journal of Systematic and Evolutionary Microbiology*, *38*(2), 223-224.

Pettersen, E. F., Goddard, T. D., Huang, C. C., Couch, G. S., Greenblatt, D. M., Meng, E. C., & Ferrin, T. E. (2004). UCSF Chimera-A visualization system for exploratory research and analysis. *Journal of Computational Chemistry*, *25*(13), 1605-1612.

Phelps, C. F., & Antonini, E. (1975). A study of the kinetics of iron and copper binding to hen ovotransferrin. *Biochemical Journal*, *147*(3), 385-391.

Pollack, J. R., Ames, B. N., & Neilands, J. B. (1970). Iron transport in *Salmonella typhimurium* : Mutants Blocked in the biosynthesis of enterobactin. *Journal of Bacteriology*, *104*(2), 635-639.

Qin, X., Dong, R., He, S., Zhou, X., Zhang, Z., Cui, Y., Shi, C., Liu, Y., & Shi, X. (2020). Characterization of the role of ybgC in lysozyme resistance of *Salmonella* Enteritidis. *Food Control*, *109*, 106732.

Qin, X., He, S., Zhou, X., Cheng, X., Huang, X., Wang, Y., Wang, S., Cui, Y., Shi, C., & Shi, X. (2019). Quantitative proteomics reveals the crucial role of YbgC for *Salmonella enterica* serovar Enteritidis survival in egg white. *International Journal of Food Microbiology*, *289*, 115-126.

Raffa, R. G., & Raivio, T. L. (2002). A third envelope stress signal transduction pathway in *Escherichia coli* . *Molecular Microbiology*, *45*(6), 1599-1611.

Rana, F. R., Sultany, C. M., & Blazyk, J. (1991). Determination of the lipid composition of *Salmonella* Typhimurium outer membranes by 31P NMR. *Journal of microbiological methods*, 14(1), 41-51.

Raspoet, R., Appia-Ayme, C., Shearer, N., Martel, A., Pasmans, F., Haesebrouck, F., Ducatelle, R., Thompson, A., & Immerseel, F. V. (2014). Microarray-Based Detection of *Salmonella* enterica Serovar Enteritidis Genes Involved in Chicken Reproductive Tract Colonization. *Applied and Environmental Microbiology*, *80*(24), 7.

Redhead, K., Hill, T., & Chart, H. (1987). Interaction of lactoferrin and transferrins with the outer membrane of *Bordetella Pertussis* . *Microbiology*, *133*(4), 891-898.

Réhault-Godbert, S., Guyot, N., & Nys, Y. (2019). The golden egg : Nutritional value, bioactivities, and emerging benefits for human health. *Nutrients*, *11*(3), 3.

Réhault-Godbert, S., Labas, V., Helloin, E., Hervé-Grépinet, V., Slugocki, C., Berges, M., Bourin, M.-C., Brionne, A., Poirier, J.-C., Gautron, J., Coste, F., & Nys, Y. (2013). Ovalbumin-related Protein X Is a Heparin-binding Ov-Serpin Exhibiting Antimicrobial Activities. *Journal of Biological Chemistry*, *288*(24), 17285-17295.

Robinson, D. S., & Monsey, J. B. (1972). Changes in the composition of ovomucin during liquefaction of thick egg white. *Journal of the Science of Food and Agriculture*, *23*(1), 29-38.

Robinson, D. S., & Monsey, J. B. (1975). The Composition and proposed subunit structure of egg-white P-ovomucin. *Biochemical Journal*, *147*(1), 55-62.

Roer, L., Hendriksen, R. S., Leekitcharoenphon, P., Lukjancenko, O., Sommer Kaas, R., Hasman, H., & Aarestrup, F. M. (2016). Is the evolution of *Salmonella enterica* subsp. Enterica linked to restriction-modification systems? *American Society for Microbiology*, *1*(3).

Samuelson, K. J., Rupnow, J. H., & Froning, G. W. (1985). The effect of lysozyme and ethylenediaminetetraacetic acid on *Salmonella* on broiler parts. *Poultry Science*, *64*(8), 1488-1490.

Sandrini, S., Masania, R., Zia, F., Haigh, R., & Freestone, P. (2013). Role of porin proteins in acquisition of transferrin iron by enteropathogens. *Microbiology*, *159*(Pt_12), 2639-2650.

Sato, Y., Hayakawa, S., & Nakamura, R. (1976). Studies on factors of solubilization of insoluble ovomucin during thick white thinning. *Journal of Agricultural and Food Chemistry*, *24*(4), 798-803.

Sauveur, B. (1988). *Reproduction des volailles et production d'oeufs*. Quae.

Schwyn, B., & Neilands, J. B. (1987). Universal chemical assay for the detection and determination of siderophores. *Analytical Biochemistry*, *160*(1), 47-56.

Shade, A. L., & Caroline, L. (1944). Raw hen egg white and the role of iron in growth inhibition of *Shigella dysenteriae*, *Staphylococcus aureus*, *Escherichia coli* and *Saccharomyces cerevisiae*. *Science*, *100*, 14-15.

Shah, P., Hsiao, F. S.-H., Ho, Y.-H., & Chen, C.-S. (2016). The proteome targets of intracellular targeting antimicrobial peptides. *PROTEOMICS*, *16*(8), 1225-1237.

Sharp, P. F., & Powell, C. K. (1931). Increase in the pH of the white and yolk of hens' eggs. *Industrial & Engineering Chemistry*, *23*(2), 196-199.

Silhavy, T. J., Kahne, D., & Walker, S. (2010). The Bacterial cell envelope. *Cold Spring Harbor Perspectives in Biology*, *2*(5), a000414.

Simons, R. W., Houman, F., & Kleckner, N. (1987). Improved single and multicopy lac-based cloning vectors for protein and operon fusions. *Gene*, *53*(1), 85-96.

Skare, J. T., Ahmer, B. M., Seachord, C. L., Darveau, R. P., & Postle, K. (1993). Energy transduction between membranes. TonB, a cytoplasmic membrane protein, can be chemically cross-linked in vivo to the outer membrane receptor FepA. *Journal of Biological Chemistry*, *268*(22), 16302-16308.

Smith, T. (1894). *The hog-cholera group of bacteria*. *6*, 6-40.

Solovyev, V., & Salamov, A. (2011). *Automatic annotation of microbial genomes and metagenomic sequences* (Robert W. Li, pp). Nova Science.

Stadelman, W. J., & Cotterill, O. J. (1995). *Egg Science and Technology* (4th Edition). CRC Press.

Suzuki, T., Yamauchi, K., Kawase, K., Tomita, M., Kiyosawa, I., & Okonogi, S. (1989). Collaborative bacteriostatic activity of bovine lactoferrin with lysozyme against *Escherichia coli* 0111. *Agricultural and Biological Chemistry*, *53*(6), 1705-1706.

Tan, A. T., & Woodworth, R. C. (1969). Ultraviolet difference spectral studies of conalbumin complexes with transition metal ions. *Biochemitry*, *8*(9), 3711-3716.

Tan, A. T., & Woodworth, R. C. (1970). Differences in absorption and emission properties of conalbumin and metal-saturated conalbumin. *Journal of Polymer Science Part C: Polymer Symposia*, *30*(1), 599-606.

Tittsler, R. P., & Sandholzer, L. A. (1936). The Use of semi-solid agar for the detection of bacterial motility. *Journal of Bacteriology*, *31*(6), 575-580.

Tranter, H. S., & Board, R. G. (1984). The influence of incubation temperature and pH on the antimicrobial properties of hen egg albumen. *Journal of Applied Bacteriology*, *56*(1), 53-61.

Troxell, B., & Hassan, H. M. (2013). Transcriptional regulation by Ferric Uptake Regulator (Fur) in pathogenic bacteria. *Frontiers in Cellular and Infection Microbiology*, *3*, 59.

Trüper, H. G. (2005). The type species of the genus Salmonella Lignieres 1900 is Salmonella enterica (ex Kauffmann and Edwards 1952) Le Minor and Popoff 1987, with the type strain LT2T, and conservation of the epithet enterica in *Salmonella* enterica over all earlier epithets that may be applied to this species. Opinion 80. *International Journal of Systematic and Evolutionary Microbiology*, *55*(1), 519-520.

Turner, J., Cho, Y., Dinh, N.-N., Waring, A. J., & Lehrer, R. I. (1998). Activities of LL-37, a cathelin-associated antimicrobial peptide of human neutrophils. *Antimicrobial Agents and Chemotherapy*, *42*(9), 2206-2214.

Valenti, P., Stasio, A., Mastromerino, P., Seganti, L., Sinibaldi, L., & Orsi, N. (1981). Influence of bicarbonate and citrate on the bacteriostatic action of ovotransferrin towards *staphylococci* . *FEMS Microbiology Letters*, *10*(1), 77-79.

Valenti, P., Visca, P., Antonini, G., & Orsi, N. (1985). Antifungal activity of ovotransferrin towards genus *Candida* . *Mycopathologia*, *89*(3), 169-175.

Valenti, P., Visca, P., Antonini, G., & Orsi, N. (1986). Interaction between lactoferrin and ovotransferrin and Candida cells. *FEMS Microbiology Letters*, *33*, 271-275.

Valenti, P., Visca, P., Antonini, G., Orsi, N., & Antonini, E. (1987). The effect of saturation with Zn2+ and other metal ions on the antibacterial activity of ovotransferrin. *Medical Microbiology and Immunology*, *176*(3), 123-130.

van Dijk, A., Veldhuizen, E. J. A., & Haagsman, H. P. (2008). Avian defensins. *Veterinary Immunology and Immunopathology*, *124*(1), 1-18.

Vollmer, W., Blanot, D., & De Pedro, M. A. (2008). Peptidoglycan structure and architecture. *FEMS Microbiology Reviews*, *32*(2), 149-167.

Vrancken, K., Van Mellaert, L., & Anné, J. (2008). Characterization of the *Streptomyces lividans* PspA Response. *Journal of Bacteriology*, *190*(10), 3475-3481.

Waggoner, A. S. (1979). Dye indicators of membrane potential. *Annual Review of Biophysics and Bioengineering*, *8*(1), 47-68.

Wall, E., Majdalani, N., & Gottesman, S. (2018). The Complex Rcs Regulatory Cascade. *Annual Review of Microbiology*, *72*, 111-139.

Wang, X., & Quinn, P. J. (2010). Lipopolysaccharide : Biosynthetic pathway and structure modification. *Progress in Lipid Research*, *49*(2), 97-107.

Ward, L. R., de Sa, J. D. H., & Rowe, B. (1987). A phage-typing scheme for *Salmonella* enteritidis. *Epidemiology and Infection*, *99*(2), 291-294.

Warner, R. C., & Weber, I. (1953). The metal combining properties of conalbumin. *Journal of the American Chemical Society*, *75*(20), 5094-5101.

Wehland, M., & Bernhard, F. (2000). The RcsAB Box : Characterization of a new operator essential for the regulation of exopolysaccharide biosynthesis in enteric bacteria. *Journal of Biological Chemistry*, *275*(10), 7013-7020.

Weiner, L., Brissette, J. L., & Model, P. (1991). Stress-induced expression of the *Escherichia coli* phage shock protein operon is dependent on sigma 54 and modulated by positive and negative feedback mechanisms. *Genes & Development*, *5*(10), 1912-1923.

Weiner, L., & Model, P. (1994). Role of an *Escherichia coli* stress-response operon in stationary-phase survival. *Proceedings of the National Academy of Sciences*, *91*(6), 2191-2195.

Wellawa, D. H., Allan, B., White, A. P., & Köster, W. (2020). Iron-Uptake systems of chicken-associated *Salmonella* serovars and their role in colonizing the avian host. *Microorganisms*, *8*(8), 8.

Wellman-Labadie, O., Picman, J., & Hincke, M. T. (2008). Antimicrobial activity of cuticle and outer eggshell protein extracts from three species of domestic birds. *British Poultry Science*, *49*(2), 133-143.

Wesierska, E., Saleh, Y., Trziszka, T., Kopec, W., Siewinski, M., & Korzekwa, K. (2005). Antimicrobial activity of chicken egg white cystatin. *World Journal of Microbiology and Biotechnology*, *21*(1), 59-64.

Whitehead, M. L., & Roberts, V. (2014). Backyard poultry : Legislation, zoonoses and disease prevention. *Journal of Small Animal Practice*, *55*(10), 487-496.

WHO, & FAO. (2002). *Risk assessments for Salmonella in eggs and broiler chickens : Interpretative summary*. World Health Organization.

Wiegert, T., Homuth, G., Versteeg, S., & Schumann, W. (2001). Alkaline shock induces the *Bacillus subtilis* σW regulon. *Molecular Microbiology*, *41*(1), 59-71.

Williams, J. (1968). A comparison of glycopeptides from the ovotransferrin and serum transferrin of the hen. *Biochemical Journal*, *108*(1), 57-67.

Wittwer, C. (2001). Rapid Cycle Real-Time PCR : Methods and Applications. In S. Meuer, C. Wittwer, & K.-I. Nakagawara (Éds.), *Rapid Cycle Real-Time PCR: Methods and Applications* (p. 1-8).

Xie, X., Zhang, H., Zheng, Y., Li, A., Wang, M., Zhou, H., Zhu, X., Schneider, Z., Chen, L., Kreiswirth, B. N., & Du, H. (2016). RpoE is a putative antibiotic resistance regulator of *Salmonella* enteric serovar Typhi. *Current Microbiology*, *72*(4), 457-464.

Yoshioka, R., Fujii, T., & Ito, Y. (1966). On electrophoretic resolution and densitometric determination of apo-transferrin and iron-bound transferrin. *Biochemical and Biophysical Research Communications*, *24*(2), 203-207.

Appendices

Appendix 1. Construction of *S*. Enteritidis (pBBC129).

The *lacZ* gene of *E. coli* MG1655 (F^-, λ^-, *ilvG*$^-$, *rfb*-50, *rph*-1) (Blattner et al., 1997) was amplified by PCR using the Fidelio polymerase (Ozyme, Saint-Cyr-L'Ecole, France), and the primers TAGCTCACTCATTAGGCAC and AATGGATTTCCTTACGCG. The PCR was carried out according to the manufacturer's instructions. The amplified PCR fragment (3226 bp) was purified using the QIAquick gel extraction kit (Qiagen, Les Ulis, France) and ligated into the pBR322 plasmid (Bolivar et al., 1977) linearised at the *Eco*RV site. The ligation mixture was transformed into electrocompetent cells of *E. coli* DH5α (F^-, *endA1, glnV44, thi-1, recA1, relA1, gyrA96, deoR, nupG, purB20,* φ80d*lacZ*Δ*M15* Δ(*lacZYA-argF*)*U169, hsdR17*(rK^-mK^+), λ^-) (Meselson & Yuan, 1968). Transformants were selected on LB with ampicillin (100 µg/mL), 40 µM X-gal, and 1 mM IPTG (Isopropyl-β-D-thiogalactopyranoside, Sigma). Plasmid DNA was extracted from Lac^+ Amp^R transformants (QIAprep Spin Miniprep Kit – Qiagen) and the identity of the isolated plasmids was verified by restriction digestion analysis and was designated pBBC129. The *S.* Enteritidis strain NCTC13349 was transformed with the plasmid pBBC129. The new strain obtained was called *S.* Enteritidis pBBC129 and expresses β-lactamase and β-galactosidase in the periplasm and cytoplasm, respectively. The behaviour of this strain in the various media used in this study was checked and is comparable to that of *S.* Enteritidis NCTC13349 (data not shown). This strain was used to study outer and inner membrane permeabilisation.

Appendix 2. Measure of viscosity. The viscosity of egg white (blue) and SM with 10% of egg white (green) was measured using a rheometer (Discovery Hybrid Rheometer, DHR Serie, TA Instrument, New Castle, USA). A progressive shear rate from 1 to 100 (1/s) was applied to a volume of 22 mL of each medium. The experiment was performed with two technical replicates.

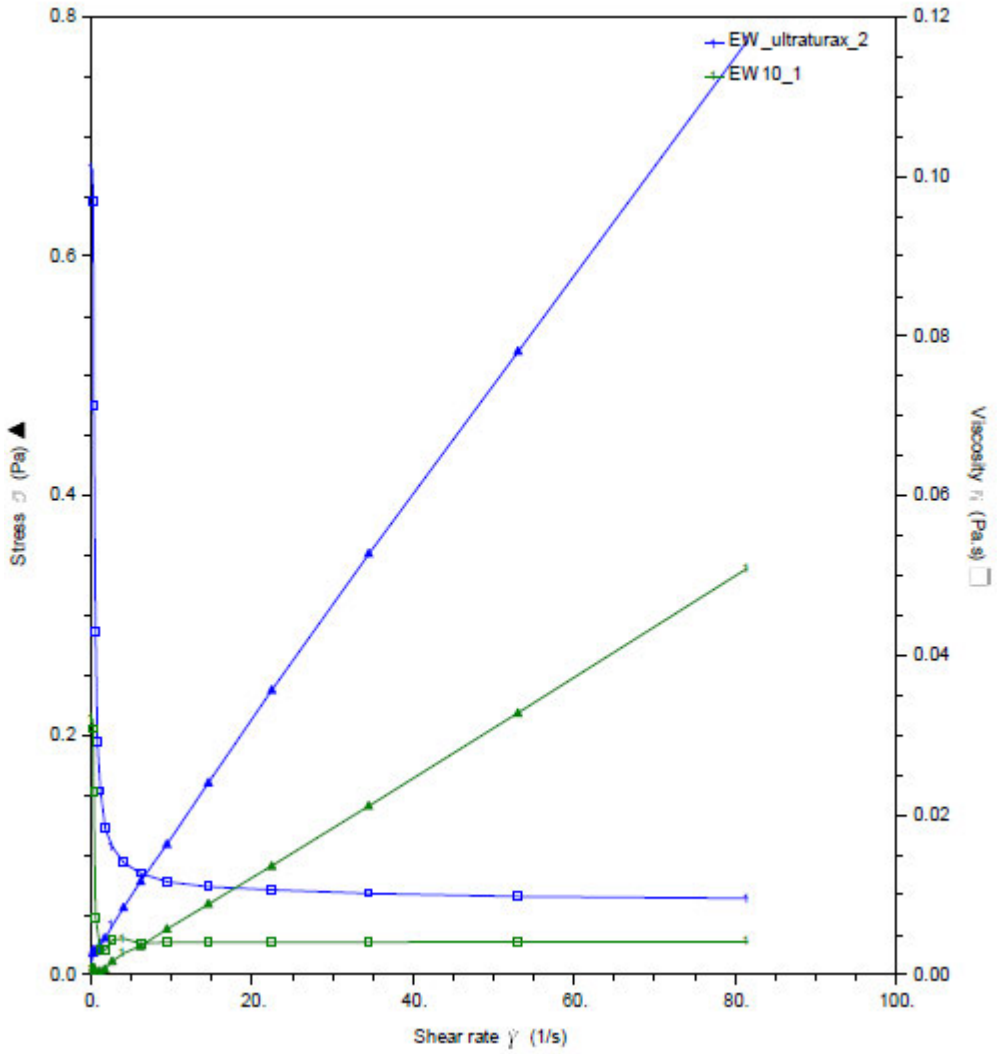

Appendix 3. – Regions amplified from S. Enteritidis NCTC13349 and cloned into pRS1274. (A) *pspF*, (B) *pspA* and (C) *pspG*. Enzyme restriction sites were highlighted in yellow, start codon in blue and stop codon in green.

A

*Bam*HI
GGATCCCCAGCGTATCTTCCATCTCCTGAATCATCAGGCGCACCAGCTTCTGCGGATCTT

CCGCTTTTTCCAACAACGCATTGATATTGGCGTTCACGATGTCGGCAAAACGAGAAAAAA

pspA
TACCCATAATTCAATCCTCACATAATGTTCTGATAACGGGCGATGCCCTGCTACATGGTT

AATACAATTTGCGTGCCAACTTTTTATACCACTGATAGTAAAGGAATTATTTCGTTTTAC

pspF
CTCGCCAGCAAAAAAGGATAAAGTGGTGAAAAACACTAACAAGTGGCGATTTTCATCATG

GCTGAATTTAAAGATAACCTGCTCGGCGAGGCAAACCGTTTTCTTGAAGTACTGGAACAA

*Eco*RI
GTCTCCCGGAATTC

B

*Bam*HI
GGATCCCGGGAGACTTGTTCCAGTACTTCAAGAAAACGGTTTGCCTCGCCGAGCAGGTTA

pspF
TCTTTAAATTCAGCCATGATGAAAATCGCCACTTGTTAGTGTTTTTCACCACTTTATCCT

TTTTTGCTGGCGAGGTAAAACGAAATAATTCCTTTACTATCAGTGGTATAAAAAGTTGGC

ACGCAAATTGTATTAACCATGTAGCAGGGCATCGCCCGTTATCAGAACATTATGTGAGGA

pspA
TTGAATTATGGGTATTTTTTCTCGTTTTGCCGACATCGTGAACGCCAATATCAATGCGTT

GTTGGAAAAAGCGGAAGATCCGCAGAAGCTGGTGCGCCTGATGATTCAGGAGATGGAAGA

*Eco*RI
TACGCTGGGAATTC

C

*Bam*HI
GGATCCCGATGTATCCCTATATTGAGCGTGAATTGAGCCAGGGAGCGTATCTGGGGCATA

TCACTCGCCATATGCTGGGGTTGTTCCAGGGCATTCCCGGCGCGCGACAGTGGCGTCGCT

ATCTGAGCGAAAACGCCCATAAAGCTGGCGCGGATGTTGCTGTACTGGAGCAGGCGCTAA

yjbN stop codon
AACTGGTAGCAGACAAGCGTTAAAAGTTCGCCAAAAATTAGTCAATCTCACCACGCTCTG

TGCAGTCTTGCAGGGCGTTTTCTTTATATATCAAAAACATAAATATTGGCATGATTTTTG

TAATAGCTTACCTGACCAGACCCGGTAAGCGCCGTGCCGCCGGGCAATGCCATCTTTATG

pspG
GGGAGCGACTATGCTGGAACTACTTTTTGTGCTTGGCTTTTTTCTGATGTTAATGGTGAC

*Eco*RI
GGGCGTCTCCTTGCTGGGCATTCTGGAATTC

Appendix 4. **RNA amplification by PCR.** A few samples of RNA were used as PCR templates to check the absence of gDNA contamination. Lane (M) contains high range RNA ladder (200 – 6000 bases) (ThermoScientific™). Lanes 1 to 12 contain RNA extracted after 45 min in SM, SM with 10% EW, SM with OT 1.3 g/L and SM with OT 13 g/L. The electrophoresis was performed for 1 h at 80 V on a 1.2% agarose gel.

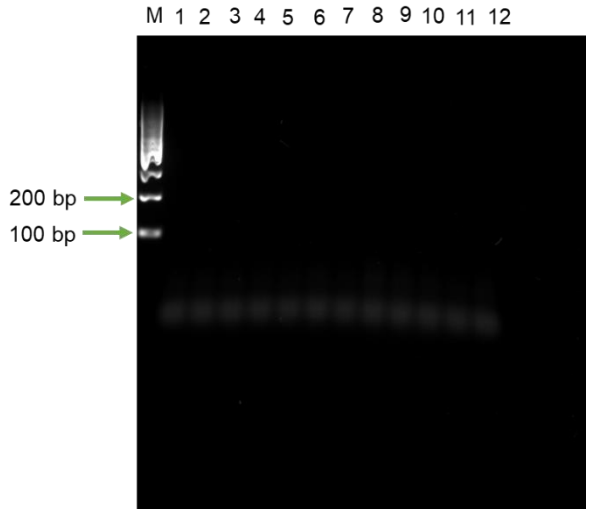

Titre : L'ovotransferrine, une protéine multifonctionnelle impliquée dans l'immunité passive du blanc d'œuf

Mots clés : Ovotransferrine ; Blanc d'œuf ; *Salmonella* Enteritidis ; Fer ; Perturbations membranaires

Résumé : L'ovotransferrine (OT) est la protéine antimicrobienne la plus abondante du blanc d'œuf (BO). Les œufs et ovoproduits étant souvent impliqués dans des épidémies de salmonelloses, cette étude visait à mieux comprendre (i) le rôle de l'OT sur la croissance et les fonctions membranaires de *Salmonella* Enteritidis et (ii) la capacité des bactéries à contrecarrer l'activité antimicrobienne de cette protéine. Il a été confirmé que l'activité chélatrice de fer de l'OT était responsable de l'activité antimicrobienne du BO contre *S.* Enteritidis. L'importance des sidérophores pour soutenir la croissance de *S.* Enteritidis lordque l'OT est entièrement saturée en fer a été suggérée. Cependant, en absence de fer, la production de sidérophores ne semble pas conférer un avantage à la croissance bactérienne. La production insuffisante de sidérophores et/ou la séquestration d'enterobactin par les lipocalines pourraient expliquer cette observation. La capacité de l'OT à induire des dommages membranaires à *S.* Enteritidis, indépendamment de son activité chélatrice de fer a fortement été observée. Ainsi, l'OT est capable de perméabiliser la membrane externe de *S.* Enteritidis et participer à la dépolarisation de la membrane interne. Le maintien de l'intégrité membranaire est assuré par l'expression de différents syst-mes tels que les Phage Shock protein genes (Psp). Dans cette étude, l'expérience des gènes psp semble être étroitement liée au pH alcalin du milieu utilisé. Cependant, le BO et l'OT semblent avoir un rôle dans la réponse aux gènes psp, dépendant de la concentration employée et du temps d'exposition. Cette étude confirme l'action antimicrobienne de l'OT contre *S.* Enteritidis dans le BO (activité de chélatrice de fer, perturbation membranaires).

Title: Ovotransferrin, a multifunctional protein involved in the passive immunity of egg white

Keywords: *Ovotransferrin; Egg white; Salmonella Enteritidis; Iron; Membrane damage*

Abstract: Ovotransferrin (OT) is the most abundant antimicrobial protein of egg white (EW). As eggs and egg products are often involved in salmonellosis outbreaks, this study aimed to gain a better understanding of (i) the role of OT in disturbing the growth and membrane functions of *Salmonella* Enteritidis and (ii) the ability of the bacteria to counteract the antimicrobial activity of this protein. The metal-chelating activity of OT was confirmed to be responsible for the antimicrobial activity of EW against *S.* Enteritidis. The importance of siderophores to support *S.* Enteritidis growth when OT is fully saturated was suggested. However, in the absence of iron the production of siderophores does not seem to confer any advantage for bacterial growth. The insufficient production of siderophores and/or the sequestration of Ent by lipocalins could explain this observation. The capacity of OT to induce *S.* Enteritidis membrane damage independently of its metal-chelating activity was strongly observed. Thus, OT can permeabilise the outer membrane and participate in the depolarisation of the inner membrane. The maintenance of membrane integrity is supported through the expression of different systems such as the Phage Shock Protein (Psp) genes. In this study, the expression of the *psp* genes seemed to be closely related to the alkaline pH of the medium employed. However, both EW and OT appeared to have only modest roles in the *psp* response, which depended on the concentration employed and the time of exposure. This study confirms the antimicrobial action of OT against *S.* Enteritidis in EW (metal-chelating activity, membrane perturbations).